

Further titles in this series:

1. *G. SANGLERAT*
THE PENETROMETER AND SOIL EXPLORATION
2. *Q. ZARUBA AND V. MENCL*
LANDSLIDES AND THEIR CONTROL
3. *E.E. WAHLSTROM*
TUNNELING IN ROCK
4. *R. SILVESTER*
COASTAL ENGINEERING, I and II
5. *R.N. YOUNG AND B.P. WARKENTIN*
SOIL PROPERTIES AND BEHAVIOUR
6. *E.E. WAHLSTROM*
DAMS, DAM FOUNDATIONS, AND RESERVOIR SITES
7. *W.F. CHEN*
LIMIT ANALYSIS AND SOIL PLASTICITY
8. *L.N. PERSEN*
ROCK DYNAMICS AND GEOPHYSICAL EXPLORATION
Introduction to Stress Waves in Rocks
9. *M.D. GIDIGASU*
LATERITE SOIL ENGINEERING
10. *Q. ZARUBA AND V. MENCL*
ENGINEERING GEOLOGY
11. *H.K. GUPTA AND B.K. RASTOGI*
DAMS AND EARTHQUAKES
12. *F.H. CHEN*
FOUNDATIONS ON EXPANSIVE SOILS
13. *L. HOBST AND J. ZAJIC*
ANCHORING IN ROCK
14. *B. VOIGT (Editor)*
ROCKSLIDES AND AVALANCHES, 1 and 2
15. *C. LOMNITZ AND E. ROSENBLUETH*
SEISMIC RISK AND ENGINEERING DECISIONS
16. *A.C.A. BAAR*
APPLIED SALT-ROCK MECHANICS, I
The in-situ Behavior of Salt Rocks
17. *A.P.S. SELVADURAI*
ELASTIC ANALYSIS OF SOIL-FOUNDATION INTERACTION
18. *J. FEDA*
STRESS IN SUBSOIL AND METHODS OF FINAL SETTLEMENT CALCULATION
19. *Á. KÉZDI*
STABILIZED EARTH ROADS
20. *E.W. BRAND AND R. P. BRENNER*
SOFT-CLAY ENGINEERING

Developments in Geotechnical Engineering 21

THE BEARING CAPACITY OF BUILDING FOUNDATIONS

PROF. DR. ING. ALOIS MYSLIVEC, DRSc.

*Corresponding Member
of the Czechoslovak Academy of Sciences, Prague*

ING. ZDENĚK KYSELA, CSc.

*Senior Research Fellow
Institute of Theoretical and Applied Mechanics of the Czechoslovak Academy of Sciences,
Prague*



ELSEVIER SCIENTIFIC PUBLISHING COMPANY

Amsterdam

Oxford

New York

1978

Published in co-edition with SNTL Publishers of Technical Literature, Prague

Distribution of this book is being handled by the following publishers:

for the USA and Canada

Elsevier/North-Holland, Inc.

52 Vanderbilt Avenue

New York, 10017

for the East European Countries, China, Northern Korea, Cuba, Vietnam and Mongolia

SNTL Publishers of Technical Literature, Prague

for all remaining areas

ELSEVIER SCIENTIFIC PUBLISHING COMPANY

335 Jan van Galenstraat

P. O. Box 211, Amsterdam, The Netherlands

Library of Congress Cataloging in Publication Data

Myslivec, Alois.

The bearing capacity of building foundations.

(Developments in geotechnical engineering ; 21)

Revised and updated translation of Unosnost
základů staveb.

Bibliography: p.

Includes index.

I. Foundations. I. Kysela, Zdeněk, joint
author. II. Myslivec, Alois. Unosnost základů
staveb. III. Title. IV. Series.

TA775.M9413 1978 624'.15 78-6172

ISBN 0-444-99794-0

Series ISBN 0-444-41662-5

With 78 illustrations and 57 tables

Translation © by Ing. John Eisler

Copyright © 1978 Prof. Dr. Ing. Alois Myslivec DrSc and Ing. Zdeněk Kysela CSc

All rights reserved. No part of this publication may be reproduced, stored in a retrieval system, or transmitted in any form or by any means, electronic, mechanical, photocopying, recording, or otherwise, without the prior written permission of the publisher

Printed in Czechoslovakia

SYMBOLS USED

a	acceleration of vibration; relative coefficient of compressibility
A	foundation surface
A_f, A_r	work necessary for the mobilization of τ_f, τ_r
\bar{A}	coefficient of springing
b	distance of foundation from edge of slope
B	width of foundation; mean width of two foundations
B_1, B_{11}	width of foundation I and II
c	cohesion
c'	effective cohesion
c_f	peak cohesion
c_r	residual cohesion
c_u	total cohesion
c_v	coefficient of consolidation
c_1, c_2	cohesion of upper level of soil 1 and lower level of soil 2
\bar{c}	cohesion between soil and structure
$C, (C_0)$	coefficient of compressibility (absolute)
C_1, C_2	components of total cohesion for a length l_1, l_2
d	height of slope
d_1, d_2	coefficients of the soil friction influence on the sides of a foundation
d_γ, d_q, d_c	coefficients of the soil influence above the foundation level
d_p	height of plastic range
d_1	height of influence of horizontal force on column
D	depth of foundation
D'	effective depth of foundation
D_1, D_{11}	depth of foundation of foundation I and II
e	eccentricity; void ratio
e_{\max}	largest permissible eccentricity
E	elastic modulus
E_1	elastic modulus of upper layer of soil or cushion
E_2	elastic modulus of lower layer of soil
E_a	active earth pressure
E_0	modulus of deformation; earth pressure at rest
E_p	passive resistance of soil

f	coefficient of friction; frequency in Hz
F	safety factor
g	acceleration due to gravity ($g = 9,80665 \text{ m s}^{-2}$)
h	height of soil layer
\bar{h}	depth of groundwater elevation below surface
h_k	height of capillary rise of water
H	horizontal force acting in foundation line; thickness of upper layer of soil under foundation line; height of foundation
H_{eq}	equivalent height of soil
H'	vertical distance of the edge of the foundation from the sliding surface
i, \bar{i}	number of layers, points, elements
i_γ, i_q, i_c	coefficients of the influence of the load resultant inclined at an angle to the vertical
J	hydraulic slope
k	coefficient of permeability; uniformity coefficient
K_a	coefficient of active earth pressure
K_0	coefficient of earth pressure at rest
K_p	coefficient of passive earth pressure
K_t	coefficient of foundation rigidity
l	axial distance of adjacent foundations
L	length of foundation
L_k	distance over which a sliding slope comes to rest
m	coefficient of the reliability of a calculation; number of sectors of a circle
m'	degree of mobilization of the shearing strength of soil
\bar{m}	number of pulses
m_1, m_2	correction coefficients
M	bending moment, tilting moment
\bar{M}	weight of released part of slope
M'	coefficient of moment caused by horizontal load
M_0	oedometric modulus of deformation
M_m	ultimate moment
M_x	moment related to point X
n	porosity of soil; number of annuli, layers
\bar{n}	coefficient of load
$N_\gamma, N_q, N_c, N_{cq}$	
\bar{N}_c	coefficients of bearing value
N_s	factor of slope stability
\bar{N}	normal force
O	circumference of foundation

p	pressure on soil surface
p_k	internal stress
P	horizontal force
P_m	ultimate horizontal force
q	load on foundation soil
Δq	load increment
\bar{q}	load in the vicinity of a foundation at the foundation line
q_b	bulking pressure
q_d	permissible load
q_f	calculation stress of foundation soil
q_m	bearing capacity in foundation line
q_{m1}	bearing capacity of upper soil layer
q_{m2}	bearing capacity of lower soil layer
q_{ms}	bearing capacity of soil layer on bedrock
q_0	derived normative stress of soil; estimated mean load at foundation line
q_p	permissible load of foundation soil
Q	force acting in foundation line
\bar{Q}	weight of released part of slope
Q_m	ultimate vertical load acting in foundation line
Q_1, Q_2	components of the weight of the soil
r, R	radius of circular foundation; directrix of logarithmic spiral
r_0	initial directrix of logarithmic spiral
R_1, R_2	components of friction on yield surface in the subgrade of a foundation
s	settlement of a foundation
s_γ, s_q, s_c	coefficients of the influence of the shape of the foundation
S	separation of foundations
t	time
i	depth of capillary water menisci beneath the ground surface
T	distance of the lowest point of the yield surface from the plane of the foundation line; time factor
T	displacement force
u_a	pore air pressure
u, u_w	pore water pressure
v	velocity of movement
w	water content of soil; wind pressure
w_s	shrinkage limit
w'_s	water content of soil after a period of drying out
W	cross-section modulus
x	length

y	amplitude of vibration
z	depth beneath ground level
z_{eq}	equivalent depth beneath ground level
\bar{z}	depth of point X
Z	separation of ground levels in the vicinity of foundations
Z_1, Z_2	components of resultant forces on sliding surfaces
I	the foundation for which the bearing capacity or permissible load is determined
II	the foundation adjacent to foundation I
$\alpha, \alpha_\gamma, \alpha_q, \alpha_c$	factors of interaction of adjacent foundations
$\alpha^\circ, \alpha', \bar{\alpha}, \alpha_r$	angle
$\bar{\alpha}$	coefficient of the shape and rigidity of a foundation
β	gradient; inclination of the resultant load to the vertical
$\beta^\circ, \beta', \bar{\beta}$	angle
γ	unit weight of soil with natural-water content
γ_d	unit weight of dry soil
γ_n	unit weight of water-saturated soil
γ_s	specific weight of soil particles
γ_w	specific weight of water
γ'	unit weight of soil beneath groundwater level
γ_1	unit weight of soil beneath foundation
γ_2	unit weight of soil above foundation line
δ	angle of wall friction
Δh	compression of soil in oedometer
Δs	difference in settlement
Δl	displacement during shearing test
Δl_{crit}	displacement during shearing test where a peak value of strength τ_f was reached
Δl_r	displacement during shearing test where a residual strength τ_r was reached
Δh_t	permanent compression
Δh_p	elastic compression
Δw	change in the water content of soil
$\Delta D = D_1 - D_{11}$	difference in the depth of foundation of adjacent foundations
$\Delta \sigma_z$	vertical stress increment
ε	relative deformation
ζ, η	lengths
ϑ	factor of bedrock influence; angle
Θ	angle
λ	reduction coefficient
μ	degree of consolidation

ν	Poisson's ratio (< 1)
$\sigma_1, \sigma_2, \sigma$	stress
σ_n	normal stress on a yield surface
σ_z	vertical stress
σ'	effective stress
σ_{st}	static stress
σ_d	dynamic stress
$\bar{\sigma}$	static stress during failure
σ_k	consolidation stress
σ_o	normal stress on a general plane
τ	shearing stress; shearing strength
τ_0	shearing stress on a general plane; initial shearing strength
τ_f	peak shearing strength
τ_r	residual shearing strength
Φ	angle
Φ'	effective angle of internal shearing resistance of the soil
Φ_f	peak angle of internal shearing resistance of the soil
Φ_r	residual angle of internal shearing resistance of the soil
Φ_u	total (acting) angle of internal shearing resistance of the soil
Ψ	angular acceleration
ω	circular frequency
Ω_f, Ω_r	modulus of mobilization of τ_f, τ_r
	$\bar{B}; E_1; f(D_1 - D_{11}); f_{ayi}; f_{byi}; G; K; l_c; l_q; S_c; S_q; U; v; V; Y;$ $\beta_1; \beta_2; \beta_c; \beta_q; \Gamma; \bar{\eta}; \psi; \bar{\lambda}; \varkappa$ main auxiliary functions.

INTRODUCTION

In foundation engineering, the main factor to be determined is the permissible soil pressure. This used to be done on the basis of experience with existing buildings. The permissible load was given for each type of soil but at that time no allowance was made for the width and depth of the foundation. Also, the definition of soil was inaccurate. For cohesive soils the permissible soil pressure values were given according to their consistency, this being classified as soft, firm, solid, hard, etc., but there were no rules for distinguishing between these types of soils. The composition of cohesionless soils was classified as sand, gravel or gravel-sand. Even today, permissible load values are given in tables and building codes and are still used in simple cases if the soil is homogeneous and the building has a maximum of three floors. These values also serve for orientation in the designing of large buildings and buildings in complicated geological conditions. With growing knowledge about the behaviour of soil during loading, the building-code permissible pressure values have been complemented with the influence of the depth of foundation, foundation breadth and the groundwater level.

A further step towards the determination of the permissible soil pressure has been provided by loading tests made in a trench at the level of the proposed foundation line. It was assumed that when the ultimate bearing capacity q_m is reached, the soil would be displaced from beneath the loaded surface to the sides causing the foundation to sink — this would appear as a break on the compression curve. Soil deformation caused by the load was not considered. When the load tests were made on compact sand, it was found that the relationship between the load and the impression was at first linear with increased load, the compression increment of the soil increased and the relationship had the form of a curve, and when the ultimate bearing capacity was reached the loaded surface sank to a depth where the resistance against displacing the subsoil was equal to the acting stress (Fig. 1). When the load $q_{m,a}$ was increased, after a larger settlement, the foundation again sank slightly. A loading test made in this way showed the influence caused by the depth of the loaded surface below ground level.

When the loading tests were made on clays, a continuous curve was obtained (Fig. 2). With increased load, the loading disc sank gradually and increasingly into the soil, while at the same time the resistance against the displacement increased with increasing depth. It is difficult to determine the ultimate bearing

capacity on such a continuous curve. The construction for its determination is given in Fig. 1. Sometimes a load which caused a previously defined settlement – for example 3 mm – was taken as the ultimate bearing capacity. Loading tests showed that the magnitude of the ultimate bearing capacity is influenced by the size of the loaded surface. When the relationship between the load and settlement for loading discs of various sizes was determined, it was found that

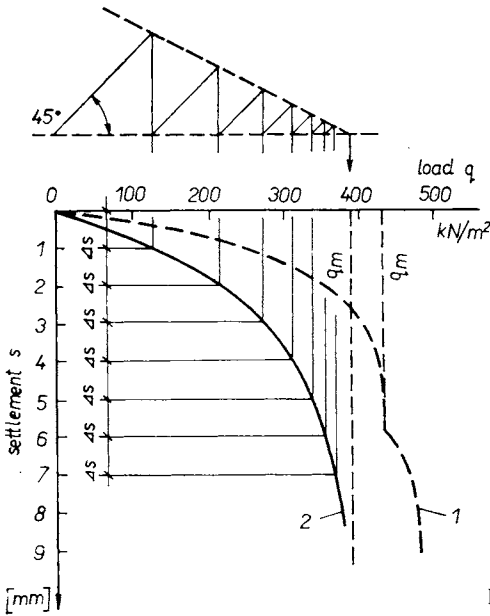


Fig. 1 Loading test: 1. on sand; 2. on clay

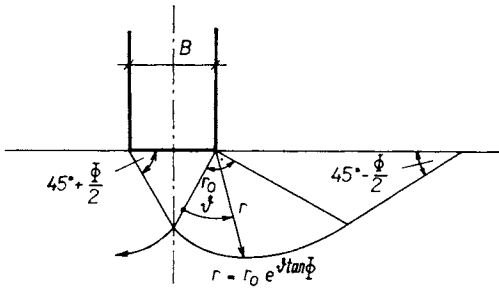


Fig. 2 Collapse mechanism according to Prandtl

a circular loading disc with a size of approximately 1000 cm² has the minimum settlement. When the disc was larger the settlement increased since the stress caused by the load penetrated to a greater depth and therefore a greater layer of soil was compressed. With a small loading surface the soil was displaced-outwards. For a larger loading surface, the previously determined soil compression was considered for a smaller loading surface. A loading disc with a very

small surface sank under a very small load and therefore the permissible settlement was obtained for a very small load.

To determine the influence of the foundation depth, a loading test used to be made in some countries in such a way that the loading disc was placed inside a tube, which was surrounded with earth to a height where the ratio of the foundation depth D to the foundation width B was the same as for the proposed building. The ultimate bearing capacity determined by the loading test was divided by a safety factor $F \doteq 2$ giving a permissible load $q_d = q_m/F$.

The loading test has many disadvantages if it is used to determine the ultimate bearing capacity. Nowadays, field loading tests are made, which allow the determination of in situ soil parameters, i.e. the deformation modulus, the angle of internal shearing resistance Φ and the cohesion c . For this test, two discs of different size are used.

The third way of determining the ultimate bearing capacity was theoretical. Here it was assumed that when the ultimate bearing capacity was reached sliding surfaces would be created under the foundation, along which the soil would be displaced towards the surface causing the foundation to sink. The first authors started from very simplified assumptions, for example that the bearing value of a foundation is a vertical load giving the result that under the foundation a horizontal stress, equal to the passive resistance of the soil, is created. By this reasoning, the bearing value of cohesionless soil on the surface would be equal to zero since there the passive pressure is equal to zero — a conclusion obviously in disagreement with reality. Later a more realistic assumption was made, that after reaching the bearing value of a foundation, collapse mechanisms would be created on one or both sides, by which the earth would be displaced outwards. Some authors assumed complex-plane collapse surfaces, which are kinematically impossible. Prandtl (1920) derived theoretically the shape of the collapse surfaces on the assumption that the unit weight of matter under the foundation is equal to zero. For the solution he used Kötters equation, which gives the relationship between the shape of the collapse surface and the distribution of the stresses along it. He was in fact solving the case of a bolt pressed into metal. The unit weight of the displaced metal is small compared with the resistances, so that this simplifying assumption was justifiable. According to Prandtl, a solid wedge is formed under the foundation. The angle between the side of the wedge and the foundation surface is $45^\circ + \Phi/2$. Further on, the collapse surfaces take the shape of a logarithmic spiral which changes into a plane inclined at an angle of $45^\circ - \Phi/2$ to the horizontal surface (Fig. 2). The angle formed by the walls of the solid wedge and a horizontal plane, when the unit weight of the soil $\gamma > 0$, was actually smaller than $45^\circ + \Phi/2$ and therefore many authors (Berezancev, Rossinski and others) assume an angle of 45° — Terzaghi uses the angle Φ . Buismann

added to Prandtl's equation the weight of the displaced soil, this enabling the bearing capacity of a foundation on homogeneous soil to be determined theoretically. The Prague-born K. Terzaghi made a large number of tests and derived an equation for the calculation of the bearing value of a strip foundation on homogeneous soil. He made the tests on the surface and replaced the influence of the earth above the foundation level by a uniform vertical load $\bar{q} = \gamma D$, where γ is the unit weight of soil and D the foundation depth. He expressed the influence of friction in the foundation level by a solid wedge of soil. The sides of the wedge, which originate at the edges of the foundation, form an angle of friction of the soil Φ with the foundation surface (Fig. 3). He therefore

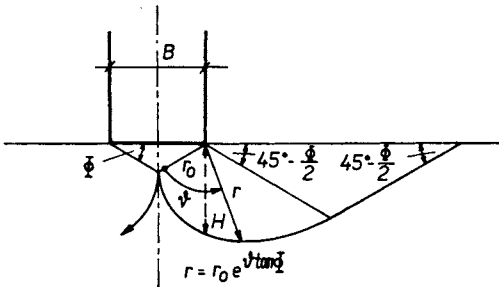


Fig. 3 Collapse mechanism according to Terzaghi

assumed that the soil above the foundation level manifests itself only by its weight and has no shearing strength. For this reason, his equation is valid only to approximately a foundation depth D equal to the foundation width B . For larger depths D , where the shearing strength of soil above the foundation level is already important, Terzaghi's equation gives smaller values. Terzaghi found it difficult to determine the ultimate bearing capacity of a foundation on clay since the compression curve is continuous. He therefore recommends that the values $(2/3) \tan \Phi$ and $2/3$ of cohesion c should be used in this equation.

Terzaghi's equation was adapted by Meyerhof (1951), who assumed yield surfaces which extend right to the surface, and resistances which act along the whole yield surface. In the case of deep foundations, according to Meyerhof, the yield surfaces envelop the foundation and do not reach the surface (Fig. 4). Brinch Hansen (1955) considered the influence of the foundation depth, the groundwater level and the inclination of the load acting on the foundation. Terzaghi's equation has been simplified by some authors for foundations on clay which has a small angle of internal shearing resistance, in such a way that the logarithmic spiral was replaced by a circle. Przeddecki-Rossinski (1961) solved the ultimate bearing capacity of a foundation on a cohesionless soil graphically, replacing the logarithmic spiral by a non-continuous curve formed by straight lines. The ultimate bearing capacity of a foundation determined

graphically in this way usually gives values slightly larger than those determined according to other authors.

In practice, cases more complicated than that of a homogeneous subgrade and a separately standing foundation arise. Usually there is an adjacent foundation at a greater or smaller distance from the foundation considered. Therefore

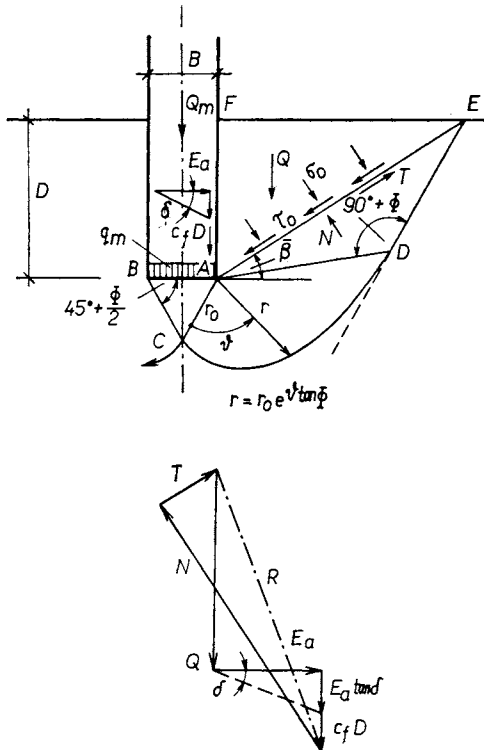


Fig. 4 Collapse mechanism according to Meyerhof

in this book we also study these special cases. The influence of the adjacent foundation can be positive, i.e. the bearing value of the foundation considered can be increased, or negative, if the value is decreased by the adjacent foundation. This depends on the separations of the foundations.

In old foundations we often find that the excavation gets narrower with depth and in section has the shape of an obtuse wedge; the width B at the bottom is smaller than at the top. The authors also describe this case.

Bridge pillars are often founded near the edge of a slope or on a slope and so the authors also study the influence of the angle of a slope on the ultimate bearing capacity of a foundation. A foundation is often loaded by an inclined resultant force, which can be resolved into vertical and horizontal components. For this reason the authors consider the effect of a horizontal force acting

on a foundation. The foundation soil is often stratified. We consider a situation where, beneath the foundation level in the zone of influence of the foundation there are two layers of soil, including the case where the second, lower layer is formed by incompressible rock. The case where the subgrade consists of a number of heterogeneous strata of soil is also considered.

In former times, buildings were built on marshy soils with a low bearing value, by covering these with a sufficiently thick layer of gravel or sand. As the load creates the greatest stress directly beneath the foundation and therefore the greatest resistance against displacement, the authors replace the low bearing-value soil by a gravel-sand bed just beneath the foundation and describe a graphical method for the determination of the ultimate bearing capacity of a foundation on such a bed.

For completeness, we consider the determination of the permissible load of a foundation and the safety factor, and also the contact stress in the foundation line, as this has a great influence on the dimensioning of foundation slabs.

The authors have not covered all the complicated cases found in building practice, but they feel that the most common have been included in such a form that the reader may make use of them in calculations.

1. SETTLEMENT OF FOUNDATIONS

1.1 VERTICAL STRESS IN SOIL DUE TO ITS WEIGHT

For the calculation of settlement or of the bearing value of foundations, it is necessary to know the effective vertical stress σ' , which acts between the grains of the foundation soil at a given depth. The total vertical stress σ is made up of the effective stress σ' , which acts between the grains of the soil, the neutral stress of water u_w in the pores of the soil, which may be either compressive or tensile, and finally of the neutral air pressure u_a . The total stress is

$$\sigma = \sigma' \pm u_w + u_a$$

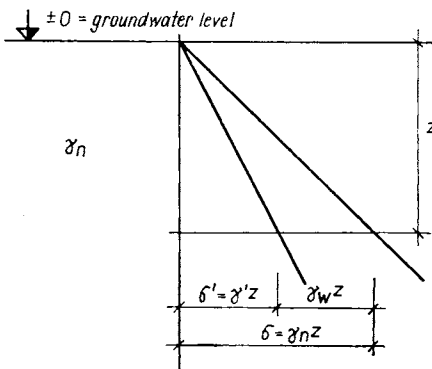


Fig. 1.1 Total and effective vertical stress in soil, if the water level is on the surface of the soil

The stresses carried by water or air are called neutral as neither water or air bear shearing stresses.

Let us consider a case where the water level is on the surface. The total vertical stress at a depth z is $\sigma = \gamma_n \cdot z$ (Fig. 1.1) The neutral stress at a depth z is $u_w = \gamma_w \cdot z$.

The effective stress

$$\sigma' = \sigma - u_w = z(\gamma_n - \gamma_w) = z\gamma' \quad (1.1)$$

with γ_n the density of waterlogged soil,
 γ_w the unit weight of water and
 γ' the weight of submerged soil.

Let us determine the vertical stress at a depth z , if the groundwater level is at a depth $\bar{h} \leq h_k$, where h_k is the capillary rise of water (Fig. 1.2). On the surface, the water menisci cause a capillary tension $u_w = -\gamma_w \cdot h$. The soil below the capillary level is waterlogged and therefore $u_a \doteq 0$. The neutral stress at a depth z is

$$u_w = \gamma_w(z - \bar{h}).$$

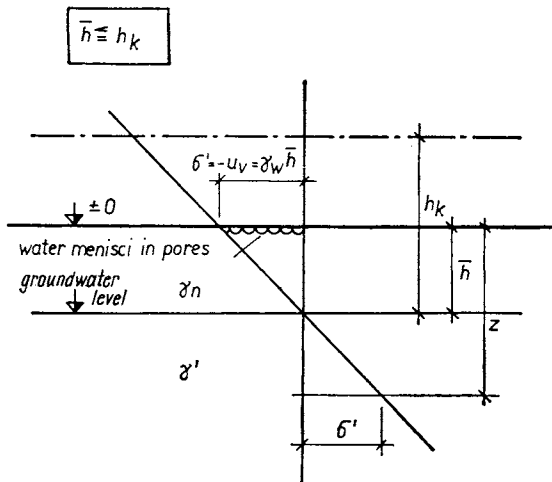


Fig. 1.2 Vertical stress in soil for $\bar{h} \leq h_k$

The effective stress

$$\sigma' = (\gamma_n - \gamma_w)z + \gamma_w \bar{h} = \gamma'z + \gamma_w \bar{h} \quad (1.2)$$

If one considers, for example, the effective stress at the groundwater level, i.e. for $z = \bar{h}$, then the neutral stress $u_w = \gamma_w(\bar{h} - \bar{h}) = 0$. On the surface the water pressure is equal to zero. The effective stress at the groundwater level is

$$\sigma' = \gamma_n \bar{h}.$$

The capillary rises h_k for various types of soil are given in Table 1.1.

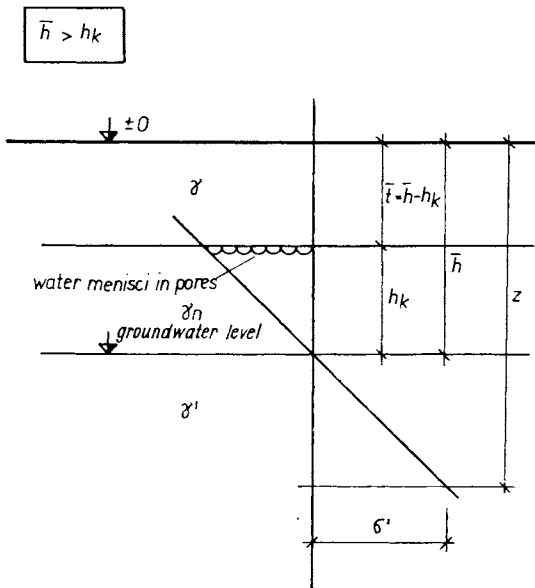
Data concerning capillary rises greater than 10 m are interpreted differently by a number of authors. Many see a given capillary height as a water head with which the capillary water acts upon the grains. For example, clay is left to shrink and the porosity at the shrinkable limit, i.e. after shrinkage, is measured. Then the soil is left to consolidate in an oedometer under a variable load and the porosity of the consolidated soil is determined. Under these conditions the equivalent load with which the soil would have to be compressed to attain a porosity equal to the porosity at the shrinkage limit, is for a sandy

loam 250 kN/m^2 , for loam 3.0 MN/m^2 and for clay 9.0 MN/m^2 . These values correspond to capillary heights of 25 m, 300 m and 900 m. The present authors see this height as a water head which would cause the same decrease in porosity as the evaporation of water.

TABLE 1.1

Capillary height h_k of water

Type of soil	Capillary height [m]
sand	0.03—0.1
fine sand	0.1—0.5
loamy sand	0.5—2.0
loess loam	2.0—5.0
loam	5.0—15.0
clayey loam	15.0—50.0
clay	over 50.0

Fig. 1.3 Vertical stress in soil for $\bar{h} > h_k$

Let us consider a case when the surface is at a height \bar{h} above the groundwater level, when $\bar{h} > h_k$. In such a case the pores of the soil are not fully waterlogged, as the capillary surface does not reach the ground surface (Fig. 1.3 and II.1). Let us determine the stress at a depth z . We designate $\bar{i} = \bar{h} - h_k$.

The neutral stress at a depth z is

$$u_w = \gamma_w(z - \bar{i} - h_k) = \gamma_w(z - \bar{h})$$

The effective stress at a depth z is

$$\begin{aligned} \sigma' &= \sigma - u_w = \gamma \bar{i} + \gamma_n(z - \bar{i}) - \gamma_w(z - \bar{i} - h_k) = \gamma \cdot \bar{i} + \\ &+ \gamma'(z - \bar{i}) + \gamma_w h_k \end{aligned} \quad (1.3)$$

where γ is the density of unsaturated soil.

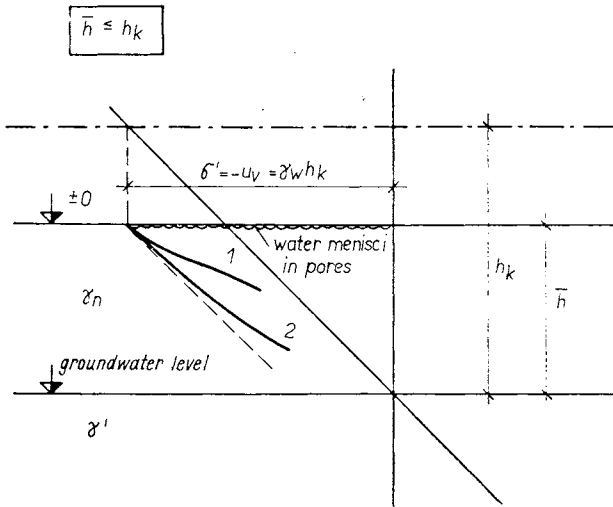


Fig. 1.4 Effective vertical stress in soil, if water evaporates intensely from the soil. Curve 1 corresponds to a more permeable soil than curve 2

In nature, we frequently encounter a situation where the capillary rise of water is above the surface of the area and the soil is therefore waterlogged. As a result of evaporation during sunny weather, the menisci bend and the soil particles are subjected to the full capillary pressure (Fig. 1.4). The neutral stress in a depth z under the surface of the area is

$$u_w = \gamma_w z - \gamma_w h_k = -\gamma_w(h_k - z)$$

The effective stress at a depth z is $\sigma' = \gamma_n z + \gamma_w(h_k - z)$.

The effective stress is larger by $\gamma_w(h_k - z)$, being a maximum on the surface where z equals zero. This must be taken into account when calculating the settlement. The consolidation pressure measured for an agrillaceous sandy soil by the Tower of Pisa is given in Fig. 1.5. The acting consolidation stress was at least three times greater than $\sigma_z = \gamma z$ (the groundwater level is at a

small depth below the surface of the area) and reached to a depth of about 17 m.

The consolidation pressure is usually determined according to Casagrade by a compressibility test in an oedometer. Fig. 1.6. The compressibility curve for an overconsolidated soil is almost linear at first, then it curves, and then becomes a straight line having a steeper gradient than the low-load straight line. The tangent of the angle to the vertical is the coefficient C of oedometric compressibility. We make a circle at the point of the greatest curvature of the

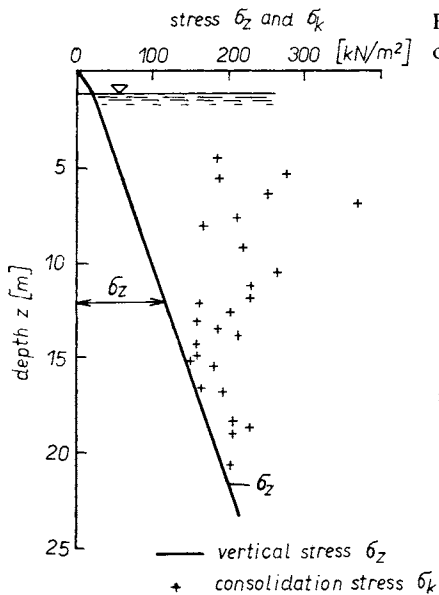


Fig. 1.5 Vertical and consolidation stress of the Tower of Pisa

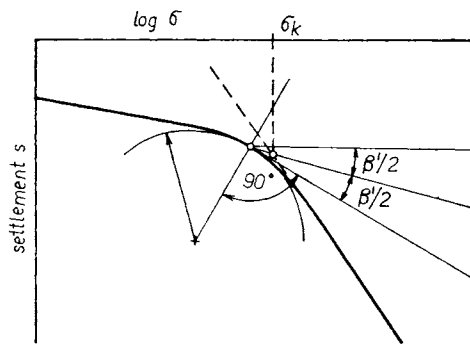


Fig. 1.6 Determination of the consolidation pressure σ_k as determined by Casagrande

compression curve. At the point of contact with the compression curve, a tangent and a straight line are drawn. These form an angle β' . This angle is then bisected and the intersection point of the disector with the extrapolation of the compression line gives us the magnitude of the consolidation pressure σ_k .

Stress in soil is also caused by the load on a foundation and depends on its rigidity and shape. These problems and some methods for calculating the stress in the soil are described in Chapter 4.

1.2 COMPRESSIBILITY OF SOIL

When subjected to a load, the soil is compressed and settles, the relationship is at first linear. As the load increases the settlement increment grows. Let us consider a sand which is not waterlogged. The load is transferred to particles on the contact surfaces, the grain surfaces are crushed and the grains are forced into the gaps between them, i.e. the pores. When the resistance against further compaction of the grains into the pores is equal to the acting stress, settlement ceases. As a result of an outer load in soil, there is not only a vertical stress σ_z , which compresses the soil, but also a horizontal stress σ_x , which forces the soil to the sides.

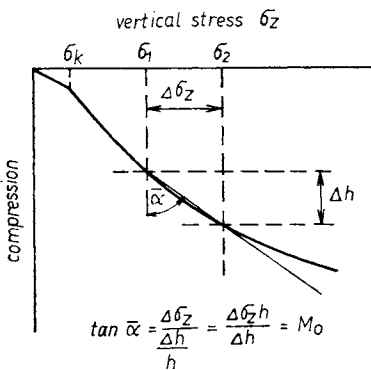


Fig. 1.7 The relationship between load and compression in the oedometer used for the determination of the deformation modulus M_0

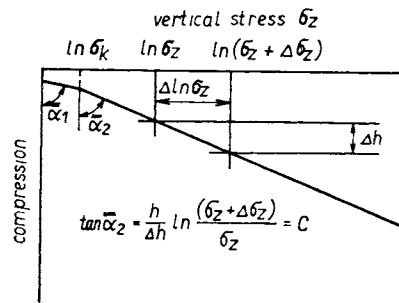


Fig. 1.8 The relationship between load and relative compression in the oedometer used for the determination of coefficient C

Compressibility is measured in an oedometer. This is a cylinder with a piston, which creates a vertical load. So that water can be drained from the tested sample there are porous drainage plates above and below the sample. The test is made in such a way that an undisturbed sample is taken from the soil and placed in the apparatus. When the sample is taken out of the extracting apparatus the horizontal stress, which was acting in the soil and could exceed the vertical stress relaxes. When talking of an undisturbed sample we bear in mind that the structure should be undisturbed, whereas the stress ratios in the oedometer may be very different from natural conditions. For this reason the measured values of compression and thence the calculated settlement do not always correspond to the true values. Therefore current compressibility tests are being made in a triaxial apparatus, which maintains a stress $\sigma_2 = \sigma_3$ having the same value as the stress in the soil.

If we plot the relationship of the vertical stress σ_z and the compression on a normal scale, we obtain a curve, and for an overconsolidated soil two curves. This curve is replaced in the section which corresponds to a stress increment $\Delta\sigma_z$ by a secant. The tangent of the angle of the secant and the vertical is called the modulus of oedometric deformation M_0 , Fig. 1.7. With a growing stress σ_z , the deformation modulus $M_0 = \tan \bar{\alpha}$ increases. The compression of a soil layer with thickness h caused by a stress $\Delta\sigma_z$ is

$$\Delta h = h\Delta\sigma_z/M_0 \quad (1.4)$$

On the compression curve there is usually a discontinuity at a point which corresponds to the stress σ_k which caused the soil to consolidate.

If we plot this relationship on a semilogarithmic scale we usually obtain two straight lines, where one line suddenly changes into the other straight line (Fig. 1.8). The coefficient of oedometric compressibility $C = \tan \bar{\alpha}$. When the load is less than the consolidation load, the soil is compressed elastically. For a load $\sigma > \sigma_k$ it is compressed both non-elastically and elastically, the non-elastic compression being the larger

$$\tan \bar{\alpha}_1 = \bar{A} > \tan \bar{\alpha}_2 = C$$

The compression of a layer with thickness h is then

$$\Delta h = \frac{h}{C} \ln \frac{\sigma_z + \Delta\sigma_z}{\sigma_z} \doteq \frac{h}{C} 2.3 \log \left(1 + \frac{\Delta\sigma_z}{\sigma_z} \right) \quad (1.5)$$

where the mean vertical stress σ_z acts and the mean load increment $\Delta\sigma_z$ is created in this thickness h . The values of the coefficient of compressibility are given in Table 1.2.

Compared to the coefficient of compressibility, the oedometric deformation modulus M_0 is variable, depending on the size of the vertical stress σ_z . With a growing stress σ_z , M_0 increases. It is therefore necessary to state the vertical stress for which the oedometric deformation modulus was determined.

The coefficient of compressibility C and the oedometric deformation modulus M_0 characterize the compressibility of a soil without taking into account its

TABLE 1.2

Values of coefficients of compressibility C for various soil types

Soil	Peat	Loam	Clay	Sand	Gravel-sand
coefficient of compressibility C	3—7	15—25	30—120	150—250	250 and more

lateral deformation. The settlement of a soil beneath a foundation with possible lateral deformation is characterized by the deformation modulus E_0 , which like M_0 is not constant. The moduli M_0 and E_0 are related by

$$E_0 = \left(1 - \frac{2\nu^2}{1 - \nu}\right) M_0$$

where ν is Poisson's ratio; for cohesionless soils $\nu \doteq 0.3$, for silty soils $\nu \doteq 0.35$ and for clayey soils $\nu \doteq 0.4$.

Using the preceding equation it is possible to convert the coefficient of compressibility to the secant modulus M_0 , or rather, to the deformation modulus E_0 , and vice versa. If we know the deformation modulus M_0 , the stream σ_z and the load increment $\Delta\sigma_z$, then the coefficient of compressibility is

$$C = M_0 2.3 \log(1 + \Delta\sigma_z/\sigma_z)/\Delta\sigma_z \quad (1.6a)$$

Similarly the deformation modulus knowing the coefficient of compressibility C , is

$$M_0 = C\Delta\sigma_z/2.3 \log(1 + \Delta\sigma_z/\sigma_z). \quad (1.6b)$$

The exact determination of the true values of Poisson's ratio ν is difficult and therefore calculated values based on estimated values of Poisson's ratio are approximate. To investigate the variation of the oedometric modulus of compressibility M_0 with loads 100–500 kN/m², its mean values were calculated for various soil types. These values are given in Table 1.3, which shows the magnitude of the influence of the acting load on the value of the deformation modulus of the same soil.

TABLE 1.3

Values of the moduli of deformation M_0 of various soils for a different load increment caused by the building σ_z and an initial stress $\Delta\sigma_z$ in the soil

Type of soil	Initial stress σ_z kN/m ²								
	20			60			100		
	Load increment $\Delta\sigma_z$ kN/m ²								
	100	300	500	100	300	500	100	300	300
Peat	280	540	760	510	840	1 120	730	1 080	1 390
Loam	1 120	2 160	3 060	2 040	3 360	4 480	2 900	4 320	5 560
Clay	4 200	8 100	11 500	7 700	12 600	16 800	10 900	16 200	20 900
Sand	11 200	21 600	30 600	20 400	33 600	44 800	29 000	43 200	55 800
Gravel-sand	28 000	54 000	76 000	51 000	84 000	112 000	72 500	108 000	139 000

As can be seen, the deformation moduli change with the acting stress σ_z and the load increment $\Delta\sigma_z$. To make a comparison of soils in terms of their compressibility, a modulus of compressibility $E_{0.50}$ is used. This value expresses the $\tan \bar{\alpha}$ of a secant passing through the beginning and the point, which corresponds to the maximum $(\sigma_1 - \sigma_3)$, on the compression-stress curve for a sample tested in a triaxial apparatus (see Fig. 1.9).

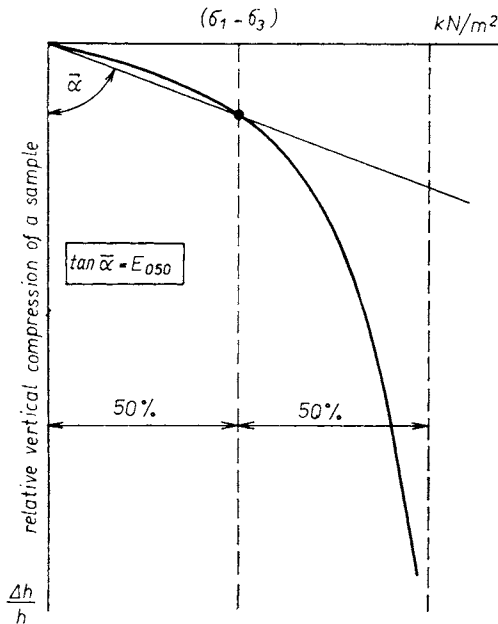


Fig. 1.9 Determination of deformation modulus $E_{0.50}$ during a shearing test in a triaxial apparatus

In some countries the relationship between the stress σ and the void ratio e is derived from the oedometric test. A load decreases the original void ratio e_0 to a value of

$$e = e_0 - C_0 \ln \frac{\sigma_z + \Delta\sigma_z}{\sigma_z} \quad (1.7)$$

σ_z is the initial mean stress in the layer, which has a porosity $n_0 = e_0/(1 + e_0)$

$$e_0 = n_0/(1 - n_0)$$

$\Delta\sigma_z$ is the mean load increment in the layer due to loading. If we know from the oedometric test the relationship between e and σ , then the absolute coefficient of oedometric compressibility

$$C_0 = \frac{e_0 - e}{\ln \frac{\sigma_z + \Delta\sigma_z}{\sigma_z}} = (1 + e_0)/C \quad (1.8)$$

As mentioned, the lateral deformation of the soil to the sides is not taken into account. If the theory of an elastic half-space is used, then the settlement of a rigid circular surface with a radius r , caused by a uniform load q is

$$s = \frac{1 - \nu^2}{E_0} \frac{\pi r q}{2} = \frac{1 - \nu^2}{E_0} \frac{Q}{2r} \quad (1.9)$$

where Q is the total load.

Let us designate the term $\frac{E_0}{1 - \nu^2} = E_0^*$ and call it the reduced deformation modulus. Then the settlement $s = Q/2rE_0^*$. Since Poisson's ratio $0 < \nu < 0.5$, E_0^* can have a maximum value of $1.33E_0$, so the settlement calculated from E_0^* can only reach 0.75 of the value calculated from E_0 . As it is difficult to determine Poisson's ratio for a soil, we may calculate the deformation modulus from the following equation

$$E_0^* = \frac{Q}{2rs} = \frac{\pi r q}{2s} \quad (1.10)$$

The value E_0^* is easily determined by a loading test.

As a result of drying out, the soil nearer to the surface is usually compressed by a stress greater than $\gamma \cdot z$, at a depth z beneath the surface, for wide foundations or slab foundations, the soil is compressed at a depth where it has not overconsolidated. Finally we must note that for clays the loading test speed is critical, i.e. the soil may or may not have time to consolidate during the test. The depth of the oversoil is also important and loading tests made to determine the deformation modulus should be made in such a way that this influence is taken into account. We therefore consider that the calculations of settlement give us assumed or expected settlement values and not exact values.

As regards the settlement of the soil with respect to time, the calculation is based on the final settlement s , multiplied by the degree of consolidation μ , giving the settlement over a period t as a percentage of the final settlement. The degree of consolidation is a function of the time factor T . For 90% consolidation, $T = 1$. The time factor

$$T = \frac{1 - n}{n_0 - n} \frac{\Delta\sigma_z}{\gamma_w} \frac{kt}{h^2} = \frac{c_v t}{h^2} = \frac{M_0 kt}{\gamma_w h^2} \quad (1.11)$$

depends on the distribution of stress in depth and on the possibility of water percolation from the soil, upwards alone or both upwards and downwards into a permeable layer. In equation (1.11)

n_0 is the initial porosity,

n is the porosity after consolidation as a result of a stress increment $\Delta\sigma_z$,

k is the coefficient of permeability,

t is time

h is the depth of the layer and

c_v is the coefficient of consolidation—see Sec. 1.6.

The calculation of consolidation does not assume a change in the coefficient of permeability k during consolidation; it assumes that the soil is isotropic, and therefore produces only an expected time settlement. For $k < 10^{-10}$ m/s the calculated time settlement corresponds to real values.

For each building where the foundation soil is to be fully used, the following three conditions must be fulfilled:

(a) there must be a high enough safety factor—see Sec. 2 and 3,

(b) the settlement of a building must not exceed a particular value which would make proper use of the building impossible (see Table 3.1, Sec. 3.1),

(c) differences in the settlement of various parts of the building must not exceed a particular value since this would result in the creation of fissures.

It is therefore very important to predict the magnitude of the settlement of a building, as it enables us to propose foundations, which often have various sizes and shapes such that the building will, as far as possible, settle uniformly.

The total settlement is calculated using the coefficient of compressibility C , or from the deformation moduli M_0 and E_0 .

1.3 CALCULATION OF TOTAL SETTLEMENT USING COMPRESSIBILITY COEFFICIENT C

When the total settlement is calculated using coefficients of compressibility C , the grade is divided into layers such that each layer contains soil of the same kind and the value of the coefficient of compressibility C for the different layers are determined from undisturbed samples in a laboratory. The settlement s for both a uniform and stratified subgrade of the foundations (with the exception of unstable volume soils, which bulk or subside) is, according to Terzaghi-Buisman

$$s = \int_0^{h_i} \frac{2.3}{C} \log \left(1 + \frac{\Delta\sigma_z}{\sigma_z} \right) dh \doteq \sum_1^i \frac{h}{C} 2.3 \log \left(1 + \frac{\Delta\sigma_z}{\sigma_z} \right) \quad (1.12)$$

In this equation, i is the number of layers with depth h into which the subgrade was divided. The initial mean vertical consolidation stress acting at the centre of each layer before the building process is σ_z . For overconsolidated soils $\sigma_k > \gamma \cdot z$ and therefore, in the calculation of the total settlement, it is assumed that $\sigma_z = \sigma_k$. The vertical stress increment $\Delta\sigma_z$, created at the centre of each layer when it assumes the load of the building, surface works, adjacent objects,

the load due to the lowering of the groundwater level, etc., is usually determined on the basis of elastic half-space theory. A uniform subgrade of a foundation, reaching to a depth at least equal to two and a half times the foundation width, can be taken as such a half-space (See Sec. 4 and appendixes). As the maximum vertical-stress increment is directly beneath the foundation, this is where the maximum settlement occurs. The settlement of a strip foundation to a depth $z = B$ amounts to more than 60 % of the total settlement. For this reason, this depth is described as the effective depth and its determination is described in appendix II. When calculating the total settlement, it is sufficient to take into account the settlement of the soil to a depth of $2.0 B$ beneath the foundation level. If the subgrade of the foundation is uniform or consists of several layers of different types of soil with varying compressibility, then in calculating the settlement these are usually divided into at least six layers, so that, for the purposes of calculation we obtain a sufficiently accurate value of the vertical stress increment $\Delta\sigma_z$ which decreases unevenly with increasing depth. The vertical stress σ_z and its increment $\Delta\sigma_z$ are determined below the characteristic point of the foundation. For a circular foundation, this point lies at a distance of $0.845r$ from the centre of the foundation, and for a rectangular foundation ($B \times L$), it lies at the intersection of straight lines lying $0.37 B$ and $0.37 L$ from the centre of the foundation. The stress in the soil due to a loaded foundation is divided unevenly. The maximum stress is in the axis of the foundation and it decreases with distance from the axis of the foundation in the form of a bell-shaped curve. The mean stress in the space within the sides of the foundation is in the so-called characteristic points, and therefore the settlement is calculated for the stress on a vertical line passing through the characteristic points. Only the settlement caused by the vertical-stress increment $\Delta\sigma_z$ is taken into account during calculation. The influence of the horizontal-stress increment $\Delta\sigma_x$ is neglected. This stress forces the soil to the sides and is very pronounced for larger values of $\Delta\sigma_x$, for example in the case of stock-yard crane tracks.

When the load on the foundations is larger and approaches the ultimate bearing capacity, the settlement of the foundations is caused not only by the compression of the soil, but also by the creation of plastic ranges and by forcing out the soil from beneath the foundation to the sides. The permissible load for foundations is usually less than a half or a third of their ultimate bearing capacity.

The rigidity of the foundation results in the redistribution of the stress, which is larger at the edges and smaller in between. The exact calculation of the contact stress is only possible in idealized cases. These problems were studied theoretically by Boussinesq (1888), Sadowski (1928), Gastev (1937), Jegorov (1938) and others. It can be stated that the more flexible the foundation, the

smaller the difference between the distribution of the stress in the foundation line and that of the acting load. Small foundations are usually rigid (for example footings, strip foundations under walls, etc.). Questions dealing with stress in the foundation line and in the subgrade are discussed briefly in Chapter 4.

Real values of settlement are usually smaller than calculated values. When the soil above the foundation level, which is subjected during settlement to tension and other influences, contributes, the real settlement value amounts to about 1/2 to 3/4 of the calculated value. For a more exact determination of the settlement, it is wise to begin with the distribution of the stress in the foundation line, which is not really uniform and depends especially on the rigidity of the foundation and of the upper part of the building.

1.4 CALCULATION OF TOTAL SETTLEMENT USING DEFORMATION MODULI E_0 AND M_0

As mentioned previously, the lateral movement of the soil to the sides, caused by the horizontal-stress increments $\Delta\sigma_x$, $\Delta\sigma_y$, is neglected in the calculation of the settlement of a building according to Terzaghi. On the basis of the theory of stress and strain in an elastic half-space, we get the following relative deformations along the axes

$$\varepsilon_x = \frac{1}{E} [\sigma_x - \nu(\sigma_y + \sigma_z)] \quad (1.13)$$

$$\varepsilon_y = \frac{1}{E} [\sigma_y - \nu(\sigma_x + \sigma_z)] \quad (1.14)$$

$$\varepsilon_z = \frac{1}{E} [\sigma_z - \nu(\sigma_x + \sigma_y)] \quad (1.15)$$

If the stress condition is uniaxial $\sigma_x = \sigma_y = 0$, then $\varepsilon_z = \delta_z/E$, which is Hook's law.

According to the law of supervision, if we divide any loaded surface into smaller surfaces, then at the centre of gravity of each of these surfaces a vertical force, proportional to the size of the surface, is applied. The settlement of the foundation is the sum of the settlements due to the forces acting on each surface. The settlement to a depth z , caused by a single load is

$$s = \frac{Q(1 + \nu)}{2\pi E_0} \left[\frac{2(1 - \nu)}{R} + \frac{z^2}{R^3} \right] \quad (1.16)$$

$$R^2 = r^2 + z^2 \quad (1.17)$$

where r is the horizontal distance of the considered point from the loading point of force Q . The settlement caused by a uniform load q , for a rigid circular foundation with radius r is

$$s = \frac{1 - \nu^2}{E_0} \frac{\pi r q}{2} \quad (1.18)$$

If we apply the reduced deformation modulus $E_0^* = E_0/(1 - \nu^2)$, then the settlement of a circular surface is

$$s = \pi r q / 2 E_0^* \quad (1.19)$$

In the building code ČSN 73 1001 Foundation Soil beneath Shallow Foundations, the settlement for a uniform soil is calculated according to the following equation

$$s = \frac{\bar{q}}{E_0} B \bar{\alpha} 1.25 m_1 (1 - \nu^2) \quad (1.20)$$

where q is the load increment in the foundation line in kN/m^2 ,

B is the width of the foundation in cm,

$\bar{\alpha}$ is the coefficient of the shape and rigidity of the foundation according to Table 1.4,

E_0 is the deformation modulus in kN/m^2

$m_1 = 0.7$ for cohesionless soils and $m_1 = 0.5$ for cohesive soils with the exception of volume-unstable soils, which either bulk with water or subside, i.e. loess,

ν is Poisson's ratio.

TABLE 1.4

Coefficient $\bar{\alpha}$ of the shape and rigidity of a foundation (According to ČSN 73 1001)

Shape of foundation	Perfectly rigid foundation	Centre of non-rigid foundation	Edge of non-rigid foundation
Circle	0.79	1.00	0.64
Square	0.88	1.12	0.56
Rectangle $L/B = 1.5$	1.08	1.36	0.68
2	1.22	1.53	0.77
3	1.44	1.78	0.89
5	1.72	2.10	1.05
10	2.12	2.53	1.27
50	2.12	3.54	1.77

If the soil under the foundation is stratified, the total settlement of the foundation is

$$s = \sum_{i=1}^n \frac{\Delta\sigma_z h_i 1.25m_2}{M_0} \quad (1.21)$$

where $\Delta\sigma_z$ is the load increment caused by the building in the centre of the soil layers indexed i , and m_2 is the corrective coefficient used for the simplification of the calculation. For a greatly overconsolidated soil, if the consolidation stress σ_k is at least twice as large as the acting vertical stress σ_z , then $m_2 = 0.5$. In other cases $m_2 = 0.8$. During the calculation of the total settlement, soils to a depth of up to $2B$ below the foundation level are taken into account. The thickness of either of the first two layers below the foundation should not exceed $B/2$.

The disadvantage of the previously mentioned equations is that they do not take into account more accurately the initial stress condition in the soil. The influence of the foundation depth is incorporated in the value of the deformation moduli. The equation for the calculation of settlement includes Poisson's ratio, which is difficult to determine and thus its value is estimated. Therefore it is advantageous to determine the deformation modulus E_0 by a loading test of the foundation soil using the same ratio $\frac{D}{B}$ as for the building.

During the loading of the foundation soil, the soil settles not only directly under the foundation but also in its vicinity. Žemočkin and Sinicyn (1947) mathematically solved the settlement s_J of a point J , which is at a distance x from the centre of the foundation on its axis of symmetry. They formulated the solution for a rectangle and a circle, when the whole foundation, based on the ground surface, was loaded by a unit load $Q = 1$. The settlement of a real foundation exceeds that calculated according to the derived equations greatly, since the real acting load is greater than $Q = 1$. The subgrade is assumed to be uniform and elastic. For a rectangular foundation (Fig. 1.10), the load on the foundation line is $q = Q/BL = 1/BL$, where B is the width of the foundation and L its length. The settlement s_J is calculated from the differential equation

$$d^2 s_J = \frac{d\xi d\eta (1 - \nu^2)}{BL\pi M_0 r} \quad (1.22)$$

and its size is

$$s_J = \int_{\xi=x-B/2}^{\xi=x+B/2} 2 \int_{\eta=0}^{\eta=L/2} \frac{1 - \nu^2}{BL\pi M_0 r} d\xi d\eta \quad (1.23)$$

H. Siemer (1973) describes the influence of depth by a reduction coefficient κ . The settlement of a foundation at a depth D is $s_D = \kappa s$, if the settlement is calculated according to equations (1.16), (1.18), (1.20) to (1.25) (see Table 1.7).

TABLE 1.7

Reduction coefficient κ as a function of the depth of foundation D
(According to Siemer)

Depth of foundation $\frac{D}{B}$	0.0	0.5	1.0	1.5	2.0
Coefficient κ for a strip foundation*)	1.0	0.78	0.64	0.55	0.50
Coefficient κ for a circular footing	1.0	0.60	0.42	0.33	0.29

*) It is also possible to take $\kappa \doteq e^{-D/3B}$ for $D \leq 5B$

1.5 INFLUENCE OF A VERTICAL MOMENT IN THE FOUNDATION LINE ON THE INCLINATION OF THE FOUNDATION

The determination of the deformation modulus has the advantage that it permits the solution of problems whose solution was derived for an elastic half-space defined by the elastic modulus and Poisson's ratio, for example the inclination of a circular foundation caused by an acting moment. In the equations we assume that the elastic modulus E is the deformation modulus E_0 . If we know the oedometric modulus of deformation M_0 , then $E_0 = \left(1 - \frac{2\nu^2}{1-\nu}\right) M_0$. If $\nu = 1/3$, then $E_0 = 0.667 M_0$, for $\nu = 0.4$ we get $E_0 \doteq 0.5 M_0$. Let us assume that we have a circular foundation with a radius R on the surface of an elastic half-space, which is characterized by deformation characteristics (E, ν) . At its centre it is loaded by a moment in a vertical plane. According to Fröhlich, the distribution of stress in the foundation line is

$$\sigma_z = \frac{3}{2\pi} \frac{M}{R^3} \frac{x}{\sqrt{R^2 - r^2}} \quad (1.26)$$

where r is the distance of the surface dA from the centre of the foundation and x is the perpendicular projection of the distance r onto the axis X (Fig. 1.11a).

Let us substitute this distribution of the stress by a system of elementary loads $dP = \sigma dA = \sigma r dr d\varphi$, according to Fischer. Since $x = r \cos \varphi$, we get

$$dP = \frac{3}{2\pi} \frac{Mr^2 \cos \varphi}{R^3 \sqrt{R^2 - r^2}} dr d\varphi \quad (1.27)$$

The acting load dP , which acts on the surface dA , causes the settlement of the centre of the foundation

$$d \left[\frac{d\bar{s}}{dr} \right] = \frac{1 - \nu^2}{\pi E_0} \left[\frac{1}{r^2} - \frac{r}{\sqrt{(z^2 + r^2)^3}} - \frac{3}{2(1 - \nu)} \frac{z^2 r}{\sqrt{(z^2 + r^2)^3}} \right] dP \quad (1.28)$$

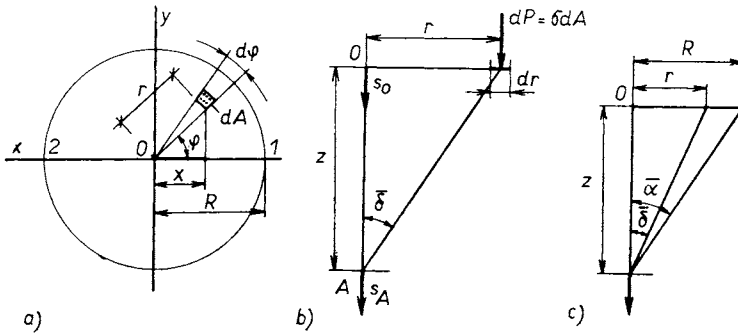


Fig. 1.11 Diagram for the calculation of stress beneath a circular slab, loaded by a moment M acting in a vertical plane

The expression

$$\left[\frac{1}{r^2} - \frac{r}{\sqrt{(z^2 + r^2)^3}} - \frac{3}{2(1 - \nu)} \frac{z^2 r}{\sqrt{(z^2 + r^2)^3}} \right]$$

we designate as K , so that

$$d \left[\frac{d\bar{s}}{dr} \right] = \frac{1 - \nu^2}{\pi E_0} K dP \quad (1.29)$$

\bar{s} is the difference between the settlement of the centre of the foundation s_0 and the settlement s_A of the point A at a depth z , Fig. 1.11b.

This term serves to determine the difference in settlement

$$d \left[\frac{d\bar{s}}{dx} \right] = d \left[\frac{d\bar{s}}{dr} \frac{dr}{dx} \right] = d \left[\frac{d\bar{s}}{dr} \cos \varphi \right] = \frac{1 - \nu^2}{\pi E_0} dPK \cos \varphi \quad (1.30)$$

By summing all the elementary loads we get

$$\frac{1 - \nu^2}{\pi E_0} \int_{\varphi=0}^{2\pi} \int_{r=0}^R dPK \cos \varphi = \frac{3(1 - \nu^2)}{2\pi E_0} \frac{M}{R^2} \times \\ \times \int_{r=0}^R \left[\frac{1}{r^2} - \frac{r}{\sqrt{(z^2 + r^2)^3}} - \frac{3}{2(1 - \nu)} \cdot \frac{z^2 r}{\sqrt{(z^2 + r^2)^3}} \right] \frac{r^2 dr}{\sqrt{R^2 - r^2}} \quad (1.31)$$

The partial integrals in parentheses are

$$\int_0^R \frac{dr}{\sqrt{R^2 - r^2}} = \pi/2 \quad (1.32)$$

$$\int_0^R \frac{r^3 dr}{\sqrt{(z^2 + r^2)^3 (R^2 - r^2)}} = J_2 \quad (1.33)$$

$$\int_0^R \frac{z^2 r^3 dr}{\sqrt{(z^2 + r^2)^3 (R^2 - r^2)}} = J_3 \quad (1.34)$$

Since $r = z \tan \bar{\delta}$; $R = z \tan \bar{\alpha}$ (Fig. 1.11. c), then

$$J_2 = \cot \bar{\alpha} \int_{\bar{\delta}=0}^{\bar{\delta}=\bar{\alpha}} \frac{\sin^3 \bar{\delta} d\bar{\delta}}{\cos^2 \bar{\delta} \sqrt{1 - \cot^2 \bar{\alpha} \tan^2 \bar{\delta}}} \quad (1.35)$$

$$J_3 = \cot \bar{\alpha} \int_{\bar{\delta}=0}^{\bar{\delta}=\bar{\alpha}} \frac{\sin^3 \bar{\delta} d\bar{\delta}}{\sqrt{1 - \cot^2 \bar{\alpha} \tan^2 \bar{\delta}}} \quad (1.36)$$

The solution of these integrals gives us

$$J_2 = R - \sin \bar{\alpha} \cos \bar{\alpha} \quad (1.37)$$

$$J_3 = \frac{2}{3} \sin^2 \bar{\alpha} \cos \bar{\alpha} \quad (1.38)$$

and the total integral is

$$J = \left(\frac{\pi}{2} - \bar{\alpha} \right) + \sin \bar{\alpha} \cos \bar{\alpha} \left(1 - \frac{\sin^2 \bar{\alpha}}{1 - \nu} \right) \quad (1.39)$$

so that the inclination

$$\left[\frac{d\bar{s}}{dx} \right] = (1 - \nu^2) \frac{3}{2\pi} \frac{M}{R^3 E_0} \left[\left(\frac{\pi}{2} - \bar{\alpha} \right) + \sin \bar{\alpha} \cos \bar{\alpha} \left(1 - \frac{\sin^2 \bar{\alpha}}{1 - \nu} \right) \right] \quad (1.40)$$

The boundary values are:

- (a) $z = 0; \bar{\alpha} = \pi/2; d\bar{s}/dx = 0$
 (b) $z = \infty; \bar{\alpha} = 0; d\bar{s}/dx = (1 - \nu^2) \frac{3}{4} \frac{M}{R^3 E_0}$

as derived by Fröhlich.

Equation (1.40) which gives the inclination can be rearranged into the following expression

$$\left[\frac{d\bar{s}}{dx} \right] = \frac{M}{R^3 E_0} F(\nu; \bar{\alpha}) \quad (1.41)$$

where function

$$F(\nu; \bar{\alpha}) = (1 - \nu^2) \frac{3}{2\pi} \left[\left(\frac{\pi}{2} - \bar{\alpha} \right) + \sin \bar{\alpha} \cos \bar{\alpha} \left(1 - \frac{\sin^2 \bar{\alpha}}{1 - \nu} \right) \right] \quad (1.42)$$

The situations arising in the case of soils are:

- (a) $\nu = 1/2$

$$F\left(\frac{1}{2}; \bar{\alpha}\right) = \frac{9}{8\pi} \left[\left(\frac{\pi}{2} - \bar{\alpha} \right) + \sin \bar{\alpha} \cos \bar{\alpha} (1 - 2 \sin^2 \bar{\alpha}) \right]$$

- (b) $\nu = 1/3$

$$F\left(\frac{1}{3}; \bar{\alpha}\right) = \frac{4}{3\pi} \left[\left(\frac{\pi}{2} - \bar{\alpha} \right) + \sin \bar{\alpha} \cos \bar{\alpha} \left(1 - \frac{3}{2} \sin^2 \bar{\alpha} \right) \right]$$

- (c) $\nu = 1/4$

$$F\left(\frac{1}{4}; \bar{\alpha}\right) = \frac{45}{32\pi} \left[\left(\frac{\pi}{2} - \bar{\alpha} \right) + \sin \bar{\alpha} \cos \bar{\alpha} \left(1 - \frac{4}{3} \sin^2 \bar{\alpha} \right) \right]$$

The calculated values of the function $F(\nu; \bar{\alpha})$ for various ratios $\frac{z}{R}$ are given in Table 1.8 and in Fig. 1.12. The given equations are valid for the cases where $e \leq R/3$. If $e > R/3$ the foundation will lift on one side.

For a uniform subgrade reaching to a depth $z > 8R$, we assume that $z/R = \infty$. K. Fischer suggests a procedure for a case where the soil is stratified. The inclination is determined for each layer, taking into account the deformation modulus, and the sum of these is the total inclination.

$$\Delta_1 \left(\frac{d\bar{s}}{dx} \right) = \frac{M}{R^3 E_{01}} \Delta_1 F(v; \bar{\alpha}) = \frac{M}{R^3 E_{01}} [\bar{F}_1(v; \bar{\alpha}) - \bar{F}_2(v; \bar{\alpha})] \quad (1.43)$$

$$\Delta_2 \left(\frac{d\bar{s}}{dx} \right) = \frac{M}{R^3 E_{02}} \Delta_2 F(v; \bar{\alpha}) = \frac{M}{R^3 E_{02}} [\bar{F}_2(v; \bar{\alpha}) - \bar{F}_3(v; \bar{\alpha})] \quad (1.44)$$

TABLE 1.8

Values of function $\bar{F}(v; \bar{\alpha})$

Ratio $\frac{z}{R}$	Function $\bar{F}(v; \bar{\alpha})$		
	$v = 1/2$	$v = 1/3$	$v = 1/4$
0.5	0.080	0.163	0.196
1.0	0.282	0.387	0.427
1.5	0.416	0.523	0.562
2.0	0.482	0.589	0.627
2.5	0.516	0.621	0.659
3.0	0.533	0.638	0.676
3.5	0.543	0.648	0.685
4.0	0.549	0.654	0.691
4.5	0.553	0.657	0.694
5.0	0.555	0.660	0.696
5.5	0.557	0.661	0.698
6.0	0.558	0.663	0.699
∞	0.563	0.667	0.703

The total inclination is then

$$\tan \beta' \approx \Sigma \Delta \left(\frac{d\bar{s}}{dx} \right) = \frac{M}{R^3} \sum_{i=1}^n \frac{\Delta_i F(v; \bar{\alpha})}{E_{0i}} \quad (1.45)$$

The equation was derived for a circular foundation and it can be used with sufficient accuracy for foundations of a different shape (square, rectangular) if the surface of the foundation is converted to a circular surface.

Example 1.1

The Tower of Pisa, which is 58 m high, produces a tilting moment resulting from inclination $Qe = 318\,000$ kNm. The deformation modulus E_0 of clay is $2\,400$ kN/m² to a depth of 42 m. Below this there is sand, found even at a depth of 60 m, which was the depth of the bore-

holes. The weight of the tower $Q = 144\,540$ kN. Poisson's ratio $\nu = 1/3$. The radius of the foundation of the tower $R = 9.8$ m. For a depth $z = 42$ m we have $\frac{z}{R} = \frac{42}{9.8} = 4.29$ and the value of function $\bar{F}\left(\frac{1}{3}; \bar{\alpha}\right) = 0.655$.

The inclination $\tan \beta' = \frac{M}{R^3 E_0} \bar{F}(\nu; \bar{\alpha}) = \frac{318\,000}{9.8^3 \cdot 2\,400} \cdot 0.655 = 0.091$. The deflection of the 58 m high tower is $58.0 \cdot 0.091 = 5.3$ m. The actual deflection is 5.7 m so that we get sufficient correspondence between the calculated and measured deflection. The calculated angle of inclination $\beta' = 5^\circ 12'$. The real angle of inclination $\beta' = 5^\circ 36'$.

Example 1.2

The following is an example of the inclination of a foundation, when the soil beneath the foundation is stratified. In the subgrade we have a 6.60 m deep layer of sand $E_{01} = 20\,000$ kN/m², under which lies a 13.20 m deep layer of clay $E_{02} = 7\,000$ kN/m², which rests on gravel. The compressibility of the gravel can be neglected. The foundation is square with sides $B = L = 10.7$ m. The moment $Qe = 28\,000 \cdot 1.5 = 42\,000$ kNm, for $Q = 28\,000$ kN. The foundation surface $A = B^2 = 10.7^2 = 114$ m². We replace the square surface with a circular surface of radius $R = \sqrt{\frac{A}{\pi}} = 6$ m.

The ratio $\frac{M}{R^3} = \frac{42\,000}{216} = 194.5$ kN/m²

The inclination in the upper layer of sand $\left(\frac{z_1}{R} = \frac{6.60}{6.0} = 1.1\right)$

$$\bar{F}_1(1/3; \bar{\alpha}) = 0.414; \bar{F}_0(1/3; \bar{\alpha}) = 0; \Delta_1 \bar{F}(1/3; \bar{\alpha}) = 0.414$$

$$\Delta_1 \left(\frac{d\bar{s}}{dx}\right) = \frac{M}{R^3 E_{01}} \Delta_1 \bar{F}(1/3; \bar{\alpha}) = \frac{194.5}{20\,000} \cdot 0.414 = 0.0040$$

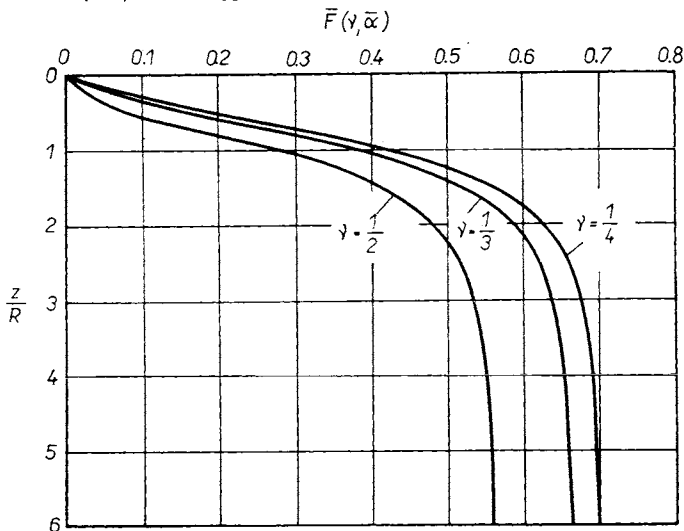


Fig. 1.12 Function $\bar{F}(\nu; \bar{\alpha})$ in relation to z/R

The inclination caused by the layer of clay $\left(\frac{z_2}{R} = \frac{19.8}{6.0} = 3.3 \right)$

$$\bar{F}_2(1/3; \bar{\alpha}) = 0.644; \bar{F}_1(1/3; \bar{\alpha}) = 0.414; \Delta_2 \bar{F}(1/3; \bar{\alpha}) = 0.644 - 0.414 = 0.230$$

$$\Delta_2 \left(\frac{d\bar{s}}{dx} \right) = \frac{M}{R^3 E_{02}} \Delta_2 F(1/3; \alpha) = \frac{194.5}{7000} 0.230 = 0.0064$$

$$\tan \beta' = 0.0040 + 0.0064 = 0.0104$$

The settlement of one edge of the foundation compared to the other is

$$B \tan \beta' = 10.7 \cdot 0.0104 = 0.111 \text{ m} \doteq 11 \text{ cm}$$

If the settlement of a circular foundation were considered, we would get $2R \tan \beta' = 2 \cdot 600 \times 0.0104 = 12.4 \text{ cm}$. The difference in the settlement of the edges of the square foundation compared to that of the circular foundation is negligible.

1.6 TIME—SETTLEMENT CURVE

Particles are pressed into the pores as a result of loading. Friction and resistance of water or air against expulsion from the pores act against their movement. In permeable soils—for example sand—the resistance against this expansion is small and acts only for a short while so that the whole stress, which is created in the soil, is borne only by the particles. Soil, which is not very permeable and especially soils such as clay which are virtually watertight, behave quite differently. At first, all the stress created in the soil is borne by the water alone as the particles cannot be forced into the pores while the water remains there at least partially. The water is under pressure. A hydraulic gradient $I = h/l$, i.e. the ratio of the pressure head h to the path l of the water particle, is created and causes the water to start escaping from the pores; the soil begins to be compressed and the foundation subsides. The size of the settlement s at any given moment is equal to the height of the water expelled from the soil if it is completely waterlogged — nearly always the case with clay. When some of the water has left the pores, the grains partially fill the pores of the soil. The friction between the particles increases, they then take up some of the stress, the remaining part of the stress being carried by the water. Gradually with time more and more water is expelled from the pores of the soil, the stress borne by the water decreases and that by the particles increases. When the friction between the particles takes the whole load from the foundation and the water is only under hydrostatic pressure or capillary tension, the soil is consolidated. During a test in the oedometer, the magnitude of the settlement s is plotted on a normal scale and time is plotted on a logarithmic scale (Fig. 1.13). As a result of loading, a soil with height h in the oedometer is immediately compressed by a value Δs_1 . This is caused by the unevenness

of the soil surface, the compression of the soil into the pores of the porous plate and by the partial expulsion of the water from the pores, since on both the soil surfaces which are in contact with the permeable porous plates, the path of the water particle $l = 0$ and the hydraulic gradient $\frac{h}{l} \rightarrow \infty$. The expulsion of the water takes a certain time longer if the soil is less permeable and if the height of the compressed soil is greater.

The time of settlement of a soil during an oedometer test is divided into primary and secondary settlement, see Fig. 1.13, which shows the primary settlement. Settlement takes an infinite time. The secondary settlement is greater than calculated, because the grains of the soil are compressed as a result

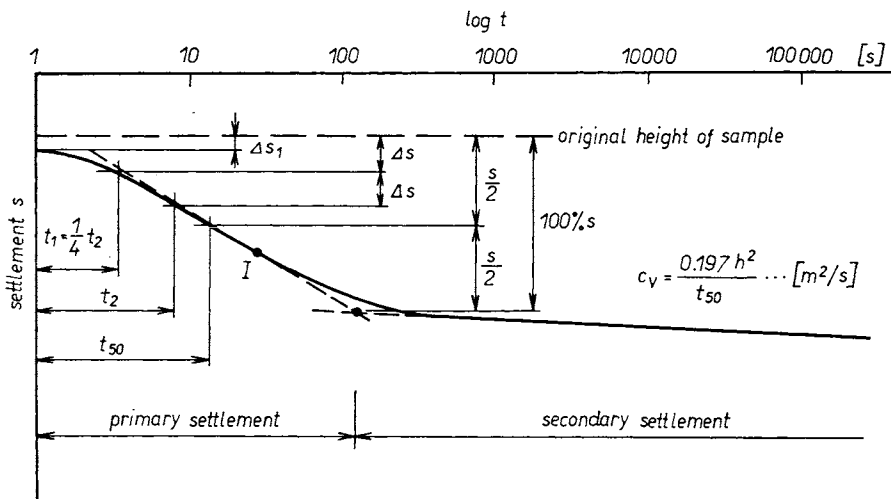


Fig. 1.13 Consolidation curve

of the crushing of extremities on the surface. The contact stress on these projections is usually large and as a result they are crushed. This transfers the stress to other particles. Between particles of the soil, zones with an increased concentration of stress are formed, beneath which the grains are only subjected to a small stress. When the particles which form the void are disturbed, the void collapses and a new void is formed which lasts for a certain time. The span and shape of the void, as well as the stress acting on the particles, change in time and the soil continues to settle. The total settlement is caused by the expulsion of the water from the pores and the deformation of the particles. In Fig. 1.14 the magnitudes of the stress resulting from loading, which acts between the particles, is marked by lines. The actual magnitude of the stress is given by the density of the line. These lines were obtained by the photo-

elasticimetric method. The particles were modelled by circular discs and were in a frame with variable vertical and horizontal load. It can easily be shown that zones with a concentration of stress are formed in the soil, if we model the soil with the help of balls between two parallel glasses.

The consolidation caused by the deformation of particles was studied. The resulting compression was found to be $s_s = h\alpha_s \log t$ for a load between 50 and 300 kN/m². The value of the consolidation coefficient for dry gravel (ϕ 3 cm) and for organic clay or peat ($\gamma = 11$ kN/m³) was $\alpha_s = 0.03$, for

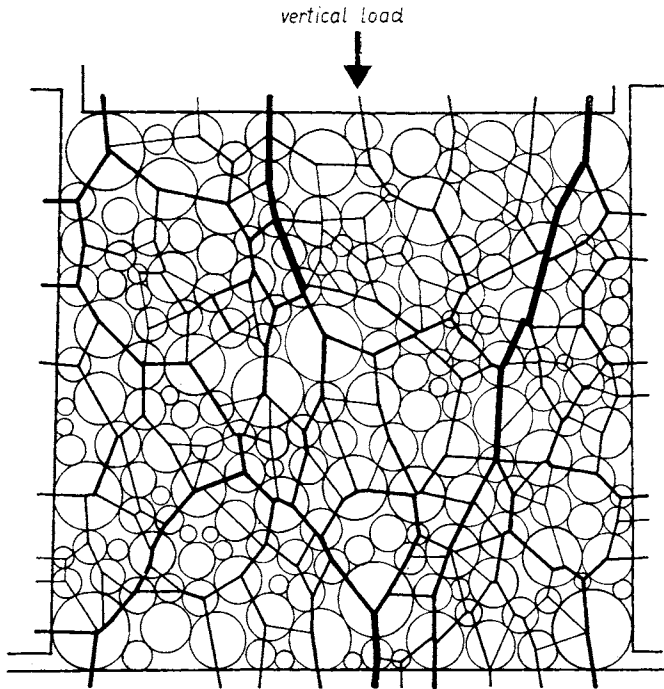


Fig. 1.14 Stress between grains, expressed as the weight of the lines (G. de Josselin de Jong)

fine dry gravel $\alpha_s = 0.007$, for water-saturated greywacke fill $\alpha_s = 0.0002$, for dry greywacke fill $\alpha_s = 0.0001$, for dry clay particles $\alpha_s = 0.001$, for dry particles of loess loam $\alpha_s = 0.0005$ and for fine silicate sands E J F and N II $\alpha_s = 0.00004$. The formula is also valid for permanent and repeated loads with a very low frequency, where t (sec) is the total time of application of the load. If for example we know, in the case of a wheel passing over a point on a road, the time t during which the load has been applied, we can estimate the settlement of the surface of the road after \bar{m} loadings, i.e. for a total time $t = \bar{m} \cdot \bar{t}$. The effective depth h is considered (see appendix II). For roads

this is up to 0.7 m. At the same time a very simplifying assumption is made, i.e. that for a low frequency of the repeated load the coefficient of consolidation α_s is not dependent on acceleration, the elastic deformation of the surface or the frequency of the load.

The consolidation of relatively impermeable soils was first studied by K. Terzaghi, who assumed that the seepage of water from the soil is linear and came to the following differential equation

$$\frac{k(1 + e_0)}{\gamma_w a} \frac{\partial^2 \sigma'}{\partial z^2} = \frac{\partial \sigma'}{\partial t} \quad (1.46)$$

if the effective stress

$$\sigma' = \sigma - u_w,$$

e_0 is the void ratio before a load increment is effected

$a = \frac{\Delta e}{\Delta \sigma_z}$ gives the ratio of the void ratio decrement Δe to the load increment $\Delta \sigma_z$.

The term $\frac{k(1 + e_0)}{\gamma_w a} = c_v$ is the coefficient of consolidation, and for cohesive soils ($\nu = 0.4$) the following is valid

$$c_v = \frac{2E_0 k}{\gamma_w} = \frac{M_0 k}{\gamma_w} \quad (1.47)$$

E_0 is the deformation modulus, k is the coefficient of permeability. Similarly

$$\frac{\partial w}{\partial t} = c_v \frac{\partial^2 w}{\partial z^2} \quad (1.48)$$

K. Terzaghi solved this function using a dimensionless quantity $T = c_v t / h^2$, which is called the time factor. For a certain value of the time factor, the degree of consolidation μ is determined; the settlement after a time t is $s_t = \mu s$, where s is the final settlement and μ is the degree of consolidation. The relationship between the degree of consolidation and the time factor is described in Fig. 1.15. (Some authors do not base their solution on a unidirectional, but on a spatial, flow of water.) For a 90 % consolidation $\mu = 0.9$ and

$$T = \frac{c_v t}{h^2} = 1.$$

Terzaghi's equation was formulated for cases where the load increment created in the soil is constant and has a rectangular shape, curve 1. This is the case if the soil is loaded over a large area with an embankment of an equal

height. Then a solution was sought for case 2, where the stress increment has a triangular shape. The real stress surface under the foundation can be transposed to such a shape if the soil is uniform to a great depth. In the next case 3, the increment takes the form of a triangle with a base at the bottom. We find this situation where a soil has been alluviated and left to consolidate.

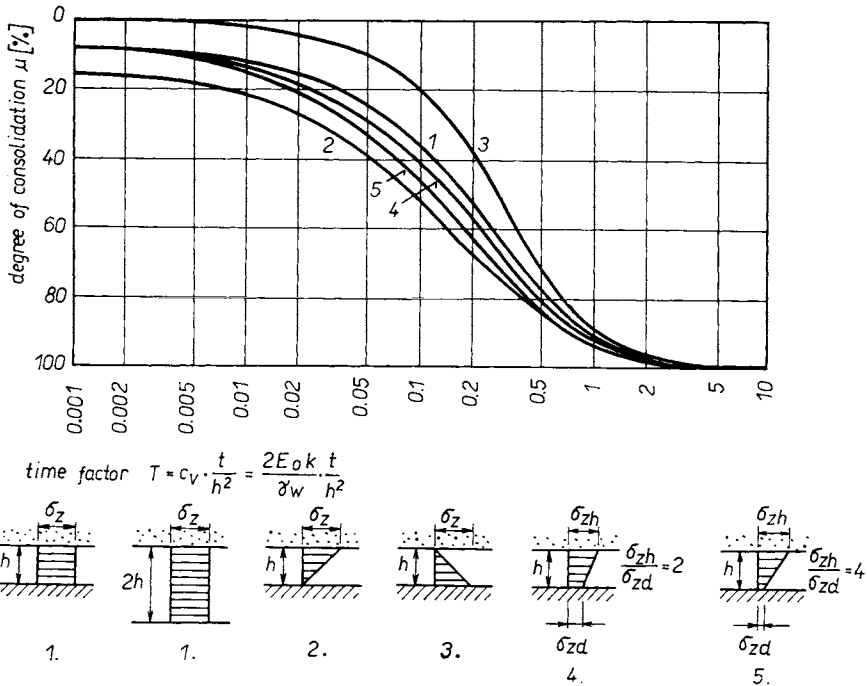


Fig. 1.15 The degree of consolidation μ as a function of the time factor T

Next, a case 4 was solved in which the load increment in a consolidating layer of clay has a trapezium form; then the stress at the top is σ_{zh} and the stress at the bottom σ_{zd} . Curve 4 is applicable to a case where $\sigma_{zh}/\sigma_{zd} = 2$, and finally curve 5 is for a case where this ratio is equal to 4. If the water can escape in one direction, then h is the height of the impermeable layer which is consolidating. If the water can escape in two directions (up and down) into a permeable layer, its height is $2h$. Height h is substituted in the equation.

The coefficient of consolidation can also be determined according to Taylor from the consolidation curve located by a oedometer test (Fig. 1.13). The soil is loaded and the settlement is measured after 4, 10, 20, 40, 80, 200, 400, 800, 2 000, 4 000, 20 000 and 86 400 (one day) seconds. A time $t_2 < t_{50}$ and a time $t_1 = t_2/4$ are chosen. The settlement Δs in the period $t_2 - t_1$ is plotted against the settlement for a period t_1 , and thus the initial height of the sample,

from which the settlement (compression) is being measured, is determined. At the inflection point I of the settlement curve, a tangent is drawn and the lower part of the compression curve is extrapolated. The intersection point of the two curves divides the period of consolidation into a primary and secondary consolidation and at the same time gives a 100 % value of the settlement s .

We locate a half of the settlement $\frac{s}{2}$ and the time corresponding to this 50 %

settlement is t_{50} . The coefficient of consolidation $c_v = \frac{0.197h^2}{t_{50}} m^2/s$. The inflection point on the compression curve is usually located for a 68 % consolidation (Naylor – Daran 1948).

The coefficient of consolidation c_v is usually calculated from equation (1.47), if we know the coefficient of permeability k and the oedometric modulus of deformation M_0 . Usually the coefficient of permeability is given in m/s or m/min , the deformation modulus is given in kN/m^2 and therefore the unit weight γ_w must be given in kN/m^3 . To enable the calculation of the coefficient of consolidation, the values of the coefficients of permeability are given in Table 1.9.

TABLE 1.9
Coefficients of soil permeability

Type of soil	Coefficient of permeability k [m/min]
Fine sand	10^{-1} — 10^{-3}
Clayey sand	10^{-4} — 10^{-5}
Loess loam	10^{-5} — 10^{-7}
Loam	10^{-7} — 10^{-8}
Clayey loam	10^{-8} — 10^{-9}
Clay	10^{-9} — 10^{-10}

The modulus of deformation M_0 is determined for a given load in the oedometer, which makes it easy to calculate the coefficient of consolidation c_v .

For normal foundations on clayey loam with a width from 1 to 2 m, the effective layer of soil is, in terms of settlement, about 2 m and a 90 % consolidation takes a little over a year if the water seeps only upwards (Table 1.10). Only for wider foundations is the time-settlement relationship more pronounced.

TABLE 1.10

The period required for a 90 % consolidation of a layer of clayey loam ($k = 6 \cdot 10^{-9}$ m/min, $M_0 = 10\,000$ kN/m²)

Height of clayey loam layer [m]	Period t (years) of consolidation if water seeps	
	upwards and downwards	upwards
1	0.08	0.32
2	0.32	1.28
3	0.72	2.88
4	1.28	5.12
5	2.88	11.50
6	6.45	25.80

Example 1.3

The magnitude of the settlement of the soil under an embankment after 3 months is to be determined. A layer of loam, with a height of $h = 6$ m is uniformly loaded by an embankment with of height of 10 m, which produces a uniform load $q = 200$ kN/m². The coefficient of permeability $k = 1 \cdot 10^{-8}$ m/s and the oedometric modulus of deformation $M_0 = 6000$ kN/m².

The total settlement of the layer $s = \frac{q \cdot h}{M_0} = \frac{6 \cdot 200}{6000} = 0.2$ m. The coefficient of consolidation $c_v = \frac{kM_0}{\gamma_w} = \frac{10^{-8} \cdot 6 \cdot 10^3}{10} = 6 \cdot 10^{-6}$ m²/s = $6 \cdot 10^{-6} \cdot 8.64 \cdot 10^4 = 0.518$ m²/day.

For a period $t = \frac{1}{4}$ of a year the time factor $T = \frac{c_v t}{h^2} = \frac{0.518 \cdot 365}{4 \cdot 36} = 1.31$.

According to curve 1 (see Fig.1.15), the corresponding degree of consolidation for this time factor is $\mu = 0.95$, so that after a quarter of a year the compression of the layer will be $20 \cdot 0.95 = 19.0$ cm.

Example 1.4

Let us consider the Tower of Pisa, which has a circular plan with a diameter $2R = 2 \cdot 9.8 = 19.6$ m. The stress almost disappears at a depth of $3 \cdot 19.6 = 58.8$ m. At a depth of 42 m there is sand, above which are strata of clay and nearer to the surface are thin layers of clays and sands. The coefficient of permeability of clay is usually given as $2 \cdot 10^{-10}$ m/s and for layers of sand and clay as $2 \cdot 10^{-6}$ m/s. The deformation modulus $E_0 = 2\,400$ kN/m² and the oedometric modulus of deformation $M_0 = 3\,600$ kN/m². The mean load is 500 kN/m². The total weight of the tower is $144\,540$ kN. The settlement

$$s = \frac{\pi r q}{2E_0} (1 - \nu^2) = \frac{(1 - \nu^2) Q}{E_0 2R} = \frac{(1 - 0.33^2) \cdot 144\,540}{2\,400 \cdot 2 \cdot 9.8} = 2.7 \text{ m}$$

The mean settlement estimated from the level of the sill at the entrance to the tower and at the entrance to the dome, is 2.4 m. The agreement between the calculated settlement and that estimated in this way is satisfactory.

The coefficient of consolidation $c_v = \frac{M_0 k}{\gamma_w} = \frac{3\,600 \cdot 2 \cdot 10^{-10}}{10} = 7.2 \cdot 10^{-8} \text{ m}^2/\text{s} = 0.006\,22 \text{ m}^2/\text{day}$.

As water can escape both upwards and downwards from a layer of clay then $42 \text{ m} = 2H$.

The time factor for one year $T = \frac{c_v t}{h^2} = \frac{0.006\,22 \cdot 365}{21^2} = 0.0051$ and the corresponding

degree of consolidation $\mu = 10\%$. During one year, assuming that the tower was built completely at one time, the mean settlement would be $0.10 \cdot 2.7 = 0.27 \text{ m}$. For 10 years the time factor $T = 0.051$ and the corresponding degree of consolidation $\mu = 26\%$, the settlement would be $0.26 \cdot 2.7 = 0.7 \text{ m}$. The building was completed in A.D. 1350 and it took 176 years to build. Since then $1973 - 1350 = 623$ years have passed. To this we add half the

building period and get $623 + 88 = 711$ years. For this period $T = \frac{0.006\,22 \cdot 365 \cdot 711}{21^2} =$

$= 3.65$ and the corresponding degree of consolidation $\mu = 99 \div 100\%$. In fact the Tower of Pisa is no longer setting but only toppling by 1 mm per year.

If the building process is such that the soil is loaded uniformly during the building period t_s , then the settlement after a period t (from the completion of the building) is equal to the settlement after a period $(t + t_s/2)$.

1.7 SETTLEMENT CAUSED BY SOIL SHRINKAGE. BULKING AND SUBSIDENCE OF SOIL

Buildings standing mainly on clay, peaty soils or other very shrinkable soils can settle during a prolonged drought as a result of shrinkage. In the case of brick buildings with shallow foundations, the corners of the building which face south and southwest tear away and cease to carry the load of the building as a result of soil shrinkage. In our conditions the influence of clay shrinkage reaches to a depth of approximately 1.5 m; in special cases to a depth of 4 m. For buildings with a foundation depth larger than the shrinkage depth, the influence of shrinkage is not apparent. However, shrinkage can reach to a greater depth if the subgrade is being dried out by the building, for example in the case of brickworks, coking plants, furnaces, etc. Drying out of the soil can also be caused by trees in the vicinity of a building (especially poplars) as they drain of water very quickly.

The settlement of a building caused by soil shrinkage can be calculated from the decrease of the moisture content of the soil after shrinkage. Soil dries out and shrinks until its moisture content drops to the shrinkage limit w_s . During further drying out, the soil no longer shrinks even if the moisture content of the soil drops below w_s . After the drying out of the soil during a drought period, the lowest moisture content is on the surface and with increasing depth

it increases tangentially to the initial moisture content. For the calculation of the settlement s of a building, the subgrade is divided into layers of height h . For each layer we take the mean decrease of the moisture content

$$\Delta w = w - w'_s \quad (1.49)$$

where w is the moisture content before shrinkage,
 w'_s is the moisture content after drying out.

If $w'_s < w_s$, the following decrease of the moisture content is considered

$$\Delta w = w - w_s \quad (1.50)$$

since for a decrease of the moisture content below w_s there is no further shrinkage. A uni-directional shrinkage Δh of a soil layer with thickness h is

$$\Delta h = h \frac{\gamma_s \cdot \Delta w}{\gamma_w + \gamma_s w} \doteq h \gamma_s \frac{\Delta w}{1 + \gamma_s w} \quad (1.51)$$

where γ_s is the density of the soil grains. On average $\gamma_s = 27 \text{ kN/m}^3$. The settlement of a building caused by shrinkage is

$$s = \sum_1^i h_i \frac{\gamma_s \Delta w}{1 + \gamma_s w} \quad (1.52)$$

This equation is valid provided no fissures are formed in the soil. Water would evaporate in the fissures and we would obtain a shrinkage in both a vertical direction and in directions perpendicular to the fissures. According to this equation, the settlement s of a soil layer with a thickness of 1 m with an initial moisture content w and a decrease of the moisture content caused by drying out Δw , was calculated. The calculated values are given in Table 1.11.

So far, the settlement due to the decrease of the moisture content caused

TABLE 1.11

The settlement s in cm of a soil layer with a thickness of 1 m for a decrease of the moisture content caused by drying out from w [%] by a difference Δw [%]

Initial moisture content w	Settlement of layer with thickness 1 m for a decrease of the moisture content					
	$\Delta w = 2 \%$	4 %	6 %	8 %	10 %	12 %
30 %	3.0	6.0	9.0	12.0	15.0	18.0
40 %	2.6	5.2	7.8	10.4	13.0	15.6
50 %	2.3	4.6	6.9	9.2	11.5	13.8

by drying out has been studied. In our conditions, drying out reaches to a depth of 1.5 m. If the building is founded on clays shallower than 1.5 m, then it is assumed that the shrinkage up to the shrinkage limit reaches to a depth of 50 cm (measured from the surface). At a greater depth the moisture content increases linearly and reaches the initial moisture content at a depth of 1.3 m. From these data it is possible to calculate the settlement of soil under a foundation, as we know the decrease of the moisture content. An example of the changes of the moisture content of a soil at various depths is shown in Fig. 1.16.

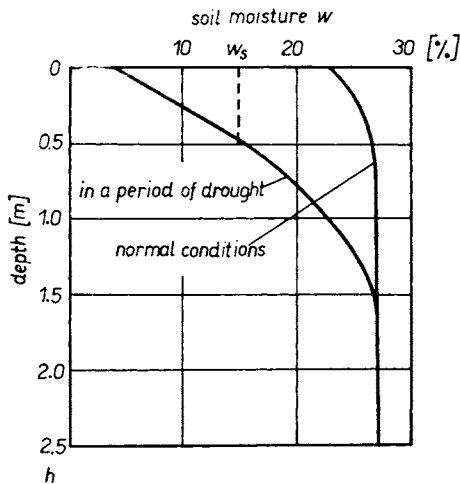


Fig. 1.16 Course of soil moisture content during drying out

We know from experience the depth reached by the decrease of humidity under ceramic and brick furnaces; this decrease of course, depends on the period of function. This depth is about 2 to 3 m beneath the foundation of the furnace. On the contact surface, the moisture content drops to the shrinkage limit or below at a depth of about 20 to 50 cm. At a greater depth we assume a linear increase of the moisture content from the initial state, which is reached at a depth of 2 to 4 m. Calculation gives the magnitude of the settlement, which is usually 10 to 20 cm. The shrinkage is not uniform and results in the formation of fissures caused by non-uniform settlement. (We must therefore take suitable precautions, for example by providing a ventilated or irrigated gravel-sand cushion, which enables the water to evaporate from the gravel and not from the clay (which therefore does not shrink), or the furnace may be founded on a hollow box, which is ventilated.

The raising of building foundations

The opposite of soil shrinkage is its expansion; we come across this phenomenon especially in solid tertiary overconsolidated clays. Soil, previously loaded with a greater vertical stress which even caused a part of the absorbed water to be expelled, increases its content of absorbed water during the access of humid air to its initial volume, soil grains move apart again, the moisture content increases and the shear strength decreases. The load q_b which is in equilibrium with the internal forces of the bulking soil is called bulking pressure. When measured in the oedometer it was found for some clays to be as much as $q_b = 40 \text{ kN/m}^2$. If water has the possibility of access to a soil which is liable to bulk, then for a load $q < q_b$ the soil bulks and the building lifts. Non-uniform lifting causes the formation of fissures on buildings. This is a long-term process. In the case of tunnel engineering, layers of clay bulk and press on the timbering. If the load $q > q_b$, the soil is compressed.

We can also find that foundations are raised during the winter time, as a result of the fact that the soil beneath the foundation freezes. In a case where the soil is saturated with water, the freezing causes an immediate raising of the soil surface as a result of an increase in water volume by

$$\Delta h = 0.09nh \tag{1.53}$$

where h is the depth of the freezing zone and n is the porosity of the soil. If the level of the capillary water is higher than the lower limit of the freezing zone, more water is carried into the freezing zone this water in turn freezes and the surface continues to rise. This process is made possible by the fact that in the capillaries, water freezes at temperatures lower than -5 to -6°C as a result of vapour tension and the tension of the large volume of adsorbed water (for example in a capillary with a diameter of 0,24 mm water freezes at -13.3°C). The usual depths of the freezing zone for our conditions are given in Table 1.12 as a function of height above sea level.

Soils which present the greatest danger as regards freezing consist of grains of varying diameter as shown by the dotted plan in Fig. 2.39. From a mineralogical point of view these soils are kaolinitic. Montmorillonite clays are less critical as they are not very permeable.

TABLE 1.12

Freezing zone in Czechoslovakia

Height above sea level in m	less than 250	250—400	400—700	700—900
Depth of freezing zone in m	0.75—0.85	0.8—0.95	0.9—1.15	1.1—1.3

Freezing increases the bearing value of the soil. On the other hand, during spring with an increase of temperature, the soil may thaw faster than it can consolidate. The soil may have taken in so much water that after thawing it becomes slurry and the bearing value decreases. Therefore it is necessary to avoid freezing of the foundations, preferably by sufficiently deep loading.

Another type of soil where settlement is not guided by the laws of consolidation and creeping are subsiding soils, especially loess and some of the loess loams. These soils have macropores and are loose. Particles on contact surfaces are bound by lime. When these soils are waterlogged, usually when the groundwater level rises, the structure of the soil is disturbed as the lime on the contacts is dissolved and the foundation suddenly subsides.

The subsidence of loess resulting from waterlogging can be avoided if a layer of loess, for example with a thickness of 1 m, is removed and gradually compacted. This was done during the building of the cellulose works in Braile in Rumania. There were fears that if the water mains should fail, the loess in the subgrade might subside.

To prevent subsidence, loess loams were sometimes subjected to a pressure exceeding 300 kN/m^2 . Thus the loess was compacted and its structure was broken down in such a way that after waterlogging it subsided very little. However, the subsidence caused by a load $q > 300 \text{ kN/m}^2$ was large and harmful.

Finally some special situations are to be found in the case of chemical works when a pipe containing some solution bursts. The solution then saturates the soil and during drying out starts to crystalize. This has been found to cause the raising of foundations by 50 cm or more, the raising depending on the nature of the solution. Technological equipment, which acts on low-temperature subgrade ($\ll 0^\circ\text{C}$), has a similar effect if the groundwater freezes near the surface. For these reasons it is necessary to consider such problems in the case of chemical works.

Soils which bulk and subside are volume-unstable and it is not possible to build foundations on them without careful consideration. For volume unstable soils it is not sufficient to calculate the settlement according to Sec. 1.3 – 1.6.

2. BEARING CAPACITY OF FOUNDATIONS

2.1 SHEARING RESISTANCE OF SOILS

The law of shearing strength was discovered by Coulomb (1773) on the basis of tests he made. According to him the shearing strength of cohesionless soils is

$$\tau = \sigma \tan \Phi \quad (2.1)$$

and of cohesive soils

$$\tau = c + \sigma \tan \Phi = c + \sigma f \quad (2.2)$$

where Φ is the angle of internal shearing resistance,
 $\tan \Phi = f$ is the coefficient of friction,

c is the cohesion and gives the shearing strength value if $\sigma = 0$.

The general expression of shearing strength is

$$\tau = m\sigma^n;$$

In Coulomb's equation $m = \tan \Phi$, $n = 1$ (for cohesionless soils).

The shearing strength of a soil is determined in a box apparatus (of the Casagrande type) or in a rotation apparatus (of the Hvorslev type). A test made with this equipment determines the shearing strength τ for a normal stress σ_n for a sliding surface or in the rupture zone, whose thickness depends on the diameter of the grains. Another type of apparatus used for the determination of the shearing strength is the triaxial apparatus in which the soil sample is enveloped in a rubber container. At the bottom and sometimes at the top there are porous plates for drainage of the soil. The sample is contained in a chamber and is surrounded by water. This enables the measurement of the horizontal stress $\sigma_2 = \sigma_3$, which is maintained during the test at a constant level. The sample is subjected to a vertical stress $\sigma_1 - \sigma_3$, which is increased up to the failure point. This is observed when on the sample one or two sliding surfaces, or an infinite number, all of which intersect, are created and the soil swells out into a barrel-like shape. Usually a noticeable drop is measured on the compression curve during failure. Tests are made with unconsolidated, undrained soil and the pore water pressure u_w is measured (the shearing of an unconsolidated soil is rapid); or they are made with consolidated, undrained

soil (the soil is left to consolidate and the loading of the sample is made rapidly, allowing no time for consolidation during the test); or they are made with consolidated, drained soil (the test on the consolidated sample is made so slowly that the pore pressure $u_w = 0$). Tests are made for different values of σ_3 . In the evaluation of the tests, circles are constructed over the components of stress ($\sigma_1 - \sigma_3$). The envelope of these (Fig. 2.1) intersects the vertical axis at the point which from the beginning gives the initial shearing strength (cohesiveness); the angle between the envelope and the horizontal is the angle of internal shearing resistance Φ . Therefore the shearing strength expressed by effective parameters is in general

$$\tau = \tau'_0 + \sigma' \tan \varphi' \quad (2.3)$$

A triaxial shearing apparatus is also used, where the value of the three main stresses $\sigma_1 \neq \sigma_2 \neq \sigma_3$, can be independently changed, until a failure of the prism-shaped sample is obtained. The advantage of the triaxial apparatus is that the shearing surface (or the failure zone) is created at the places of least resistance and the soil need not shear on the shearing surface defined in advance by the construction of the apparatus. To determine the cohesion of soils, it is also possible to use an apparatus, simple pressure tests, etc.

For soil failure there are several failure criteria. The most often used Mohr-Coulomb criterion (when expressed in the effective main stresses) is for cohesive soils

$$\frac{\sigma'_1 - \sigma'_3}{\sigma'_1 + \sigma'_3 + 2c' \cot \Phi'} = \sin \Phi' \quad (2.4a)$$

For cohesionless soils

$$\frac{\sigma'_1 - \sigma'_3}{\sigma'_1 + \sigma'_3} = \sin \Phi' \quad (2.4b)$$

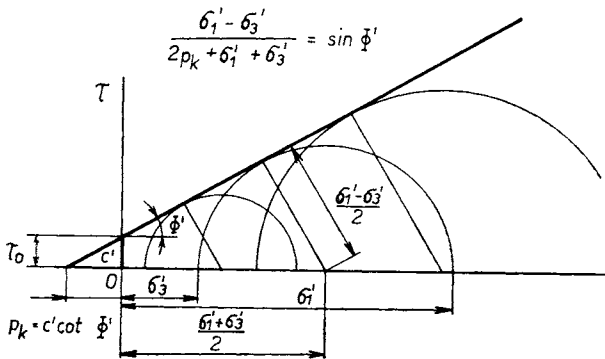


Fig. 2.1 Coulomb—Mohr's criterion for the shearing failure of soil

Then there is the so-called extended criterion of Tresco

$$|\sigma'_1 - \sigma'_2| = f_{T_1}(\Phi') \left(\frac{\sigma'_1 + \sigma'_2 + \sigma'_3}{3} \right) + f_{T_1}(c') \quad (2.5)$$

$$|\sigma'_2 - \sigma'_3| = f_{T_2}(\Phi') \left(\frac{\sigma'_1 + \sigma'_2 + \sigma'_3}{3} \right) + f_{T_2}(c') \quad (2.6)$$

$$|\sigma'_3 - \sigma'_1| = f_{T_3}(\Phi') \left(\frac{\sigma'_1 + \sigma'_2 + \sigma'_3}{3} \right) + f_{T_3}(c') \quad (2.7)$$

where $f_T(\Phi')$ is a function of the angle of internal shearing resistance of the soil Φ' , $f_T(c')$ is a function of the cohesion of the soil c' . Next there is the so-called extended criterion of Mises, which may be written in the following form

$$\begin{aligned} & [(\sigma'_1 - \sigma'_2)^2 + (\sigma'_2 - \sigma'_3)^2 + (\sigma'_3 - \sigma'_1)^2]^{1/2} = \\ & = f_M(\Phi') \left(\frac{\sigma'_1 + \sigma'_2 + \sigma'_3}{3} \right) + f_M(c') \end{aligned} \quad (2.8)$$

where $f_M(\Phi')$ is a function of the angle of internal shearing resistance of the soil Φ' , $f_M(c')$ is a function of the cohesion of the soil c' . Tests made on apparatus, when $\sigma'_1 \neq \sigma'_2 \neq \sigma'_3$, did not confirm the validity of the Tresco and Mises criteria as the calculated angle of friction was larger by approximately 10° than found in reality. For that reason the criterion of Coulomb–Mohr remains valid for the determination of the failure of soil by shearing.

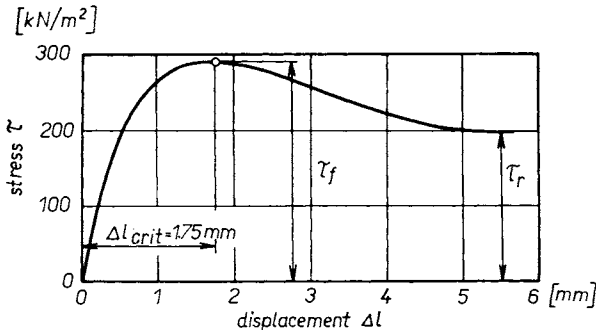


Fig. 2.2 Example of the dependence of stress τ on displacement Δl

If a compact sand shears in a box-shearing apparatus, the working diagram of the shearing stress τ against the displacement Δl forms a curve (Fig. 2.2) where for a critical displacement Δl_{crit} there is a peak value, which gives the peak shearing strength τ_f . For an acting shearing stress τ , the soil is deformed both in a horizontal and vertical sense until the peak shearing strength τ_f is reached. During further shearing, when a shearing zone has been created in

cohesionless soils or a sliding surface in cohesive soils, the shearing strength decreases until it settles on a residual value τ_r . In German sources, the term peak value is translated as Scherfestigkeit (shearing strength), whereas the residual stress is translated as Gleitwiderstand (yield resistance). In physics the following two expressions are also used: friction at rest and friction during movement, where friction during movement is always the smaller. Residual yield resistance is smaller than peak-value shearing strength by 30 percent or more. The fall from peak-value shearing strength to residual resistance is very important for the calculation of the bearing value as we must use a greater safety factor $F \geq 2$, so that the shearing stress is much smaller than the peak-value shearing strength.

TABLE 2.1

Residual angle of friction Φ'_r

$I_p = w_l - w_p$	Montmorillonite content %	Residual angle of friction Φ'_r	Author and location
58	40	9.6°	Taylor I (Lameport, Texas)
38	0	9.3°	Strawn (Proctor Dam, Texas)
91	45	5.5°	Kincaid (Cooper Dam, Texas)
132	15	6.3°	Bearpaw (Fort Peck Dam, Montana)
320	60	3.3°	Pierre (Oake Dam, South Dakota)

When the soil in the shearing apparatus is loaded, the stress is at first carried by the soil grains and water or air. But only the soil grains have a shearing strength. Therefore in the calculation of the angle of friction we take into account the effective stress σ' between the grains, as a result of which we obtain the effective angle of friction Φ' and the effective cohesion c' . The peak-value shearing strength expressed in the effective values is

$$\tau_f = c' + \sigma' \tan \phi'_f \quad (2.9)$$

For a normally consolidated clay $c' = 0$. Borowicka explains the cohesion of clay by overconsolidation.

The residual resistance

$$\tau_r = \sigma' \tan \phi_r' \quad (2.10)$$

For a residual yield resistance the cohesion $c' = 0$. According to F. C. Townsend and P. A. Gilbert a residual angle of friction was measured in clay with a variable index of plasticity I_p , as given in Table 2.1.

Tests were made in a box-and-annulus apparatus with the same results. A cohesive soil which has sheared never joins up on the shearing surface; it has a cohesion $c' = 0$ and the angle of friction is Φ_r' . An attempt was made to determine the relationship between the plasticity index I_p and the residual angle of friction Φ_r' . The measured results were very scattered and many authors (Kenney 1967) are of the opinion that the residual resistance cannot be expressed in this way and that the mineralogical composition must also be considered.

If the surface of a sample during a shearing test in a box apparatus is observed, it is found that with compact sands the surface rises or falls a little at first and then rises. This phenomena is called dilatancy. If the surface rises it is a positive dilatancy and if it falls it is a negative dilatancy (contractancy). Dilatancy makes it possible for grains in the shearing zone of cohesionless soils to turn and roll over each other during shearing, thereby effecting rolling friction which is smaller then dragging friction. If the soil in the apparatus settles at first, it is caused by the fact that the total applied stress in the soil has increased. Later, when the shearing surface begins to form, the surface of the soil rises and the negative dilatancy becomes positive. The size of displacement with which the fallen surface reaches the initial level is of no mechanical importance. For a large load, for example $\sigma_z > 20\,000 \text{ kN/m}^2$, the resistance of grains against lifting would be greater than their resistance against crushing, and therefore shearing due to a large load causes the grains to be crushed and the surface does not rise. The measured peak angle Φ' is smaller than for a small load as the crushed grains have a smaller angle of friction.

The shearing strength τ consists of resistances which act during a macro-dilatancy τ_m , during which the grains in the shearing zone rise in such a way that the grains can roll over each other and a rolling friction is effected in the soil. Then there are the resistances during microdilatancy τ_{mm} where the grains, which slide over each other and are wedged together between protrusions, partially rise and then the protrusions are broken off. The resistance encountered in the breaking away of the grains can be designated τ_t . Further, there are the resistances caused by the speed of the deformation of the soil during shearing τ_p . The slower the rate of performing the test, the smaller the angle of internal shearing resistance Φ_r' . Lastly there are the resistances due to the mutual attraction of the grains τ_c . This depends on the type of the minerals, the degree

of electrochemical saturation, the polarity of the adsorbed ions, the diagenetic strengthening, etc. Therefore, we can say that the shearing strength

$$\tau = \tau_m + \tau_{mm} + \tau_l + \tau_p + \tau_c \quad (2.11)$$

Attempts have been made to express the individual resistances separately. When a shearing surface is created in clay, the grains are laid in the shape of small tablets or rods in the direction of the shearing surface. In their original position, the grains of the clay formed a house-of-cards structure, and after shearing they are laid over each other slab-wise. As the residual angle of friction Φ'_r has very small values, as shown in Table 2.1, the cohesion c is equal to zero. In further considerations only the residual angle of friction Φ'_r is applied.

The angle of friction Φ' in cohesionless soils depends on the shape of the grains, their size, compactness and non-uniformity. According to Chen, the angle of friction in cohesionless soils is

$$\Phi' = 36^\circ + \Phi'_1 + \Phi'_2 + \Phi'_3 + \Phi'_4 \quad (2.12)$$

Φ'_1 expresses the influence of the grain shape; for grit sands $\Phi'_1 = 1^\circ$, for not very angular sands $\Phi'_1 = 0$, for rounded grains $\Phi'_1 = -3^\circ$ and for round grains $\Phi'_1 = -5^\circ$

Φ'_2 expresses the influence of the size of the grains; for a medium sand $\Phi'_2 = 0$, for a coarse sand $\Phi'_2 = 1^\circ$ and for gravel $\Phi'_2 = 2^\circ$

Φ'_3 expresses the influence of uniformity; for a uniform sand $\Phi'_3 = -3^\circ$, for a medium non-uniform sand $\Phi'_3 = 0$ and for a non-uniform sand $\Phi'_3 = +3^\circ$

Φ'_4 expresses the influence of compactness; for a loose sand $\Phi'_4 = -6^\circ$, for a medium compact sand $\Phi'_4 = 0^\circ$, for a compact sand $\Phi'_4 = +6^\circ$.

Kérisel expressed the influence of the coefficient of friction $\tan \Phi'$ on the void ratio e in the following way

$$\tan \Phi' = \frac{0.5 \div 0.6}{e} = \frac{0.5 \div 0.6}{n} (1 - n) \quad (2.13)$$

The smaller the porosity, the greater the angle of friction Φ' . This finding has been confirmed by tests made by Kamenov, Feda and others. During shearing, the porosity in the shearing zone changes. After reaching the peak angle Φ'_f , the porosity n continues to increase and settles on the critical porosity n_{crit} , which is independent of the initial porosity. If the initial porosity $n < n_{crit}$, the soil in the shearing zone loosens, and dilatancy is observed if the vertical load is not too great and the resistance against lifting is smaller than the resistance against the crushing of the grains. If $n > n_{crit}$, the soil is compacted during shearing, there is a negative dilatancy. The critical porosity has a different value for a dynamic load than for a static load.

If a sand is compact and its porosity $n < n_{crit}$, the grains in the shearing zone must rise a little, so that the friction can be lowered partially, thus becoming a rolling friction. With compact sands the initial shearing strength τ_0 is measured for $\sigma = 0$. For example, a Zbraslav sand has an initial shearing strength $\tau_0 = 9 \text{ kN/m}^2$ with an initial porosity $n = 35\%$, for a Žatec sand $\tau_0 = 6 \text{ kN/m}^2$ with an initial porosity $n = 39\%$, for a Vltava sand $\tau_0 = 12 \text{ kN/m}^2$ with an initial porosity $n = 32\%$. For a flat-grained gravel with a grain thickness of about 1 mm and a length of about 4 to 6 mm, whose grains were placed in the box apparatus at right angles to the shearing surface, an initial shearing strength $\tau_0 = 20 \text{ kN/m}^2$ was measured. Cohesionless soils have a shearing strength

$$\tau = \tau_0 + \sigma \tan \varphi \quad (2.14)$$

and for cohesive overconsolidated soils

$$\tau = c + \sigma \tan \varphi \quad (2.15)$$

The equations have the same form. According to Coulomb the initial shearing strength is called cohesion and it must not be confused with the force of attraction, which acts mutually between the grains.

In cohesionless soils subjected to a load, water and air can escape easily from the pores and therefore the neutral stress in permeable soils is not very noticeable. Between grains an effective stress is applied and for the calculation of the bearing value of foundations we use the effective values of the shearing parameters. However, in cohesive soils the water escapes from the pores slowly and sometimes it takes years after the completion of the building for the neutral stress in the pores to disappear. If the loading of the soil continues faster than its consolidation, which is usual in the case of clay and clayey soils, then we must take into account the total stress σ and the total values of the shearing parameters.

The usual values of the density of soils and their shearing parameters are given in Table 2.2.

Tests made by Anders Heiner (1975) have shown that low temperatures have a very great influence on the initial shearing strength τ_0 . For a loamy sand of the Swedish moraine, the grading curve is given in Fig. 2.39 at a temperature of -5°C $\tau_0 = 300 \text{ kN/m}^2$ for a water content $w = 5\%$ and $\tau_0 = 1\,260 \text{ kN/m}^2$ for $w = 10\%$. For a temperature of -10°C $\tau_0 = 400 \text{ kN/m}^2$ when $w = 5\%$ and $\tau_0 = 1\,800 \text{ kN/m}^2$ for $w = 10\%$. For temperatures below freezing point, an unconfined compression strength of up to $10\,500 \text{ kN/m}^2$ for -10°C and $w = 10\%$ was measured; under the same conditions a tensile strength of $2\,700 \text{ kN/m}^2$ was measured.

Until now in tests of shearing strength we have been observing shearing

TABLE 2.2

Usual values of density and the shearing parameters of some soils

Soil	Density kN/m ³ γ	Peak cohesion kN/m ²	Angle of internal shearing resistance of soil	
			peak	residual
Dense cohesionless soils with natural moisture content		Effective values		
		c'_f	Φ'_f	Φ'_r
Crushed gravel	18—20	0	39—44	37—38
River gravel	18—21	0	36—41	34—35
Grit	18—21	0	38—43	32—34
Sand with rounded grains	18—21	0	31—35	30—33
Damp cohesive soils		Total values		
		c_{uf}	Φ_{uf}	Φ_{ur}
Loess loam	16—18	10—50	22—28	16—22
Non-yielding clay	20—22	50—100	10—18	10—18
Form clay	19—21	50	0	0
Soft clay	18—20	25	0	0

strength in relation to normal stress on a shearing surface or zone. We shall now observe the work necessary to achieve the failure of soils on a yield surface. Let us designate Δl_{crit} the displacement of the soil along the rupture surface, during which the peak shearing strength τ_f is mobilized. Similarly let us designate Δl_r the displacement of the soil along the rupture surface, during which the residual shearing strength τ_r was reached. The work A_f (Fig. 2.3) required if we are to achieve during a stable effective normal stress σ'_n on a unit rupture surface (for example 1 m²), the mobilization of the peak shearing stress τ_f , is

$$A_f = \int_0^{\Delta l_{crit}} \tau \, d(\Delta l) \quad (2.16)$$

This integral describes the size of the dotted surface in Fig. 2.3. The work A_r necessary for the mobilization of the residual shearing strength τ_r by a stress σ'_m on a unit surface is

$$A_r = \int_0^{\Delta l_r} \tau \, d(\Delta l) \quad (2.17)$$

Tests made in a box-shearing apparatus have shown that the work A_f , A_r , of the outer forces, which is necessary for the mobilization of the shearing strength τ_f or τ_r on a shearing surface, is proportional to the effective normal stress σ'_n acting on the shearing surface. The work also depends on the type and porosity of the soil, and in some cases on the degree of consolidation. The work is determined from the diagram of the shearing test by the measurement of the appropriate surface, for example in Fig. 2.3 the work A_f is equal to the dotted surface. Tests made with a stress σ'_n of up to 360 kN/m² have shown that the following is valid

$$A_f \approx \sigma'_n \Omega_f \quad (2.18)$$

$$A_r \approx \sigma'_n \Omega_r \quad (2.19)$$

For a cohesionless soil of a given porosity or for a cohesive soil with a given degree of consolidation, the factors Ω_f , Ω_r are constants of proportionality between the work and the normal stress on a yield surface when the shearing strength has been reached.

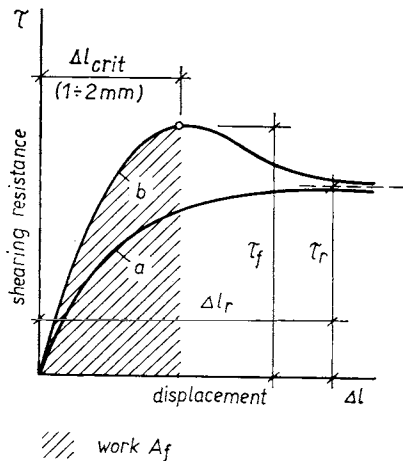


Fig. 2.3 The expression of work A_f from a diagram of a shearing test. Sand: a) loose, b) compact

For this reason these factors have been called the mobilization moduli of peak (Ω_f) and residual (Ω_r) shearing strength. The dimension of the moduli Ω_f , Ω_r is length as is apparent from equations for the unit rupture surface (for example the dimension of work corresponding to a unit yield surface is $[A_f] = \text{kNm/m}^2 = \text{kNm}^{-1} \text{m}$ the dimension of the normal stress is $[\sigma'_n] = \text{kN/m}^2$ and therefore the dimension of the modulus $[\Omega_f] = \text{m}$, i.e. length).

During shearing tests, the mobilization modulus of shearing strength achieved values from $\Omega_f = 0,5 \text{ mm}$ for a peak shearing strength of very compact cohesionless soils, to $\Omega_r = 5 \text{ mm}$ for a residual shearing strength of medium compact cohesionless soils. For loose cohesionless soils and for cohesive soils

the modulus Ω_f and also Ω_r reached values between these extreme values. Some of the measured values of the mobilization moduli of shearing strength are given in Table 2.3.

TABLE 2.3

Ω_f, Ω_r of the mobilization of shearing strength τ_f, τ_r

Soil	Ω_f [mm]	Ω_r [mm]
Sand NII; $n = 40.7\%$	1.2	4.6
Sand NII; $n = 44.0\%$	—	1.6
Sand EJP; $n = 38.8\%$	0.7	3.7
Sand EJP; $n = 46.0\%$	—	1.9
MOST clay; normally consolidated	—	1.5
MOST clay; consolidated $\sigma_k = 312 \text{ kN/m}^2$	1.6	3.1

The failure of a soil by shearing occurs if the acting stress τ reaches shearing strength. To reach the shearing strength the outer forces must do work, i.e. must transfer a certain amount of energy to the soil. The amount of energy necessary for the mobilization of the peak or residual shearing strength of the soil on a unit rupture surface, if the effective normal stress σ'_n is stable, is equal to the work A_f or A_r . The shearing strength of soils can change substantially as a result of dynamic loading as opposed to static loading. The problem has been researched for example by Barkan (1962), Finn (1967), Litvinovič (1970), Seed and Chan (1966). Published results of tests of total shearing parameters under the influence of shocks have shown that, as a result of vibrations, shearing parameters of a soil decrease in relation to amplitude, frequency and the function time of an exciter oscillating force. In cohesionless soils the decrease of the shearing strength is faster than in cohesive soils. The results of tests made by Barkan, Goodman and Seed show that as a result of shocks (vibration) in the soil, a shearing strength lower than the static peak shearing strength τ_f is applied. In a dry medium sand, as a result of shocks, the angle of internal shearing resistance comes nearer to the residual value Φ_r in proportion to the increment of the amplitude y of the oscillation and the increment of the circular frequency w (Fig. 2.4). The more intense the shocks, the faster the fall of the peak shearing strength τ_f to the residual value Φ_r . If for example the ratio of the acceleration of the oscillating movement to the gravitational acceleration when the shocks started was $a/g = 0.75$, and after a short while it was $a/g = 0.3$, then the residual strength of the sand would be reached after just three oscillations. In moist and waterlogged soil the influence of dynamic forces is even greater and more complicated.

The interaction of static and dynamic loading of soils has been measured in several cases by Seed and Chan (1966). The results of tests with a silty-clayey loam are shown in Fig. 2.5, which points out what combination of static stress σ_{st} and dynamic stress σ_d for a variety of number of pulses \bar{m} causes a failure in the soil. The static and dynamic stress is expressed as a percentage of the static stress $\bar{\sigma}$, which alone causes a failure in the soil.

Cohesionless loose soils and medium compact soils are compacted by vibrations with very small amplitudes and as a result their shearing strength increases. Amplitudes of the vibrations acting in soils are at a maximum on the level of earthquakes of the lowest degree. Piles are also driven into the soil by vibrations.

Of the dynamic influences on the mechanical properties of soils, the results of tests on the effects of earthquakes having various degrees of intensity according to the MCS (Mercalli-Cancani-Sieberg) scale have been proceeded. The

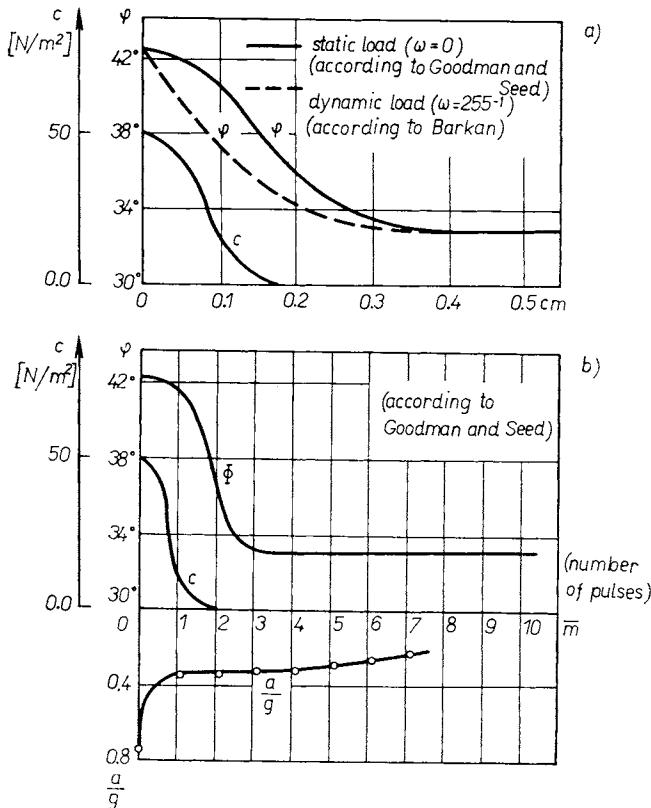


Fig. 2.4 Shearing strength of dry sand during vibration after reaching a peak strength (a) and as a function of the number of pulses (b)

values of the deflection amplitudes and soil acceleration for various degrees of earthquake intensity are given in Table 2.4.

The vibrations of the soil caused by earthquake have a very different character. Near the epicentre, vertical vibrations predominate but further away the horizontal vibrations have a more critical influence. The effects of an earthquake are greatly influenced by the geological composition of the area through

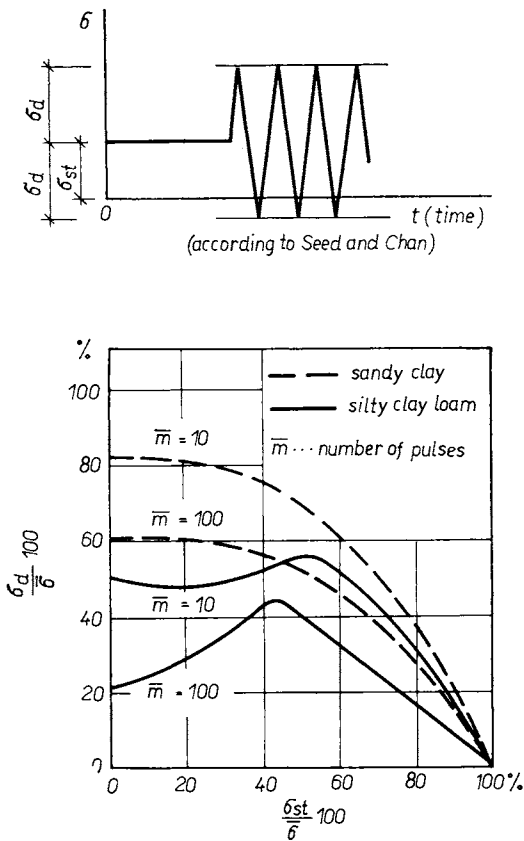


Fig. 2.5 The number of pulses which cause failure of the soil during a combined load

which the earthquake is spreading. For example the speed with which the longitudinal earthquake waves spread in different types of rocks varies by more than an order of magnitude (for example in sand it is 500 to 1 000 m/s, in basalt 5 000 to 8 000 m/s).

An effect similar to that of an earthquake is observed in the case of shocks caused by traffic, with the difference that these have higher frequencies and are very often repeated. The frequencies of traffic shocks are usually 30 to 150 Hz and their amplitudes are very small, reaching several thousandths

TABLE 2.4

Amplitude y and the maximum acceleration a for various degrees of intensity of earthquakes in °MCS

°MCS Degree of earthquake intensity	Amplitude y [mm]	Maximum acceleration a [ms^{-2}]
0 calm	0	0
1 unfelt earthquake	0.05—0.1	$g/4000$
2 very weak earthquake	0.1—0.2	$g/2000$
3 weak earthquake	0.2—0.5	$g/1000$
4 mild earthquake; felt by almost everyone in enclosed spaces	0.5—1	$g/400$
5 rather strong earthquake; felt even by people outdoors	1—2	$g/200$
6 strong earthquake	2—4	$g/100$
7 very strong earthquake	4—8	$g/50$
8 stormy earthquake	8—16	$g/25$
9 devastating earthquake	16—32	$g/12$
10 destructive earthquake		
11 catastrophic earthquake		
12 absolutely catastrophic earthquake		

TABLE 2.5

Values of shearing parameters Φ_u and c_u , which have to be considered in seismic regions, in the case of dry and naturally moist soils (According to Fift and Kysela, 1972)

°MCS Degree of earthquake intensity	Total angle of internal shearing resistance of soil	Total cohesion
1	Φ_{uf}	c_{uf}
2	Φ_{uf}	c_{uf}
3	Φ_{uf}	c_{uf}
4	Φ_1	$0.8c_{uf}$
5	Φ_2	$0.33c_{uf}$
6 and more	Φ_{ur}	0

$$\Phi_1 \dots \tan \Phi_1 = \tan \Phi_{ur} + 0.80(\tan \Phi_{uf} - \tan \Phi_{ur})$$

$$\Phi_2 \dots \tan \Phi_2 = \tan \Phi_{ur} + 0.33(\tan \Phi_{uf} - \tan \Phi_{ur})$$

of a millimetre. As a result, traffic shocks influence the mechanical properties of soils to a much smaller degree than earthquakes but their influence on the settlement of soil is not negligible.

The values of shearing parameters, which must be introduced into the calculation of the ultimate bearing capacity of foundations when considering earthquakes of various degrees of intensity MCS , are given in Table 2.5, which is valid for dry and naturally moist soils.

The parameters of the shearing strength of a soil do not change if the degree of intensity of the earthquake does not exceed 3. For a greater intensity, the angle of friction Φ_{uf} and the cohesion c_{uf} decrease as the degree of intensity grows. For a degree of intensity 6 or more, the cohesion $c_{uf} = 0$ and the angle of friction decreases to the residual angle of friction Φ_{ur} .

2.2 FRICTION BETWEEN SOIL AND STRUCTURE

In building engineering it is sometimes necessary to know the angle δ of friction between the soil and the building structure or the bedrock, for example in the case of deep foundations, foundations for columns, in the case of a stratified subgrade, etc. Tests were made to determine the amount of friction between a cohesionless soil and rigid bodies. During these tests the angle of friction δ of a Zbraslav sand moving on a solid base was measured. The tests were made in a box-shearing apparatus. The sand grains had a diameter of 1 mm, 1 to 2 mm and 2 to 4 mm. Each test was made both with a soil which was compacted so that its angle of internal friction was close to $\Phi_f = 42^\circ$, and with a loose soil with an angle of internal shearing resistance of approximately $\Phi_r = 33^\circ$. The values of the angle of surface friction δ , which were measured for a sand with grains of a maximum diameter of 1 mm, are given in Table 2.6. During the tests no significant difference was observed between the angles determined for grains of sand with a diameter of up to 1 mm and up to 2 mm. During tests with a diameter of the grains from 2 mm to 4 mm the measured values were on average smaller by 3° .

The values of the angle of surface friction for a compact and loose sand are not noticeably different, with the exception of the angle of friction of a soil with very rough concrete.

The problem of friction between a cohesive soil and smooth concrete was studied with a view to the calculation of the bearing value of deep foundations by Caquot and Kérisel (1967). They made tests on the vertical boundary between the structure and clay ($\Phi_{uf} = 0$, $c_{uf} \neq 0$) to determine a coefficient β^* . With this coefficient the total peak cohesion c_{uf} must be reduced to obtain the peak cohesion c_f , which was measured during the critical displacement

Δl_{crit} of the soil on the structure. The values of the reduction coefficient β^* for various cohesion values c_{uf} are given in Table 2.7.

$$c_f = \beta^* c_{uf} \quad (2.20)$$

TABLE 2.6

Angle of surface friction angle δ of Zbraslav sand

Base	Angle δ for	
	dense sand $\Phi_f = 42^\circ$	loose sand $\Phi_r = 33^\circ$
Smooth metal sheet, greasy	$0.36\Phi_f$	$0.36\Phi_f$
Smooth metal sheet, dry	$0.50\Phi_f$	$0.50\Phi_f - 1^\circ$
Beech and pine wood	$0.66\Phi_f$	$0.66\Phi_f - 2^\circ$
Smooth concrete (from mould)	$0.70\Phi_f$	$0.70\Phi_f - 2^\circ$
Rough concrete	$= \Phi_f$	$= \Phi_r$

TABLE 2.7

Reduction coefficient β^* in relation to the cohesion c_{uf} of soil

Cohesion of soil c_{uf} [kN/m ²]	10	30	50	100	200
Reduction coefficient β^*	0.95	0.66	0.5	0.25	0.2

If the concrete structure is very rough, a rupture surface, which envelops the projections of the uneven structure, is created and therefore, in the case of rough concrete on the boundary with a cohesive soil we must consider cohesion c_f to equal c_{uf} . This situation is encountered for example in the case of a foundation poured directly into an open trench in the soil.

If a cohesive soil has an angle of internal shearing resistance $\Phi_{uf} \neq 0$, then the largest shearing stress τ_f , which can act on the vertical boundary between a vertically loaded structure and a cohesive soil, is according to Caquot and Kérisel determined from the equation

$$\tau_f = d_2 c_f = d_2 \beta^* c_{uf} \quad (2.21)$$

where the coefficient d_2 depends on the angle of internal shearing resistance of the cohesive soil. The values of d_2 are given in Table 2.8.

TABLE 2.8

Coefficient d_2 in relation to the angle of internal shearing resistance Φ_{uf} of a cohesive soil

Φ_{uf}	0°	10°	15°	20°	25°	30°
d_2	1.00	1.60	2.06	2.70	3.62	5.01

This equation is valid provided that no changes in the mechanical properties of the soil, for example by shaking, etc., have occurred during the building process.

2.3 BEARING CAPACITY OF FOUNDATIONS — HOMOGENEOUS FOUNDATION SOIL

During the loading of soil by a foundation, a vertical stress σ_z , horizontal stresses σ_x , σ_y and shearing stresses τ_{xy} , τ_{xz} , τ_{yz} are created at a given point. As a result of stress σ_z the soil is compressed in a vertical direction, as a result of stresses σ_x , σ_y it is forced to the side and the shearing stresses are taken up by the shearing strength of the soil. At the edges of the foundation, where the shearing stress τ reaches the shearing strength, plastic ranges begin to form. When the load increases, the plastic ranges spread increasingly beneath the foundation. When they spread over the whole area beneath the foundation, a system of sliding surfaces, along which the soil is forced out from beneath the foundation to the surface, is created and the foundation sinks. The load which is in equilibrium with the resistance of the foundation soil against displacement is called the ultimate bearing capacity of a foundation.

The ultimate bearing capacity of a foundation was determined by Rankine (1857). He assumed that the horizontal stress in a vertical plane passing through the edge of a foundation is equal to the passive pressure of the soil at the foundation depth D . According to this assumption, the ultimate bearing capacity is

$$q_m = \gamma D \tan^4 (\pi/4 + \Phi/2) + c \cdot \cot \Phi (\tan^4 (\pi/4 + \Phi/2) - 1) \quad (2.22)$$

where q_m is the ultimate bearing capacity,

γ is the density of the soil,

D is the depth of foundation

Φ is the angle of internal shearing resistance of the soil,

c is the cohesion of the soil.

This equation does not include the influence of the width of the foundation and for cohesionless soils with $c = 0$, we get for foundations on the surface $q_m = 0$, which is in contradiction with true values.

Therefore we base the calculation of the ultimate bearing capacity of the foundation soil on the rupture surfaces, derived theoretically by Prandtl (1920). These are the end yield surfaces. From these towards the foundation there is a system of further yield surfaces. Beneath the end yield surface the soil does not move. The rupture surface caused by a vertical load is created either on one side of the foundation or on both sides. The settlement of a foundation when the ultimate bearing capacity is reached manifests itself as the sinking of the foundation to a depth in which the settlement stops (as the depth D has increased). Photographs of the rupture surfaces by various authors (Muhs 1965, Caquot and Kérisel 1967, Kysela 1971 and others) show that at one particular moment the rupture surface is usually created only on one side of the foundation. The formation of yield surfaces on both sides of the foundation occurs only after a greater settlement of the building, as the mobilization of the shearing strength on two rupture surfaces needs more energy. This energy is released into the soil by the sinking of the building, i.e. by the decrease of the potential energy of the building.

According to Prandtl (see Fig. 2), a wedge forming an angle $(45^\circ + \Phi/2)$ with the foundation is created under the foundation. The wedge follows up with a transient range in the form of a logarithmic spiral, whose shape is given by the equation

$$r = r_0 \exp(\vartheta \tan \Phi) \quad (2.23)$$

where r is the directrix,

r_0 is the initial directrix,

ϑ is the angle between r and r_0 .

The rupture surface intersects the horizontal surface at an angle $(45^\circ - \Phi/2)$. Prandtl did not take into account the weight of the displaced material below the loaded surface and the weight of the mass above the foundation surface. Caquot and Buismann incorporated both these influences for an infinitely long strip foundation, leaving the shape of the rupture surfaces in the form derived by Prandtl. According to them, the ultimate bearing capacity is

$$q_m = \gamma D E_1 + 0.5 \gamma B \tan(45^\circ + \Phi/2) (E_1 - 1) + c \cdot \cot \Phi (E_1 - 1) \quad (2.24)$$

where $E_1 = e^{\pi \tan \Phi} \tan^2(45^\circ + \Phi/2)$.

These equations for the determination of the ultimate bearing capacity of foundations are no longer used as they were not derived specifically for soils. Terzaghi, Meyerhof, Brinch Hansen, Caquot and Kérisel and others based

their work on the conditions created in the soil when the ultimate bearing capacity is reached, and all consider the mechanical properties of the foundation soil during the calculation of the ultimate bearing capacity. In its determination, Terzaghi assumed a state where the soil above the foundation level has no friction or cohesion and acts only by its weight. Therefore his equation is valid only to a foundation depth equal to the width of the foundation. The Meyerhof method incorporates the influence of the shearing strength of the soil above the level of the foundation line into the calculation of the ultimate bearing capacity, which is very important in the case of deep foundations. The most generally valid is the method of Brinch Hansen who also started from the Terzaghi method, adding his own new findings and those of other authors. In comparison with Terzaghi's method in its basic form, it also incorporates the influence of various shape of the foundation surface, the inclination of the acting load, the eccentricity of the load and the foundation depth. For deep foundations the Caquot and Kérisel method is especially suitable as it takes into account the friction between the soil and the sides of the foundation. All these methods consider the influence of groundwater as well as shown in Sec. 2.3.3.

2.3.1 The method of Terzaghi

Terzaghi (1943) assumed rupture surfaces (see Fig. 3 in the introduction) and expressed the friction in the foundation line with the help of a soil wedge beneath the foundation. The angle formed by the walls of the wedge and the foundation plane is the angle of internal shearing resistance of the soil. The ultimate bearing capacity of a strip foundation is

$$q_m = \frac{Q_m}{B \cdot L} = \frac{1}{2} \gamma_1 B N_\gamma + \bar{q} N_q + c N_c \quad (2.25)$$

where Q_m is the ultimate load (the bearing value of the foundation),

B is the width of the foundation,

L is the length of the foundation,

γ_1 is the unit weight of the soil beneath the foundation plane level

γ_2 is the unit weight of the soil above the foundation plane level

$\bar{q} = \gamma_2 D + p$ is the vertical stress in the vicinity of the foundation at the foundation plane level

p is the load on the ground surface

N_γ, N_q, N_c are the bearing-value coefficients

$$N_q = e^{\pi \tan \Phi} \tan^2 (45^\circ + \Phi/2) \quad (2.26)$$

$$N_c = (N_q - 1) \cot \Phi \quad (2.27)$$

The magnitudes of coefficient N_γ were derived semi-empirically

$$N_\gamma \doteq 1.8N_c \tan^2 \Phi \quad (2.28)$$

The numerical values of the bearing-value coefficients according to Terzaghi are given in Table 2.9.

TABLE 2.9

Bearing-value coefficients N_γ , N_q , N_c for a vertical load

Φ [°]	According to Terzaghi		
	N_γ	N_q	N_c
0	0.000	1.000	5.14
5	0.089	1.568	6.49
10	0.467	2.471	8.34
15	1.419	3.940	10.98
20	3.54	6.40	14.83
25	8.11	10.66	20.72
27.5	12.12	13.94	24.85
30	18.08	18.40	30.10
32.5	27.04	24.58	37.00
35	40.7	33.3	46.1
37.5	61.9	45.8	58.4
40	95.4	64.2	75.3
42.5	149.9	91.9	99.2
45	241.0	134.9	133.9

The influence of the soil above the foundation line is replaced by a uniform load $\bar{q} = \gamma_2 D$ acting at the foundation line level, if $p = 0$.

The coefficient of the ultimate bearing capacity N_γ for a given foundation was calculated by Houska (1959) from a balance of forces on a vertical passing through the edge of the foundation to the yield surface (marked by dash line in Fig. 3). He left the shape of the rupture surfaces according to Terzaghi without modification. For the calculation of the other bearing-value coefficients N_q and N_c J. Houska proceeded from the general expressions as derived by Janbu:

$$N_q = K_p/K_a \quad (2.29)$$

In the calculation according to Rankin, $K_p = 1/K_a$, which gives $N_q = K_p^2 = 1/K_a^2$, i.e. $K_p = N_q^{0.5}$ and $K_a = N_q^{-0.5}$. The values of K_p calculated in this way have been found to be in good agreement with the values of K_p given for $\delta = 2\Phi/3$ by Shields and Tolunay (1973). For $\delta \doteq \Phi$ they give higher values ($K_p \doteq 18$ for $\Phi = 45^\circ$; $K_p = 2.7$ for $\Phi = 20^\circ$) and for $\delta \doteq 0$ lower values

($K_p = 5.8$ for $\Phi = 45^\circ$; $K_p = 2$ for $\Phi = 20^\circ$). On a vertical side at a depth z below the horizontal surface, a horizontal stress is applied during a passive resistance $\sigma_{xp} = \gamma z K_p + 2cK_p^{0.5}$ and during active pressure $\sigma_{xa} = \gamma z K_a - 2cK_a^{0.5}$. In cohesive soils with a horizontal surface, a vertical wall of an excavation is retained to a depth $d = 2cK_p^{0.5}/\gamma$ for a certain time (until the soil becomes soaked or its strength is lowered as a result of vibrations caused by traffic, etc.).

$$N_y = (N_q - 1) H/B = 0.5(N_q - 1) \sec \Phi e^{(\pi/2 - \Phi) \tan \Phi} \quad (2.30)$$

$$N_c = (N_q - 1)/\tan \Phi \quad (2.31)$$

where K_p is the coefficient of passive soil pressure and K_a the coefficient of active soil pressure acting on the vertical H , which passes through the edge of the foundation to the yield surface

$$K_a = \cos^2 \Phi e^{-(\pi - 2\Phi) \tan \Phi} \quad (2.32)$$

$$K_p = 2 \sin^2 (\pi/4 + \Phi/2) e^{(\pi/2 + \Phi) \tan \Phi} \quad (2.33)$$

By substituting into equations 2.29 and 2.30 we get

$$N_q = 0.5 \sec^2 (\pi/4 + \Phi/2) e^{(3\pi/2 - \Phi) \tan \Phi} \quad (2.34)$$

$$N_y = 0.5 \{0.5 \sec^2 (\pi/4 + \Phi/2) e^{(3\pi/2 - \Phi) \tan \Phi} - 1\} \cdot \sec \Phi e^{(\pi/2 - \Phi) \tan \Phi} \quad (2.35)$$

The calculated values of the bearing-value coefficients are given in Table 2.10. The value of the bearing-value coefficients according to Houska are larger than those of Terzaghi.

TABLE 2.10

Bearing-value coefficient N_y , N_q , N_c for a vertical load, according to Houska

Φ [°]	N_y	N_q	N_c
0	0.000	1.000	5.712
5	0.367	1.641	7.337
10	1.100	2.694	9.605
15	2.533	4.446	12.861
20	5.344	7.439	17.690
25	10.974	12.720	25.134
30	22.676	22.456	37.163
35	48.342	41.440	57.754
40	108.970	81.270	95.662
45	267.130	173.240	172.240

The influence of the inclination of the load resultant from the vertical was studied by Lebegue (1972); he considers both a horizontal foundation surface and a foundation surface at right angles to the resultant of the acting inclined load on the foundation.

If the foundation surface is horizontal and β is the inclination of the load resultant from the vertical (Fig. 2.6a) the ultimate bearing capacity of a strip foundation can be determined from Terzaghi's equation. The bearing-value coefficients have a varying magnitude, which depends on the size of the angle β and the angle of internal shearing resistance of the soil Φ . These values, for cohesionless soils, are given in Table 2.11.

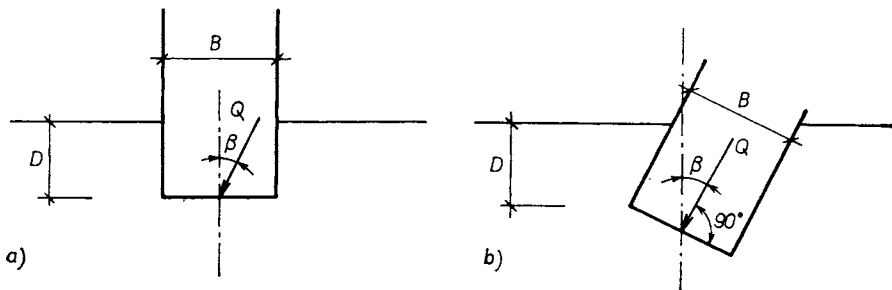


Fig. 2.6 Two types of foundations loaded by an inclined force

When considering cohesive soils, the cohesive soil is replaced by a cohesionless soil, which is under a vertical stress $p_k = c \cot \Phi$. The load increment p_k acts in the foundation-line surface together with the load $\bar{q} = \gamma_2 D + p$. However, as the load increment p_k acts both around the foundation and in the foundation line, the vertical load increment p_k must be added to the inclined load on the foundation. The resultant of these forces is inclined to the vertical by an angle β_c which we must take into account when determining the bearing-value coefficients N_γ , N_q from Table 2.11. The following relationship is valid

$$\cot \beta_c = \cot \beta + p_k / (q \cdot \sin \beta) \quad (2.36)$$

where q is the mean inclined load in the foundation line. The inclination of the load direction from the vertical decreases the values of the bearing-value coefficient and therefore also the ultimate bearing capacity in direct proportion to the increment of the inclination β .

The bearing value of a foundation may be increased if the foundation line is set at right angles to the resultant of the load. The ultimate bearing capacity of such a strip foundation is also calculated from Terzaghi's equation in which B is the width of the foundation measured in the plane of the inclined foundation surface (Fig. 2.6b). The depth of the foundation D is the smaller of the distances

TABLE 2.11

Bearing-value coefficient N_γ , N_q for inclined loading of a foundation if the foundation surface is horizontal (cohesionless soil).

Bearing-coefficient	Angle of internal shearing resistance of soil ϕ	Inclination β of the load from the vertical					
		0°	10°	20°	30°	40°	50°
N_γ	10°	1.0	0.0	—	—	—	—
	15°	2.3	0.2	0.0	—	—	—
	20°	5.0	1.3	0.0	—	—	—
	25°	10.4	3.8	0.4	0.0	—	—
	30°	21.8	9.2	2.3	0.0	—	—
	35°	48.0	21.1	7.3	0.7	0.0	—
	40°	113.0	51.0	18.6	4.1	0.0	—
	45°	297.0	131.0	50.0	14.0	1.5	0.0
N_q	10°	2.5	1.5	0.0	—	—	—
	15°	3.9	2.8	0.0	—	—	—
	20°	6.4	4.7	2.2	0.0	—	—
	25°	10.7	7.8	4.9	0.0	—	—
	30°	18.4	13.1	8.5	3.2	0.0	—
	35°	33.3	23.1	14.8	8.0	0.0	—
	40°	64.0	44.0	27.2	15.1	4.5	0.0
	45°	135.0	87.0	52.0	29.2	13.3	6.3

of the foundation from the ground surface. Lebegue made and evaluated many model loading tests of foundations with a inclined foundation surface positioned at right angles to the resultant of the acting forces and determined the values of the coefficients N_γ , N_q , N_c (Table 2.12).

2.3.2 The method of Meyerhof

Meyerhof starts from Terzaghi's basic equation for the determination of the ultimate bearing capacity of the soil beneath the foundation, but he takes into account the shear strength of the soil above the foundation line along the whole length of the yield surface. According to Meyerhof the rupture surface has a shape as shown in Fig. 4 (see Introduction). The size of angle β depends on the angle Φ of internal shearing resistance of the soil, the ratio of the foundation depth to the width of the strip foundation and the degree m' of mobilization of shear strength on the surface AE , as this surface is not the same as the rupture surface. He replaces the effect of the soil in the wedge AEF by a normal stress σ_0 and a shearing stress τ_0 uniformly distributed along the whole length AE .

TABLE 2.12

Bearing-value coefficients N_γ , N_q , N_c for inclined loading of a foundation with a foundation surface positioned at right angles to the resultant of the acting forces

Coefficient of bearing value	Angle of internal shearing resistance of soil ϕ	Inclination β of the load from the vertical					
		0°	10°	20°	30°	40°	50°
N_γ	10°	1.0	1.0	1.0	1.0	1.0	1.0
	15°	2.3	2.2	2.1	1.9	1.8	1.6
	20°	5.5	4.4	3.9	3.4	2.9	2.5
	25°	10.4	8.7	7.2	5.9	4.8	3.9
	30°	21.8	17.2	13.3	10.4	8.0	6.0
	35°	48.0	35.2	25.8	18.9	13.4	9.6
	40°	113.0	76.8	52.5	35.6	24.2	16.0
	45°	297.0	181.0	115.0	72.6	45.0	27.4
N_q	10°	2.5	2.3	2.2	2.1	1.9	1.8
	15°	3.9	3.6	3.3	3.0	2.7	2.5
	20°	6.4	5.6	5.0	4.4	3.8	3.4
	25°	10.7	9.2	7.7	6.5	5.6	4.7
	30°	18.4	15.0	12.3	10.0	8.2	6.7
	35°	33.3	25.9	20.4	15.9	12.5	9.8
	40°	64.0	47.7	35.7	26.5	19.8	14.8
	45°	135.0	95.1	67.1	47.4	33.4	23.5
N_c	10°	8.4	7.5	6.7	6.0	5.3	4.6
	15°	11.0	9.7	8.5	7.4	6.4	5.5
	20°	14.8	12.7	10.9	9.3	7.8	6.6
	25°	20.7	17.7	14.4	11.9	9.8	8.0
	30°	30.1	24.3	19.6	15.5	12.5	9.9
	35°	46.1	35.6	27.7	21.3	16.4	12.6
	40°	75.3	55.7	41.4	30.4	22.4	16.5
	45°	134.0	94.1	66.1	46.4	32.4	22.6

In reality, this assumption is not completely fulfilled. Table 2.13 is used for the determination of the angle $\bar{\beta}$.

The value $m' \doteq 0$ is valid for a shallow foundation on a horizontal base. The value $m' \doteq 1$ is valid for very deep foundations. The value of coefficient m' is determined in the following way. To start with a certain value m' is shown and the appropriate angle $\bar{\beta}$ is located in Table 2.13. Next the weight Q of the soil wedge AEF is calculated (see Fig. 4) in the following way.

$$Q = 0.5\gamma_2 D^2 \cot \bar{\beta} \quad (2.37)$$

An active pressure of a cohesive soil is assumed on the side surface of the foundation ($E_a \geq 0$ always)

$$E_a = 0.5\gamma_2 D^2 \tan^2 (45^\circ - \Phi/2) - 2cD \tan (45^\circ - \Phi/2) \quad (2.38)$$

as during the displacement of the soil from beneath the foundation, the soil in the area $ADEF$ is drawn away from the side wall of the foundation by forces acting on surface AD . On the foundation wall AF , friction and cohesion are taken into account, i.e. the adhesion of the soil to the foundation

$$E_a \tan \delta + c_f D = E_a \tan \delta + \beta^* c_{uf} D \quad (2.39)$$

Friction and cohesion apply during the sinking of the foundation into the soil; δ is the angle of friction of the soil on the walls of the foundation (see Par. 2.2, Table 2.7).

The resultant R of these forces is determined graphically, and distributed into the component normal force N , which is at right angles to the surface AF , and the component tangential force T . The mean stresses σ_0 and τ_0 acting on surface AE (see Fig. 4 in the Introduction) are

$$\sigma_0 = N \sin \bar{\beta}/D \quad (2.40)$$

$$\tau_0 = T \sin \bar{\beta}/D \quad (2.41)$$

TABLE 2.13

Angle $\bar{\beta}$ in degrees

D/B	$m' = 0$					$m' = 1$				
	Angle of internal shearing resistance of the soil Φ									
	0	10	20	30	40	0	10	20	30	40
0.0	0	0	0	0	0	0	0	0	0	0
0.2	11	7	4.5	2.5	1.5	17	10	6	3.5	1.4
0.4	23	15	9	5	3	35	19	11	6.5	3.5
0.6	36	22	13	8	4	55	30	17	9.5	5
0.8	52	28	16	9.5	5.5	90	40	22	13	7
1.0	85	35	21	12	7	90	50	27	15	8
2.0	90	85	40	23	14	90	90	50	28	16
4.0	90	90	75	40	22	90	90	90	46	27
6.0	90	90	90	55	30	90	90	90	67	35
8.0	90	90	90	68	37	90	90	90	90	44
10.0	90	90	90	90	45	90	90	90	90	53
20.0	90	90	90	90	70	90	90	90	90	87

The degree of mobilization of shearing is, according to Meyerhof,

$$m' = \frac{\tau_0}{\sigma_0 \tan \Phi + c} \tag{2.42}$$

If the calculated value m' is substantially different from the value chosen at the beginning of the calculation, then the calculation is repeated. An agreement between the chosen and calculated m' is found for a certain angle $\bar{\beta}$, used as a basis for the calculation of the ultimate bearing capacity of the foundation. The ultimate bearing capacity of a strip foundation is, according to Meyerhof,

$$q_m = 0.5\gamma_1BN_\gamma + \gamma_2DN_q + cN_c \tag{2.43}$$

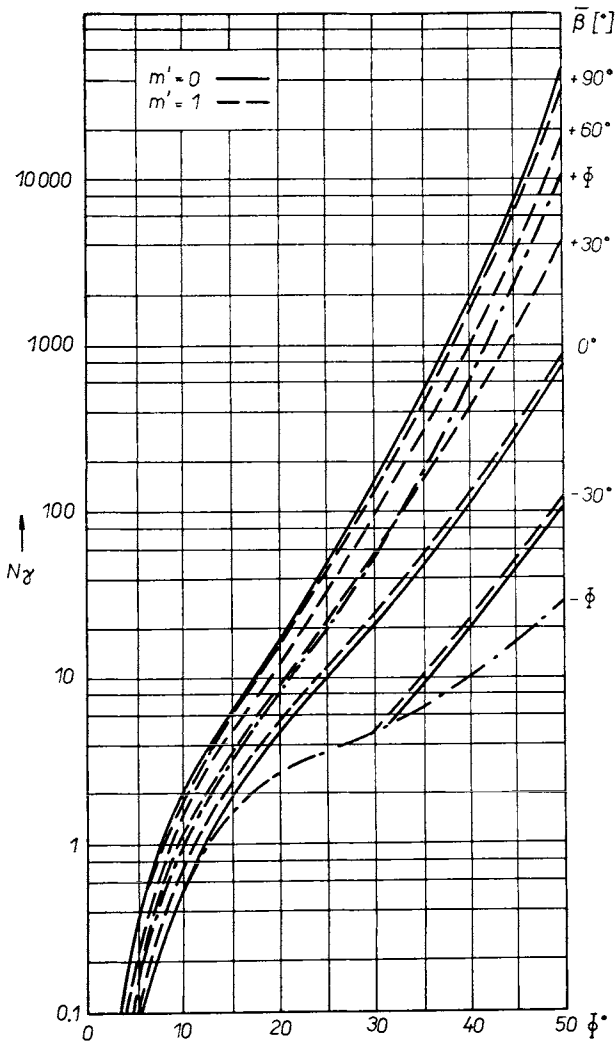


Fig. 2.7 Coefficient N_γ according to Meyerhof

The bearing-value coefficients N_γ , N_q , N_c depend on the size of the angle $\bar{\beta}$ and on the value of the degree of mobilization of the shearing stress m' . Their values are determined from the diagrams in Fig. 2.7, 2.8 and 2.9, and they can be also used for the determination of the ultimate bearing capacity of a foundation on a slope or embankment, which has a cross-sectional shape as shown in Fig. 2.10. In such a case the angle $\bar{\beta}$ has a negative value and the bearing-value coefficients, determined for a negative angle $\bar{\beta}$, are used for a calculation of the ultimate bearing capacity of a foundation on a slope crest with the help of equation (2.43). Foundations on a slope must be on the safe side against sinking and also the whole slope, which is loaded by the building, must have a sufficient safety factor against sliding. (See also Sec. 2.6.)

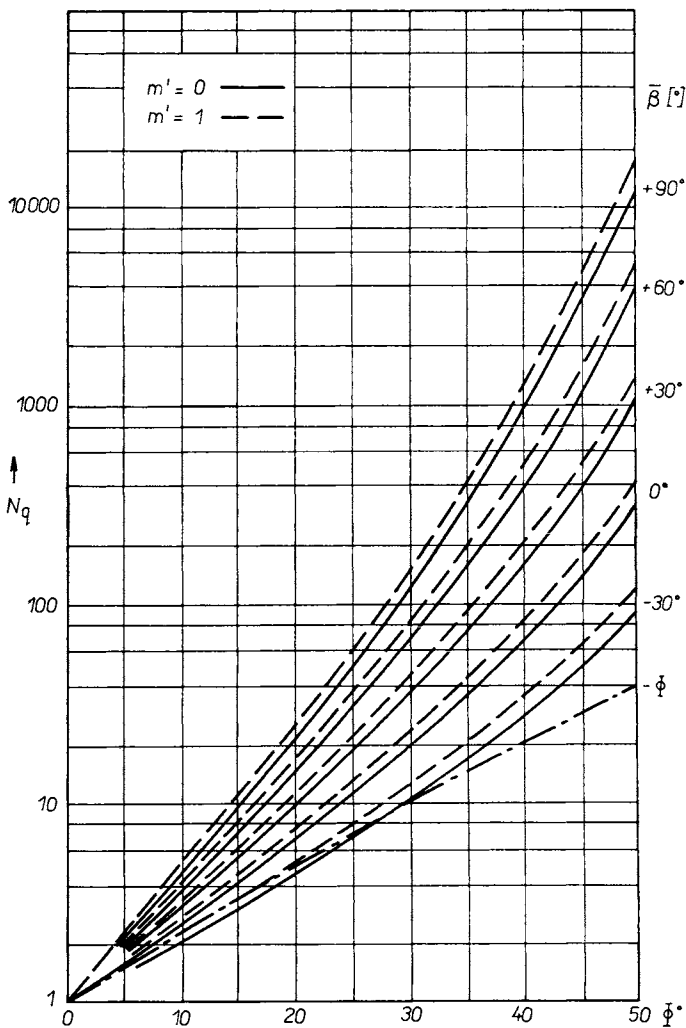


Fig. 2.8 Coefficient N_q according to Meyerhof

2.3.3 The method of Brinch Hansen

Brinch Hansen (1961) also started from the basic equation of Terzaghi to which he added the influence of the foundation depth, the shape of the horizontal foundation surface and the deflection of the resultant of the load from the normal to the base. The ultimate bearing capacity of the foundation is

$$q_m = \frac{1}{2} \gamma_1 B N_{\gamma} s_{\gamma} d_{\gamma} i_{\gamma} + \gamma_2 D N_q s_q d_q i_q + N_c s_c d_c i_c \quad (2.44)$$

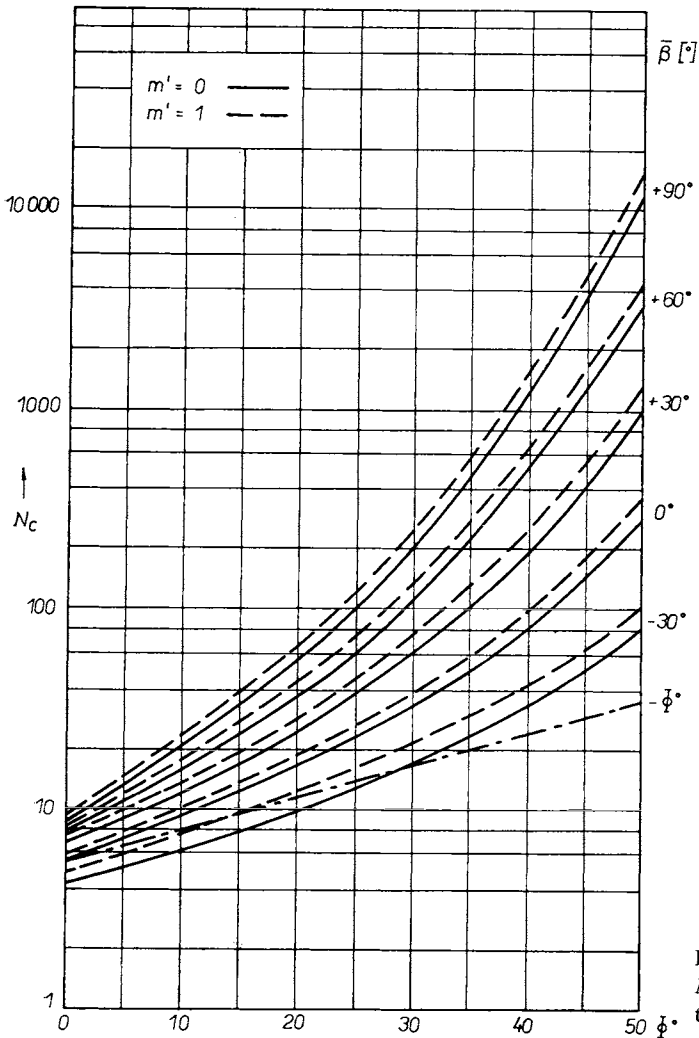


Fig. 2.9 Coefficient N_c according to Meyerhof

The coefficients s_γ, s_q, s_c express the influence of the shape of the foundation, coefficients d_γ, d_q, d_c express the influence of the foundation depth and coefficients i_γ, i_q, i_c express the influence of the inclination β of the load resultant from the vertical. The bearing-value coefficients N_γ, N_q, N_c have the same magnitude as in Terzaghi's case (Table 2.9 or 2.10). Recently Brinch Hansen mentions (1968) an approximate relationship $N_\gamma \doteq 1.5N_c \tan^2 \Phi$. The coefficient of form

$$s_\gamma \doteq 1 - 0.5 (0.2 + \tan^6 \Phi) B/L \tag{2.45}$$

or approximately

$$s_\gamma \approx 1 - 0.4B/L \tag{2.46}$$

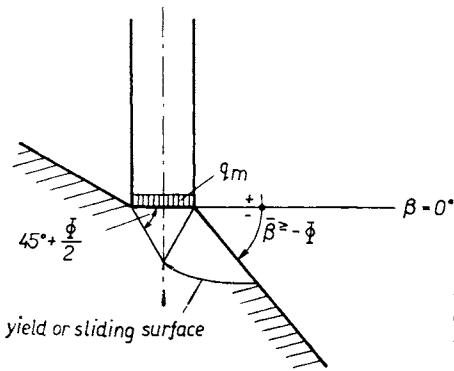


Fig. 2.10 Diagram of the loading of a slope using nomograms from Figs. 2.7 to 2.9 to determine q_m

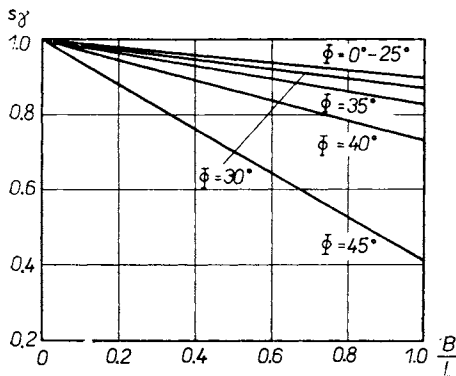


Fig. 2.11 Values of the shape factor s_γ

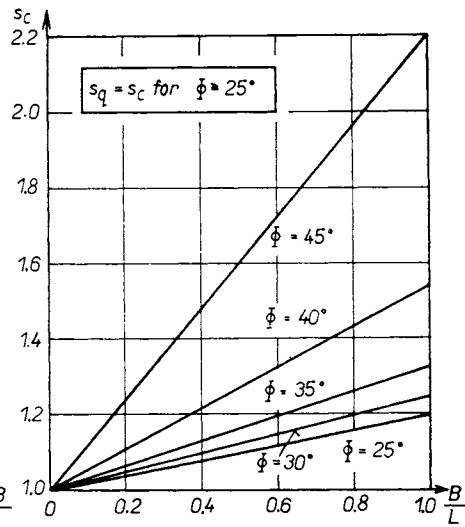


Fig. 2.12 Values of the shape factor s_c

The coefficient of form s_y is determined from the diagram in Fig. 2.11

$$s_q = s_c - \frac{s_c - 1}{N_q}; \quad s_q = 1 \quad \text{for } \Phi = 0^\circ; \quad s_q = s_c \quad \text{for } \Phi \geq 25^\circ \quad (2.47)$$

$$s_c \doteq 1 + (0.2 + \tan^6 \Phi) B/L \quad (2.48)$$

Coefficient s_c is determined from the diagram in Fig. 2.12 or calculated from the following equation

$$s_q \doteq s_c \approx 1 + 0.2B/L \quad (2.49)$$

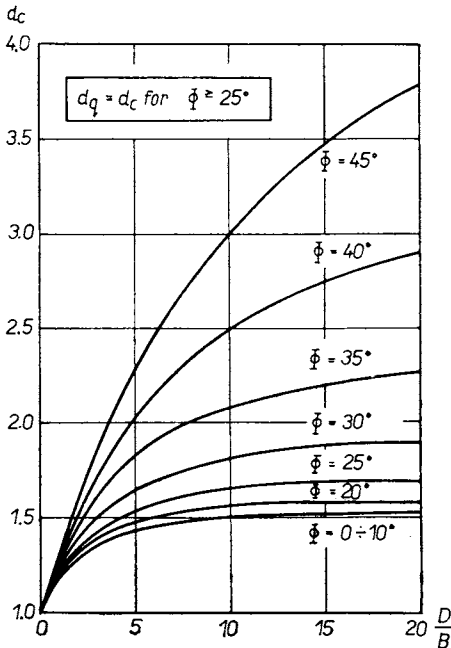


Fig. 2.13 Values of the depth factor d_c

The depth coefficient

$$d_c \doteq 1 + \frac{0.35}{B/D + 0.6/(1 + 7 \tan^4 \Phi)} \quad (2.50)$$

The depth factor d_c can be determined from the nomogram in Fig. 2.13

$$d_q = d_c - \frac{d_c - 1}{N_q}; \quad d_q \doteq d_c \quad \text{for } \Phi \geq 25^\circ \quad (2.51)$$

$$d_y = 1 \quad (2.52)$$

The influence of the depth can also be approximately calculated from equation

$$d_q = d_c \approx 1 + 0.35D/B \quad (2.53)$$

The coefficient of inclination

$$i_q = \frac{1 + \sin \Phi \sin (2\bar{\alpha} - \Phi)}{1 + \sin \Phi} e^{-(\pi/2 + \Phi - 2\bar{\alpha}) \tan \Phi} \quad (2.54)$$

The factor i_q can be determined from the nomogram in Fig. 2.14

$$i_c = i_q - \frac{1 - i_q}{N_q - 1}; i_c = 1 \text{ for } \Phi = 0^\circ \quad (2.55)$$

$$i_\gamma = i_q^2 \quad (2.56)$$

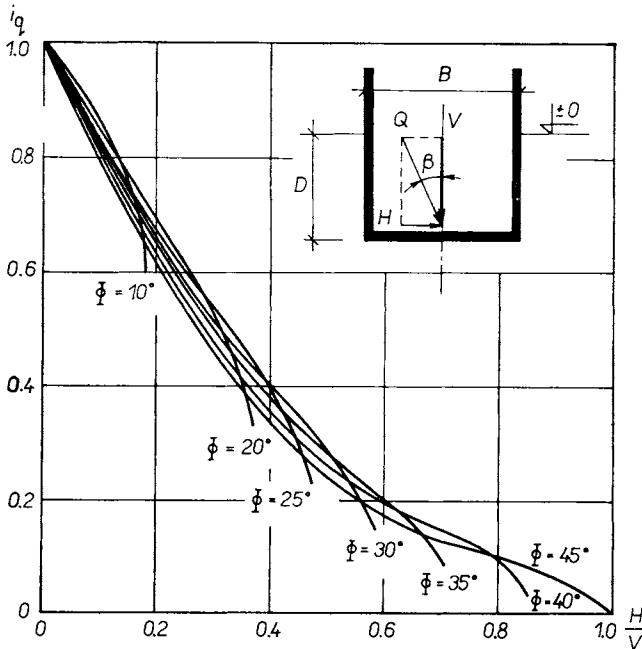


Fig. 2.14 Values of the inclination factor i_q

or calculated from equation

$$i_\gamma \doteq \left(1 - \frac{H}{V + Ac \cot \Phi} \right)^4 \quad (2.57)$$

Recently Brinch Hansen (1968) mentioned an approximate relationship

$$i_\gamma = \left(1 - \frac{0.7H}{V + Ac \cot \Phi} \right)^5 \text{ and } N_\gamma \doteq 1.5 N_c \tan^2 \Phi \quad (2.58)$$

The inclined resultant Q is distributed into a horizontal component H and a vertical component V . A condition to be fulfilled is that the horizontal forces $H < (Ac_f + V \tan \delta)$, where A is the area of the foundation and c_f the cohesion of the soil with the foundation (see Sec. 2.2). The angle of friction of the

soil against the foundation is δ . The auxiliary angle $\bar{\alpha}$ in equation (2.54) is calculated using the expression

$$\tan(\bar{\alpha} - \Phi/2) = \frac{\sqrt{1 - (\tan \beta \cot \Phi)^2} - \tan \beta}{1 + \tan \beta / \sin \Phi} \quad (2.59)$$

if the angle β is the inclination of the resultant of the load on the foundation from the vertical. If H is the horizontal and V the vertical component of the resultant Q of the forces acting in the foundation line, then $\tan \beta = \frac{H}{V}$. For a vertical load we get $i_y = i_q = i_c$. For deeper foundations, the horizontal forces H would be also absorbed by the passive pressure of the soil on the sides of the foundation, if the foundation were displaced by about $0.02 D$.

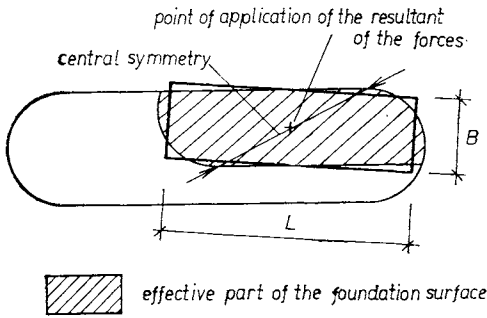


Fig. 2.15 Effective and equivalent parts of the foundation surface

For a smaller displacement there is a pressure close to the active pressure. In view of the displacement necessary to mobilize the pressure of the soil, it is not taken into account.

If the resultant of the load acts on the foundation eccentrically, an effective part of the foundation area is taken into account (Fig. 2.15). For its determination the following is valid:

1. The resultant of the forces acting on the foundation passes through the centre of gravity of the effective part of the foundation surface.

2. The inner outline of the effective part of the foundation surface is radially symmetrical; the centre of symmetry is at the point of application of the resultant of the forces acting on the foundation surface.

If the shape of the foundation surface (or the shape of the effective foundation surface) is complicated, the ultimate capacity is determined for an equivalent rectangular (square) surface (Fig. 2.15). The equivalent surface and the original surface have:

1. the same centre of gravity,
2. the same main orthogonal axes,
3. the same size of the surface and
4. the ratio of the main dimensions (length and width) is maintained as far as possible.

Usually it is stated that the greatest permissible eccentricity for the least favourable combination of the effects of the load is a third of the dimension of the foundation for cohesionless soils, and a sixth of the dimension of the foundation for cohesive soils. These conditions should provide a safety factor of at least one and a half against tipping over. This does not take into account the influence of the compressibility of the subgrade. If the foundation tilts, the stress on the edge increases and as a result we get a compression increment and a further inclination and a further increase of the eccentricity. This can cause failure by tipping over.

As far as the influence of the level of the groundwater beneath the foundation is concerned, its influence is taken care of by the introduction of a substitute density of soil

$$\bar{\gamma}_1 = \gamma'_1 + \frac{\bar{h} - D}{B} (\gamma_1 - \gamma'_1) \dots \quad \text{for } 0 \leq (\bar{h} - D) \leq B \quad (2.60)$$

where \bar{h} is the depth of the groundwater level beneath the surface and γ'_1 is the density of the submerged soil. If $(\bar{h} - D) = B$ then $\bar{\gamma}_1 = \gamma_1$. If $(\bar{h} - D) > B$ the groundwater exerts no influence.

If the groundwater level is above the level of the foundation line, i.e. $(\bar{h} - D) < 0$, the substitute densities are $\bar{\gamma}_1 = \gamma'_1$ and $\bar{\gamma}_2 = [\gamma'_2(D - \bar{h}) + \gamma_2\bar{h}]/D$, if γ'_1 and γ'_2 are the densities of the submerged soil below and above the foundation line.

2.3.4 The method of Caquot and Kérisel

The advantage of the method worked out by Caquot and Kérisel (1967) for the calculation of the ultimate bearing capacity of foundations is that it can be used also for deep foundations, for example wells, piles, etc. Basically it is derived from Terzaghi's method to which it gives more precision and adds the influence of friction and cohesion of the soil on the sides of the foundation. In the description of the Caquot and Kérisel method, the designations used here are similar to those used in the other methods for the calculation of the ultimate bearing capacity of the foundation soil and therefore differ from the designations used by the authors of the method.

The ultimate bearing capacity of a foundation loaded vertically is

$$q_m = \frac{1}{2} \gamma_1 B N_{\gamma} s_{\gamma} + \gamma_2 D N_q s_q + c N_c s_c + \frac{1}{2} \gamma_3 \frac{D'^2 O}{A} d_1 + c_f \frac{D' O}{A} d_2 \quad (2.61)$$

The first term of the equation expresses the influence of the resistance of the soil beneath the foundation, the second term takes into account the cohesion of the soil, the fourth term expresses the influence of the friction of the soil on the sides of the foundation and the last term gives the influence of the cohesion acting on the sides of the foundation.

The width of the foundation or its diameter is B , the depth of the foundation is D , the length of the foundation is L , the circumference of the foundation is O and the area of the foundation is A . In the calculation of the friction of the soil against the sides of the foundation we consider the effective depth of the foundation D' , which is

$$D' = D - \bar{d} - d_p \quad (2.62)$$

if for a strip foundation with a width B

$$d_p = N_{q_{\max}}^{2/3} B/2 \quad (2.63)$$

and for a circular foundation with a diameter B

$$d_p = N_{q_{\max}}^{2/3} B/4 \quad (2.64)$$

The values of the expression $N_{q_{\max}}^{2/3}/2$ are given in Table 2.15 for various values of Φ . If $D' \leq 0$, the friction of soil or its cohesion on the sides of the foundation are not taken into account,

- \bar{d} is the depth of the surface layer which is not effective as far as lateral pressure is concerned (top soil, soil with fissures, etc.),
- $N_{q_{\max}}$ is the maximum value of coefficient N_q – see Table 2.14,
- γ_1 is the density of the soil beneath the level of the foundation line
- γ_2 is the density of the soil above the level of the foundation line to a height d_p ,
- γ_3 is the density of the soil in a depth from $D = 0$ to $(D - d_p)$,
- c_f is the cohesion (adhesion) between the soil and the foundation – see Sec. 2.2, equation (2.20),
- δ is the angle of friction of the soil between the soil and the foundation – see Sec. 2.2,
- d_1, d_2 are the coefficients expressing the influence of the friction of the soil on the sides of the foundation,

s_y, s_q, s_c are the coefficients expressing the influence of the shape of the foundation. For a strip foundation $s_y = 1$; for a square $s_y = 0,8$; for a circle $s_y = 0,6$; for a rectangle $s_q = s_c = 1 + 0,2B/L$ and for a circle $s_q = 1, s_c = 1,3$.

It is assumed, that when the ultimate bearing capacity is reached, plastic ranges are created along the foundation surface. These reach to a height d_p above the foundation line. In this part of the foundation the friction against the sides of the foundation is not considered.

The bearing-value coefficient N_y depends on the angle of internal shearing resistance of the soil and on the size of the angle α' , formed by the sides of the triangular soil wedge below the foundation with the foundation surface. For rigid foundations and a very compact cohesionless soil it is usually assumed that $\alpha' = 45^\circ + \Phi/2$; for imperfectly rigid foundations in usual geological conditions Caquot and Kérisel suggest the use of a coefficient N_y given for $\alpha' = \Phi$; for very yielding foundations on the ground surface (for example loaded sheet metal reservoirs, the pressure of water acting on soil through isolating dividing membranes, etc.) one counts with $\alpha' = 0^\circ$.

TABLE 2.14

Coefficients N_y, N_q, d_1, d_2 according to Caquot and Kérisel

Coefficient		Φ Angle of internal shearing resistance of the soil							
		for	10°	15°	20°	25°	30°	35°	40°
N_y	$\alpha' = 0^\circ$	0.34	0.78	1.66	3.48	7.38	16.4	39.3	104.8
	$\alpha' = \Phi$	0.88	1.78	3.51	7.24	14.8	33.4	78.1	172.5
	$\alpha' = 45^\circ + \Phi/2$	1.60	3.00	5.69	11.4	22.7	49.8	114.0	307.5
N_q	$D = 0$	2.50	4.03	6.67	11.4	20.4	38.5	78.6	178.0
	$D = d_p/2$	3.20	5.68	11.3	21.7	47.8	110.5	286.1	866.0
	$D \geq d_p$	3.44	6.23	12.8	26.2	56.9	134.5	355.5	1 096.0
d_1	$\delta \doteq \Phi$	0.29	0.57	1.03	1.81	3.21	5.85	11.3	23.7
	$\delta \doteq 2\Phi/3$	0.19	0.36	0.64	1.10	1.88	3.27	5.90	11.4
d_2		1.60	2.06	2.70	3.62	5.01	7.27	—	—
For $D' \leq 0, d_1 = d_2 = 0$									
$N_{q \max}^{2/3}/2$		1.14	1.69	2.73	4.40	7.40	13.1	25.0	53.0

The coefficient N_q depends on the angle of internal shearing resistance Φ of the soil and on the ratio of the foundation depth D to the height d_p of the plastic ranges in the vicinity of the foundation. The smallest value of N_q is obtained for foundations founded on the surface. The largest value of N_q is obtained for a foundation depth $D = d_p$; when the foundation depth increases the value of N_q does not change any more.

Coefficients d_1 and d_2 also depend on the angle Φ . The size of the coefficient d_1 also depends on the size of the angle of friction δ of the soil on the structure.

The values of coefficients N_γ , N_q , d_1 , d_2 are given in Table 2.14.

The bearing value coefficient N_c is calculated from the equation

$$N_c = (N_q - 1) \cot \Phi \quad (2.27)$$

When calculating deep foundations according to this method, it is possible to consider as many as three types of soil if one layer of soil reaches to a depth $(D - d_p)$, the second is from $(D - d_p)$ to D and the third is still deeper. In equation (2.61), we then in the first term of the equation consider the shear parameters and the density of the lowest layer of soil. In the second and third term we take the properties of the central layer of soil. In the last two terms, which deal with the effect of the friction of the soil on the sides of the foundation, we take the properties of the uppermost soil layer.

2.3.5 Graphical determination of the ultimate bearing capacity of foundations

The ultimate bearing capacity of a strip foundation in cohesionless and cohesive soils can also be determined graphically. The geographical method is very concise and it is also suitable for the determination of the ultimate bearing capacity in special cases such as when the ground surface is sloping or when the footing is founded on a gravel-sand cushion. When the ultimate load is reached a collapse mechanism, which is always the route of least resistance, is created under the foundation. The graphical method enables the selection of several collapse mechanisms, of which one is chosen that leads to the determination of the minimum bearing capacity.

The best correlation with model test results for a foundation depth $D = 0 \div 2.5B$ is obtained with the collapse mechanism used by Przedeczki and Rossiński for vertical loads (Fig. 2.16). In this mechanism a solid wedge I of soil is assumed beneath the foundation. The sloping side of the wedge, which forms a part of the main sliding surface, is inclined at an angle $(\beta^\circ + \Phi/2)$ while the other face is at an angle $\pi/2 - \beta^\circ$ to the horizontal during vertical loading.

If the resultant of the applied force is inclined to the vertical by an angle β , then the value of the angle β° depends on the angle of internal shearing resistance of the soil and the angle β . The values of the angle β° expressed as a function of the above two parameters, are given in Table 2.15.

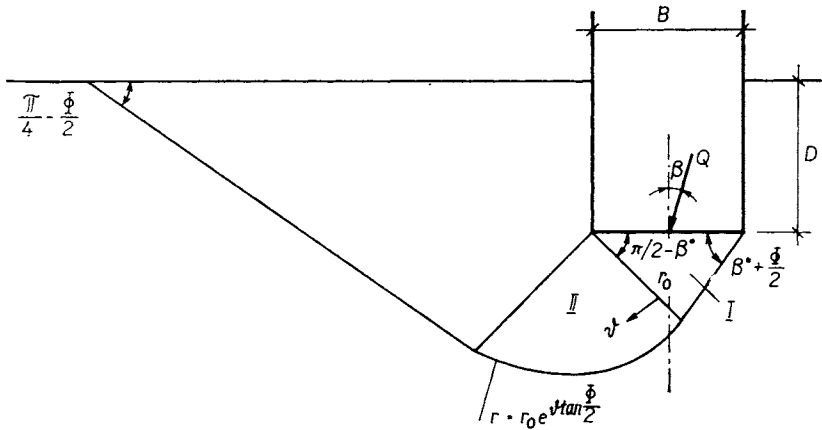


Fig. 2.16 The collapse mechanism assumed during the graphical determination of the bearing value of a foundation

TABLE 2.15

Values of angle β° in relation to the inclination β of the resultant of the load from the vertical for various angles Φ of internal shearing resistance of the soil

Φ	β				
	0°	10°	20°	30°	40°
0°	$\beta^\circ = 45^\circ$	—	—	—	—
10°	$\beta^\circ = 45^\circ$	$\beta^\circ = -5^\circ$	—	—	—
20°	$\beta^\circ = 45^\circ$	$\beta^\circ = 22^\circ$	$\beta^\circ = -10^\circ$	—	—
30°	$\beta^\circ = 45^\circ$	$\beta^\circ = 27^\circ$	$\beta^\circ = 8^\circ$	$\beta^\circ = -15^\circ$	—
40°	$\beta^\circ = 45^\circ$	$\beta^\circ = 31^\circ$	$\beta^\circ = 15^\circ$	$\beta^\circ = 0^\circ$	$\beta^\circ = -20^\circ$

The following condition $F \tan \beta \leq \tan \Phi$ must be fulfilled for cohesionless soils, where F is the safety factor against the sliding of the foundation.

Beyond the solid wedge I , the main sliding surface assumes the form of a logarithmic spiral

$$r = r_0 \exp (\vartheta \cdot \tan (\Phi / 2)) \quad (2.65)$$

Beyond this zone, another wedge *III* completes the collapse mechanism. One side of the wedge *III* forms the continuation of the main sliding plane and is tangential to the range bounded by the logarithmic spiral. The angle between the sliding plane and the horizontal is $(45^\circ - \Phi/2)$. The soil in *II* and *III* bounded by the logarithmic spiral and the sliding plane is in a plastic state.

The graphical solution of the ultimate loading of a strip foundation is known for cohesionless soils (Przeddecki-Rossiński et al. 1961). This method can be extended to apply to cohesive soils. In the graphical solution, the area above the main sliding surface is divided into smaller triangular areas in such a way that the length of their bases approximates to the length of the actual curved sliding surface. To clarify this method an example is given where the ultimate loading of a strip foundation with a width of 1 m and a foundation depth of 1 m is determined. The foundation soil is a cohesive soil and its $\Phi_{uf} = 20^\circ$, $c_{uf} = 10 \text{ kN/m}^2$ and $\gamma = 20 \text{ kN/m}^3$.

When the ultimate state of equilibrium is reached the weight of the soil Q_1 acts in area *III* (Fig. 2.17) and the reactions on the walls are R_1 and Z_1 . These forces are inclined at an angle of internal shearing resistance Φ to the normals of the sliding surfaces. Cohesive forces $C_1 = c \cdot l_1$ and $C_2 = c \cdot l_2$ act on the walls in a direction opposing the soil movement. The length of segment \overline{ab} is l_1 , and of segment \overline{bd} l_2 . If we sum forces Q_1 , C_1 and C_2 we obtain a resultant force, which can be resolved in the direction of reactions R_1 and Z_1 , thus defining their size. During the solution of the next triangular zone, we assume at the boundary with area *II* forces Z_1 and C_1 . Again, we add the weight Q_2 of the soil wedge \overline{bde} , the cohesive force C_3 on the sliding surface and the cohesive force C_4 with the next soil wedge to force C_2 . The resultant force is again resolved in the known directions R_2 and Z_2 and their size is obtained at the point of intersection. We proceed thus until, for the last wedge directly beneath the foundation, the resultant of known forces Q_4 , Z_3 , C_6 , C_7 is resolved to find the size of reaction R_4 and the vertical ultimate load Q_m of the foundation. In this example the value of the ultimate load $Q_m = 492 \text{ kN}$. The ultimate bearing capacity of the foundation soil is $q_m = Q_m/A = 492 \text{ kN/m}^2$, if $A = 1 \text{ m}^2$ is the area of the examined element of the foundation.

Similarly, a graphical solution for the same foundation with a width of 1 m and a foundation depth $D = 4 \text{ m}$ yielded an ultimate bearing capacity $q_m = 1500 \text{ kN/m}^2$. The ultimate bearing capacities for depths $D = 1 \text{ m}$ and 4 m obtained using the various methods mentioned in Sec. 2.3 are given in Table 2.16.

In Fig. 2.17 the area bounded by the logarithmic spiral was divided in two triangles for the sake of clarity. For practical purposes it is suggested that this area be divided into at least 4–6 triangular parts.

The listed values show good correspondence of the ultimate bearing capaci-

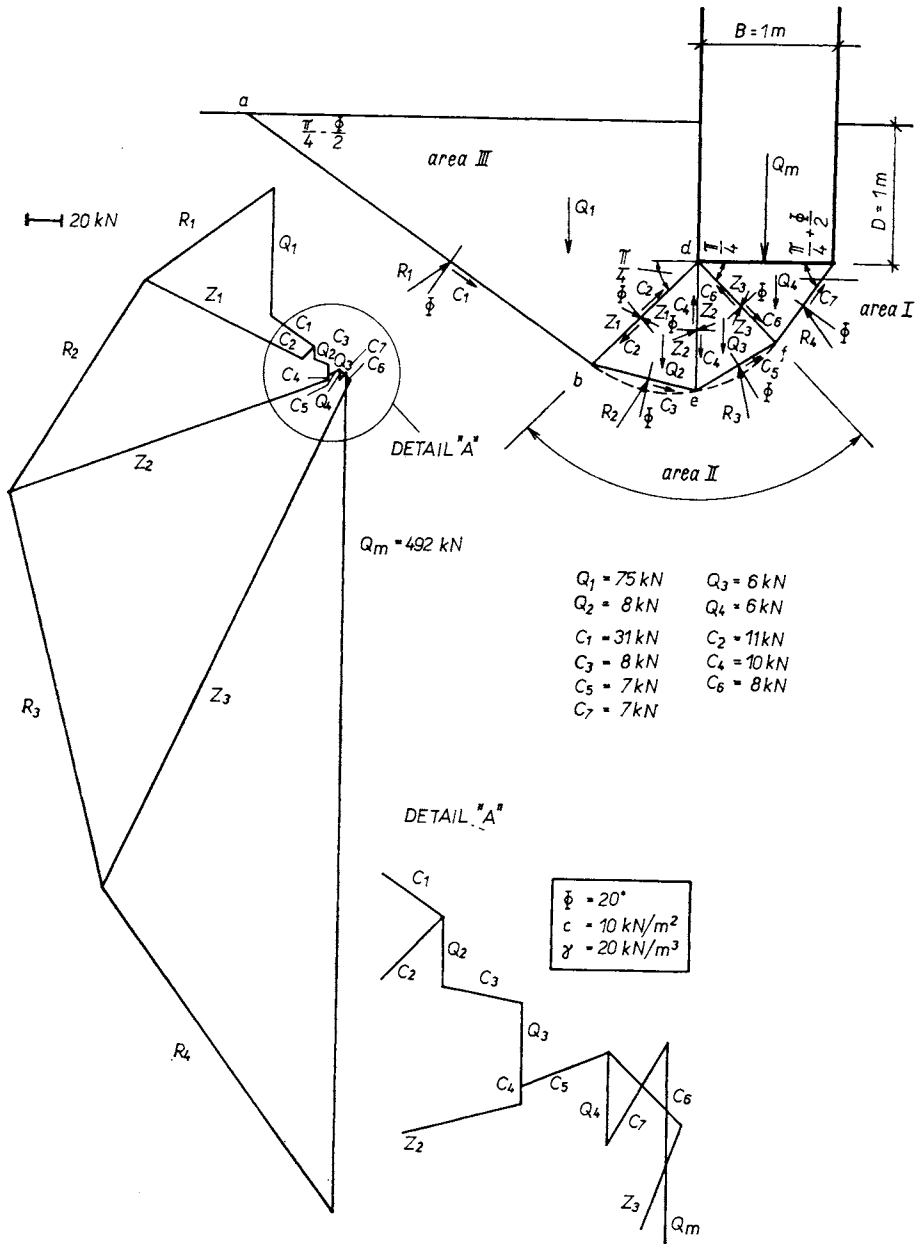


Fig. 2.17 The graphical determination of the ultimate bearing capacity of a strip foundation

ties of foundations determined according to the methods of Meyerhof and Caquot and Kérisel, and the graphical method. These methods are suitable for shallow- and medium-depth foundations. The methods of Meyerhof, Caquot and Kérisel also give good results for deep foundations, i.e. for $D \leq 20B$. Furthermore, the second of these two methods is suitable for the determination of the bearing value of individual piles. The Brinch-Hansen method gives very low ultimate load values, thus not sufficiently utilizing the bearing capacity of the foundation. The advantage of the method is that the calculation can deal with a combination of horizontal and vertical loads on a foundation. The method of Terzaghi gives the lowest bearing capacity values for a foundation, as it does not take into account the influence of the shear strength of the soil above the foundation level. Therefore this method is suitable only for foundations where the foundation depth $D < B$.

TABLE 2.16

The ultimate bearing capacity q_m in kN/m^2 of a strip foundation with a width $B = 1 \text{ m}$, $\Phi_{uf} = 20^\circ$, $c_{uf} = 10 \text{ kN/m}^2$, $\gamma = 20 \text{ kN/m}^3$

Depth of foundation D	The ultimate bearing capacity q_m [kN/m^2] according to				
	Terzaghi	Meyerhof	Brinch Hansen	Caquot and Kérisel	the graphical method
1 m	320	510	340	420	490
4 m	690	1 580	990	1 180	1 500

It should be noted that some authors assume a shape of the collapse mechanism which differs from that given in Fig. 2.16 and Table 2.15 (for example, Lebeque 1972). In the soil, various systems of sliding surfaces, partly linear in vertical section and partly in the shape of a logarithmic spiral, are assumed. In reality, all the sliding surfaces have a complex curvature. As the shape of the sliding surface, for a case where the dead weight of the soil is taken into account, has not been theoretically determined, the authors chose an experimentally determined shape for the collapse mechanism (Fig. 2.16 and Table 2.15).

A sliding surface of almost the same shape was obtained from tests made by Reimberts (1974), who measured the angles of the sliding curves. Range *I* (below the foundation) is symmetrical, compared to the axis of the strip foundation, if the load is central and vertical. The angles of the foundation line are $45^\circ + \Phi/3$. The logarithmic spiral in range *II* continues according to equation $r = r_0^{8 \tan(2\Phi/3)}$ and the linear continuation of the sliding surface is at an angle of $45^\circ - \Phi/3$ to the surface.

Each method used for the determination of the ultimate bearing capacity of a foundation is based on specific assumptions, and therefore the design engineer is left to choose the method of calculation which will best suit the specific conditions. For this reason, different methods of calculation are described in Chapter 2.3.

Calculation of the ultimate bearing capacity q_m , using the methods of the various authors, gives values of different magnitude. This also applies to tests where a large experimental scatter is obtained. An example of such known loading tests are those made in the DEGEBO (Deutsche Gesellschaft für Bodenmechanik). The scatter of the results was considerable, even although the sand was carefully compacted and the angle of friction Φ was controlled. Consequently, we try to use a large number of loading tests and the measured bearing values are processed statistically. During calculations we then use the safest of the limits of the confidence interval¹⁾ (usually 95 %) of the sought value q_m .

2.4 INFLUENCE OF ADJACENT FOUNDATIONS

The problem of the interaction of adjacent foundations was studied by the following authors: Stuart (1962), Biarrez (1963), Mandel (1963), West and Stuart (1965), Kos (1967), Myslivec and Kysela (1968, 1969 and 1971), Dembicky et al. (1971) and others. Usually they studied a case where the foundations were of the same width and their foundation depth was the same. Until now the situation where the foundations have a different width, a different foundation depth and their distance from one another varies while their length remains the same, has not been considered. The solution of such a case for two adjacent foundations with a rectangular section is presented on the following pages.

Bearing capacity tests were made on a model with a homogeneous grain sand EJF with a grain diameter of 0.05 to 0.2 mm. For a qualitative assessment of the shape of the failure ranges in the subgrade a sand NII (grains from 0.2 to 2.0 mm) was used. The sand was compacted to a volume weight of 16.2 kN/m³,

¹⁾ For a confidence of 95 % and Students distribution in 5 measurements of q_{mi} , the confidence interval is

$$\bar{q}_m - K \leq q_m \leq \bar{q}_m + K$$

where

$$\bar{q}_m = 0.2 \sum_{i=1}^5 q_{mi}$$

$$K = 1.388 \sqrt{0.25 \left(\sum_{i=1}^5 q_{mi}^2 - 0.20 \left(\sum_{i=1}^5 q_{mi} \right)^2 \right)}$$

for which the measured angle of internal shearing resistance was $\Phi'_f = 32^\circ 12' \pm \pm 1^\circ 03'$ with a probability of 90 %. The models of the foundations were made of metal and their dimensions were 1×10 , 1.5×10 , 2×10 , and 4×10 cm. The surface friction angle of the soil against the sides of the foundations was, for individual series of tests, $0.36 \Phi'_f$, $0.5 \Phi'_f$, $0.66 \Phi'_f$, $1.00 \Phi'_f$. The influence of the ratio of the grain size to the foundation width on the measured bearing value was also observed during the tests. Deviations in the measured values of the bearing value were not statistically important when different types of sand

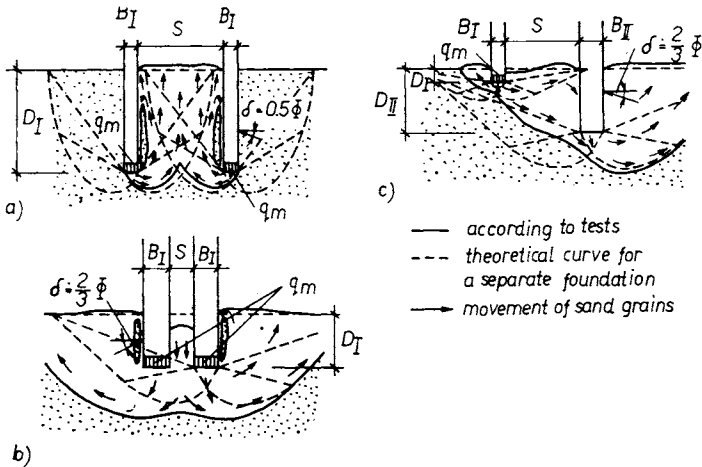


Fig. 2.18 Yield surfaces of interacting foundations

were used if the sand grains did not exceed $1/25$ th of the width B of the foundation. Both foundations were pressed into the sand simultaneously with a velocity of 0.066 mm/s and for each foundation the acting load and the vertical settlement were measured. The ultimate bearing capacity was reached when there was a load decrement in connection with a large increment of the settlement of the foundation. The ultimate bearing capacity was usually reached when the foundation was depressed by 0.5 to 1.5 mm . The same results have also been measured by L'Hermier et al. (1965) and Dembicky et al. (1971). During the evaluation of the model test results, consideration was given to the increment of the foundation depth caused by the depression of the foundation up to the point where the ultimate bearing capacity was reached.

During the tests, the shape of the sliding surfaces was photographed. 354 further bearing capacity tests on pairs of foundations having various sizes and arrangements were statistically processed. The widths of the foundations are designated B_I and B_{II} , the mean width $B = (B_I + B_{II})/2$, the foundation depths are D_I and D_{II} , the difference of foundation depth $\Delta D = (D_I - D_{II})$

the clear distance between the foundations is S the axial distance of adjacent foundations is $l = S + B$ and the length of the foundations is L . The index I relates to the foundation whose ultimate bearing capacity is being determined and index II designates values corresponding to the adjacent foundation.

For a distance $S > 8 \div 10 B$, a failure range developed under each of the foundations, as though they were standing separately. When the distance $S = 6 \div 8 B$, the sliding surfaces created under the foundations intersected, and the soil between the foundations was forced upwards by both foundations (Fig. 2.18a). The upward movement of the soil is the route of least resistance and therefore no sliding surfaces are created on the outer side of either foundation. Adjacent to the wall of the foundation, the soil moved downwards as a result of friction. The smoother the walls of the foundation, the more intense was the forcing upwards of the soil between the foundations. The bearing value of each foundation was slightly smaller than the value of the foundation standing separately. For the above separation of the foundations $S = 6 \div 8 B$, the bearing value of the foundations did not decrease if their surface was rough. For a distance $S < 5 B$, sliding surfaces were formed only on the outer side of the foundations (Fig. 2.18b). The friction on the walls caused the sand to move downwards at a slightly slower rate than both the foundations. At the foundation level not only did the weight of the sand press on the subgrade but it also produced a force resulting from the friction on the walls of the foundations. The resulting failure ranges under the foundations were larger than for separately standing foundations. We conclude that in this case the ultimate bearing capacity of both foundations is larger than the sum of the ultimate bearing capacities of two separately standing foundations.

Tests were also made with foundations having different widths and foundation depths. When the difference of the foundation depth $\Delta D = 2B_1$, a sliding surface was formed under the higher-placed foundation and this surface spread beneath the second, lower foundation. This resulted from the soil between the foundations being pulled downwards by the friction on the lower foundation and the loading of the higher foundation (Fig. 2.18c). As a result, the bearing value of the higher foundation was smaller than had it been standing separately. Horizontal forces in the soil resulting from the shallower foundation increase friction on the surface of the deeper foundation and the failure range of the deeper foundation is larger than for a separately standing foundation. Therefore the measured bearing value of the deeper foundation was greater than for a separately standing foundation.

From the bearing value Q_m of the foundation, the ultimate bearing capacity $q_m = Q_m/A$ was calculated, where A is the surface of the foundation. The measured ultimate bearing capacities of foundations having the same width and foundation depth D are depicted in Fig. 2.19. The greatest increment of the ultimate

bearing capacity of a pair of foundations was obtained for a distance $S = 0.6B$; it amounted to 160 % of the value for a separately standing foundation. The increment was smaller as the foundation depth increased, and for a depth $D_1 = 6B_1$ it fell to 50 % (Fig. 2.20). In comparison, for a separation of the foundations $S = 6.2B$ the greatest decrement of the ultimate bearing capacity was measured and it amounted to -7% of that of a separate foundation, when the angle δ of the surface friction of the soil on the sides of the foundation was $2/3 \Phi_f$. This decrement of the ultimate bearing capacity caused by an adjacent foundation is almost negligible, whereas the increment is important and can be made use of in foundation engineering.

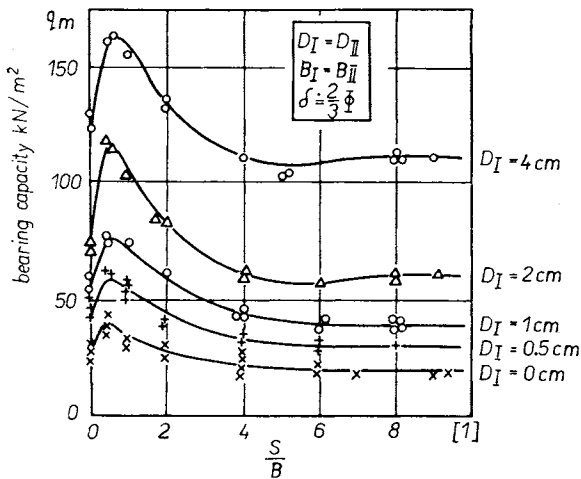


Fig. 2.19 The ultimate bearing capacity q_m of each of two foundations having the same depth. Here D_I , D_{II} are the depths of the models of foundations at the beginning of the test but not when q_m was reached

The results of one series of tests with foundations, where the width $B_I = 0.5B_{II}$, the distance of the foundations $S = 0.5B$ and where the foundation depth D and the difference in the depths of foundation ΔD vary, are given in Fig. 2.21. The established coefficient α expresses how the ultimate bearing capacity of the examined foundation exceeds that of a separately standing foundation.

When the examined foundation was placed higher than the second foundation, its bearing value was smaller than when standing separately if the difference in depth $\Delta D < -B_I$. The decrement of the ultimate bearing capacity was as much as 40 %. This was the case when $\Delta D = -3B_I$. When the foundation was placed deeper than the adjacent foundation its ultimate bearing capacity was greater than when standing separately in inverse proportion to

the decrease of the difference in the depth of foundation ΔD and the shallowness of the placing of the examined foundation. For example, for $D_I = 4B_I$ and $\Delta D = 1.5B_I$, the ultimate bearing capacity increment was 35%. The decrement and increment in these cases is significant and should be considered in foundation engineering.

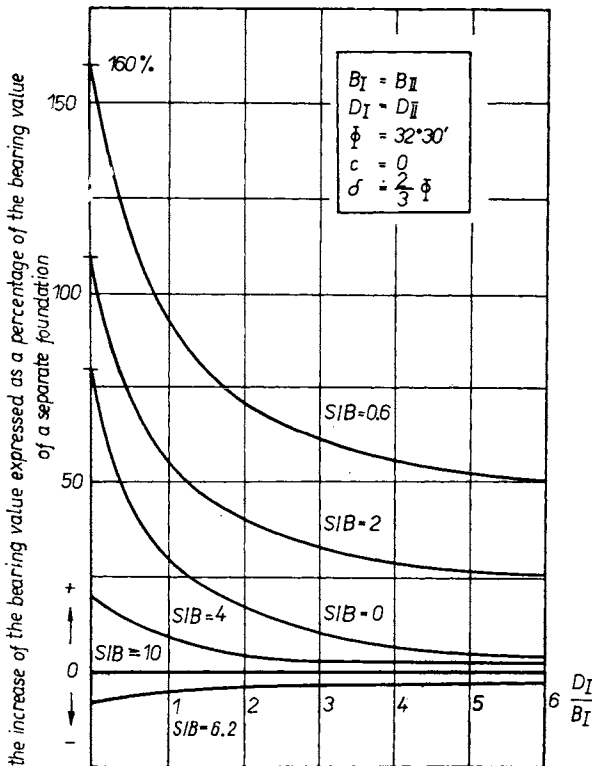


Fig. 2.20 The change in the bearing value of a foundation as a function of the relative depth of foundation D_I/B_I . Here D_I, D_{II} are the depths of the models of foundations at the beginning of the test but not when q_m was reached

For a small separation of the foundations and a small difference in their depth of foundation, the bearing value of each is greater than the bearing value of separately standing foundations. For foundations of the same width, the bearing value of the deeper foundation is somewhat larger than that of the shallower foundation.

Qualitative and quantitative evaluation was made for all tests where the sand had an acceptable mean porosity. Multiplication by the coefficient α , which tells us by how much the bearing value of the examined foundation

exceeds the ultimate bearing capacity q_{m1}^1 of the same foundation when standing separately, quantitatively describes the influence of the adjacent foundation on the ultimate bearing capacity q_{m1} of the examined foundation. The influence of scale (model: reality) on the absolute size of the measured ultimate bearing capacity appears in α equally in both numerator and denominator and thus the value of α is independent of the scale of the model. The coefficient α obtained in tests for different foundation depths and different widths of foundation is expressed by three partial coefficients $\alpha_\gamma, \alpha_q, \alpha_c$. These allow the calculation

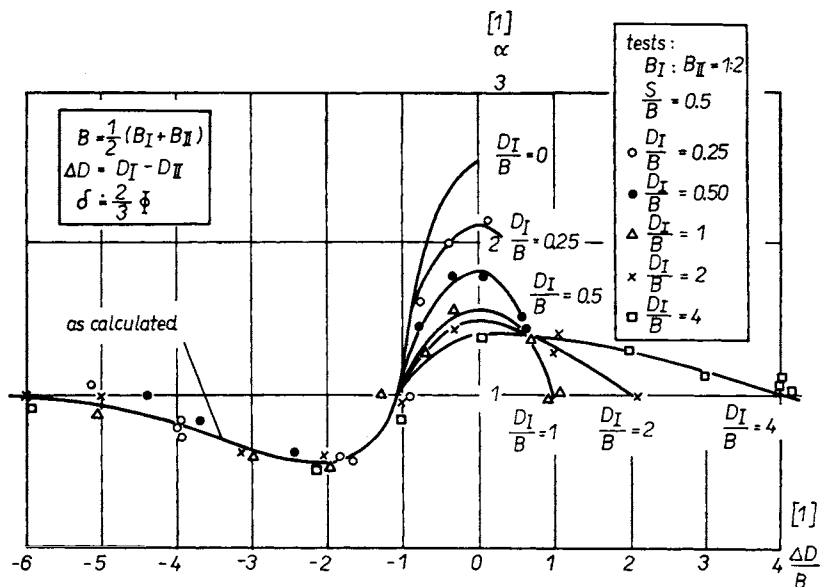


Fig. 2.21 The ultimate bearing capacity q_m of foundations with various depths of foundation, if the foundations have varying widths. Here D_I, D_{II} are the depths of foundations of the models of foundations at the beginning of the test, but not when q_m was reached

of the ultimate bearing capacity of interacting foundations using equations for the calculation for individual foundations (for example the equations given in Chapter 2.3). The individual terms of the basic equations are multiplied by the coefficients $\alpha_\gamma, \alpha_q, \alpha_c$. For example, according to the equation of Brinch Hansen, the ultimate bearing capacity of a foundation influenced by another foundation is

$$\bar{q}_{m1} = \alpha q_{m1}^1 = 0.5\gamma_1 B_1 N_\gamma s_\gamma d_\gamma i_\gamma \alpha_\gamma + \gamma_2 D N_q s_q d_q i_q \alpha_q + c N_c s_c d_c i_c \alpha_c \quad (2.66)$$

For foundations of the same length $L > 3.5B$, with a foundation depth $D < 7B$, for a ratio B_1/B_2 of the widths of the adjacent foundations from 1 : 4 to 4 : 1 and the angle of contact friction of the soil on the walls of the

foundations $\delta = 2\Phi/3$, the factors α_γ , α_q , α_c , which describe the influence of the adjacent foundation are

$$\alpha_\gamma = 1 + \frac{\sin(0.6S/B + 0.2)\bar{\eta}}{e^{(0.6S/B + 1,3 - \pi)}} (1 - \beta_1)(B_{II}/B_I)^\psi + \beta_2(B_{II}/B_I)^{\psi/3} \quad (2.67)$$

The coefficient α_q is derived from equations:

$$\text{a) if } f(D_1 - D_{II}) \leq -1 \text{ then } \alpha_q = 1 + \beta_2 \quad (2.68)$$

$$\text{b) if } f(D_1 - D_{II}) > -1 \text{ then}$$

$$\alpha_q = 0.54 K \text{ for } K \geq 1/0.54 \quad (2.69)$$

$$\alpha_q = 1.00 \text{ for } K < 1/0.54 \quad (2.70)$$

The auxiliary function K is given by the expression

$$K = 1 + \frac{\sin(0.6S/B - 0.2)\bar{\eta}(1 - \beta_1)}{e^{(0.6S/B + 1,3 - \pi)}} \quad (2.71)$$

The factor α_c was derived from the relationship (2.27)

$$N_c = (N_q - 1) \cot \Phi$$

$$N_c \alpha_c = \alpha_c (N_q - 1) \cot \Phi \quad (2.72)$$

$$N_c \alpha_c = (N_q \alpha_q - 1) \cot \Phi \quad (2.73)$$

After subtraction and rearrangement we get

$$\alpha_c = \frac{N_q \alpha_q - 1}{N_q - 1} \quad (2.74)^1$$

Similarly, if we start from equation (2.44), then

$$\alpha_c = \frac{N_q \alpha_q s_q d_q i_q - 1}{N_q s_q d_q i_q - 1} \quad (2.75)^1$$

In these equations, the terms have the following meanings

$$B = (B_I + B_{II})/2 \quad (2.76)$$

$$\text{The exponent } \Psi = 1.5^{-S/B} \quad (2.77)$$

The auxiliary function

$$f(D_1 - D_{II}) = \Delta D/D_1 \text{ for } D_1/B_1 > 1, \text{ if simultaneously } \Delta D > 0 \quad (2.78)$$

$$\text{in the other cases } f(D_1 - D_{II}) = \Delta D/B_1 \quad (2.79)$$

¹⁾ For $\Phi < 10^\circ$ we assume $\alpha_c = 1$. For $\Phi \geq 25^\circ$ it is sufficiently accurate to take $\alpha_c \approx \alpha_q$.

The auxiliary function β_2 has the following values:

$$\beta_2 = 0 \text{ if } f(D_I - D_{II}) > -1 \quad (2.80)$$

$$\beta_2 = \frac{e^{(0.5\Delta D/B_I + 0.5 + \pi)} \sin(0.5\Delta D/B_I + 0.5)\bar{\eta}}{10 + 0.08(S/B)^3} \quad (2.81)$$

$$\text{for } f(D_I - D_{II}) \leq -1$$

For the solution of the equations, auxiliary functions $\bar{\eta}$ and β_1 are also used. These depend on the mutual separation S of the foundations. If the distance $S = 0$, then

$$\bar{\eta} = 0.834 \quad (2.82)$$

$$\beta_1 = 1.00 \quad (2.83)$$

If the separation of the foundations $S > 0.6B$, then $\bar{\eta} = \tan \Phi$; but at most $\bar{\eta} = \tan 35^\circ$ for $B_I/B_{II} = 1 : 2$ to $2 : 1$

and at most $\bar{\eta} = \tan 37.5^\circ$ for the other values of B_I/B_{II} (2.84)

$$\beta_1 = 1 \text{ for } f(D_I - D_{II}) \leq -1 \quad (2.85)$$

$$\beta_1 = (|f(D_I - D_{II})|^{3/2}) \text{ for } f(D_I - D_{II}) > -1 \quad (2.86)$$

In a general case, the factors $\alpha_y \neq \alpha_q \neq \alpha_c \neq 1$; only when the foundations do not influence each other $\alpha_y = \alpha_q = \alpha_c = 1$.

For parallel strip foundations of the same width and same foundation depth, it is possible to assume that they do not influence their respective bearing value and settlement if their axial distance $l \geq 6B$ and $10^\circ \leq \Phi \leq 40^\circ$. The corresponding radius of the zone of influence, which is used sometimes, is then: $x_{\max} = 3B$. In more accurate calculations of the bearing value, it is necessary to consider values of factors $\alpha_y, \alpha_q, \alpha_c$ and in the calculation of the settlement it is necessary to consider the influence of the foundation and the influence of the adjacent foundation at the same time (see appendices).

The equations were derived for a situation where the surface levels outside and between both foundations are the same. If the difference between the surface levels outside both the foundations is smaller than their mean width, and if the surface between the foundations is not higher than the surface outside the foundations, we can, with sufficient accuracy, use the calculated factors $\alpha_y, \alpha_q, \alpha_c$. To determine their values, we consider the depths of foundation D_I and D_{II} relative to the level of the surface between the foundations (Fig. 2.22). For the calculation of the ultimate bearing capacity, the smaller of the foundation depths, measured on both sides of the foundation, is substituted for D . More complicated cases must be solved experimentally as the mathematical solution is not known.

To simplify calculations, values of factors α_γ and α_q were calculated and tabulated. In Table I two directly adjacent foundations are considered, $S = 0$. In this case the factors α_γ , α_q are not influenced by the angle of internal shearing resistance of the soil Φ . The values of factor α_γ for different width ratios B_I/B_{II} and the values of factor α_q are arranged in the columns of the table. The values of both factors for one ratio of the function $f(D_I - D_{II})$ are given in the rows of the table.

Tables II to VI give the values of factors α_γ , α_q for cases where the separation of the foundations $S > 0.6 B$. The tables are arranged in five groups for foundation-width ratios $B_I/B_{II} = 4 : 1, 2 : 1, 1 : 1, 1 : 2, 1 : 4$. Each of these groups includes tables for angles of internal shearing resistance of the soil equal to $10^\circ, 20^\circ, (25^\circ), 30^\circ, 35^\circ$, and in some cases $37,5^\circ$. Each column

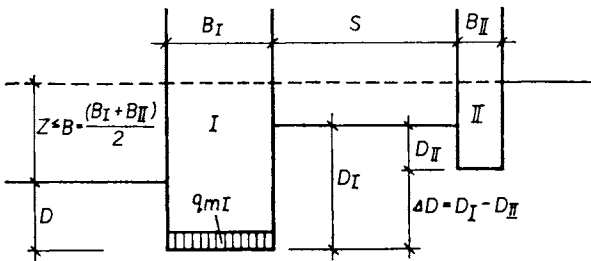


Fig. 2.22 Notation for interacting foundations in a group

relates to a different ratio S/B and each double row gives values for different sizes of $f(D_I - D_{II})$. The upper line gives the value of factor α_γ and the value of factor α_q is given on the lower line.

The equations described and the tables in the supplement can be used directly if the ultimate bearing capacity of both foundations is used in the same way, i.e. if the ratio of the actual load acting on foundation I to the load acting on foundation II is the same as the ratio of their ultimate bearing capacities $\overline{q_{mI}} : \overline{q_{mII}}$. In such a case the mutual influence exerted by the adjacent foundations is the most intense. The other extreme is the theoretical case, where foundation II, adjacent to foundation I, does not produce any load on the soil. In such a case the ultimate bearing capacity of foundation I is not influenced by the adjacent foundation and its value is the same as if the foundation was standing separately.

Let us establish the following designations:

- I the foundation for which the ultimate bearing capacity is being calculated,
- II the adjacent foundation,

$\overline{q_{mI}}$ the ultimate bearing capacity of foundation I, when the adjacent foundation II is acting with its ultimate capacity $\overline{q_{mII}}$,

$\overline{q_{mII}}$ the ultimate bearing capacity of foundation II, when the foundation I is acting with its ultimate bearing capacity $\overline{q_{mI}}$,

q_{mI}^1 the ultimate bearing capacity of foundation I, when standing separately,

q_{mI} the ultimate capacity of foundation I, when the foundation II is acting with a load q_{II} ,

q_I the maximum true load on foundation I

q_{II} the minimum true load on foundation II

For possible extreme cases, the following relations are valid:

$$q_{mI} = q_{mI}^1 \dots \text{ if } q_{II} = 0 \quad (2.87)$$

$$q_{mI} = \overline{q_{mI}} \dots \text{ if } q_{II} \cdot \overline{q_{mI}} = q_I \cdot \overline{q_{mII}} \quad (2.88)$$

In general, if two adjacent strip foundations of the same length $L > 3.5B$ are loaded, the real size of the ultimate bearing capacity of foundation I can be determined by a linear interpolation between extremes (2.87) and (2.88) according to equation

$$q_{mI} = (\overline{q_{mI}} - q_{mI}^1) \frac{q_{II} \overline{q_{mI}}}{q_I \overline{q_{mII}}} + q_{mI}^1 \quad (2.89)$$

For low-rise non-rigid buildings the critical state is that of an idealized least favourable state, when the load acting on the examined foundation is the maximum q_I (for example permanent and live load) and the load on the adjacent foundation is the minimum q_{II} (permanent load only). For higher buildings it is possible to assume for the adjacent foundation a load larger than q_{II} , but not the full load for this foundation, as in higher buildings it is probable that at least on some of the floors above the adjacent foundation there will be some live load. Apart from that, in higher buildings the load is also transferred by the structure to those foundations which do not carry the full load directly. The static engineer decides in what proportion and for which of the foundations the live load must be taken into account, depending on the character of the load, the type of the structure and on the way in which it interacts with the subgrade. For very rigid and very tall buildings it can be assumed that all foundations carry the same portion of the permanent and live load. In such a case, for the determination of the ultimate bearing capacity, the reduction according to equation (2.89) need not be made and therefore $q_{mI} = \overline{q_{mI}}$.

A more general case than that of two interacting adjacent foundations is where we have three interacting foundations. In order to determine the relationships, loading tests were made in the same way and with the same equipment as was developed for the testing of the bearing value of foundations in a pair.

This equipment on the one hand enabled the measurement of the sum of the bearing values of foundations I + II and their settlement, and on the other hand the bearing value of foundation III and its settlement.

Tests were made first of all with three foundations of the same width and an equal foundation depth. The arrangement of the tests is apparent from Fig. 2.23. When the separation of foundations was the same $S = 2B$, bearing values $(Q_{mI} + Q_{mII}) \doteq 2 Q_{mIII}$ were measured. The bearing value of all three foundations was almost the same as that of each of the foundations in a pair with equal separation S/B . When the separations of the foundations were unequal,

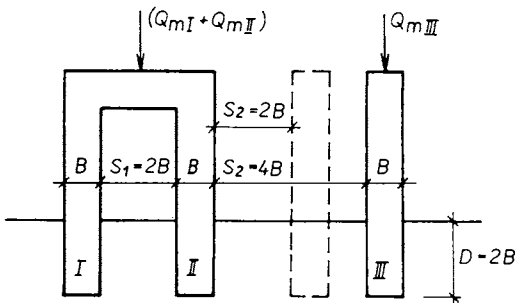


Fig. 2.23 A tested group of three foundations for $D_I = D_{II} = D_{III}$

$S_1 = 2B$ and $S_2 = 4B$, then, for the central foundation, the interaction with foundation I, which was nearer, was critical. The bearing value of the considered foundations was the same as for a group of two foundations with a clearance between the foundations of S_1 . The more distant foundation III had almost the same bearing value as if it had been paired with foundation II with a clearance of S_2 , but the settlement of foundation III, when the ultimate bearing capacity was reached, was noticeably greater.

As the next step, tests were made with foundations of the same width and having a separation of $S_1 = S_2 = 2B$. The foundation depth of the first two foundations was $D_I = D_{II} = 2B$ (Fig. 2.24). When foundation III was located on the surface, the bearing value of foundations I + II was approximately 8% lower than their value uninfluenced by foundation III. This would seem to suggest an influence of foundation III, although it is not very conclusive owing to the dispersion of the model test results. The bearing value of foundation III was the same as if it had been interacting with foundation II alone. When the foundation depth of foundation III was $4B$, its bearing value was also the same as when interacting with foundation II, but the cumulative bearing value of foundations I + II was again significantly smaller. Calculations established that the measured bearing value of the pair of foundations I + II corresponds to the calculated bearing value if the bearing value of foundation I is assumed to be interacting with foundation II alone. The bearing value of

Foundation II is taken as the mean value of the bearing values determined for its interaction with foundation I and with foundation III.

Finally, similar tests were made, but with the difference that the separation of foundations II and III was only $S_2 = B$. When foundation III was on the surface it had almost the same bearing value as when interacting with foundation II alone, i.e. it was smaller than for the test described above. The bearing value of the pair of foundations I + II was not decreased in this case. However, we should note that the values of factors α_γ and α_q for foundation II are almost the same both for its interaction with foundation I alone, as with foundation III alone. Therefore it can be assumed that the bearing value of foundation I can be calculated from a consideration of the interaction with foundation II alone,

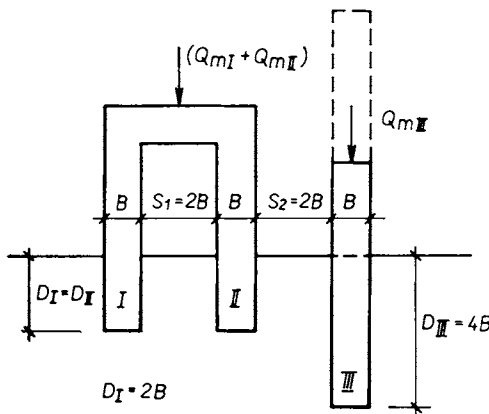


Fig. 2.24 A tested group of three foundations for $D_I = D_{II} \neq D_{III}$

and the bearing value of foundation II can be then determined either from the influence of foundation III alone or it can be taken as the mean value of the bearing values determined for the interaction with foundations I and III. When foundation III had a foundation depth $D_{III} = 4B$, its bearing value was the same as when it interacted with foundation II alone. The bearing value of the pair of foundations I + II was smaller than in the case described earlier (for $S_2 = 2B$). The measured bearing value was determined mathematically when the interaction of foundation II with foundation III was taken into account, and when the ultimate bearing capacity of foundation I was determined for an interaction with foundation II, which had a smaller load as a result of the influence of foundation III (reduction according to equation (2.89)).

These tests showed that foundations in a group interact with that foundation which has a stronger influence, usually a foundation which is nearer (S/B is smaller), if the difference between the depths of foundation is not too great. When the reduced separation S/B of the foundations is the same, the inner

foundation is influenced by both adjacent foundations, and its bearing value can be determined as the mean of the bearing values calculated for successive interacting pairs of foundations. In a group of foundations we can find that one foundation decreases the ultimate bearing capacity of the second foundation, which then has a smaller bearing value than it would have if it were interacting with another, third foundation alone. The bearing value of the third foundation must be reduced as a result of the smaller bearing value of the second foundation, which is caused by the first foundation. Thus the first foundation can influence not only the adjacent foundation but also the next one.

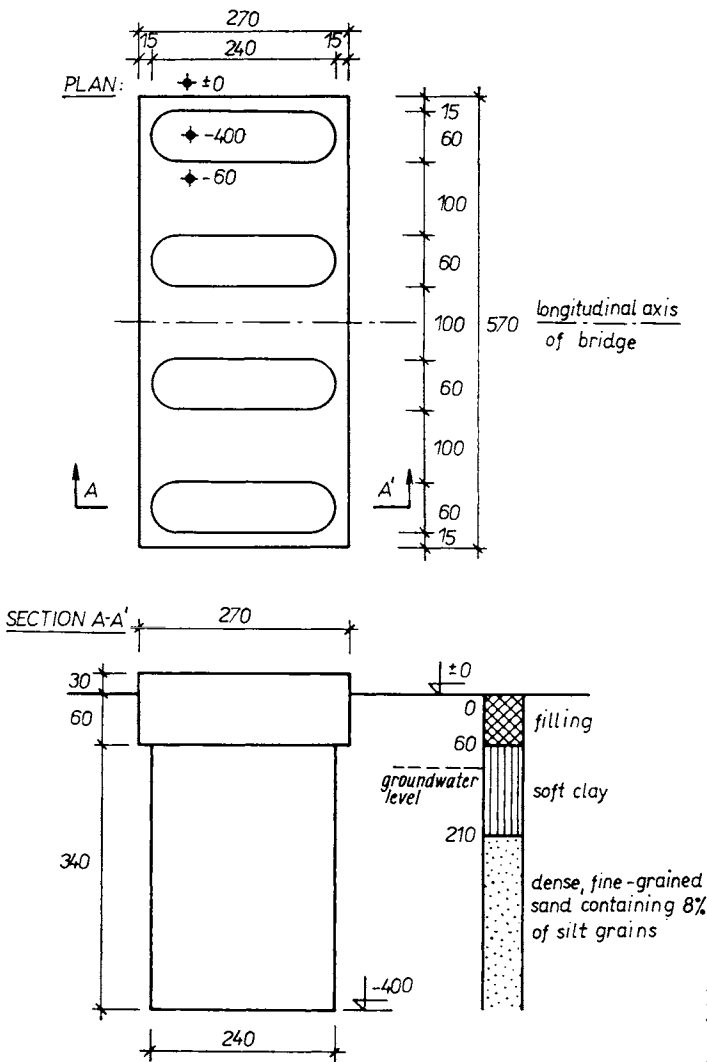


Fig. 2.25
The foundation
in Example 2.1

The results of the model tests were mathematically formulated and verified by several field loading tests. The bearing values of foundations, determined mathematically, were in good agreement with the test results:

Example 2.1

For the transportation of ore, conveyor belts in steel bridge structures are used. The longitudinal forces in the bridge elements are taken over by four towers: 1 driving, 2 tensioning and 1 reversible. Between these the bridge structure is carried by swinging supports, which have a foundation as shown in Fig. 2.25. The steel supports act on the foundation with a maximum vertical force of 1 540 kN (the permanent load is 1 220 kN). Wind produces a horizontal force of ± 97 kN and a moment of $\pm 1 060$ kNm in a direction at right angles to the axis of the bridge. All the forces act on the upper surface of the reinforced concrete slab having dimensions of 2.7×5.7 m and a thickness of 0.9 m, which transfers them to four underground walls with a profile of 0.6×2.4 m. The foundation depth is 4 m. On the site there is a filling to a depth of 0.6 m. To a depth of 2.1 m there is a soft, non-bearing clay and lower down there is a compact, very fine grain sand with a 8% proportion of silt grains. The groundwater level is 0.9 m below the surface. The sand has an angle of internal shearing resistance $\Phi'_f = 26^\circ$ and a density $\gamma = 20$ kN/m³.

As a result of its ability to yield, the bridge structure is not sensitive to differences in settlement. As a result it is sufficient to judge the foundation only from the point of view of safety against sinking. To do this we only consider the bearing value of the underground walls at their foundation lines at a level of -4 m. The skin friction in soft clay is negligible and if we omit its effect the calculation is simplified and we get a slightly safer result. We cannot reckon with the interaction of the upper, load distributing slab, because of the great compressibility of the soft clay.

The actual weight of the foundation:

slab	$2.7 \times 5.7 \times 0.9 \times 25$	350 kN
piles	$2.4 \times 0.6 \times 3.4 \times 2.5 \times 4$	490 kN
— lifting	(hydrostatic)	
force	$2.4 \times 0.6 \times 3.1 \times 10 \times 4$	-180 kN
		660 kN

The original weight of the soil in the space of the foundation:

slab	$2.7 \times 5.7 \times 0.6 \times 20$	185 kN
piles	$2.4 \times 0.6 \times 3.4 \times 20 \times 4$	395 kN
— lifting	(hydrostatic)	
force	$2.4 \times 0.6 \times 3.1 \times 10 \times 4$	-180 kN
		400 kN

Load increment in foundation line at a level of -4.0 m:

actual weight of foundation (660 — 400)	260 kN
vertical load from upper part of building	1 540 kN
	1 800 kN

The horizontal force $H = 97$ kN is reliably taken up by the pressure and friction of the soil on the narrow front face and sides of the underground walls. The following is valid: $H/Q = 97/1800 = 0.054$. The bending moment $M = \pm 1060$ kNm corresponds to an eccentricity

$e = M/Q = 1\,060/1\,800 = 0.59$ m. For a coincident action of moment M and load Q , the effective length of the foundation is $5.7 - 2e \doteq 4.5$ m. This means that the whole load is taken up by just the three outer piles, and we make a simplifying assumption that the piles are loaded almost in the same way. Therefore it is not necessary to take into account the reduction of the ultimate bearing capacity caused by the unequal utilization of adjacent foundations. The ultimate bearing capacity of each of the three active piles, according to equation (2.66), is

$$q_m = 0.5\gamma_1 B_1 N_\gamma s_\gamma d_\gamma i_\gamma \alpha_\gamma + \gamma_2 D N_q s_q d_q i_q \alpha_q$$

if

$$\begin{aligned} \gamma_1 &= 10 \text{ kN/m}^3 & \gamma_2 &= (4 \cdot 10 + 0.9 \cdot 10)/4 = 12.2 \text{ kN/m}^3 \\ B &= B_1 = 0.6 \text{ m} & D &= D_1 = 4.0 \text{ m} \\ N_\gamma &= 10.0 \text{ (Table 2.9)} & L &= 2.4 \text{ m} \\ N_q &= 12.4 \text{ (Table 2.9)} & B/L &= 0.6/2.4 = 0.25 \\ s_\gamma &= 0.97 \text{ (Fig. 2.11)} & D/B &= 4.0/0.6 = 6.7 \\ s_q &= 1.06 \text{ (Fig. 2.12)} & H/Q &= 97/1800 = 0.054 \\ d_q &= d_c = 1.64 \text{ (Fig. 2.13)} & B_I/B_{II} &= 1 : 1 \\ d_\gamma &= 1 \text{ (equation (2.52))} & S &= 1.0 \text{ m} \\ i_q &= 0.92 \text{ (Fig. 2.14)} & S/B &= 1/0.6 = 1.66 \\ i_\gamma &= i_q^2 = 0.84 \text{ (equation (2.56))} \end{aligned}$$

The foundations have the same depth of foundation, therefore $f(D_I - D_{II}) = 0$. From the tables in the supplement in group $B_I/B_{II} = 1 : 1$ (for $\Phi = 25^\circ$; $\Phi = 30^\circ$ and $S/B = 1.5$; $S/B = 2.0$) we obtain, using linear interpolation factors

$$\alpha_\gamma = 2.09 \quad \alpha_q = 1.11$$

The ultimate bearing capacity of the foundation

$$\begin{aligned} q_m &= 0.5 \cdot 10 \cdot 0.6 \cdot 10.0 \cdot 0.97 \cdot 1 \cdot 0.84 \cdot 2.09 + 12.2 \cdot 4.0 \cdot 12.4 \cdot 1.06 \cdot 1.64 \cdot 0.92 \cdot 1.11 \\ &= 50 + 1\,070 = 1\,120 \text{ kN/m}^2 \end{aligned}$$

The real load at the foundation line is

$$q = 1\,800(3 \cdot 2.4 \cdot 0.6) = 420 \text{ kN/m}^2$$

The safety factor is

$$F = q_m/q = 1\,120/420 = 2.66$$

This value is quite sufficient and consistent with the geological composition of the foundation soil.

The calculation, which took into account the influence of the adjacent foundations, showed a possible load $q_k = q_m/2.5 = 450 \text{ kN/m}^2$.

Example 2.2

Consider a project for a four-floor warehouse and a five-floor office block. The structure consists of reinforced concrete frames. The columns have a modular grid of 6×6 m and they rest on 9 lateral footings forming a strip foundation each with a length of 14.2 m. The facade of the whole object, which has a flat roof, is arranged uniformly using glass and steel profiles.

The longitudinal section of the whole structure is described by the diagram in Fig. 2.26. On the site there is a filling 80 cm high and below that there is a solid silty loam. The ground-water level is at a depth of 9.5 m. The silty loam has an angle of internal shearing resistance $\Phi = 27.5^\circ$, a cohesion $c = 5 \text{ kN/m}^2$ and a density $\gamma = 21 \text{ kN/m}^3$. The continuous footings bear different loads and therefore have been designed to have different widths. Data concerning the loading of the footings, their widths and calculated settlement are given in Table 2.17. The proposed foundations must be considered from the point of view of their settlement and their safety against sinking.

The calculated values of settlement are permissible. The difference in the settlement of footings I to VI and VII to IX are also within the permissible limits. The large difference between the settlement of footing VI and VII does not matter, as the relative displacement of both parts of the building can be allowed for in the dividing joint. As we can assume that when settlement ceases, footing VII will settle by about 0.3 cm more than footing IX, which is 12 m distant, the office block will lean over a little towards the warehouse and the dividing joint at roof level will close by about 0.5 cm. Therefore the dividing joint must be at least 0.5 cm wider than if it were to act only as a dilatation joint. If, when settlement ceases, the floors on the first floor and the roofs of both parts of the building are to be on the same level, then the whole warehouse part which is heavier and has a greater settlement must be built on a level which is 2 cm higher. To start with the roof of the warehouse part will be higher by 2 cm than the roof over the office block, but as the subgrade consolidates, the difference will disappear. As far as settlement is concerned the proposed foundations are satisfactory.

TABLE 2.17

The load, width and settlement of the continuous footings in example 2.2

Continuous footing	The load increment in the foundation line for a				Width of continuous footing [m]	Settlement of continuous footing [cm]
	permanent load		permanent and live load			
	[kN/m]	[kN/m ²]	[kN/m]	[kN/m ²]		
Warehouse						
I	340	226	550	366	1.5	4.0
II	360	225	600	375	1.6	4.3
III	360	225	600	375	1.6	4.3
IV	360	225	600	375	1.6	4.3
V	360	225	600	375	1.6	4.3
VI	310	221	520	372	1.4	3.9
Office block						
VII	230	230	280	288	1.0	2.1
VIII	230	192	290	241	1.2	1.9
IX	210	210	260	260	1.0	1.7

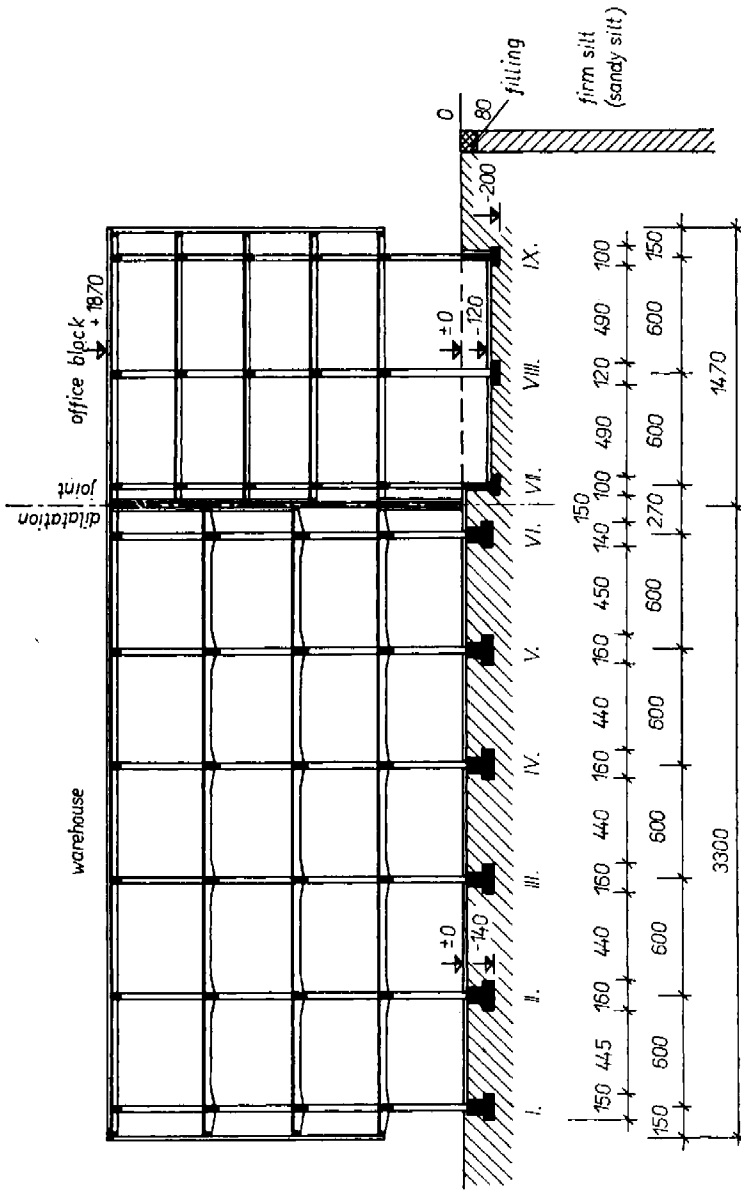


Fig. 2.26 The arrangement of frame cross-beams, joist ceilings and parameter walls of a building founded on transverse strip foundations, where each footing has a length of 14,2 m. The width of the building is 15 m

As the next step we consider the safety against sinking of the continuous footings. Since during usage, there is a live load of variable size in different parts of the low warehouse, we look at an idealized, least favourable state, during which the studied foundation is loaded with the maximum load q_I (both permanent and live load) and the adjacent foundations are loaded with the minimum load q_{II} (permanent load). We assume that the load on all foundations is central and vertical so that in equation (2.66) the factors $i_y = i_q = i_c = 1$. First of all, the ultimate bearing capacity $\overline{q_{mI}}$ of the continuous footings is determined on the assumption that the adjacent footings are also subjected to their ultimate bearing capacity. The ultimate bearing capacity q_{mI}^1 of the footing is also determined as if it were standing separately.

The calculation of $\overline{q_{mI}}$ is made using equation (2.66) and the calculation of q_{mI}^1 using equation (2.44), which is obtained from equation (2.66) for $\alpha_y = \alpha_q = \alpha_c = 1$.

Continuous footing I:

The interaction of continuous footing I with continuous footing II is considered.

$$\begin{array}{ll}
 \gamma_1 = \gamma_2 = 21 \text{ kN/m}^3 & B_I = 1.5 \text{ m} \\
 D = D_I = 1.4 \text{ m} & c = 5 \text{ kN/m}^2 \\
 N_\gamma = 12.12 \text{ (Table 2.9)} & B_I/L = 1.5/15 = 0.1 \\
 N_q = 13.94 \text{ (Table 2.9)} & D_I/B_I = 1.4/1.5 = 0.93 \\
 N_c = 24.85 \text{ (Table 2.9)} & d_y = 1 \text{ (from equation (2.52))} \\
 s_\gamma = 0.99 \text{ (Fig. 2.11)} & d_q = 1.21 \text{ (Fig. 2.13)} \\
 s_q = 1.02 \text{ (Fig. 2.12)} & d_c = 1.21 \text{ (Fig. 2.13)} \\
 s_c = 1.02 \text{ (Fig. 2.12)} &
 \end{array}$$

Determination of coefficients of cooperation α_y, α_q :

$$\begin{array}{ll}
 D_I = D_{II} = 1.4 \text{ m} & \Delta D = 0 \\
 f(D_I - D_{II}) = 0, \text{ as } \Delta D = 0 & B_I/B_{II} = 1.5/1.6 = 0.94 \\
 S = 4.45 \text{ m} & S/B = 2.87
 \end{array}$$

By linear interpolation according to the tables in the supplement for $\Phi = 27.5^\circ$ we find that coefficient $\alpha_y = 1.55$. That means that the term expressing the influence of the width of the foundation is increased by 55 % as a result of interaction, which cannot be neglected.

By substitution into equation (2.66) we get:

$$\begin{aligned}
 \overline{q_{mI}} &= 0.5 \cdot 21 \cdot 1.5 \cdot 12 \cdot 0.99 \cdot 1 \cdot 1 \cdot 1.55 + 21 \cdot 1.4 \cdot 13.94 \cdot 1.02 \cdot 1.21 \cdot 1 \cdot 1 + \\
 &+ 5 \cdot 24.85 \cdot 1.02 \cdot 1.21 \cdot 1 \cdot 1 = 293 + 507 + 154 = 954 \text{ kN/m}^2 \\
 q_{mI}^1 &= 188 + 507 + 154 = 849 \text{ kN/m}^2
 \end{aligned}$$

Continuous footing II:

The axial separations of continuous footings I, II and III are the same. Continuous footing I is narrower than continuous footing III and therefore causes a smaller increase of the ultimate bearing capacity of continuous footing II than continuous footing III. The ultimate bearing capacity of continuous footing II is determined while considering the influence of continuous footing I. The results were:

$$\begin{aligned}
 {}^{II}q_{mI} &= 978 \text{ kN/m}^2 \\
 {}^{II}q_{mI}^1 &= 857 \text{ kN/m}^2
 \end{aligned}$$

Continuous footings III and IV:

The mutual interaction of the two continuous footings is considered. As they are the same, their ultimate bearing capacities are also the same:

$$\begin{aligned} \text{III} \bar{q}_{m1} &= \text{IV} \bar{q}_{m1} = 978 \text{ kN/m}^2 \\ \text{III} q_{m1}^1 &= \text{IV} q_{m1}^1 = 857 \text{ kN/m}^2 \end{aligned}$$

Continuous footing V:

The axial distances of continuous footings IV, V and VI are the same. Continuous footing VI is narrower than continuous footing IV and therefore causes a smaller increase of the ultimate bearing capacity of continuous footing V. The ultimate bearing capacity of continuous footing V is determined while considering the influence of continuous footing VI.

$$\begin{aligned} \text{V} \bar{q}_{m1} &= 958 \text{ kN/m}^2 \\ \text{V} q_{m1}^1 &= 857 \text{ kN/m}^2 \end{aligned}$$

Continuous footing VI:

Continuous footing VII is much nearer to continuous footing VI than continuous footing V. Therefore during the determination of the ultimate capacity of continuous footing VI we consider the influence of continuous footing VII.

$$\begin{aligned} \text{VI} \bar{q}_{m1} &= 1002 \text{ kN/m}^2 \\ \text{VI} q_{m1}^1 &= 844 \text{ kN/m}^2 \end{aligned}$$

Continuous footing VII:

Continuous footing VI is much nearer to continuous footing VII than continuous footing VIII. Therefore the interaction of continuous footing VI is critical and the ultimate bearing capacity of continuous footing VII is calculated while considering the influence of continuous footing VI.

$$\begin{aligned} \text{VII} \bar{q}_{m1} &= 780 \text{ kN/m}^2 \\ \text{VII} q_{m1}^1 &= 575 \text{ kN/m}^2 \end{aligned}$$

Continuous footing VIII:

The axial separations of continuous footings VII, VIII and IX are the same and continuous footings VII and IX also have the same width. As the permanent load of continuous footing IX is smaller than the load of continuous footing VII, the influence of continuous footing IX is considered when determining the ultimate bearing capacity of continuous footing VIII. This procedure is on the safe side when compared with a more accurate calculation, where the mean values determined for the interaction with both foundations would be considered. The result of the more accurate calculation is similar but the calculation is more time-consuming.

$$\begin{aligned} \text{VIII} \bar{q}_{m1} &= 592 \text{ kN/m}^2 \\ \text{VIII} q_{m1}^1 &= 583 \text{ kN/m}^2 \end{aligned}$$

Continuous footing IX:

The ultimate bearing capacity of continuous footing IX is determined, while considering the influence of foundation VIII.

$$\begin{aligned} \text{IX} \bar{q}_{m1} &= 585 \text{ kN/m}^2 \\ \text{IX} q_{m1}^1 &= 572 \text{ kN/m}^2 \end{aligned}$$

The ultimate bearing capacity q_{mI} of each continuous footing, while influenced by the critical adjacent continuous footing, which exerts a load q_{II} , is calculated according to equation (2.89). The values necessary for the calculation of q_{mI} , established by the previous calculations and the definition of the task, are arranged in Table 2.18.

TABLE 2.18

The values substituted in equation (2.89) for the calculation of q_{mI} of the individual continuous footings

Foundation I	$\overline{q_{mI}}$ kN/m ²	q_{mI}^1 kN/m ²	q_I kN/m ²	Foundation II whose inter- action is considered when determining $\overline{q_{mI}}$	$\overline{q_{mII}}$ kN/m ²	q_{II} kN/m ²
I	954	849	366	II	978	225
II	978	857	375	I	952	226
III	978	857	375	IV	978	226
IV	978	857	375	III	978	225
V	958	857	375	VI	1 002	221
VI	1 002	844	372	VII	780	230
VII	780	572	280	VI	1 002	221
VIII	592	583	241	IX	585	210
IX	585	572	260	VIII	592	192

If we substitute the values from Table 2.19 into equation (2.89), we get the following:

$$I q_{mI} = (954 - 849) \frac{225 \cdot 954}{366 \cdot 978} + 849 = 942 \text{ kN/m}^2.$$

and similarly

$$II q_{mI} = 932 \text{ kN/m}^2$$

$$VI q_{mI} = 969 \text{ kN/m}^2$$

$$III q_{mI} = 930 \text{ kN/m}^2$$

$$VII q_{mI} = 668 \text{ kN/m}^2$$

$$IV q_{mI} = 930 \text{ kN/m}^2$$

$$VIII q_{mI} = 591 \text{ kN/m}^2$$

$$V q_{mI} = 914 \text{ kN/m}^2$$

$$IX q_{mI} = 581 \text{ kN/m}^2$$

As the last step, the safety factor F of the individual continuous footings against sinking is determined according to the relationship

$$F = q_{mI}/q_I$$

The calculated values are given in Table 2.19. The safety factor of all the foundations is satisfactory.

Table 2.19

The safety factors of the individual continuous footings against sinking

Foundation I	q_{mI} [kN/m ²] ultimate bearing capacity	q_I [kN/m ²] Maximum true load	F [1] Safety factor
I	942	366	2.57
II	932	375	2.43
III	930	375	2.52
IV	930	375	2.52
V	914	375	2.44
VI	969	372	2.60
VII	668	280	2.39
VIII	591	241	2.45
IX	581	260	2.24

Example 2.3

A reinforced concrete chimney stack with a height of 74 m and an inner lining reaching to a height of 30 m has a weight of 10 800 kN. The horizontal force caused by the loading of the chimney stack by wind $H = 430$ kN acts at a height of 31 m above the ground. The base of the stack with ash filters is circular with a diameter of 8.8 m. It rests on a foundation which

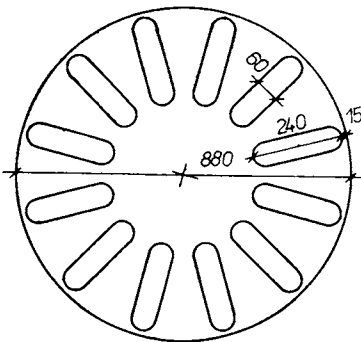


Fig. 2.27 Plan of foundation for chimney stack

consists of twelve radially arranged underground walls (Fig. 2.27). These have a profile of 2.4×0.6 m and reach to a depth of 5 m below the ground surface. On the site the soil is sand combined with loess to a depth of 4 m. Below to a depth of 4 m are fine-grained sands with a 5 % addition of silt reaching to a depth of 18 m. Under these is marl. The ground-water level is 1 m below the surface. The effective angle of internal shearing resistance of the sand is $\Phi'_f = 32.5^\circ$, its density $\gamma = 20$ kN/m³, $E = 38000$ kN/m² for a load of 1 000 kN/m², $\nu = 0.33$.

The inherent weight of the underground walls	$12 \cdot 2.4 \cdot 0.6 \cdot 5 \cdot 25$	2 160 kN
Upward hydrostatic pressure	$-12 \cdot 2.4 \cdot 0.6 \cdot 4 \cdot 10$	-690 kN
		1 470 kN
The original weight of the soil in the space of the underground walls	$12 \cdot 2.4 \cdot 0.6 \cdot 5 \cdot 20$	1 730 kN
Upward hydrostatic pressure		-690 kN
		1 040 kN
The load increment at the foundation surface at a level — 5.0 m:		
From the inherent weight of the foundation		1 470 kN
From the vertical load of the upper part of the building		10 800 kN
		12 270 kN

$$Q = 12\,270 \text{ kN}$$

The horizontal force $H = 430 \text{ kN}$ produces, at the level of the foundation line, a moment $M = 430(31 + 5) = 1\,550 \text{ kNm}$. The horizontal shear force is transferred into the soil by all twelve underground walls: the part carried by each is very small, approximately 36 kN, which is safely taken by the friction of the soil on the sides of the underground walls. The bending moment $M = 15\,500 \text{ kNm}$, corresponds to an eccentricity $e = M/Q = 15\,500/12\,270 = 1.26 \text{ m}$. For the effective diameter of the foundation of 8.5 m, the largest permissible eccentricity $e_{\max} = 8.5 : 3 = 2.84 \text{ m}$.

The effect of the moment on the load on the foundation surfaces of the underground walls can be approximately determined by replacing them with an annular-form foundation surface with diameters 8.5 and 3.7 m. The area of the annulus is

$$A = \pi(4.25^2 - 1.85^2) = 46 \text{ m}^2$$

$$\text{The section modulus } W = \frac{\pi(8.5^4 - 3.7^4)}{32 \cdot 8.5} = 58 \text{ m}^3$$

The load increment on the edges $\bar{\sigma} = M/W = 15\,500/58 = 271 \text{ kN/m}^2$.

The mean vertical stress on the annulus $\bar{\sigma} = Q/A = 12\,270/46 = 267 \text{ kN/m}^2$

The maximum stress on the lee side will have a value

$$\sigma = \bar{\sigma} + \sigma = 538 \text{ kN/m}^2$$

The load concentrated on the most-loaded foundation surface of a pile will be approximately $A \cdot \sigma/12 = 2\,060 \text{ kN}$. In the foundation line of the underground wall, there is a mean stress q_1 determined by an approximate calculation

$$q_1 = 2\,060/(2.4 \cdot 0.6) = 1\,435 \text{ kN/m}^2$$

As the underground walls are near to each other, the load on two adjacent walls will be only a little different and therefore it is not necessary to consider the reduction of the ultimate bearing capacity with a view to the unequal utilization of the bearing value of adjacent foundations. The ultimate bearing capacity is calculated from equation (2.66)

$$\gamma_1 = 10 \text{ kN/m}^3 \text{ (groundwater influence)}$$

$$\gamma_2 = (5.0 \cdot 10 + 1 \cdot 10)/5 = 12 \text{ kN/m}^3$$

$$B = 0.6 \text{ m}$$

$$D = 5.0 \text{ m}$$

$$N_y = 27.04 \text{ (Table 2.9)}$$

$$L = 2.4 \text{ m}$$

$$\begin{array}{ll}
 N_q = 24.58 \text{ (Table 2.9)} & B/L = 0.6/2.4 = 0.25 \\
 s_y = 0.97 \text{ (Fig. 2.11)} & D/B = 5/0.6 = 8.3 \\
 s_q = 1.06 \text{ (Fig. 2.12)} & H/Q = 43/1123 = 0.038 \\
 d_y = 1.00 \text{ (Equation (2.52))} & B_I/B_{II} = 1/1 \\
 d_q = 1.90 \text{ (Fig. 2.13)} & S = 1.0 \text{ m} \\
 i_q = 0.95 \text{ (Fig. 2.14)} & S/B = 1/0.6 = 1.66 \\
 i_y = i_q^2 = 0.9 \text{ (Equation 2.56)} &
 \end{array}$$

The foundations have the same foundation depth, therefore $f(D_I - D_{II}) = 0$. By linear interpolation from the tables in the supplement, we get factors

$$\alpha_y = 2.35 \quad \alpha_q = 1.25$$

This means that the influence of the width of the foundation, if we consider interaction, is larger by 135 % and the influence of the depth of foundation is larger by 135 % and the influence of the depth of foundation is larger by 25 %. By substitution into equation (2.66) we get:

$$\begin{aligned}
 \overline{q_{m1}} = q_{m1} &= 0.5 \cdot 10 \cdot 0.6 \cdot 27.04 \cdot 0.97 \cdot 1 \cdot 0.9 \cdot 2.35 + 12 \cdot 5 \cdot 24.58 \cdot 1.06 \cdot 1.9 \cdot 0.95 \cdot 1.29 = \\
 &= 167 + 3520 = 3687 \text{ kN/m}^2
 \end{aligned}$$

The safety factor

$$F = q_{m1}/q_1 = 3687/1435 = 2.57$$

which is a satisfactory value. In the foundation line of the underground walls it is permissible to have a load

$$q_p = 3687/2.5 = 1450 \text{ kN/m}^2$$

We shall calculate the settlement of the chimney stack as the compression of sand below the level of the piles and we shall consider the foundation, which consists of piles with a rectangular section, as if it were a full foundation in annular form.

According to Boussinesq, the settlement caused by the loading of a non-rigid circular surface is (for $Q' = Q - 1040 = 11230 \text{ kN}$)

$$s_0 = (1 - \nu^2) \frac{2Q'}{\pi RE} = (1 - 0.33^2) \frac{2 \cdot 11230}{\pi \cdot 4.25 \cdot 38000} = 0.039 \text{ m} \quad \text{i.e. } 3.9 \text{ cm}$$

The settlement of the outer rim of the annular surface is, according to K. Fischer, $s = s_0 \cdot f(\varrho)$; the inner diameter of the annulus

$$r = \frac{8.5 - 4.8}{2} = \frac{3.7 \text{ m}}{2}, \quad \text{so that} \quad \varrho = \frac{2r}{2R} = \frac{3.7}{8.5} = 0.43.$$

The function

$$f(\varrho) = \frac{2}{\pi} - \frac{1}{2} \varrho^2 \left[1 + \frac{1}{8} \varrho^2 + \frac{3}{64} \varrho^4 + \frac{25}{1064} \varrho^6 + \dots \right] \doteq 0.54$$

The settlement of the outer rim of the annular-shaped foundation will be $3.9 \cdot 0.54 = 2.1 \text{ cm}$. The annular pile foundation was considered as a full foundation and therefore the anticipated settlement will be a little larger.

2.5 INFLUENCE OF FOUNDATION CROSS-SECTION

The cross-sections of foundations have various forms; usually the vertical cross-section of a foundation is rectangular. When an open trench is made, the walls are not made perpendicular, therefore the foundation has a conical shape in cross-section – at the bottom and the contact surface, it is narrower than at the top. Foundations of this kind are often found in mediaeval buildings as the pit was made without sheeting and with manual excavation. Nowadays foundations are formed by reinforced concrete slabs with foundation masonry above. We shall see if the transverse shape of the foundation influences the ultimate bearing capacity.

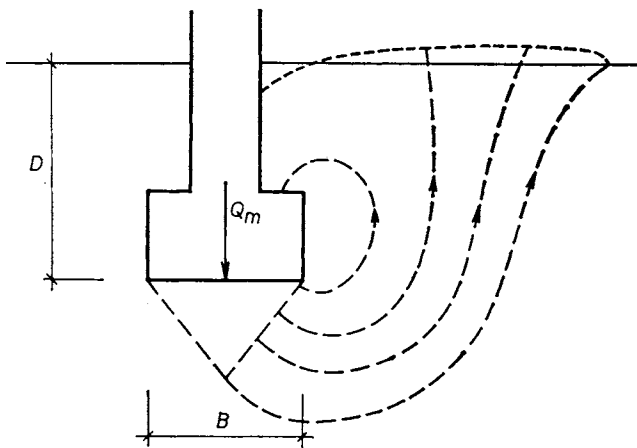


Fig. 2.28 Rupture ranges for a foundation in the shape of an inverted T

The influence of the transverse shape of the foundation on the magnitude of the ultimate bearing capacity of the soil was studied experimentally by Myslivec and Vaníček (1970). They compared the ultimate bearing capacity of a strip foundation with a rectangular section and a height-to-width ratio $D : B = 1.5$ with the ultimate bearing capacity of foundations with various sectional shapes. During all the tests, the same depth of foundation D and the same width of the foundation line B was maintained. The angle of internal shearing resistance of the sand during the tests was $\phi'_f = 37^\circ$.

When the foundation rested on a strip and therefore had a shape of an inverted T (Fig. 2.28), a decrement of the ultimate bearing capacity of about 5 %, compared to the ultimate bearing capacity of about 5 %, compared to the ultimate bearing capacity of a foundation with a total height D and a width B was measured. The decrement of the ultimate bearing capacity resulted from the displacement of the soil from the space beneath the foundation, along the

shorter sliding surfaces, to above the foundation, where a space was created as the foundation was forced in. Only part of the soil was displaced to the surface. The trajectories of the movement of the grains are marked by a dash line in Fig. 2.28. This small decrement of the bearing value is almost insignificant. If one considers that the density of the soil is smaller than the density of concrete then it becomes obvious that especially for deeper foundations the insignificant decrement of the ultimate bearing capacity in the foundation line is equalled by the smaller load increment of the lighter foundation with the inverted T shape.

Next, the influence of the conical shape of foundations, tapering upwards or downwards was determined. It was found that the ultimate bearing capacity of those foundations depends only on the contact width of the foundation

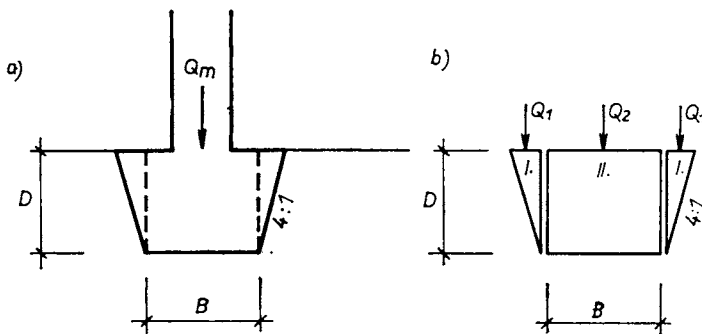


Fig. 2.29 Cross-section of a conical foundation

surface. The inclined sides of foundations with a contact width B , which widen upwards, were found to be without influence on the ultimate bearing capacity if their gradient was greater than 4 : 1 (Fig. 2.29a). This means that when concreting foundations in open trenches it is imperative to maintain not only the depth of foundation D but also the contact width of the foundation at the bottom of the trench which is most important in the calculation of the ultimate bearing capacity.

The result described is also important from the point of view of judging the interaction of adjacent foundations. It has been established by measurement that a separately standing foundation with a rectangular cross-section $D \times B$, as shown in Fig. 2.29a by a dash line, has an ultimate load Q_m during loading. A foundation which widens upwards, also has an ultimate load Q_m of the same size, also shown in the illustration. Let us now assume that the foundation is composed, according to Fig. 2.29b, of three parts and for each of these the force necessary to sink it in is measured. It follows that

$$2Q_1 + Q_2 = Q_m \quad (2.90)$$

Since forces Q_1 and Q_2 are real pressures, the following must be true

$$Q_1 < Q_m \text{ and simultaneously } Q_2 < Q_m$$

As part II of the foundation has the same shape and size as the separately standing comparative foundation with a section $D \times B$ and an ultimate load Q_m , it is obvious that when three foundations interact as shown in Fig. 2.29b, we observe a lowering of the ultimate load of foundation II from the value Q_m to the value Q_2 .

Similar results were also obtained for foundations arranged as in Fig. 2.30. In this case sand was also used, but its angle of internal shearing resistance was $\Phi'_f = 33^\circ$. In this case it was also found that, for the simultaneous sinking

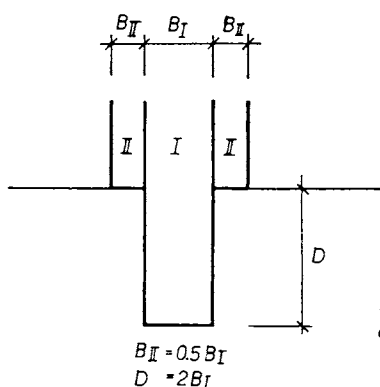


Fig. 2.30 Closely adjacent foundations having different depths of foundation

of all three foundations, a force of almost the same size is necessary as for sinking a separately standing foundation I with a width B_1 , which has a foundation depth $D = 2B_1$. We can assume, that in the case of the three interacting foundations, "wedges" of sand were created beneath foundation II near the walls of foundation I, and these were forced down together with the foundations. In this arrangement, foundation II caused a decrease in the ultimate bearing capacity of foundation I compared with the value when standing separately.

From tests made it follows that when designing foundations with varying levels of the foundation line, it is necessary to make transitions from one foundation level to another at a minimum angle. If it is necessary to have a sudden change, in the foundation level of adjacent parts of the foundations, for example where the part with a basement and the part without a basement meet, then it is necessary to consider the situation as two foundations which are adjacent and influence each other (Sec. 2.1).

2.6.1 Mathematical methods

During the calculation of the ultimate bearing capacity of a foundation influenced by a slope, it is necessary to distinguish the following situations:

- the foundation is on a slope (Fig. 2.31a),
- the foundation is near the upper rim of the slope (Fig. 2.31b),
- the foundation is near the lower rim of the slope (Fig. 2.31c).

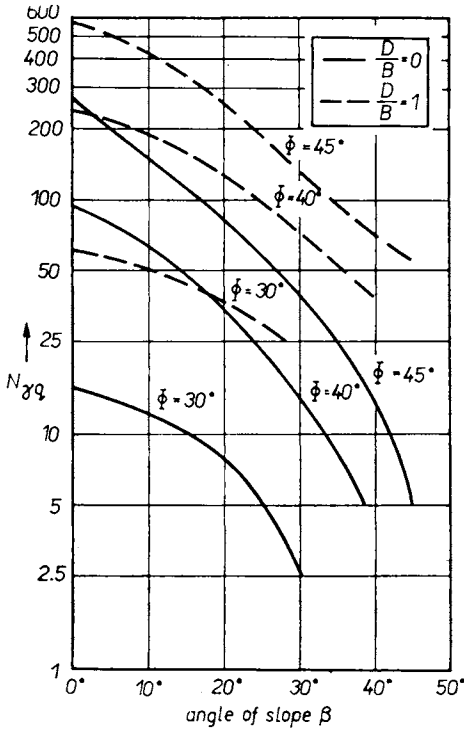


Fig. 2.32 Factor $N_{\gamma q}$ for a foundation on a slope

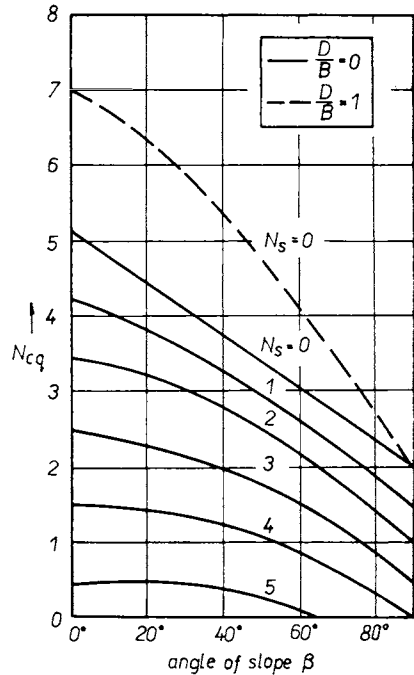


Fig. 2.33 Factor N_{cq} for a foundation on a slope

The calculation of the ultimate bearing capacity of a foundation on a slope was worked out by Meyerhof (1957). For shallow foundations, which have a depth of foundation $D < B$, the ultimate bearing capacity

$$q_m = 0.5\gamma N_{\gamma q} + cN_{cq} \tag{2.91}$$

where $N_{\gamma q}$ and N_{cq} are resultant bearing-value factors. Their values depend on the angle Φ of internal shearing resistance of the soil, on the slope gradient β , on the ratio D/B of the depth of foundation to the width of the foundation and also, for cohesive soils, on the factor $N_s = \gamma d/c$ of the stability of the slope,

where γ is the density of the soil, d is the height of the slope and c is the cohesion of the soil. The value of the bearing value factor $N_{\gamma q}$ is located in the nomogram in Fig. 2.32 and the factor N_{cq} is located in the nomogram in Fig. 2.33.

When the foundation is nearer to the upper rim of the slope in a cohesionless soil ($c = 0$), we also use Meyerhof's equation (2.91) for the calculation of the ultimate bearing capacity of the foundation. However, in comparison with the previous case, the size of the bearing-value factor also depends on the distance b of the foundation from the upper rim of the slope (Fig. 2.31b).

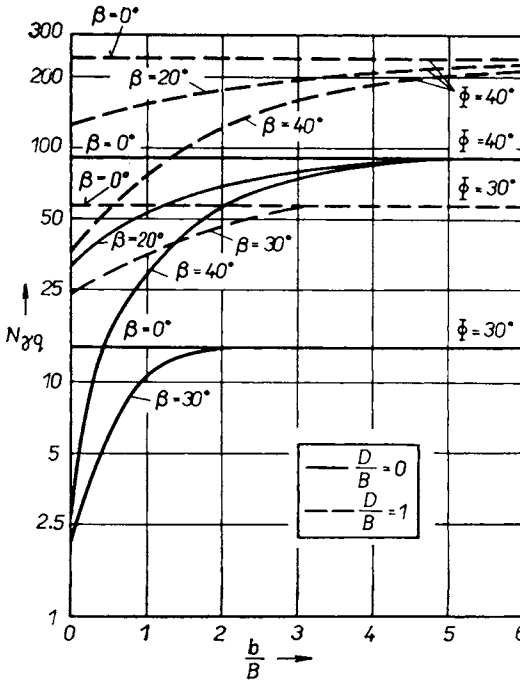


Fig. 2.34 Factor $N_{\gamma q}$ for a foundation on a flat surface near the upper rim of a slope

The bearing-value factor $N_{\gamma q}$ is determined from the nomogram in Fig. 2.34. The intermediate values are determined by linear interpolation.

If the foundation is adjacent to the upper rim of the slope, so that $b = 0$, it is possible to determine the ultimate bearing capacity of the foundation on the surface ($D = 0$) using the basic Meyerhof method, described in Sec. 2.3.2. The angle β , which characterizes the rupture surface (see Fig. 4), is in this case $\bar{\beta} = -\beta$ and for the determination of the ultimate bearing capacity we use equation (2.43). The bearing-value factors N_{γ} and N_c are determined from the nomograms in Fig. 2.7 and 2.9.

If the foundation is nearer to the lower rim of the slope, its ultimate bearing capacity is calculated as though in the vicinity of the foundation, the ground

surface was only horizontal. We can then use, for example, one of the equations given in Sec. 2.3, 2.4. But even in this case it is necessary to evaluate the stability of the slope above the foundation, to avoid the possibility of the slope sliding down and endangering the building. Some slopes are potentially dangerous due to the fact that they are in a state of equilibrium, but as a result of various mechanical and natural processes their safety factor decreases. In a slope, the resulting stress acts upon the horizontal plane at an angle, and can be divided into a vertical stress σ_z and a horizontal stress σ_x . There is also a shearing stress τ , which acts in this plane. When an open trench is made, a deformation of the slope is caused by the action of σ_x and τ . After a displacement of a certain magnitude Δl_{crit} , the peak shearing strength is reached; if the displacement

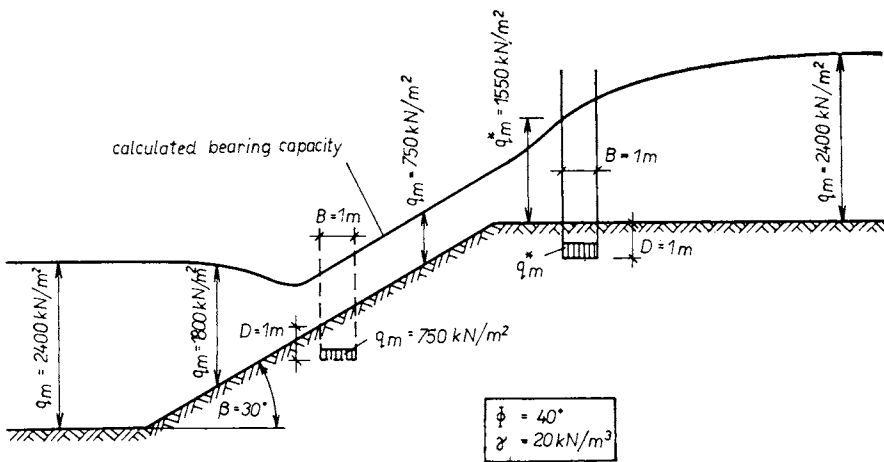


Fig. 2.35 The ultimate bearing capacity of a foundation in various positions on and near a slope

$\Delta l > \Delta l_{crit}$, the shearing strength decreases to a residual value. In a slope, a range is formed where Φ_r is applied on a yield surface, the fissure broadens and in time the slope slides down. As a result of seismic shocks we also find, apart from force effects, changes in the mechanical properties of the soils so that the slope may become unstable.

To clarify the extent and distance to which the slope influences the ultimate bearing capacity of a foundation we present a mathematical solution of a case, where a slope with a gradient $\beta = 30^\circ$ in a sandy soil ($\Phi = 40^\circ$, $\gamma = 20\text{ kN/m}^3$) influences a foundation with a width $B = 1\text{ m}$ and a foundation depth $D = 1\text{ m}$. Various positions of the foundation on the slope, on the surfaces above and below the slope were chosen. The ultimate bearing capacity of the foundation was calculated for each of the chosen positions and these were plotted on a ver-

tical over the slope in Fig. 2.35. The examined foundation, when it is on the slope, has only 1/3 of the bearing value it has when it is on a horizontal surface.

After slope failure the soil assumes a new stable position. During this process the soil is transferred from the original toe of the slope by a distance L_k (Fig. 2.31c). To prevent the instable slope from endangering the building even after slope failure, the distance b of the building from the toe of the slope must be

$$b \geq FL_k \quad (2.92)$$

The magnitude of L_k for a cylindrical failure surface in a cohesive soil was determined by Kysela and Firt (1972), Fig. 2.31c. If the stability of a slope is disturbed (for example as a result of over-loading, interference in the slope, as a result of earthquakes or other natural causes or mechanical influences), a slope failure results. In cohesive soils the loosened part of the slope moves along a yield surface. If it is assumed that the loosened soil moves along a rotary surface with a diameter r for a certain distance beyond the toe of the slope, then during the movement a resultant \bar{N} of centrifugal forces acts at the centre of gravity \bar{O}_m . The value of \bar{N} is

$$\bar{N} = \bar{M}\bar{v}^2/r_M \quad (2.93)$$

where \bar{M} is the total mass of the loosened part of the slope,

r_M is the distance of the centre of gravity \bar{O}_m from the centre \bar{O} of the yield surface.

\bar{v} is the velocity of the movement of the centre of gravity.

Along the yield surface the loosened soil is subjected to the action of tangential forces $\Sigma \bar{T}_{pi}$ and normal forces $\Sigma \bar{N}_i$, which replace in i strips the effect of the weight \bar{Q} of the loosened part of the slope. (Fig. 2.31c). On the yield surface, movement is opposed by tangential forces

$$\Sigma \bar{T}_{pi} = \Sigma \bar{N}_i \tan \Phi_r \text{ and a reaction}$$

$$T = \bar{N} \tan \Phi_r = \bar{M}r_M \left(\frac{d\Theta}{dt} \right)^2 \tan \Phi_r \quad (2.94)$$

Apart from these forces, the loosened soil is subjected to a resultant of inertial forces $M d^2s/dt^2$,¹⁾ whose moment related to the centre \bar{O} of the rotary movement of the soil is

$$\Psi J_0 = (J_M + \bar{M}r_M^2) \frac{d^2\Theta}{dt^2} \quad (2.95)$$

1) The expression d^2s/dt^2 is the acceleration of mass M , which is moving along a trajectory s , shown in Fig. 2.31c.

if Ψ is the rotary acceleration,

J_0, J_M are the polar moments of inertia related to point \bar{O} and the centre of gravity \bar{O}_m of the loosened soil,

Θ is the angle which determines the momentary position of the centre of gravity \bar{O}_m . Prior to the slope movement, $\Theta = 0$.

The moment condition for point \bar{O} has the following form

$$r \Sigma \bar{T}_{ai} - r \Sigma \bar{T}_{pi} - \Psi J_0 - rT = 0 \quad (2.96)$$

We designate

$$Z(\Theta) = \Sigma \bar{T}_{ai} - \Sigma \bar{T}_{pi} \quad (2.97)$$

and for the examined slope we express the given function (2.97) by Lagrange's polynomial of an n -th degree

$$Z(\Theta) = p_0 + p_1\Theta + \dots + p_n\Theta^n \quad (2.98)$$

The coefficients of the polynomial are determined in such a way that the values of function (2.98) are equal to the values obtained from equation (2.97) for various positions of the slope, which are given by the selected values of Θ . In the majority of cases it is sufficient to consider two or three terms of the equation (2.98).

The velocity \bar{v} of the movement of the loosened part of the slope was expressed by a linear differential equation for \bar{v}^2 . The solution of the equation, when assuming the initial conditions of the movement ($\bar{v} = 0$, if $\Theta = 0$) has the following form

$$\bar{v}^2 = \frac{r_M}{\bar{M} \tan \Phi_r} \left[Z(\Theta) - \frac{Z'(\Theta)}{\bar{k}} + \frac{Z''(\Theta)}{\bar{k}^2} - \dots - \frac{Z^{(n)}(\Theta)}{\bar{k}^{(n)}} - \left(p_0 - \frac{1! p_1}{\bar{k}} + \frac{2! p_2}{\bar{k}^2} - \dots - \frac{n! p_n}{\bar{k}^n} \right) e^{-\bar{k}\Theta} \right] \quad (2.99)$$

where

$$\bar{k} = \frac{2\bar{M}r r_M}{J_M + \bar{M}r_M^2} \tan \Phi_r \quad (2.100)$$

The velocity \bar{v}_p of the loosened soil on the yield surface is $\bar{v}_p = \bar{v}r/r_M$. The angle Θ_k , which defines the final position of the centre of gravity of the slipped soil is calculated from equation (2.99) if we take $\bar{v} = 0$. The slope stops at a distance $L_k = r\Theta_k$ measured from the toe of the slope. The slope must therefore move so far that the created resistances are equal to the active forces which put the soil in motion, and that the kinetic energy of the moving soil mass is

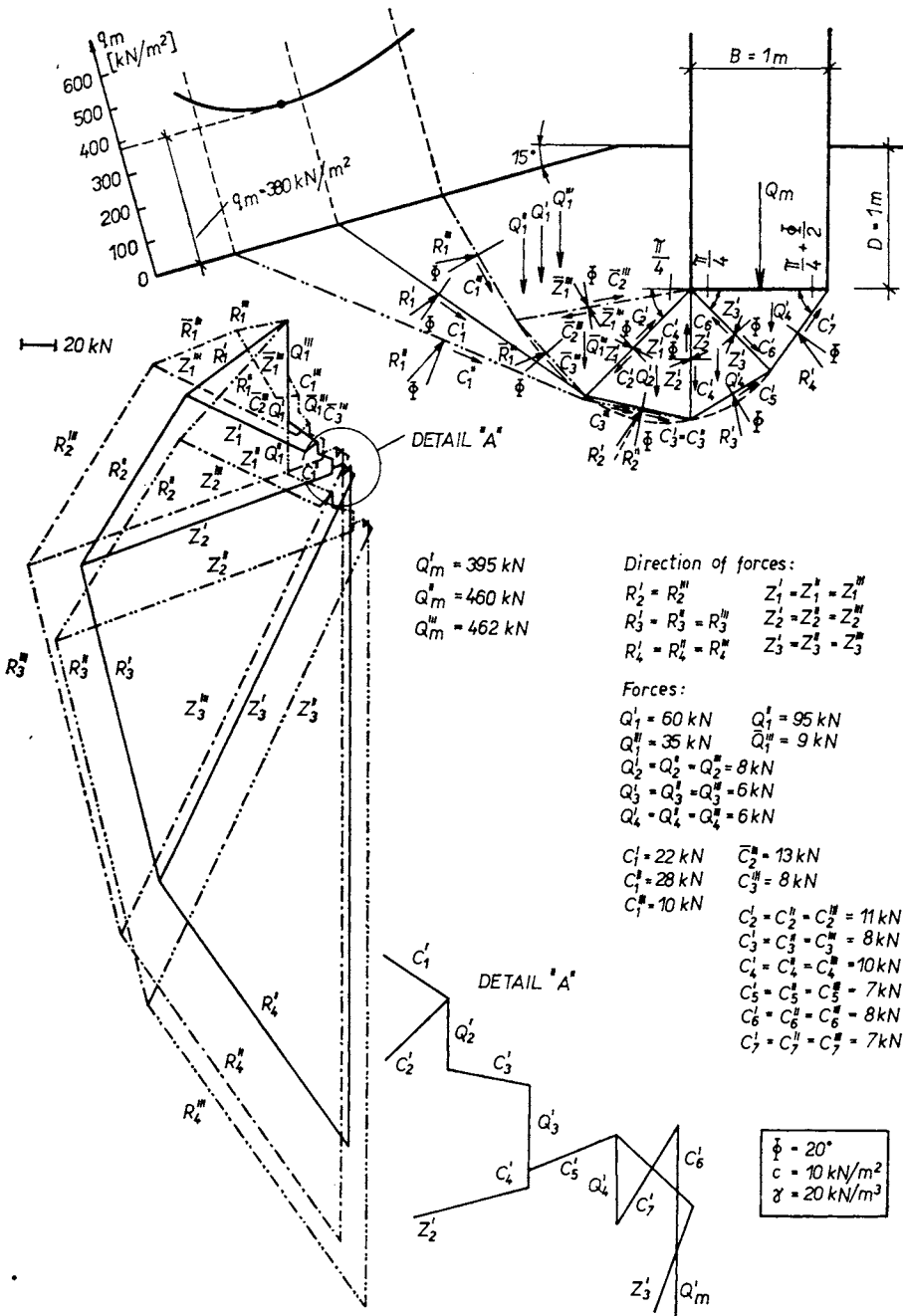


Fig. 2.36 The determination of the ultimate bearing capacity of a foundation influenced by a slope

absorbed. Therefore after slope failure (when the kinetic energy is equal to zero), the safety factor is greater than one; usually $F = 1.1$ to 1.2 . During the process of sliding the soil loosens and its shearing stress decreases.

2.6.2 Graphical method

The ultimate bearing capacity of a foundation influenced by a slope in a cohesionless or cohesive soil can be determined graphically. The procedure is described in Sec. 2.3.5. It is only necessary to locate the position of the planar, outlet part of the yield surface, which is the route of least resistance. Therefore several yield surfaces, which intersect the slope and are joined to the logarithmic spiral tangentially, are selected and for each of them the bearing capacity of the foundation is determined graphically (Fig. 2.36). We assume that the yield surface, which is directly beneath the foundation, is the same as if the surface in the vicinity of the foundation was horizontal.

For each of the outlets of the selected yield surfaces we plot the values of the graphically determined ultimate bearing capacities at right angles to the surface and thus obtain a curve, whose minimum value gives us the size of the ultimate bearing capacity of the foundation and locates the position of the yield surface of least resistance. Along this surface the soil shears when the ultimate bearing capacity is reached. In such a way the rupture surface can be found even if a foundation is lying directly on a slope.

Fig. 2.36 describes the solution of the ultimate capacity of a foundation with a width $B = 1$ and a foundation depth of 1 m, if at a distance $B/2 = 0.5$ m from the face of the foundation there is a ridge from which the ground slopes at an angle of 15° . The subgrade is homogeneous and is formed by a cohesive soil with an angle of internal shearing resistance $\Phi_{uf} = 20^\circ$, a cohesion $c_{uf} = 10$ kN/m² and a density $\gamma = 20$ kN/m³. Three positions of the outlet part of the rupture surface were examined. For these yield surfaces the ultimate bearing capacities are $q'_m = 395$ kN/m², $q''_m = 460$ kN/m² and $q'''_m = 462$ kN/m². These values were connected up by a curve at the outlets of the yield surfaces. The minimum of the curve gave the true value of the ultimate bearing capacity $q_m = 380$ kN/m² of a foundation lying near a slope. If the surface is horizontal the ultimate bearing value of the foundation $q_m = 490$ kN/m². The decrease of the ultimate bearing capacity of the foundation on a slope was in this case 22,5 %.

2.7 FOUNDATION LOADED BY HORIZONTAL FORCE

A rigid foundation is often subjected to a load acting at an angle and in such cases there is a danger that the foundation will be uprooted. This is often the case of foundations for columns carrying electricity and lighting, of anchoring blocks which take over horizontal forces at ground level, of columns carrying crane tracts, etc. In all of these cases the weight of the foundation itself is small in comparison with the bending moment of the horizontal force produced by the outer load. It was found that when a horizontal force reaches the ultimate bearing capacity, the initially vertical axis of the foundation is inclined by 3° to 5° in compact, firm soils; in loose, soft soils the inclination is as much as 11° . When the ultimate horizontal force is reached, the soil on that side of the foundation which faces the direction of the acting force, is forced out to the surface, on the opposite side the surface of the soil subsides and at the sides of the foundation we observe a movement of soil along yield surfaces of a rotary type. The stability of foundations for columns loaded by a horizontal force and their moment belongs to those tasks in the field of soil mechanics, which must be solved as spatial problems. The problem has been studied by many authors, for example Sulzberger (1945), Jaropolski (1954), Berio (1944), Brinch Hansen (1961), Boucraut (1964), Dietrich (1964), Narbut (1965), Dembicky et al (1971, 1976).

(a) The method of Brinch Hansen and Dietrich

Brinch Hansen derived a theory based on model tests, which solves the stability of rigid foundations for columns as a spatial task. He looks upon the foundation for a column as a short pile, which is subjected only to a horizontal force P at a height d_1 above a reference plane, which lies at a depth d_2 below ground level; d_2 is the surface soil layer, which does not exert lateral pressure. This method allows the calculation of the ultimate horizontal load P_m for rectangular foundations for columns in a homogeneous soil. In the equation Φ is the angle of internal shearing resistance of the soil, c is the cohesion, γ is the density, B is the width of the foundation measured at right angles to the direction of the acting force, L is the length of the foundation, D' is the effective foundation depth (Fig. 2.37).

$$D' = D - d_2 \quad (2.101)$$

if D is the depth of foundation measured from the surface of the area. The ultimate horizontal force is

$$P_m = BD'^2 K_q I_q S_q + cBD' K_c I_c S_c \quad (2.102)$$

where $K_q, l_q, S_q, K_c, l_c, S_c$ are dimensionless coefficients, whose magnitude depends on the angle of internal friction of the soil Φ and on the geometry of the foundation. The following functional relationships are valid:

$$K_q = f_1(\Phi; D'/B); \quad K_c = f_2(\Phi; D'/B) \text{ the values are given in Table 2.20.}$$

$$l_q = f_3(d_1/D'); \quad k_c = f_4(d_1/D') \text{ the values are given in Table 2.21}$$

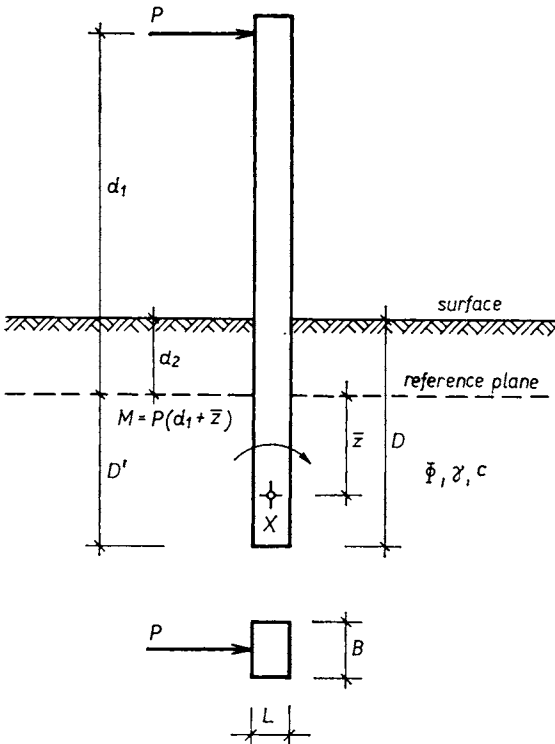


Fig. 2.37 A column loaded by a horizontal force P

The coefficients S_q and S_c depend on Φ and d_1/B and are calculated from the following equations

$$S_q = 1 + \beta_q L/B \tag{2.103}$$

$$S_c = 1 + \beta_c L/B \tag{2.104}$$

where β_q and β_c are auxiliary functions

$$\beta_q = f_5(\Phi; D'/B); \beta_c = f_6(\Phi; D'/B) \text{ the values are given in Table 2.22.}$$

The permissible horizontal load on a foundation is $P_p = P_m/F$, if the factor of safety is $F = 2$ for cohesionless soils and $F = 3$ to 4 for cohesive soils.

TABLE 2.20
Coefficients K_q and K_c

Φ	Coefficient	Ratio D'/B						
		1	2	3	4	6	8	10
0°	K_q	0.0	0.0	0.0	0.0	0.0	0.0	0.0
	K_c	3.4	3.9	4.3	4.7	5.2	5.6	6.0
10°	K_q	0.9	1.0	1.1	1.15	1.2	1.25	1.3
	K_c	4.8	5.7	6.4	6.9	7.9	8.4	9.0
20°	K_q	2.4	2.6	2.8	3.0	3.3	3.5	3.7
	K_c	7.0	8.7	10.0	11.0	12.5	13.8	14.8
30°	K_q	5.3	5.8	6.2	6.8	7.6	8.2	8.8
	K_c	11.4	15.0	18.0	20.0	24.0	27.0	29.0
40°	K_q	12.0	14.0	15.5	17.0	19.5	22.0	23.0
	K_c	19.5	28.0	35.0	41.0	52.0	62.0	70.0

TABLE 2.21
Coefficients l_q and l_c

d_1/D'	0	1	2	4	10	20
l_q	0.130	0.058	0.037	0.021	0.011	0.005
l_c	0.420	0.160	0.097	0.054	0.025	0.012

TABLE 2.22
Coefficients β_q and β_c

D'/B	Coefficient	Φ				
		0°	10°	20°	30°	40°
1	β_q	0.41	0.30	0.21	0.12	0.053
	β_c	0.70	0.57	0.38	0.27	0.160
10	β_q	0.36	0.28	0.18	0.10	0.045
	β_c	0.46	0.34	0.25	0.18	0.120

(b) The method of Dembicky

Dembicky et al (1971, 1976) made an analysis of older methods for the determination of the ultimate bearing capacity of foundations for columns loaded by a moment from a horizontal force P . For better correspondence between calculations and reality, wide-scale research was made with models of a rectangular plan in scales ranging from 1 : 2 to 1 : 20, mainly in cohesionless soils. One part of the tests was made on an analogue model of the Taylor-Schneebeli type, which enabled the shape of the rupture range in the vicinity of the foundation when the state of failure was reached, to be studied. The results obtained were analysed on the assumption that

- the foundations are perfectly rigid,
- the vertical load on the foundation surface may be neglected,
- the soil in the vicinity of the foundation is in an ultimate state of equilibrium
- the angle of friction of the soil on the sides of the foundation $\sigma \doteq 2\Phi/3$.

The method derived allows the determination of the ultimate moment M_m which will cause the foundation to be uprooted. The ultimate moment

$$M_m = M' \gamma D'^4 \quad (2.105)$$

if $D' = D - d_2$ is the effective depth of foundations (see Fig. 2.37). The values of coefficients M' are given in Table 2.23 for various angles Φ of internal shearing resistance of the soil and for various ratios L/D' , B/D' and $c/\gamma D'$. The width B of the foundation is measured at right angles to the direction of the horizontal force P , or to the plane in which the moment of the horizontal force is acting.

When reviewing the safety of a foundation against uprooting, we start with the ultimate moment M_m and the real acting moment M_x related to the centre X of rotation of the foundation. The point X lies at a depth \bar{z} below the reference plane, from which the effective depth of foundation D' is measured (Fig. 2.37). The reference plane is at a depth d_2 below the ground surface where the soil is no longer loose, for example as a result of ploughing, so that the lateral pressure of the soil can be applied. The ratio \bar{z}/D' depends on the angle of internal shearing resistance Φ of the soil and on the ratios L/D' , B/D' and $c/\gamma D'$. For their various values the ratios \bar{z}/D' are given in Table 2.23.

The ultimate moment M_m also depends on the height $(d_1 + D')$ of the point of action of the horizontal force P above the foundation line. If $d_1/D' \geq 1.6$, the more accurate values of \bar{z}/D' and M' are only slightly different ($< \pm 6\%$) from the values in Table 2.23.

In view of the introduced simplifying assumptions, the safety factor of the foundation against uprooting is $F = M_m/M_x \leq 2.5$. (The values F are given in Table 3.3.)

TABLE 2.23

The values of \bar{z}/D' and M' according to Dembicki

c		$c = 0$															
		$\Phi = 10^\circ$		$\Phi = 15^\circ$		$\Phi = 20^\circ$		$\Phi = 25^\circ$		$\Phi = 30^\circ$		$\Phi = 35^\circ$		$\Phi = 40^\circ$			
γ/D'	B/D'	\bar{z}/D'	M'	\bar{z}/D'	M'	\bar{z}/D'	M'	\bar{z}/D'	M'	\bar{z}/D'	M'	\bar{z}/D'	M'	\bar{z}/D'	M'		
0.1	0.1	0.682	0.074	0.687	0.098	0.691	0.133	0.695	0.185	0.1	0.1	0.668	0.146	0.667	0.226	0.664	0.366
	0.2	0.661	0.098	0.667	0.127	0.673	0.170	0.679	0.232	0.2	0.2	0.688	0.245	0.689	0.385	0.687	0.635
	0.5	0.626	0.166	0.633	0.212	0.640	0.277	0.647	0.370	0.5	0.5	0.712	0.515	0.716	0.812	0.714	1.348
0.4	0.1	0.635	0.142	0.642	0.182	0.649	0.237	0.656	0.317	1.0	1.0	0.726	0.939	0.731	1.476	0.731	2.444
	0.2	0.606	0.190	0.615	0.240	0.624	0.308	0.633	0.405	0.2	0.1	0.669	0.145	0.668	0.223	0.664	0.361
	0.5	0.557	0.329	0.568	0.407	0.579	0.512	0.590	0.661	0.2	0.2	0.689	0.242	0.690	0.380	0.687	0.625
0.8	0.1	0.608	0.230	0.615	0.290	0.623	0.372	0.630	0.489	0.5	0.5	0.714	0.507	0.717	0.800	0.716	1.325
	0.2	0.574	0.310	0.584	0.384	0.593	0.486	0.603	0.629	1.0	1.0	0.728	0.923	0.732	1.452	0.732	2.402
	0.5	0.519	0.537	0.530	0.655	0.541	0.813	0.553	1.033	0.5	0.1	0.670	0.141	0.668	0.215	0.665	0.344
1.2	0.1	0.595	0.318	0.602	0.397	0.609	0.505	0.616	0.658	0.2	0.2	0.692	0.234	0.692	0.364	0.689	0.595
	0.2	0.559	0.428	0.568	0.527	0.577	0.662	0.586	0.850	0.5	0.5	0.719	0.486	0.721	0.765	0.719	1.260
	0.5	0.500	0.742	0.511	0.899	0.521	1.109	0.532	1.398	1.0	1.0	0.735	0.882	0.739	1.385	0.737	2.284

Example 2.4

The safety factor of a column against uprooting is to be determined. The dimensions of the foundation are 1×1 m, the foundation depth $D = 2.3$ m below the surface. The foundation is loaded at surface level by a horizontal force $P = 12$ kN and a moment $M = 100$ kNm. The angle of internal shearing resistance of the soil $\Phi'_f = 40^\circ$; the cohesion $c = 0$ kN/m², the density of the soil $\gamma = 17.5$ kN/m³. The foundation is on a site which is ploughed to a depth of as much as 0.3 m.

The effective depth of foundation $D' = D - d_2 = 2.3 - 0.3 = 2.0$ m.

The ratios:

$$L/D' = 1/2 = 0.5; \quad B/D' = 1/2 = 0.5$$

For these ratios and $\Phi = 40^\circ$ we locate the values in Table 2.23,

$$\bar{z}/D' = 0.719; \quad M' = 1.260$$

The ultimate moment, see equation (2.105),

$$M_m = 1.260 \cdot 17.5 \cdot 2^4 = 353 \text{ kNm}$$

The depth of the centre of rotation below the reference plane $\bar{z} = D' \cdot 0.719 = 1.44$ m. At the centre of rotation X there is a moment

$$M_k = P \cdot (\bar{z} + d_2) + M = 12 \cdot (1.44 + 0.3) + 100 \doteq 121.0 \text{ kNm}$$

The safety factor of the foundation against uprooting $F = M_m/M_k = 353/121 = 2.92$, which is satisfactory.

(c) Interaction of adjacent foundations loaded by horizontal force

When a foundation is loaded by a horizontal force, the resistance of the soil acts upon those sides of the foundation which are at right angles to the direction of the applied force, and friction acts on the two sides of the foundation which are parallel to the direction of the applied force.

If we have two adjacent foundations and the applied force acts at right angles to the line connecting the centres of the foundations, then both foundations produce a frontal resistance but the side friction is only applied on one side for each of the two foundations. Each of the two foundations will therefore carry a smaller load than when standing separately.

If there is a small gap between foundations with a rough surface then the gap interacts with the foundations. In this case the pair of foundations carries a greater horizontal load than two widely separated foundations.

Model tests with short piles in sand loaded horizontally, carried out by Kratěna and Kysela and Bartoš (1975), proved the above mentioned interaction of foundations. The models of the piles were square in section ($B \times B$) and the angle of surface friction of the soil on the piles $\delta \leq 0.5\Phi$. When the axial separation of the piles was $l > 5B$, the ultimate horizontal load on each was the same as if they were standing separately. (This ultimate horizontal load was about 2.5 times greater than the ultimate horizontal force for an element with a length B of an underground wall with a thickness B and the same depth as

that of the piles.) For an axial separation of the piles $l = 3B$, the ultimate horizontal load on the outer piles was greater by 10% and on the central piles by 20% than when standing separately. When several piles stood close to each other, the ultimate horizontal force of the outer piles was 20% smaller than when standing separately. The decrement for the central piles was 30% when there were three piles and 40% when there were five piles.

Tests made with models of piles with a circular diameter differed from the previous tests in that the soil barely interacted with the piles; it “flowed” around the piles as they were pressed horizontally into the soil. Circular piles (with a diameter B) did not influence each other when their axial separation $l > 4B$. (The ultimate horizontal load on a separately standing circular pile was approximately twice as large as the ultimate horizontal force on an element of an underground wall with a length B , a thickness B and having the same depth as that of the pile.) With a decrease of the axial separation of the circular piles their ultimate horizontal load decreased. When the piles were immediately next to each other, the ultimate horizontal load of the outer piles was smaller by approximately 35% than when standing separately. In the case of the central piles, the decrement was 40–50% so that their ultimate horizontal load was the same or slightly larger than the ultimate horizontal force calculated for a comparable element of an underground wall.

The method of execution of the model tests corresponded to drilled piles, pier footings, etc. but not to driven piles.

A different case was studied by Šimek (1975). Using an extensive model-research following predominantly the Beggs-Blažek method, he studied the behaviour of a short row of piles loaded horizontally along the axis of the row. The piles were connected at the top by a relatively rigid slab. He found that in a group with all the piles vertical, the piles nearer to the point of application of the horizontal force are subjected to tension and those at the other end to compression. For a group having the outer piles at an angle, it was apparent that the vertical piles took over a relatively smaller vertical load, and that as a result of the inclination of the piles, the vertical piles nearer the point of application of the horizontal load were compressed and those at the other end in tension. The inclined piles not only decreased the axial forces of the vertical piles to about a third, but also decreased the bending moment at the butt-ends of the piles by as much as 50%. The horizontal displacement of the butt-ends of all the piles was the same, as a result of the rigidity of the overhead slab. When all the piles were vertical, the horizontal force was distributed evenly between all the piles. When the outer piles were at an angle, these carried a greater part of the horizontal load—the pile nearer to the point of application of the horizontal force (i.e. pointing towards the foundation) was in tension and the inclined pile at the other end was in compression.

2.8 BEARING CAPACITY OF A FOUNDATION ON A LAYERED SUBGRADE

In nature we often find that the foundation bed is composed of several layers of different soils. Such situations can be divided into the following groups:

- A. Double-layer subgrade beneath the foundation
 - a) the angles of internal shearing resistance of the cohesive soils of both layers $\Phi = 0$, $c_1 \neq 0$, $c_2 \neq 0$,
 - b) the upper layer is soft, $\Phi = 0$, the angle of internal shearing resistance of the lower layer $\Phi > 0$,
 - c) the angles of internal shearing resistance of the soils in both layers $\Phi \neq 0$.
- B. The ultimate bearing capacity of a foundation if the soil is on bedrock.
- C. The ultimate bearing capacity of a foundation subgrade with a gravel-sand cushion.
- D. The ultimate bearing capacity of a multilayered subgrade formed by two alternating soils.

2.8.1 Double-layer subgrade beneath foundation

- a) The angles of internal shearing resistance of the cohesive soils of both layers equal zero, $c_1 \neq 0$, $c_2 \neq 0$.

This situation was studied by Button (1953) for surface-based strip foundations, and he assumed that the cohesive soils of both layers are consolidated to approximately the same degree. For the determination of the ultimate bearing capacity q_m , he assumed a cylindrical yield surface. The ultimate bearing capacity

$$q_m = c_1 \cdot \bar{N}_c \quad (2.106)$$

where the bearing-value coefficient \bar{N}_c depends on the thickness \bar{H} of the upper soil layer and on the ratio of cohesion c_2 of the lower soil layer to cohesion c_1 of the upper layer. The value of coefficient \bar{N}_c is determined from Fig. 2.38.

- b) The upper layer is soft, $\Phi = 0$, $c \neq 0$, the angle of internal shearing resistance of the lower soil layer $\Phi > 0$.

In this case of a stratified subgrade there is, directly beneath the foundation, a layer of soft soil (for example Holocene alluvium) and beneath that there is a layer with a much greater bearing value. If the load on the foundation surface is the same or greater than the ultimate bearing capacity q_m of the soil in the upper layer, then the soft soil beneath the foundation is forced to the sides as if it were a plastic material.

The soil in the lower layer, in comparison with the upper layer is almost in-compressible and therefore for the calculation of ultimate bearing capacity of the foundation we use the method derived for a soil on bedrock (Sec. 2.8.2).

c) The angles of internal shearing resistance of both layers $\Phi \neq 0$.

The ultimate load on a strip foundation on a subgrade composed of two layers of various types of soil was experimentally determined by laboratory tests. The soil layers were formed of cohesionless and cohesive soils. The grading curves of the soil are given in Fig. 2.39. During the tests some soils

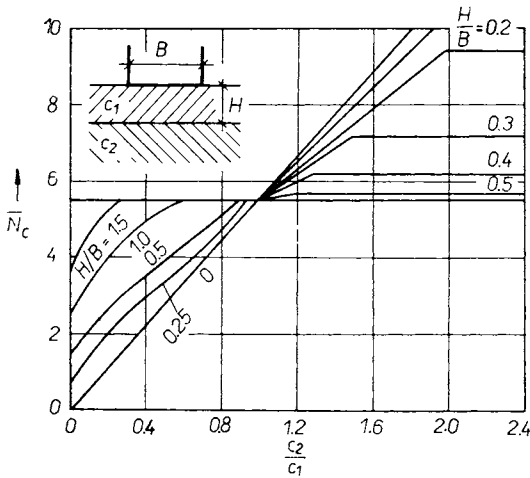


Fig. 2.38 The coefficient \bar{N}_c of the bearing value of two layers of cohesive soils if $\Phi_1 = \Phi_2 = 0$

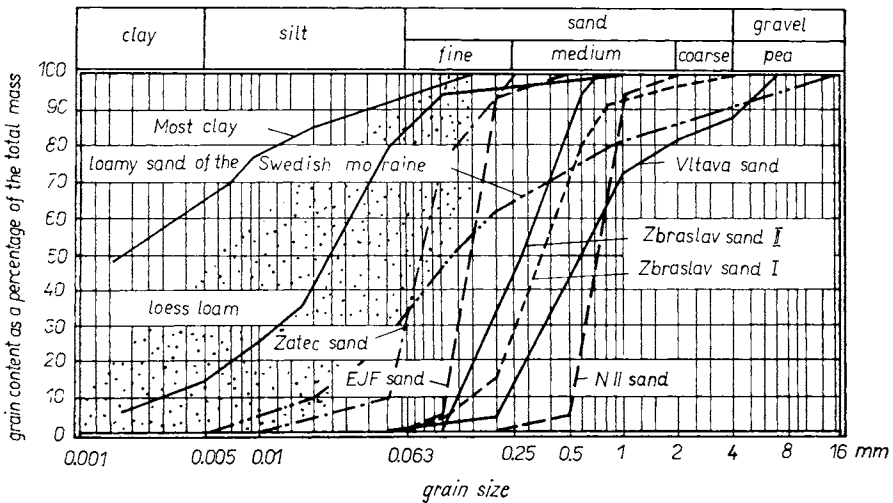


Fig. 2.39 Grading curves of soils

were compacted and others consolidated. Tests showed that the lower layer provides an almost linear influence on the ultimate bearing capacity of a foundation on the upper layer. The depth of the lower layer below the foundation level is H . The influence was continuous and it was possible to replace it, with sufficient accuracy, by one or two straight lines (Fig. 2.40).

Of critical importance in the estimation of the influence of the bottom layer, is the depth T below the foundation level to which the yield surface would reach if the subgrade was only composed of the soil of the upper level. The ratio of the depth T to the width B of the strip foundation depends on the angle Φ of internal shearing resistance of the soil and on the inclination β of the resultant of the applied load from the vertical. The measured values are given in Table 2.24 for a case when the foundation level is horizontal and the load is applied along the axis of the foundation.

TABLE 2.24

Values of ratio T/B as a function of the angle of internal shearing resistance Φ of the soil of the upper layer and the inclination β of the resultant of the load from the vertical (our measurements)

β	Φ				
	0°	10°	20°	30°	40°
0°	0.70	0.80	0.95	1.10	1.25
10°	—	—	0.60	0.80	1.00
20°	—	—	—	0.40	0.70
30°	—	—	—	—	0.35

From Fig. 2.40b it is apparent that a thin upper layer of soil with a greater bearing value over a soil with a smaller bearing value does not increase the ultimate bearing capacity of the strata group if the layer with the greater bearing value has a height of no more than $0.2B$. The layer with the greater bearing value helps to increase the ultimate bearing capacity of the strata group only when the thickness of the upper layer beneath the foundation $H > 0.2T$. The reason for this is that in the thin soil layer with a greater bearing value beneath the foundation, a yield surface with a large gradient is created when the ultimate bearing capacity is reached and the normal stress acting on this yield surface is very small. The friction in this part of the failure surface is therefore small and the thin layer contributes only a little to the increase of the ultimate bearing capacity of the strata group. If the soil layer with a greater bearing value has a thickness which is at least equal to the width

of the foundation, then the failure surface is created when the ultimate bearing capacity is reached, mainly in the soil of the upper layer. The soil of the lower layer then barely influences the ultimate bearing capacity of the foundation, and we may therefore assume it to be the same as if the foundation were standing on a homogeneous subgrade formed by the soil of the upper layer.

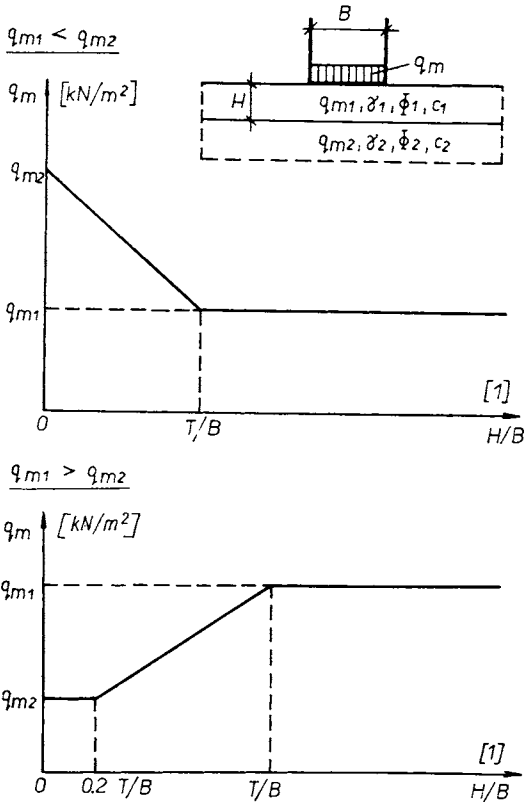


Fig. 2.40 The ultimate bearing capacity of two layers of soil with various values of Φ

When there was beneath the foundation a layer with a small bearing value and below this a layer with a greater bearing value, then the bearing value of the strata group decreased linearly as the depth beneath the foundation increased, up to a depth of $H = T$. When the depth of the upper layer with the smaller bearing value was greater, the influence was no longer apparent.

The established relationships are described in Fig. 2.40. The ratio H/B of the height H of the upper layer of the soil beneath the foundation to the width B is plotted on the horizontal axis and the values of the ultimate bearing capacities q_m are on the vertical axis.

In the calculation of the bearing value of a foundation on a double-layer

subgrade, we first calculate the ultimate bearing capacity q_{m1} of the foundation on a subgrade formed by the soil of the upper layer only, and then we calculate the ultimate bearing capacity q_{m2} of the same foundation on the soil of the lower layer (see example 2.5). For the ultimate bearing capacity q_m of the strata group the following relationships are valid:

If $q_{m1} > q_{m2}$

then for $H \leq 0.2 T$ the ultimate bearing capacity $q_m = q_{m2}$; for $0.2 T < H \leq T$ the ultimate bearing capacity

$$q_m = q_{m2} + \frac{q_{m1} - q_{m2}}{0.8} (H/T - 0.2);$$

for $T < H$ the ultimate bearing capacity $q_m = q_{m1}$.

If beneath the foundation the upper layer has a smaller bearing value than the lower layer, i.e. when $q_{m1} < q_{m2}$, then up to a depth beneath the foundation

$H \leq T$ the ultimate bearing capacity $q_m = q_{m2} - \frac{q_{m2} - q_{m1}}{T} \cdot H$, for $T < H$

the ultimate bearing capacity $q_m = q_{m1}$. The ultimate bearing capacities q_{m1} , q_{m2} of each soil layer are calculated according to Sec. 2.3.

In the same way the influence of groundwater is introduced into the calculation of the ultimate bearing capacity if the groundwater elevation is below the level of the foundation line. On the one hand the soil load beneath the ground-

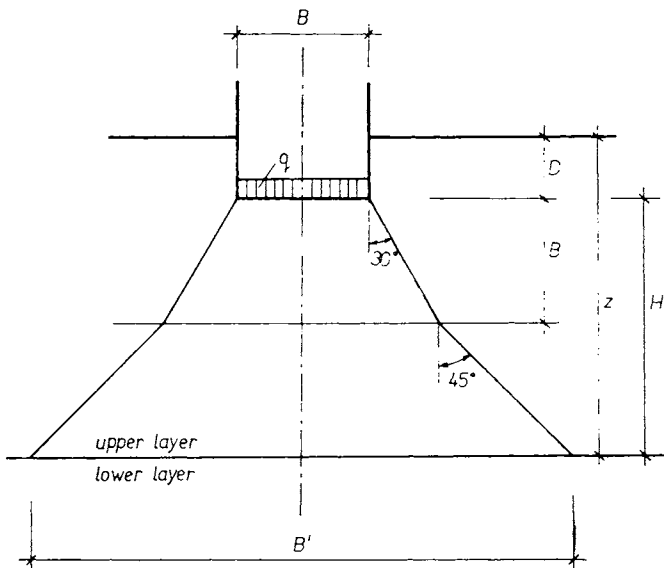


Fig. 2.41 The diagram for the determination of the ultimate bearing capacity of a strata group as determined by Kézdi

water elevation is reduced by 10 kN/m^3 , and on the other hand the water causes a decrement of the friction between the grains of the soil and thus a decrement of the angle of internal shearing resistance of the soil (in loose soils by about 1°). It is therefore more accurate to consider a homogeneous subgrade of a foundation with groundwater as a double-layer subgrade where the upper layer has different mechanical properties from the lower layer, which is below the groundwater elevation. Alternatively we can just consider a substitute density

$$\bar{\gamma} = \gamma' + \frac{h^*}{B}(\gamma - \gamma') \dots \quad \text{for } h^* \leq B \quad (2.107)$$

where h^* is the depth of the water level beneath the foundation.

In the Polish standard PN-59/B-03020, two approximate mathematical procedures are mentioned. If the soil layer with the smallest bearing value is directly beneath the foundation, the ultimate bearing capacity for this layer is determined as if the subgrade was homogeneous. In the other cases, the ultimate bearing capacity $q_m \bar{i}$ of the foundation is determined for each type of soil, the resultant ultimate bearing capacity being obtained from the expression

$$q_m = \Sigma q_m h_i / \Sigma h_i \quad (2.108)$$

where h_i is the depth of each layer beneath the foundation and $\Sigma h_i \doteq B$.

Another method for the determination of the ultimate bearing capacity of a double-layer subgrade loaded by a strip foundation is mentioned by Kézdi (1964). In this case a uniform stress on the boundary of the layers at a depth H beneath the foundation level, where H is the thickness of the upper layer of the soil beneath the foundation, is determined. The distribution of the stress is assumed according to Fig. 2.41 on a width B' . According to the author, this method is applicable in cases where the shearing strength of the upper layer is at least 50 % greater than the shearing strength of the lower layer. The second condition is that the rupture surface, which would be created under the foundation reaching the ultimate bearing capacity should encroach upon the lower layer. Whether or not the shearing surface in the upper layer of the soil reaches the lower layer can be judged from Table 2.24 in which the ratio of the distance T of the lowest point of the failure surface from the plane of the foundation level to the width B of the strip foundation in relation to the angle Φ of the internal shearing resistance of the soil of the upper layer is given. If the shearing strength of the upper layer is greater than that of the lower layer by less than 50 %, Kézdi suggests using the mean values of Φ and c and determining the ultimate bearing capacity according to one of the methods which are valid for a homogeneous subgrade.

The ultimate bearing capacity of a stratified subgrade determined according to the latter two procedures, is rather different from the values obtained in laboratory tests.

Example 2.5

The permissible vertical load on a foundation slab for a silo, whose dimensions are 12×24 m with a foundation depth of 5 m below ground level, is to be determined. From the ground level to a depth of 11 m there is a compact fine sand, to a depth of 35 m there is a firm, sandy clay, deeper still is shale. The groundwater elevation is 2.5 m below ground level. The angle of internal shearing resistance of the sand $\Phi_f = 32.5^\circ$ and its density is 20 kN/m^3 . The sandy clay has a negligible angle of internal shearing resistance ($\Phi_u = 0$), a cohesion $c_u = 50 \text{ kN/m}^2$ and a density of 21 kN/m^3 . The resultant of the load is inclined at an angle of 5° to the vertical.

As a first step we calculate the ultimate bearing capacity q_{m1} for a case where the subgrade of the foundation is formed only by the compact, fine-grained sand. According to equation (2.44), and with the use of Table 2.9, we get an ultimate bearing capacity

$$q_{m1} = 3880 \text{ kN/m}^2$$

Then we calculate the ultimate bearing capacity q_{m2} for a case when the subgrade of the foundation is formed only by the sandy clay. It is found to be $q_{m2} = 410 \text{ kN/m}^2$. Interpolation using Table 2.24, determines the corresponding ratio $T/B = 1$. The thickness of the upper layer (sand) beneath the foundation is

$$H = 11 - 5 = 6 \text{ m}$$

As $q_{m1} > q_{m2}$, and at the same time $0.2T < H < T$, the ultimate bearing capacity of the strata group is determined with the help of Fig. 2.40.

$$q_m = 410 + \frac{3880 - 410}{0.8} (6/12 - 0.2) = 1710 \text{ kN/m}^2$$

As the load is transferred by both a cohesionless and cohesive soil, a higher safety factor $F = 3$ is chosen and the permissible load of the foundation slab consistent with safety against sinking $q_k = q_m/3 = 1710/3 = 570 \text{ kN/m}^2$.

2.8.2 Soil on bedrock

Let us consider a case where the soil is on solid bedrock, which is located below the foundation at a depth H . When the ultimate bearing capacity is reached, the soil is forced to the sides. The rupture surfaces differ from the rupture surfaces in a homogeneous subgrade in proportion to the decrease of the thickness of the soil layer over the bedrock compared to the width of the foundation.

To determine how the ultimate bearing capacity of the strip foundation changes with various thickness of the soil layer on the bedrock, model tests were made, from which coefficient values expressing the influence of the depth of the (incompressible) bedrock, were derived. The influence of the bedrock

was expressed by dimensionless factors ϑ_γ , ϑ_q , ϑ_c . by which the individual terms of equations (2.25), (2.43), (2.44) for the calculation of the ultimate bearing capacity of a homogeneous subgrade, are multiplied. For example equation (2.43) has the following form after completion

$$q_{ms} = 0.5\gamma_1 B N_\gamma \vartheta_\gamma + \gamma_2 D N_q \vartheta_q + c N_c \vartheta_c \quad (2.109)$$

If the bedrock and foundation are rough, then the factors $\vartheta > 1$ always. A foundation concreted in situ can be considered as a rough foundation. Bedrock is also rough in most cases and therefore the yield surface is created in the upper soil near the bedrock. A smooth surface is rarely found, for example in the case of some types of claystone below the groundwater elevation.

Model tests were made with cohesionless soils. The results of one series of tests for the determination of the factor ϑ_γ for sand with an angle of internal shearing resistance are shown in Fig. 2.42. The value of factors ϑ_γ and ϑ_q obtained from the tests. are given in Table 2.25. The values of factor ϑ_c are calculated using equation

$$\vartheta_c = \frac{N_q \vartheta_q - 1}{N_q - 1} \quad (2.110)$$

which is derived according to Caquot in a similar way to equation (2.74).

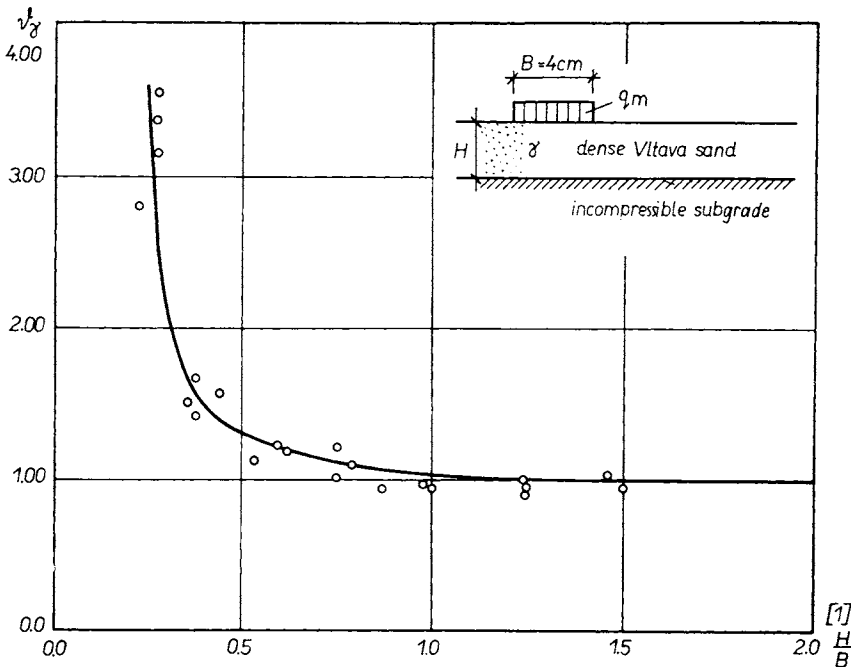


Fig. 2.42 Tests of the bearing value of sand on an incompressible subgrade

TABLE 2.25

The values of coefficients ϑ_γ and ϑ_q for a rough foundation with a width B and a rough bedrock at a depth H beneath the foundation level

Φ	ϑ	H/B						
		0.125	0.250	0.375	0.500	0.750	1.00	1.50
0°	ϑ_γ	1.00	1.00	1.00	1.00	1.00	1.00	1.00
	ϑ_q	1.15	1.10	1.05	1.00	1.00	1.00	1.00
10°	ϑ_γ	1.25	1.05	1.00	1.00	1.00	1.00	1.00
	ϑ_q	1.60	1.10	1.05	1.00	1.00	1.00	1.00
20°	ϑ_γ	2.00	1.25	1.05	1.00	1.00	1.00	1.00
	ϑ_q	5.00	1.60	1.10	1.00	1.00	1.00	1.00
30°	ϑ_γ	6.00	2.00	1.25	1.10	1.05	1.00	1.00
	ϑ_q	20.00	5.00	1.60	1.20	1.10	1.00	1.00
37°	ϑ_γ	14.00	3.50	1.60	1.25	1.10	1.05	1.00
	ϑ_q	50.00	12.00	3.00	1.60	1.20	1.10	1.00

Tests made by Obin, Mandel and Salencon (1969, 1972) show that it is possible, with sufficient accuracy, for a rough foundation and a rough bedrock to consider $\vartheta_c \approx \vartheta_q$. Also for $\Phi \rightarrow 0$ (in practice $\Phi < 10^\circ$) we assume $\vartheta_c \doteq \vartheta_q$, since in these cases equation (2.110) is not valid.

The mentioned values show that, for example, for sand with an angle of shearing resistance $\Phi < 37^\circ$, the influence of the bedrock is not apparent if the sand layer is as deep as the width of the foundation B . For other soils, with an angle of shearing resistance $\Phi < 37^\circ$, the influence of the solid subgrade disappears at a depth $H > B$. Stone paving on a concrete base is laid in sand, usually with a depth of about $H = 3$ cm. If the sand layer is deeper because of the unevennesses of the concrete or to obtain the necessary lateral gradient on the road surface, then the influence of the concrete base does not show at all and the paving behaves as if there were sand alone in the subgrade. As a result of loading by moving vehicles, the paving undulates noticeably because, beneath the paving brick the ultimate bearing capacity has been exceeded.

In the preceding paragraphs of Sec. 2.8.2, a very solid and almost incompressible bedrock with a bearing value substantially greater than the load increment, with which the stress from the foundation acts on the bedrock, has been considered. Should the bedrock not satisfy these conditions (for example as a result of pronounced decomposition, numerous faults, etc.) it would be necessary to determine the ultimate bearing capacity as for a strata group formed by two soils with different properties (Sec. 2.8.1).

2.8.3 Gravel-sand cushion

An ideal foundation soil should be composed in such a way that the upper layer, directly beneath the foundations where the greatest load is applied, would have the greatest strength. Deeper down, where the stress is smaller, the soil could have a smaller bearing value.

The greatest vertical stress in the soil is always directly beneath the foundation and with increasing depth and to the sides it decreases rapidly. If we need to make foundations for a building on a soil with a small bearing value, we make a gravel-sand cushion below the foundation. In the case of foundations on a gravel-sand cushion the original, low bearing-value soil is replaced to a depth equal to at least the width of the foundation by compacted gravel-sand as follows from tests of the ultimate bearing capacity of a double-layer subgrade where, beneath the foundation, there is a high bearing-value layer of soil and below that a low bearing-value soil. The influence of the lower layer with a smaller bearing value was hardly noticeable if the height of the upper layer with a higher bearing value was equal to the width of the foundation. The determination of the ultimate bearing capacity of a foundation on a gravel-sand cushion is a special case of the determination for a double-layer subgrade.

The ultimate bearing capacity of a foundation, beneath which there is a gravel-sand cushion is best solved by the graphical method, the principles of which were given in Sec. 2.3.5.

Let us replace the calculated ultimate bearing capacity q_m above the foundation level by an earth column with a height $h_2 = q_m/\gamma$, where γ is the density of the soil. The soil on the yield surface exerts a normal stress

$$\sigma_n \doteq \gamma(h_1 + h_2) \cos^2 \alpha^\circ,$$

where $(h_1 + h_2)$ is the total height of the soil above the position being considered on the yield surface, and α° is the angle between the tangent to the yield surface and the horizontal (Fig. 2.43). If we plot the normal components σ_n on the rupture surface we can see that the maxima are directly beneath the foundation, outside the foundation the values drop quickly and towards the surface they continue to decrease. During the calculation of the normal components, the distribution of the stress beneath the foundation was not taken into consideration and therefore the full curve in Fig. 2.43 is only approximate. On the yield surface there is no break in the distribution of the normal stress but a gradual transition as shown by the dash line. The normal stress σ_n produced by the foundation in the individual places of the rupture surface can be calculated with sufficient accuracy according to elastic-halfspace theory.

The resistance against displacement of the soil from beneath the foundation increases in proportion to the increase of the normal stress, the increase of the

angle of internal shearing resistance Φ and the increase of cohesion c . If beneath the foundation, in the places where on the rupture surface the maximum normal stress σ_n is acting, a gravel-sand cushion is created, then the bearing value of the soil is substantially increased. The cushion must reach to a depth beneath the foundation surface at least equal to the depth T (see ratios T/B in Table 2.24 in 2.8.1) as proved experimentally. For the preliminary proposal it is useful to consider a thickness of the cushion equal to the width of the foundation. Let us determine the ultimate bearing capacity of the foundation described in Sec. 2.3.5 if beneath it there is a gravel-sand cushion, which is compacted to such a degree that it has an angle of internal shearing resistance $\Phi'_f = 40^\circ$ and a density $\gamma = 20 \text{ kN/m}^3$.

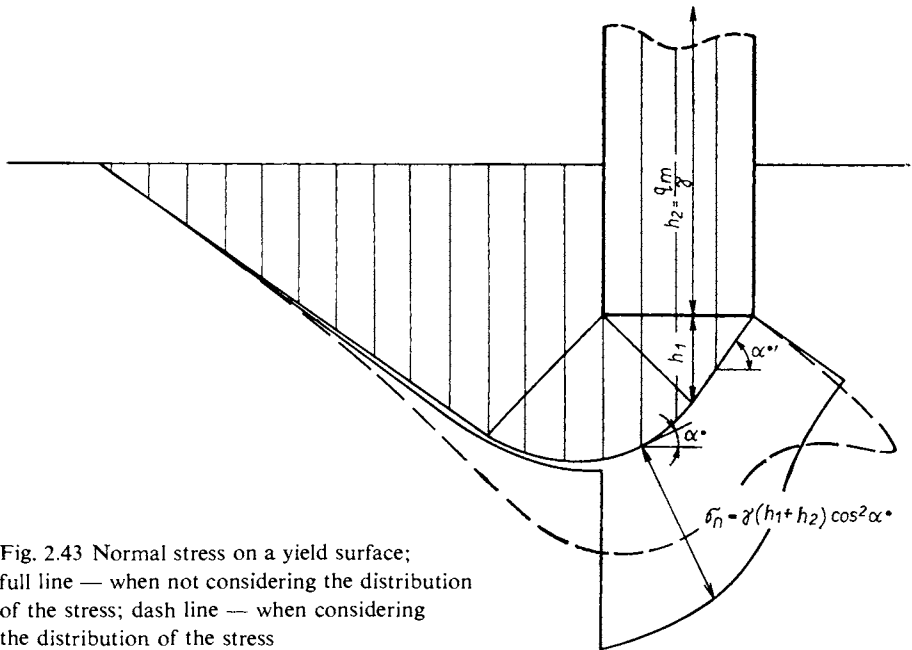


Fig. 2.43 Normal stress on a yield surface; full line — when not considering the distribution of the stress; dash line — when considering the distribution of the stress

As the rupture surface beneath the foundation on the bed passes through two types of soil, it is necessary to solve several shapes of the rupture surfaces for various Φ and find that one, which is the route of least resistance. The longer part of the rupture surface is in the cohesive soil outside the cushion and thus the rupture surface outside the cushion in the cohesive soil forms an angle of $45^\circ - \Phi/2$ with the surface, as in a cohesive soil without a gravel-sand cushion. Several shapes of the rupture surfaces for various Φ^* and ratios of the width of the cushion to the width of the foundation were examined. At the same time the shape of the yield surface in the cushion was determined for an angle of

internal shearing resistance with a minimum of 20° (the cohesive soil alone) and a maximum of 40° (the gravel-sand cushion alone). The established values are given in Fig. 2.44. The spread of the cushion to each side of the foundation B on the horizontal axis; the values of the substitute angle of internal shearing resistance Φ^* , for which the shape of the yield surfaces in the gravel-sand cushion was determined, is given on the other axis; the established ultimate bearing capacity q_m is on the vertical axis. For a cushion of the same width as the foundation, the route of

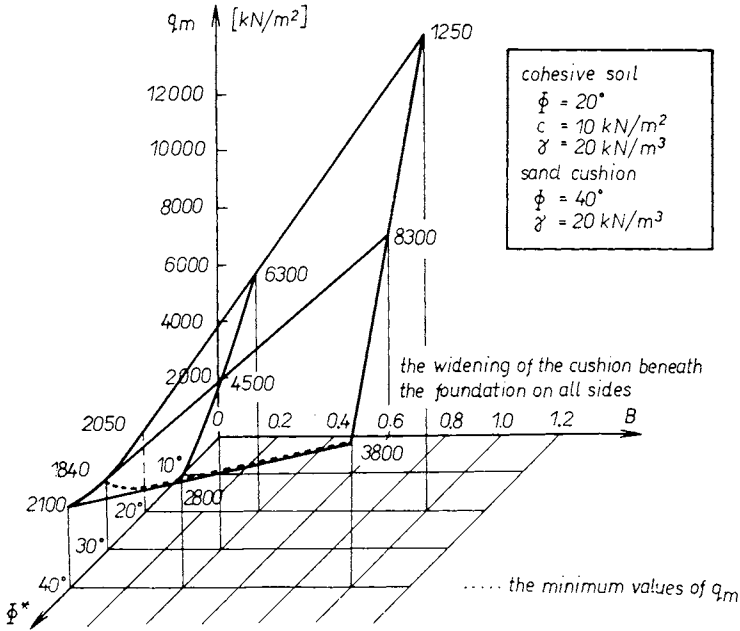


Fig. 2.44 The ultimate bearing capacity of a foundation on a gravel — sand cushion as a function of the angle and of the widening of the cushion

least resistance is a yield surface which, in the gravel-sand cushion, has a shape determined for the mean angle of internal shearing resistance of the cushion and the soil $\Phi^* = (20^\circ + 40^\circ)/2 = 30^\circ$. In such a case, the ultimate bearing capacity $q_m = 1840 \text{ kN/m}^2$. The graphical solution of the bearing value is shown in Fig. 2.45. The procedure is the same as for the case in Fig. 2.17 with the difference that the true acting forces R and cohesions c , which vary for each soil, are taken into account. (In a gravel-sand cushion $c = 0$.)

On the vertical boundary of the gravel-sand cushion and the surrounding soil one does not at first know how the angle of internal shearing resistance and the cohesion will be applied. We therefore examine several cases with different

values of Φ and c . The ultimate bearing capacity is then determined for those values which give the minimum bearing value. If on the boundary an angle of internal shearing resistance, smaller than Φ for the cushion, is considered, then

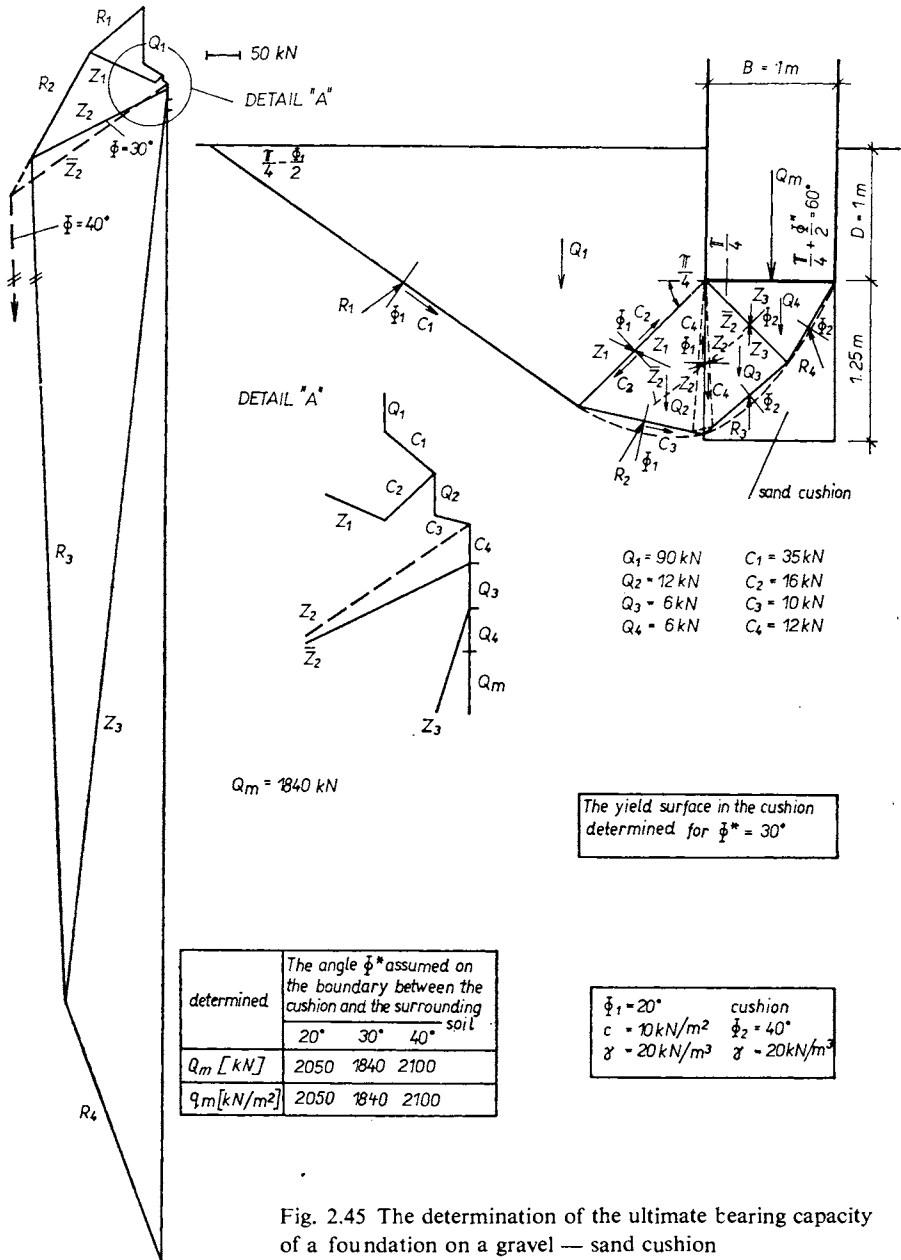


Fig. 2.45 The determination of the ultimate bearing capacity of a foundation on a gravel — sand cushion

it is assumed that the rupture surface passes partially or completely through the surrounding soil. For such a foundation the minimum values are obtained when we consider the mean angle $\Phi = 30^\circ$ and the half value $C_4/2$ of the total

- $Q_1 = 180 \times 210 = 390 \text{ kN}$ $C_1 = 55 \text{ kN}$ $C_2 = 11 \text{ kN}$
- $Q_2 = 8 \text{ kN}$ $C_3 = 8 \text{ kN}$ $C_4 = 10 \text{ kN}$
- $Q_3 = 6 \text{ kN}$ $C_5 = 7 \text{ kN}$ $C_6 = 8 \text{ kN}$
- $Q_4 = 6 \text{ kN}$ $C_7 = 7 \text{ kN}$
- $Q_5 = 25 \text{ kN}$

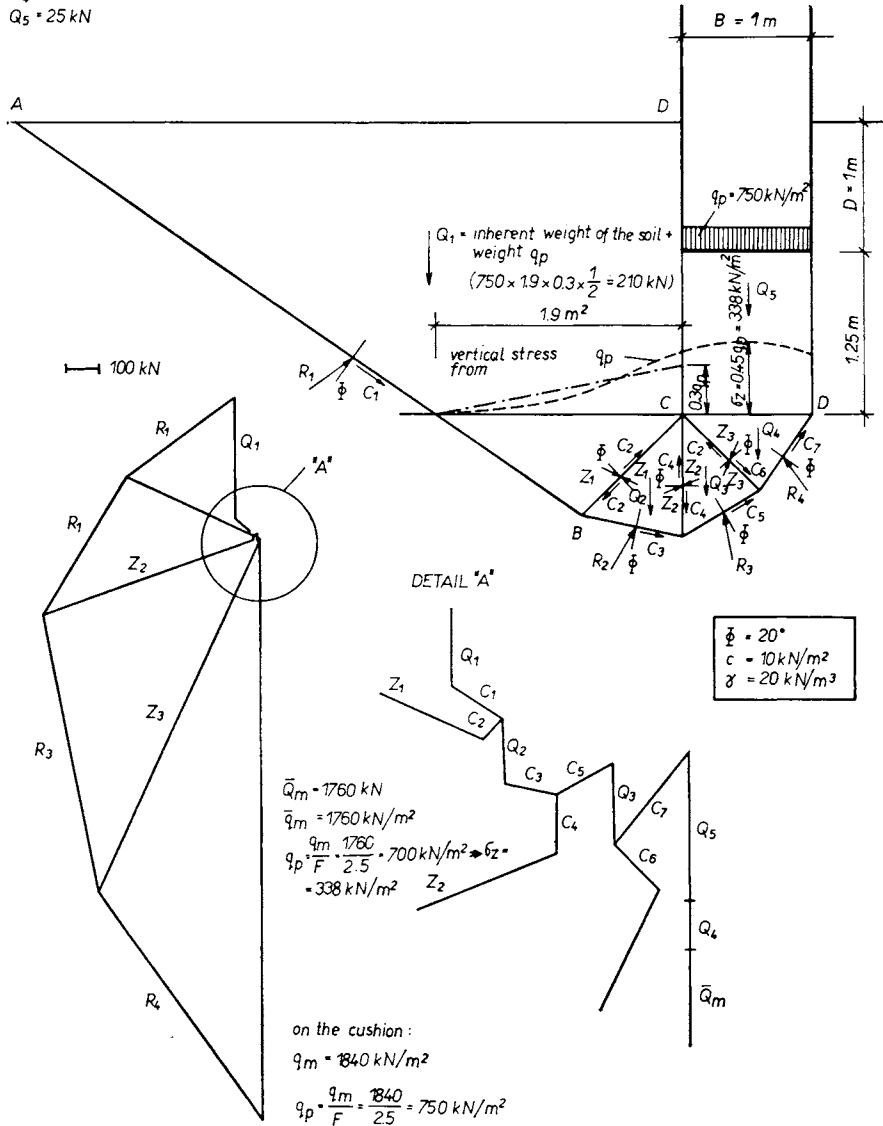


Fig. 2.46 The determination of the bearing value below the gravel — sand cushion

cohesion on the contact surface of the soil and the cushion. The ultimate bearing capacity is then $q_m = 1840 \text{ kN/m}^2$. In Fig. 2.45 the procedure for $\Phi = 30^\circ$ is drawn by a full line and the procedure for $\Phi = 40^\circ$ by a dash line.

The ultimate bearing capacity of the examined strip foundation without the cushion is 490 kN/m^2 , with the cushion $q_m = 1840 \text{ kN/m}^2$. The bearing value of the foundation with the bed is greater by 275 %. This is a very significant increase of the bearing value, and the cushion produces an effect almost as if the foundation soil was formed by gravel-sand only.

A calculation was made to find out whether or not a rupture surface will be created beneath the gravel-sand cushion (Fig. 2.46). Friction on the sides of the cushion was not taken into account. This simplification is within the safety limit as the friction on the sides of the cushion increases the safety. For a safety factor $F = 2.5$, the permissible load on the cushion $q_p = 1840/2.5 \doteq 750 \text{ kN/m}^2$. At a depth of $1.25 B$ beneath the foundation level, i.e., on the lowest level of the cushion, there is a vertical stress $\sigma_z = 0.45q_p$ when a homogeneous subgrade is assumed. Away from the axis of the foundation the stress σ_z at this depth decreases. If the curve for σ_z is replaced outside the foundation by a straight line, then on a vertical beneath the edge of the foundation we get a vertical stress $\sigma_z = 0.30q_p$. Should the ultimate bearing capacity at the level of the lower surface of the cushion be determined as if the foundation were to reach to this depth, we would get $q_m = 1760 \text{ kN/m}^2$, i.e. a value five times larger than the stress $\sigma_z = 0.45q_p = 340 \text{ kN/m}^2$ with which a foundation on a cushion can act at this level. For that reason the cushion cannot sink.

For a more accurate determination of the stress on the boundary of the cushion and the subgrade, it is possible to proceed by replacing the height H of the cushion by an equivalent layer of the soil of the subgrade according to equation

$$H_{eq} \doteq H \sqrt[3.5]{\frac{E_{o1}}{E_{o2}}} \quad (2.111)$$

where E_{o1} is the elastic modulus of the cushion and E_{o2} is the elastic modulus of the subgrade.

The stress on the boundary between the layers is then calculated as for a homogeneous subgrade at a depth H_{eq} . In our case $E_{e1} > E_{e2}$ and therefore $H_{eq} > H$, so that the true stress from the load on the foundation surface is, on the boundary between the cushion and the subgrade, even slightly smaller than $\sigma_z = 0.45q_p = 340 \text{ kN/m}^2$, which we used in calculations (see also appendix I.)

The gravel-sand cushion therefore creates a great increase of the bearing value of the foundation soil and a significant decrease of the settlement of the building. Near the foundations the calculated settlement of the soil, to a depth equal to the width of the foundation, amounts to about 60% of the total

settlement. The compressibility of compacted sand is about 10 times smaller than that of loams and at the same time there is a smaller stress in the subgrade beneath the cushion than in the case where there is no cushion. For that reason the total settlement of a foundation on a gravel-sand cushion is substantially smaller than without the cushion.

Let us also examine the influence of the width of the cushion on the increment of the bearing value of the foundation. We shall assume that the width of the cushion is larger than the width of the foundation by $0.2B$, $0.4B$, $0.6B$ and $1.0B$. The graphically determined ultimate bearing capacities q_m are given in Fig. 2.44. We can see that the widening of the cushion by 10 to 15 % does not bring a substantial increment of the bearing value of the soil. Nevertheless, it is recommended that the width of the cushion be wider by about 10 % B because of the inaccurate cutting of the trench and especially because of the large shearing stresses under the edges of the foundation.

When we design a foundation we start from an estimated permissible load q_p of the soil, as if the subgrade was formed by gravel-sand alone and for this load we calculate the dimensions of the foundation surface A . Then we determine the ultimate bearing capacity q_m of the proposed foundation graphically. The ratio q_m/q is the safety factor, which we judge from the point of view of its size (q is the true load of the foundation). If it is smaller than $F = 2.5$ then we widen the foundation and determine q_m again graphically.

The permissible vertical load of a strip foundation on a gravel sand cushion is usually 2.5 to 3.5 times larger than the permissible load of a cohesive soil without a cushion, if the angles of internal shearing resistance of the two soils differ by at least 20° to 25° . For a difference of the angles of internal shearing resistance of approximately 10° , the use of a gravel-sand cushion increases the permissible load of a cohesive soil by a factor of about 1.5 – 2.0. The permissible load of the foundation on a cushion usually does not reach the values of the permissible load of the gravel-sand from which the cushion has been made.

The solution for an inclined load is similar to the vertical-load case but the changed shape of the rupture surface, as described in Sec. 2.3.5, is taken into account.

For a permanent inclined load, it is sufficient to consider a smaller height T of the cushion than for a vertical load.

A quick approximate determination of the loads and dimensions of gravel-sand cushions with a view to their reaching the ultimate bearing value is described by Haedicke (1968). He allows a load q_{p1} on the cushion as if there were in the subgrade only gravel-sand, if the cushion has a height

$$H = B \cdot f(L/B; q_{p2}/q_{p1}) \quad (2.112)$$

while the width of the cushion at the level of the foundation line is at least $1,6B$ and at a depth H is at least B . The auxiliary function f depends on the ratio L/B of the length of the foundation to its width, and on the ratio q_{p2}/q_{p1} of the permissible load of the subgrade to the permissible load of the gravel-sand of the cushion. The values of function f are given in Table 2.26.

At the contact of the cushion with the original soil there is a danger that the finer particles of the surrounding soil will be pressed into the gravel-sand, which would lead to increased settlement of the foundation. This process is accelerated by flowing groundwater. To avoid the penetration of the soil, we must fulfil the same conditions as for a filter

$$d_{15}^C/d_{15}^S \leq 20 \text{ to } 25 \text{ and } d_{15}^C/d_{85}^S < 5 \quad (2.113)$$

Other criteria demand that $d_{50}^C/d_{50}^S = 5$ to 10 or alternatively that $d_{15}^C/d_{15}^S = 4$ to 5. These criteria are based on the grading curves of the soil of the gravel-sand cushion and of the subgrade. The term d_{15}^C designates the diameter of the gravel-sand cushion grains, when a 15% volume content of the grains is smaller than this diameter. The other terms have a similar meaning and the index S indicates that the diameter of the grains relates to the soil which is in contact with the cushion. This condition is fulfilled if at the place of contact of the soil and the cushion, a thin filtration layer is made, which fulfils the above requirements concerning the grain-size distribution.

The cushions must be made in drained trenches and at temperatures exceeding 0°C so that the gravel-sand can be well compacted.

TABLE 2.26

Values of function $f(L/B; q_{p2}/q_{p1})$

Ratio L/B	Function (f) for q_{p2}/q_{p1}				
	0.2	0.4	0.6	0.8	0.9
1.00	1.40	0.90	0.63	0.40	0.29
1.5	1.75	1.05	0.73	0.47	0.34
2.0	1.95	1.15	0.80	0.50	0.38
4.0	2.50	1.35	0.88	0.58	0.38
∞	3.30	1.50	0.90	0.58	0.38

2.8.4 Multilayered subgrade – two alternate soils

Often two soils alternate in the subgrade of a foundation. One soil forms pronounced layers which are divided by very thin layers of the other soil. The second soil has a lower shearing strength than the soil of the thicker layers

(for example in the case of thicker layers of clayey sand and clay.) Let us designate Φ_1, c_1 the angle of internal shearing resistance and the cohesion of the thicker layers and Φ_2, c_2 the angle of internal shearing resistance and the cohesion of the thinner layers. The solution of the ultimate bearing capacity of such a strata group was made by Giroud (1971) for cases where $\Phi_2 \leq \Phi_1$, $c_2 \leq c_1$, $\frac{c_1}{c_2} = \frac{\cot \Phi_2}{\cot \Phi_1}$ and when the surfaces of the layers are parallel. He found that the resultant ultimate bearing capacity q_m of such a strata group

TABLE 2.27

Reduction coefficient λ

$\Phi_1 - \Phi_2$	0°	5°	10°	15°	20°	25°	30°	35°	40°
λ	1.00	0.89	0.79	0.69	0.60	0.52	0.44	0.37	0.31

TABLE 2.28

The largest permissible values of angle κ

Φ_1	Φ_2				
	0°	10°	20°	30°	40°
10°	0°	40°	—	—	—
20°	0°	10°	35°	—	—
30°	0°	5°	11.5°	30°	—
40°	0°	2.5°	6°	10°	25°

depends almost entirely on the angles of internal shearing resistance of the two soils Φ_1 and Φ_2 and he derived a simple equation

$$q_m = q_{m1} \lambda \quad (2.114)$$

where q_{m1} is the ultimate bearing capacity of a homogeneous subgrade composed of the soil of the thicker layers, λ is the reduction coefficient whose values depend on the difference between the angles of internal shearing resistance ($\Phi_1 - \Phi_2$). The values of λ are given in Table 2.27. The equation (2.114) is valid for horizontal layers and for those which form an angle κ with the horizontal, if the size of κ does not exceed the values given in Table 2.28 in relation to angles Φ_1 and Φ_2 .

3. PERMISSIBLE LOADS ON FOUNDATIONS

The designer tries to make proper use of the building material throughout his design. Nowadays the foundation soil which carries the building is considered to be one of the building materials. The permissible load of the building is a load for which there is a sufficient safety factor against sinking (against reaching the ultimate bearing capacity), raising, pulling out, uprooting, turning over and displacement and the total settlement and the differences in the settlement of the building and the deflections of the vibrating foundation are smaller than the permissible values. It is therefore necessary to determine for each foundation both the ultimate bearing capacity q_m and the final settlement of the building, as larger differences in the settlement of the building result in the creation of fissures. The permissible load of the foundation¹⁾ must not be reached in either of the mentioned ultimate states. In the case of buildings in the vicinity of those already standing, it is also necessary to judge the influence on the adjacent buildings, so that no fissures, etc. are created in them. The reason for this is that the stress caused by the new building also spreads beneath the old building. Sand, if it is not loose, is only slightly compressible and the foundation settles very little. Therefore in the case of buildings based on cohesionless soils, it is sufficient just to calculate the ultimate bearing capacity q_m .

3.1 PERMISSIBLE VALUES OF SETTLEMENT AND SETTLEMENT DIFFERENCES

The permissible values of settlement depend on the type and rigidity of the building. The building can be designed to be very yielding, thus enabling it to bear a large non-uniform settlement. Such an approach is necessary for example in the case of buildings on embankments, in undermined areas, in regions with intense seismic activity, in the case of warehouses where the stored materials produced a large and non-uniform settlement of the building, etc. But for the majority of buildings no special arrangements for unusual settlement need be made. The permissible values of differences in settlement Δs and

¹⁾ The permissible loading of foundations is a broader term than the calculated strain on the foundation soil in the sense of ČSN 73 1001 Foundation Soil under Shallow Foundations. This also includes the important influence of adjacent foundations, contact stresses, building structures, etc.

of the mean settlement S , which should not be exceeded, are given in Table 3.1 and in Fig. 3.1 (diagram of measuring).

The dimensions of the foundation are made for a permissible load which allows the building to settle uniformly. This load is not usually reached simultaneously on all foundations, for example in the case of warehouses or in factory halls with a travelling overhead bridge-crane. The load of the crane is carried mainly by the nearest columns and the more distant columns may not be loaded by the crane at all. Thus we get a non-uniform settlement and we assume that it amounts to about 50 % of the total settlement of the building. Closer data based on measurements are given by Siemer (1973). According to him, the differences in settlement in a building on separate foundations amounts to 60 – 70 % of the total settlements. For strip foundations this value is 50 – 60 %, for a reinforced grid it is 40 – 50 %, for a foundation slab it is 30 – 40 % and for a box foundation it is about 30 % of the total settlement. The permissible difference of settlement of brickwork walls, for a ratio of the height of the wall to its length $H/L < 0.5$, is according to Siemer $L/200$ and $L/300$ and for a ratio $H/L > 1$, he permits from $L/400$ to $L/600$. The lower values of the ratios relate to cohesionless soils and the higher values relate to foundations on cohesive soils. For reinforced skeleton structures a difference in settlement of $l/500$ on cohesionless soils and $l/300$ on cohesive soils is permitted, where l is the separation of adjacent columns of the frame.

In practice we often come across a situation where the permissible or required values of settlement of one structure are a function of the settlement of another structure. The same applies to differences of settlement and sometimes also to the toleration of certain deflections of dynamically loaded foundations.

Until now we have considered only the settlement of building foundations and structures resulting from static loads or loads which change only as much as the change in the live load, which is larger or smaller than the permanent

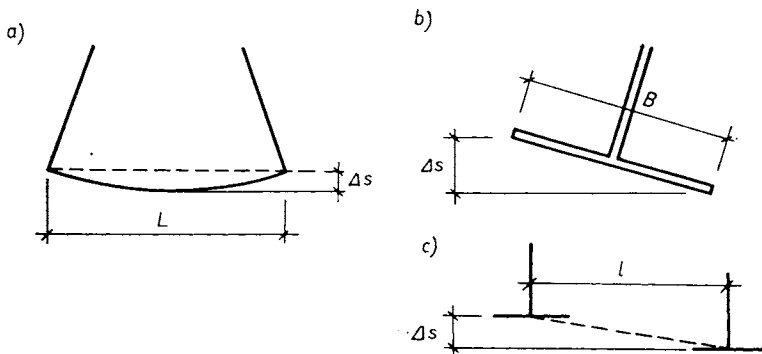


Fig. 3.1 The diagram of the measurement of the differences in the settlement of buildings

TABLE 3.1

Ultimate values of the settlement of foundations (according to ČSN 73 1001)

Type of building	The foundation soil consolidates				
	very quickly (for example, sands)		slowly (for example, clays)		
	difference of settlement	total settlement	difference of settlement	total settlement	
	$\Delta s/L$	s [cm]	$\Delta s/L$	s [cm]	
1. Buildings: panels ¹⁾	0.0005	6	0.0007	8	
	(0.002)	(7)	(0.002)	(5)	
	bricks and blocks	0.0007	6	0.001	8
	bricks, block reinforced with concrete strips	0.001	8	0.0013	10
reinforced concrete skeleton	0.0007	6	0.001	8	
	$\Delta s/l$	s [cm]	$\Delta s/l$	s [cm]	
2. Structures: statically determinate	0.003	10	0.003	10	
	statically indeterminate	0.0015	6	0.002	8
	steel	0.001	4	0.0015	6
	statically indeterminate reinforced concrete				
	$\Delta s/B$	s [cm]	$\Delta s/B$	s [cm]	
rigid and massive massive foundation	0.005	20	0.005	20	
to a height of 20 m higher than 20 m (chimneys)	0.002	10	0.002	10	
	$\Delta s/l$	s [cm]	$\Delta s/l$	s [cm]	
3. Crane tracks with bridge crane longitudinally and laterally	0.0015	—	0.0015	—	

¹⁾ Values in brackets are according to Professor Šimek, mentioned in the Proposed Code for the Foundations of Panel Housing. Difference of settlement values are used when there is strong no connection between adjacent vertical structures.

load by the same order of magnitude. We get a more complicated situation when the load alternates, i.e. when the foundation is alternatively subjected to tension and compression of such a magnitude that there is an adequate safety factor against depression, uprooting, displacement, etc. As the soil in the foundation line can only resist compression, the tension forces are borne by the soil through the friction on the sides of the foundation. To enable the foundation to transfer forces by friction on its sides, there must be a certain displacement during which particles of the soil come into contact with the irregularities of the surface of the foundation. This causes the mobilization of friction. After a change in the direction of application of the force, the soil comes into contact with the irregularities of the surface of the foundation from the other side, as the foundation is slightly displaced in the direction of the applied force. If the foundation is being pulled outwards from the soil in the previous phase, then a small gap is created at the foundation line. This gap closes after a change in the direction of the applied force. The smaller the cohesion between the soil and the foundation, and the smaller the lateral pressure, the greater the movement of the foundation. During the loading cycles the foundation moves and this alone may be not tolerable. Apart from that, the cyclic movements can cause a change in the mechanical properties of the soil near the foundation, especially if the groundwater level is higher. Usually there is a tendency to eliminate the alternating loading of the soil, for example by increasing the dead weight of the foundation, but sometimes, in the case of dynamic loading, a certain amount of movement of the foundation is allowed.

According to ON 73 1020 Foundations for Machinery with Rotating Parts, the following amplitudes y of forced oscillations of a foundation for various revolutions are permitted:

- | | |
|--------------------------|---------------|
| a) 750 rev/min (12.5 Hz) | $y = 0.10$ mm |
| b) 1 500 rev/min (25 Hz) | $y = 0.06$ mm |
| c) 3 000 rev/min (50 Hz) | $y = 0.03$ mm |

From the public health point of view vibrations with a frequency between 2 and 6 Hz are not allowed and the maximum velocity of the movement (amplitude of velocity) of the foundation should not exceed $v = 2$ mm/s, at most $v = 10$ mm/s. The following relationship between frequency f , amplitude of deflection y , amplitude of velocity v and the amplitude of acceleration a for a harmonic motion is valid

$$y = a/(2\pi f)^2 = v/(2\pi f) \quad (3.1)$$

3.2 SAFETY FACTOR AGAINST THE SINKING OF A FOUNDATION

When designing foundations the determination of the permissible load from the ultimate bearing capacity of foundations can be made in one of two ways. The ultimate bearing capacity q_m is in the first case divided by the safety factor F , so that the permissible load

$$q_p = \frac{q_m}{F} \quad (3.2)$$

and in the second case the shearing parameters of the soil and the density of the soil are decreased, and the load is increased by dividing or multiplying these values by a partial safety factor. In the first case the safety factor includes smaller shearing parameters than those which were measured in the soil samples, and the compression curve is taken into account. At first, the curve forms a straight line, then with increase of load the settlement grows first of all very slowly, then more or very suddenly as in the case of loading on sand. An adequate safety factor for a foundation soil formed by sand is $F = 2$. In the case of clay, after a short, straight-line relationship between the load and the settlement, the dependence forms a curve for which it is very difficult to determine the ultimate bearing capacity. Because of this we choose for clays a factor of safety $F = 3 - 4$. These values also include the inaccuracies contained in the determination of the shearing parameters, the density of the soil, the acting load, especially the live load, the creation of plastic ranges, the simplification of the method of calculation, etc.

In the second case, partial coefficients are used, by which the acting load, the strength of the material and the parameters of the strength of the soil are multiplied or divided. The load produced by the building can be determined with a large safety factor. The same applies for water pressure, if we know the water level, and therefore the partial safety factor in these cases $f_g = 1$. The partial safety coefficients according to the Danish standard are given in Table 3.2.

A normal load is the sum of permanent and long-term live loads and wind pressure. An unusual load is the sum of permanent and live loads including unusual loads. A transient load is an unusual load at various stages of the building process, and the load in the case of temporary buildings.

The input value is multiplied or divided by these coefficients in order to obtain less favourable values which lead to a greater safety of the structure. For example in the calculation of the bearing value of a foundation we take $\tan \bar{\Phi} = \tan \Phi / f_\Phi$, cohesion $\bar{c} = c / f_c$, wind pressure $\bar{w} = w \cdot f_w$, negative friction for piles $\tan \bar{\Phi} = \tan \Phi \cdot f_\Phi$, etc. The advantage of the partial coeffi-

cients is that their values depend on the variable reliability with which the different values can be determined.

The permissible loading of foundation soil depends on factors related not only to the subgrade of the foundations, the character and size of the load, but also to the size, shape, distribution and rigidity of the foundations themselves, as well as to the rigidity of the upper structure of the building. If during the determination of the ultimate bearing capacity of a foundation the influence of an adjacent foundation is considered, it is necessary to consider the true values of the angle of internal shearing resistance of the soil and its density. Only in this way can the static calculation be made to correspond with the real case. The interaction of adjacent foundations depends mainly on the relative

TABLE 3.2

Partial safety factors f

Symbol	The partial factor is valid for	The value of the factor if the load is		
		normal ¹⁾	unusual ²⁾	transient
f_g	dead load hydrostatic pressure	1.0	1.0	1.0
f_p	content of silos, load on surface of area live load	1.3	1.3	1.15
		1.5	1.5	1.25
f_w	wind effect	1.5	1.0	1.25
f_Φ	coefficient of friction ($\tan \Phi$) for the calculation of slope stability and earth pressure	1.2	1.1	1.1
	coefficient of friction for the calculation of flat foundations and piles	1.25	1.15	1.15
f_c	cohesion for the calculation of slope stability and earth pressure	1.5	1.4	1.4
	cohesion for the calculation of the bearing value of flat foundations	1.75	1.6	1.6
	cohesion for the calculation of the bearing value of piles	2.0	1.8	1.8
f_a	friction on the skin of piles	2.0	1.8	1.8
f_b	the bearing value of tested piles	1.4	1.25	1.25
	the bearing value of other piles	1,6	1,45	1,45

1) i.e. approximately equal to the basic combination of loads according to ČSN 7300 35

2) i.e. approximately equal to the extreme combination of loads according to ČSN 7300 35

positions of the foundations and on the shape of the rupture surfaces which are created when the ultimate bearing capacity is reached. The shape of the rupture surfaces depends on the angle of internal shearing resistance, and the foundations influence each other more and to a greater distance, in proportion

TABLE 3.3

The minimum safety factor F

Load on foundation; stability	Subgrade of foundation	F	Failure when ultimate state is reached
Vertical pressure	Loose or homogeneous or bedrock	2	Sinking
	Cohesive and homogeneous or bedrock $c < 10 \text{ kN/m}^2$	2.5	
	$10 < c < 30 \text{ kN/m}^2$	3	
	$c > 50 \text{ kN/m}^2$	4	
	Double-layer: loose and cohesive	3	
	Double-layer: both cohesive	4	
	Cohesive layer to a depth between $3B$ and D if $D > 5B$, lower down loose soil	2.5	
Gravel-sand cushion in a cohesive soil	2.5		
Vertical tensile force	Any kind, also below groundwater level	1.5	Drawing-out Raising
Horizontal force	Any kind, during earthquake	1.5	Displacement Shearing
	Any kind, in other cases	2	
Vertical force and moment	Any kind	2	Turning over
Moment; vertical and horizontal force very small	Homogeneous and loose (simplified calculation according to Dembicky)	2 (2.5)	Uprooting
	Cohesive and homogeneous $c < 10 \text{ kN/m}^2$	2.5	
	$10 < c < 30 \text{ kN/m}$	3	
	$c > 50 \text{ kN/m}^2$	4	
Stability of slope	Homogeneous soil $0 \leq c < 30 \text{ kN/m}^2$	1.2	Sliding
	$c > 50 \text{ kN/m}$	1.4	
Movement of toe of slope	Any kind, homogeneous	1.8	Displacement

to the increase of the angle Φ . The influencing of adjacent foundations of various widths and arrangements can cause not only a large increase, but also a decrease, of the bearing value. In such a case, the introduction of the reduced angle of internal shearing resistance into the calculation would lead to a decrease of the safety of the structure, since it means that we take into account a smaller decrease of the bearing value as a result of the influence of the adjacent foundation than we would get in reality. We avoid this risk if, in the calculation, we use the true values of the shearing parameters Φ and c and if, for the determination of the tolerable load of the foundation soil, we use one safety factor F . An acceptable foundation is one for which the ratio of the ultimate vertical force Q_m on the foundation surface, to the vertical component of the resultant of the outer forces, obtained from the least favourable regulation loads, is equal at least to the safety factor F , whose smallest values are given in Table 3.3. Factors F for different types of loads and for judging the stability of slopes and the foot of a slope are also given.

4. STRESS IN SOIL BENEATH BUILDING FOUNDATIONS

4.1 DISTRIBUTION OF LOADS IN THE FOUNDATION LINE

When designing foundations of buildings which behave as continuous beams or slabs, we must determine whether or not the permissible stress of the material of the foundation is exceeded for the given, least favourable load. The assessment is based on the bending moments and the shearing forces in the dangerous section of the foundation. To be able to determine these values, it is necessary to know the true distribution of the load in the foundation level. This also influences the size and distribution of the stress in the soil on which, again, the magnitude of the settlement of the building depends. The distribution of the load in the foundation line depends mainly on the rigidity of the foundation and the rigidity of the whole building.

Whether or not it is possible to consider the foundation in the direction of its width B or its length L as rigid, is determined by the rigidity coefficient of Schultze

$$K_t = \frac{E_z}{12E_0} \left(\frac{H}{B} \right)^3 = \frac{1}{12N} \quad (4.1a)$$

where H is the height of the foundation,

B is the width of the foundation when judging a foundation in a lateral sense; when judging the foundation in a longitudinal sense we substitute the length of the foundation L instead of B ,

E_z is the elastic modulus of the material of the foundation,

E_0 is the elastic modulus of the soil,

N is the rigidity number.

If the section of the foundation slab has cavities, the elastic modulus of the material is multiplied by the ratio J_z/J'_z ,

where J_z is the moment of inertia of the full profile (no cavities) of the foundation and

J'_z is the moment of inertia of the foundation profile with cavities, so that the coefficient of rigidity

$$K_t = \frac{E_z J_z}{12E_0 J'_z} \left(\frac{H}{B} \right)^3 \quad (4.1b)$$

J. Šimek (1971) made an analysis of contemporary knowledge about the distribution of the contact stresses in the foundation line. He mentions that for $K_f > > 0.25$, it is possible to consider the foundation as perfectly rigid. Grasshof starts by assuming that the foundation is rigid then determines the distribution of the loads in the foundation line for a rigid foundation and calculates the deflection of the foundation structure. If the deflection is smaller than 1/10 of the total mean settlement, the structure behaves as if it were rigid, if the soil beneath the foundation reaches to a depth which is 1.7 – 2.0 times greater than the width (diameter) of the foundation.

The distribution of the load in the foundation line is solved on the assumption that the outer load must be in equilibrium with the stress in the foundation line, and that as a result of the acting load the vertical displacement of each point of the foundation must be of the same magnitude as the settlement of the soil beneath this point. For a non-rigid foundation, it is also necessary to consider the rigidity of the upper part (German, Überbau) of the building. The distribution of the load in the foundation line is determined, for example, by the method of imaginary members, the method of Kany, or the method of Glick. These methods lead to the solution of rather extensive systems of equations, which today are solved by computer. If the foundation is not yielding, then the distribution of the load formed in the foundation line is different from the load due to the upper part of the building. The difference increases in proportion to the increase of the rigidity of the foundation. Thin foundation slabs and strip foundations are usually not perfectly rigid in a longitudinal sense, if the load acts only in some places (loading by individual columns, etc.). The rigidity of the foundation is judged according to equation (4.1), where we replace the width of the foundation B by its length L . For the determination of the contact stress below a non-rigid foundation, a comprehensive method was derived by Grasshoff (1966). A strip foundation with a width B is divided into i equal parts and the diagram of the distribution of the loads $q(y)$ is replaced by triangular loads as in Fig. 4.1. The continuous curve of the contact stresses $q(y)$ is thus replaced by a broken line given by the ordinates $q(i)$. The greater the number of parts i chosen, the more accurate the determination of the contact stress, but the calculation is more lengthy. In normal cases it is sufficient to divide the foundation into 5 to 10 parts. We start from the curve of the final subsidence s_y , which is given for each point y by the expression

$$s_y = f_{ay} - f_{by} + \left(\frac{i - y}{i} \right) s_0 + \left(\frac{y}{i} \right) s_i \quad (4.2)$$

For point $y = 2$ and for a division of the strip foundation into 10 parts ($i = 10$)

$$s_2 = f_{a2} - f_{b2} + 0.8s_0 + 0.2s_{10}$$

The deflections f_{ay}, f_{by} can be easily determined by the procedure described further on (according to Grasshoff), if the upper part of the building is statically determinate or is substantially more yielding than the foundation.

The deflections f_{ay} of a foundation (for example, a strip foundation) are determined according to building mechanics in the same way as for a simple

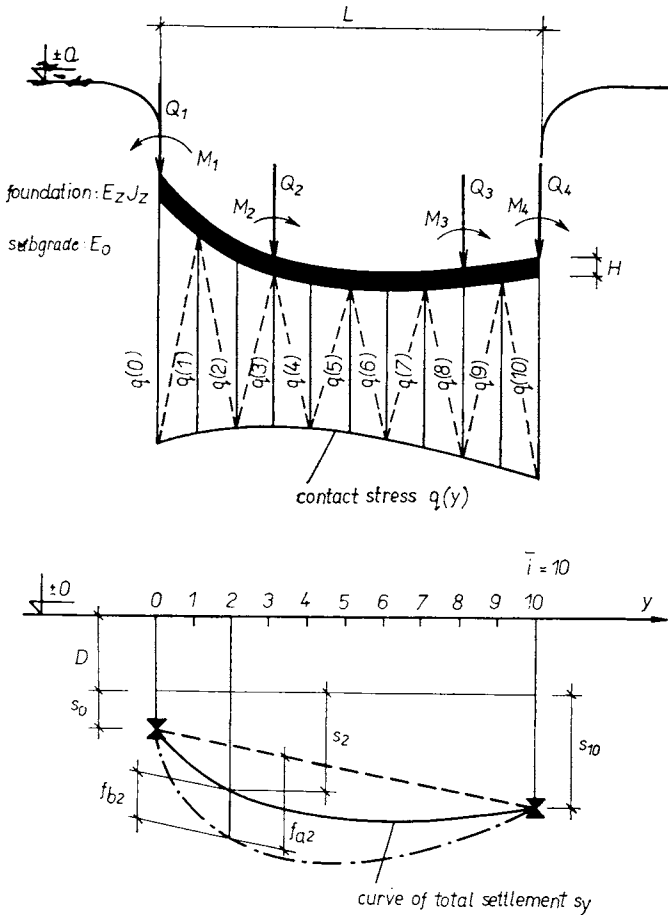


Fig. 4.1 Diagram for the calculation of the distribution of the load in the foundation line

beam supported at the extremities $y = 0$ and $y = \bar{i}$. The beam is loaded by a vertical force Q , which includes the weight of the foundation, by the moments M , and if necessary also by other loads applied to the foundation from above.

Deflections f_{by} caused by values to be determined of the contact stress in the foundation line are determined according to the same principles as the deflections f_{ay} . The load is formed by triangular loading surfaces at the points i . In

Fig. 4.1 this surface is marked by a dotted line for point $i = 2$. The deflection f_{by} at point y is the sum of the partial deflections f_{byi} . The following relationship is valid

$$f_{by} = \frac{1}{E_z} \left(\frac{L}{H} \right)^3 \sum_{i=0}^{\bar{i}} \vartheta_{yi} q(i) \quad (4.3)$$

where ϑ_{yi} is the influence factor of the deflection of point y from contact forces to be determined, distributed triangularly in the vicinity of points i . The influence factors are determined from the partial deflections f_{byi} , assuming unit ordinates, i.e. the heights of the triangular loads. If a number of parts $\bar{i} \geq 8$ is chosen, it is possible, during the calculation of ϑ_{yi} , to replace the triangular loads at points i by concentrated forces acting at points i . At point $i = 0$ and $i = \bar{i}$ we get $Q_z = L/2\bar{i}$, at other points we get $Q_z = L/\bar{i}$. For a constant rectangular section ($E_z J_z$ are constant; $B = 1$), a formula for the calculation of ϑ_{yi} in the following form was derived

$$\vartheta_{yi} \doteq 2Q_z y (\bar{i} - i) (2\bar{i}i - i^2 - y^2) / \bar{i}^4, \text{ if } y \leq i.$$

At points $y > i$ we proceed in a similar way from the other side of the beam. The calculated values $10\vartheta_{yi}/Q_z$ are given in Table 4.1 for a foundation divided into 8 parts.

TABLE 4.1

Influence factors $10\vartheta_{yi}/Q_z$ for a rectangular section; $E_z J_z = \text{constant}$; $B = 1$; $\bar{i} = 8$

y	part i								
	0	1	2	3	4	5	6	7	8
0	0	0	0	0	0	0	0	0	0
1	0	0.48	0.79	0.93	0.92	0.79	0.57	0.30	0
2	0	0.79	1.41	1.71	1.72	1.49	1.10	0.57	0
3	0	0.93	1.71	2.20	2.29	2.03	1.49	0.79	0
4	0	0.92	1.72	2.29	2.50	2.29	1.72	0.92	0
5	0	0.79	1.49	2.03	2.29	2.20	1.71	0.93	0
6	0	0.57	1.10	1.49	1.72	1.71	1.41	0.79	0
7	0	0.30	0.57	0.79	0.92	0.93	0.79	0.48	0
8	0	0	0	0	0	0	0	0	0

The subsidence s_y of point y is calculated under the characteristic points of the foundation. Here the contact stress in the direction of the width B is almost independent of the rigidity of the foundation. For strip foundations this condition is fulfilled approximately at a distance of $0,37B$ from the axis

of the foundation. The settlement beneath the characteristic point of the foundation

$$s_y = \frac{1}{E_0} \left[\sum_{i=0}^{\bar{i}} \xi_{yi} q(i) - \gamma_2 D \sum_{i=0}^{\bar{i}} \xi_{yi} \right] \tag{4.4}$$

ξ_{yi} is the influence factor of settlement in point y , caused by a contact load $q(i)$ to be determined, acting at point i . The influence factor is an E_0 multiple of the settlement at point y caused by an unit load increment acting in the foundation line in the vicinity of point i to a distance of $L/2\bar{i}$, i.e. if the load increment in the foundation line is $(1 - \gamma_2 D)$ in kN/m^2 . [For greater depths of foundation it is better to use a load increment $(10 - \gamma_2 D)$, etc.] The equation (1.12) has an universal application and the calculation is simplified, for example, by equation (1.24) or (1.25).

Table 4.2 gives the influence factors ξ_{yi}/Q_z , determined from equation (1.24) for a rectangular foundation with a ratio of sides 1 : 8, based on the ground surface, if $\bar{i} = 8$; $\nu = 0.35$; $B = 1$. The table also gives the values of factor ξ_y , according to equation (4.9). During the calculation of values ξ_{yi} and ξ_y it is necessary to start with the ration of the sides of the foundation sections in the vicinity of point i . In our case, the central sections are square and the end sections are rectangular with a ratio of the sides 0.5.

For the calculation of ordinates $q(i)$ of the contact stress at the points located by coordinates $i = 0; 1; \dots; \bar{i}$, we get by substitution from equation (4.2) a system of equations

TABLE 4.2

Influence factors ξ_{yi}/Q_z and factors ξ_y for a rectangular foundation ($L/B = 8$), if $D = 0$; $\nu = 0.35$; $B = 1$; $\bar{i} = 8$

part y	ξ_{yi}/Q_z for $i = 0$ to 8									ξ_y
	$i = 0$	1	2	3	4	5	6	7	8	
0	0.28	0.17	0.08	0.05	0.04	0.03	0.03	0.02	0.02	0.071L
1	0.15	0.56	0.17	0.08	0.05	0.04	0.03	0.03	0.02	0.130L
2	0.08	0.17	0.56	0.17	0.08	0.05	0.04	0.03	0.03	0.145L
3	0.05	0.08	0.17	0.56	0.17	0.08	0.05	0.04	0.03	0.149L
4	0.04	0.05	0.08	0.17	0.56	0.17	0.08	0.05	0.04	0.150L
5	0.03	0.04	0.05	0.08	0.17	0.56	0.17	0.08	0.05	0.149L
6	0.03	0.03	0.04	0.05	0.08	0.17	0.56	0.17	0.08	0.145L
7	0.02	0.03	0.03	0.04	0.05	0.08	0.17	0.56	0.15	0.130L
8	0.02	0.02	0.03	0.03	0.04	0.05	0.08	0.17	0.28	0.071L

$$\sum_{i=0}^{\bar{i}} (\vartheta_{yi}N + \eta_{yi}) q(i) = f_{ay}E_0/L + \kappa_y \bar{q} \quad (4.5)$$

where the auxiliary functions

$$N = \frac{E_0}{E_z} \left(\frac{L}{H} \right)^3 \quad (4.6)$$

$$\eta_{yi} = \xi_{yi} - \left(\frac{\bar{i} - y}{\bar{i}} \right) \xi_{0i} - \left(\frac{y}{\bar{i}} \right) \xi_{i\bar{i}} \quad (4.7)$$

$$\kappa_y = \xi_y - \left(\frac{\bar{i} - y}{\bar{i}} \right) \xi_0 - \left(\frac{y}{\bar{i}} \right) \xi_{\bar{i}} \quad (4.8)$$

$$\xi_y = \sum_{i=0}^{\bar{i}} \xi_{yi} \quad (4.9)$$

$$\bar{q} = \gamma_2 D \quad (4.10)$$

Apart from equations (4.5), a cumulative condition in a vertical sense is used for the calculation of the values of the distribution of the load $q(i)$

$$(q(0) + q(i))L/2\bar{i} + \sum_{i=1}^{\bar{i}-1} Lq(i)/\bar{i} + \Sigma Q = 0 \quad (4.11)$$

and if necessary also a moment condition, for example, to the end-point of the beam.

The distribution of the load, determined in this way, is non-uniform along the foundation. The calculated distribution of the load is a mean value for the width of the foundation. If it is also necessary to know the distribution of the stress accurately in a lateral direction, then this distribution must be determined separately with a view to the rigidity of the foundation in a lateral sense. The advantage of this method is that it takes into account the depth of foundation, the changes in shape and section of the foundation and the true values of settlement in the given geological conditions (the influence of the stratification of the subgrade, etc.) and also the fact that the vicinity of the foundation settles, as a result of the load increment, far less than the foundation itself.

With the exception of very thin foundation slabs beneath frame structures, foundations are usually almost rigid across their width. For rigid foundations, the determination of the stress distribution for a plastic-elastic state, introduced by Schultze (1961), is appropriate. It combines the solution for a plastic state according to Prandtl and Buisman with the solution according to Boussinesq (and if necessary as supplemented by Borowicka by the influence of the eccentricity of the load) for an elastic state of the subgrade. The procedure is as follows. Firstly, the stress for the plastic state of the soil in the subgrade, which is applied at the edges of the foundation, is determined in the foundation

line of a unit length footing. For a small eccentricity $e < 0.25B$, the value of the stress $q(x)$ in the examined point of the foundation line at a distance x from the axis of the strip foundation is

$$q(x) = \gamma_1 N_\gamma B(1 - 2x/B) + \gamma_2 DN_q + cN_c \tag{4.12}$$

In this way the stress is limited at the edge of the foundation and it can reach only a certain maximum if the soil is in a plastic state. The nearer the mean load q of the foundation is to the ultimate bearing capacity q_m , the larger the plastic ranges. If $q < q_m$, then in the vicinity of the centre of the strip foundation the distribution of the stress is calculated for an elastic state. For $e \leq 0.25B$, the value

$$q(x) = \frac{2q_0(1 + 8ex/B^2)}{\pi \sqrt{1 - (2x/B)^2}} \tag{4.13}$$

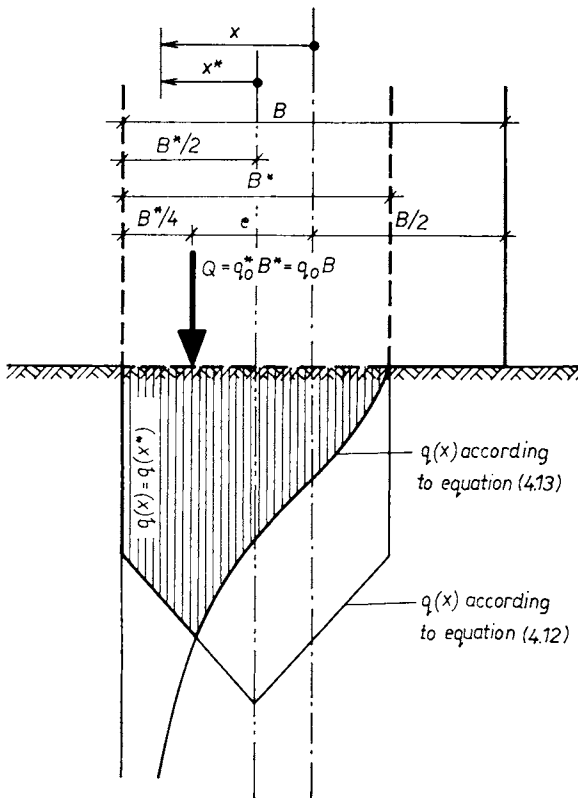


Fig. 4.2 Diagram of the distribution of the load in the foundation line of a rigid strip foundation, if the point of application of the resultant of the load Q has an eccentricity $e > 0.25B$

The diagram of the distribution of the load in the foundation line is bounded at each point by the smaller of the ordinates $q(x)$, calculated according to equations (4.12) and (4.13). The surface of the load distribution in the foundation line must be equal to the surface $q \cdot B$. To fulfil this condition we must, during the calculation of equation (4.13), estimate the size of the load in the foundation line q_0 to be able to determine the stress transferred in the central part of the foundation during an elastic state of stress. The distribution of the load and the size of this surface is determined from the estimated q_0 . If this surface is not approximately equal to the surface $q \cdot B$ then we must estimate another value of the load q_0 and determine the distribution of the load again, until adequate agreement of the surface is obtained. If the eccentricity of the load on a rigid foundation is large, the foundation is uprooted from the soil on one side. This state is found, according to Borowicka, for an eccentricity $e > 0.25B$, when the compressive stress is applied only in the effective width of the foundation line $B^* = 2(B - 2e)$. The distribution of the load in the foundation line is determined as for a foundation with a width B^* and an eccentricity of the acting load $e^* = 0.25 B^*$ (Fig. 4.2). Equations (4.12) and (4.13) are used in which we substitute e^* for e ; B^* for B ; $x^* = x + B/2 - 2e$ for x ; $q_0^* = q_0 B/B^*$ for q_0 .

Equations for the determination of the distribution of the load for a circular foundation were derived according to the same principles as for the determination of the distribution of the load under a rigid strip foundation. For a rigid circular foundation loaded centrally or with a small eccentricity $e \leq r/3$ the following is valid:

$$q(x, \bar{r}) = 1.8\gamma_1 N_y r(1 - \bar{r}/r) + \gamma_2 DN_q + 1.3cN_c \quad (4.14)$$

$$q(x, \bar{r}) = \frac{q_0(1 + 3ex/r^2)}{2\sqrt{1 - (\bar{r}/r)^2}} \quad (4.15)$$

where r is the diameter of the foundation,

\bar{r} is the radial distance of the point where the contact stress is being determined from the centre of the foundation,

x is the distance from the centre of the foundation, measured in the direction of the axis x of the point where the contact stress is being measured.

the x axis is oriented in such a way that the point of action of the resultant of the load lies upon it.

Contact stresses in the foundation line form a body above the ground-plan of the foundation, which is bounded by the smaller of the values on the ordinates, determined for individual points of the foundation surface, according to equations (4.14) and (4.15). The load q_0 , used for the determination of the

stress in the vicinity of the centre of the foundation during an elastic state of stress, is determined from the condition that the volume of the body of the contact stresses must be equal to the volume

$$V = q_0 \pi r^2 \quad (4.16)$$

if q_0 is the mean stress on the foundation surface. The volume V of the body of the contact stresses is

$$V = \int_{x=-r}^{x=r} \int_{\bar{r}=-r}^{\bar{r}=r} q(x; \bar{r}) dx d\bar{r} \quad (4.17)$$

For an approximate calculation of the integrals, the ground-plan of the foundation is divided by a grid and the mean value of the contact stress in the centre of each element of the grid is determined. The volume of the whole body of the contact stresses is equal to the sum of the volumes above the elements of the grid. To determine the vertical stresses in the subgrade, it is advantageous to use the method of Newmark (Sec. 4.2).

Example 4.1

The curves of the load distribution in the foundation line are illustrated in Fig. 4.3 which shows the load distribution for a strip foundation ($E_z = 21\,000\,000 \text{ kN/m}^2$) with a width $B = 1 \text{ m}$, a height $H = 0.5 \text{ m}$ and a length $L = 10 \text{ m}$. The strip foundation is loaded by vertical-swing stanchions, which act with a force of 250 kN at the end points of the foundation and with a force of 500 kN at the centre. The depth of foundation $D = 0$. The foundation soil is formed by firm clay, whose $\Phi = 10^\circ$, $c = 50 \text{ kN/m}^2$, $\gamma = 21 \text{ kN/m}^3$, $E_0 = 2\,630 \text{ kN/m}^2$.

In a longitudinal direction, the coefficient of rigidity

$$K_t = \frac{21\,000\,000 \cdot 0.5^3}{12 \cdot 2\,630 \cdot 10^3} \doteq 0.083 < 0.25 \quad (\text{according to Eq. 4.1})$$

so that the foundation is not rigid longitudinally. Therefore the longitudinal distribution of the load was determined according to Grasshoff (Fig. 4.3a). At the ends of the footing the soil is subjected to a load of 270 kN/m and in section $A - A'$ a load of 80 kN/m² is applied. These values are always average values for the whole width of the foundation in the examined point.

In a lateral sense, the section $A - A'$ is examined. In this section a mean load $q = 80 \text{ kN/m}^2$ is applied. The coefficient of rigidity, in the lateral sense

$$K_t = \frac{21\,000\,000 \cdot 0.5^3}{12 \cdot 2\,630 \cdot 1^3} \doteq 83 > 0.25 \quad (\text{according to Eq. 4.1})$$

which means that in the lateral sense the foundation is rigid. The distribution of the stress was determined using equations (4.12) and (4.13) and a curve, according to Fig. 4.3b, was obtained. At the centre of section $A - A'$ there is a load on the soil of 40 kN/m² and at the sides, where plastic ranges are already being created in the soil, the load is as much as 490 kN/m². Similarly it would also be possible to examine the distribution of the load in the other sections of the strip foundation.

The example shows the importance of the rigidity of the foundation for the distribution of the load in the foundation line. Although the mean load in the given example is only 100 kN/m^2 , in some places of the foundation surface there is a load as much as five times the size, and in other places it reaches less than half the value.

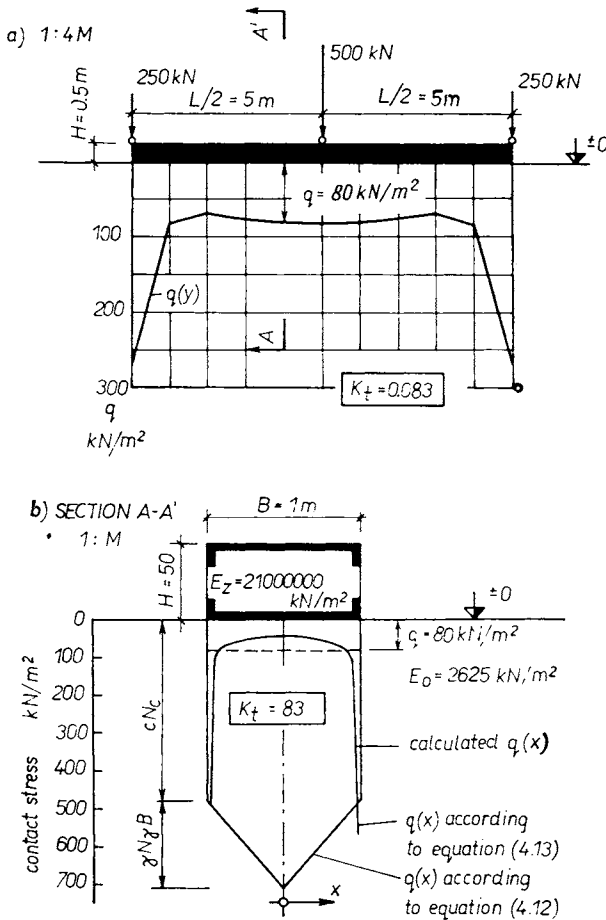


Fig. 4.3 The distribution of the load in the foundation line of a strip foundation (in Example 4.1); a) mean stress in a longitudinal direction (1 : 4M), b) distribution of the stress in cross-section A — A' (1 : M)

4.2 STRESS IN THE SUBGRADE OF FOUNDATIONS

The permissible load q_p in the foundation line is often two to three times smaller than the ultimate bearing capacity. For a load q_p , determined in this way, the relationship between the stress and strain of the foundation soil is approximately linear and the elastic state of stress is located in the extensive

central part of the foundation line. If the distribution of the stress in the foundation line is known, it is possible to determine the vertical, horizontal and shearing stress at an arbitrary point M below the level of the foundation line, according to elastic half-space theory.

For a general load $q(x)$ of a strip foundation with a width B , which is placed on the ground surface (Fig. 4.4a), there is at point M , which lies at a depth z and a distance \bar{x} from the axis of the foundation, a vertical stress

$$\Delta\sigma_z = \frac{2z^3}{\pi} \int_{\bar{x}-B/2}^{\bar{x}+B/2} q(x) \frac{dx}{(x^2 + z^2)^2} \quad (4.18)^1$$

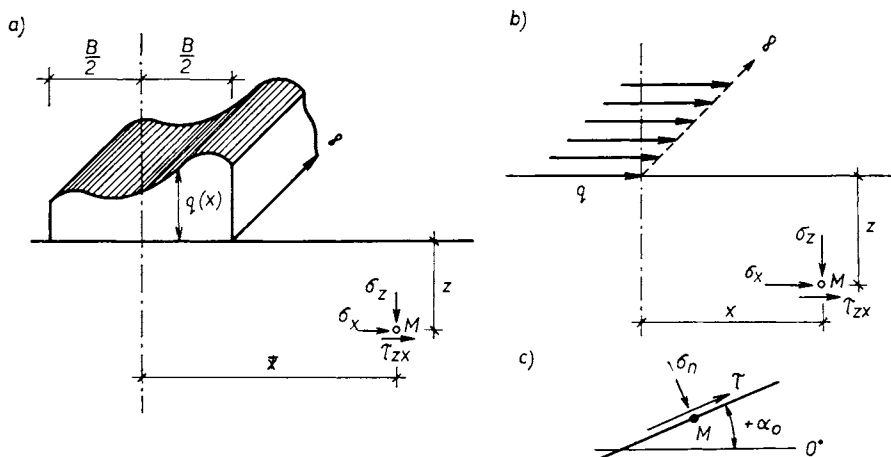


Fig. 4.4 Stress in soil for a load on the surface

a horizontal stress

$$\Delta\sigma_x = \frac{2z}{\pi} \int_{\bar{x}-B/2}^{\bar{x}+B/2} q(x) \frac{x^2 dx}{(x^2 + z^2)^2} \quad (4.19)^1$$

and a shearing stress, which is applied in a horizontal and vertical plane passing through point M

$$\Delta\tau_{zx} = \Delta\tau_{xz} = \frac{2z^2}{\pi} \int_{\bar{x}-B/2}^{\bar{x}+B/2} q(x) \frac{x dx}{(x^2 + z^2)^2} \quad (4.20)^1$$

¹) The curve $q(x)$ of the load can always be at least for certain sections of the interval $\langle \bar{x} - B/2, \bar{x} + B/2 \rangle$, replaced with sufficient accuracy by $q(x) = p_0 + p_1x + p_2x^2 + p_3x^3$. During the calculation of the stresses σ_x , σ_y , τ_{zx} we then obtain integrals of rational functions:

$$\int \frac{dx}{X^2} = \frac{x}{2z^2X} + \frac{Y}{2z^3}$$

If on the ground surface there is a horizontal line load q (Fig. 4.4b), then at point M there is a vertical stress

$$\Delta\sigma_z = \frac{2q}{\pi} \frac{z^2 x}{(x^2 + z^2)^2} \quad (4.21)$$

a horizontal stress

$$\Delta\sigma_x = \frac{2q}{\pi} \frac{x^3}{(x^2 + z^2)^2} \quad (4.22)$$

and a shearing stress

$$\Delta\tau_{zx} = \Delta\tau_{xz} = \frac{2q}{\pi} \frac{zx^2}{(x^2 + z^2)^2} \quad (4.23)$$

The total vertical stress

$$\sigma_z = \sigma'_z + u_w + \Delta\sigma_z \quad (4.24)$$

and the total horizontal stress

$$\sigma_x = K_0\sigma'_z + u_w + \Delta\sigma_x \quad (4.25)$$

where σ'_z is the effective vertical stress at a depth z ,

u_w is the neutral water stress at a depth z ,

K_0 is the coefficient of earth pressure at rest. For cohesionless soils

$K_0 = 0.4$ to 0.5 ; for cohesive soils $K_0 \doteq 0.66$; or we take, according

to Jáký $K_0 = 1 - \sin \Phi$. This is valid for normally consolidated

soils which have not been artificially compacted. At a small depth,

$$\begin{aligned} \int \frac{x \, dx}{X^2} &= -\frac{1}{2X} \\ \int \frac{x^2 \, dx}{X^2} &= \frac{Y}{2z} - \frac{x}{2X} \\ \int \frac{x^3 \, dx}{X^2} &= \frac{1}{2} \ln |X| - \frac{z^2}{2X} \\ \int \frac{x^4 \, dx}{X^2} &= \frac{x^3}{X} + \frac{3z^2 x}{2X} - \frac{3zY}{2} \\ \int \frac{x^5 \, dx}{X^2} &= \frac{x^4}{2X} + \frac{z^4}{X} - z^2 \ln |X| \end{aligned}$$

where $X = (x^2 + z^2)$

$Y = \arctan(x/z)$, i.e. $\tan Y = x/z$

as a result of compacting, overconsolidation, etc., we may get as much as $K_0 = 1/(1 - \sin \Phi)$, as shown also by field tests (Marsch 1975 and others).²⁾

From the components of the stress σ_x , σ_y , τ_{zx} at the point M , the normal stress σ_n and the tangential stress τ acting at point M on a surface inclined to the horizontal by an angle α_0 (Fig. 4.4c), are determined using the following relationships:

$$\sigma_n = \sigma_x \sin^2 \alpha_0 + \sigma_z \cos^2 \alpha_0 + \tau_{zx} \sin 2\alpha_0 \quad (4.26)$$

$$\tau = (\sigma_x - \sigma_z) \sin \alpha_0 \cos \alpha_0 + \tau_{zx} \cos 2\alpha_0 \quad (4.27)$$

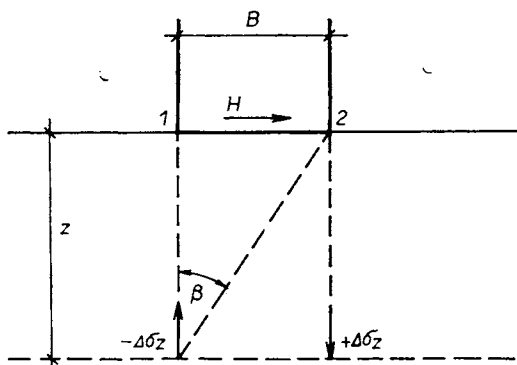


Fig. 4.5 Diagram for the determination of the vertical stresses $\Delta\sigma_z$ under the edges of a strip foundation loaded by a horizontal force H

For the vertical stress under the edges of an infinitely long strip foundation with a width B , if at the foundation line a uniform horizontal load H is applied, the following equation is derived

$$\pm \Delta\sigma_z = \pm \frac{H}{B} \frac{1}{\pi(1 + \cot^2 \beta)} = \pm \frac{H}{B} i_{wr} \quad (4.28)$$

The sense of the designations is apparent from Fig. 4.5. The stress $\Delta\sigma_z$, which is caused by the horizontal load on the foundation, is on a vertical passing through the edge 1 of the foundation negative ($-\Delta\sigma_z$) and on a vertical passing through the edge 2 of the foundation positive ($+\Delta\sigma_z$), i.e. the soil is compressed.

²⁾ Pruška (1971—1975) mentions for coefficient K_0 an interval $\tan\left(45^\circ - \frac{\Phi}{2}\right) \leq K_0 \leq \tan\left(45^\circ + \frac{\Phi}{2}\right)$

TABLE 4.3

Coefficients i_{wr} for various ratios z/B

z/B	0.0	0.25	0.50	0.75	1.000	1.50	2.00	3.00	4.0	6.0
i_{wr}	0.318	0.300	0.255	0.204	0.159	0.098	0.064	0.032	0.019	0.009

Loads are often inclined to the foundation. The load can be resolved into a vertical and horizontal component. The vertical load produces a vertical stress $\Delta^z\sigma_{zA}$ at point M_A , the horizontal component produces a vertical stress $\Delta^x\sigma_{zA}$, which has a negative value beneath the edge A of the foundation, so that below this edge the load causes a stress $\Delta\sigma_{zA} = \Delta^z\sigma_{zA} - \Delta^x\sigma_{zA}$. Below the other edge B a sum of both the stresses $\Delta\sigma_{zB} = \Delta^z\sigma_{zB} + \Delta^x\sigma_{zB}$ is applied. Further, below the edges A and B there is the vertical stress due to the soil itself $\gamma \cdot z$ (Fig. 4.6).

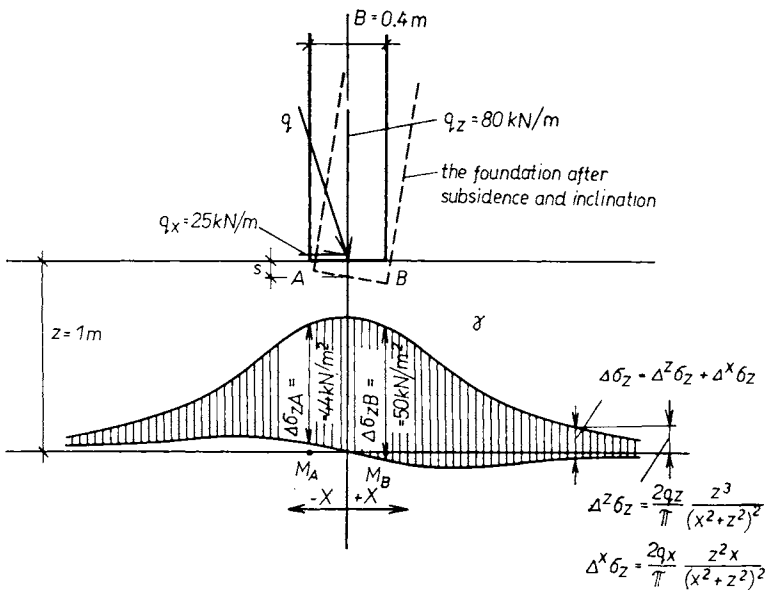


Fig. 4.6 Vertical stress at a depth z caused by an inclined line load

For a stress beneath both the edges determined in this way, the compression of the soil and the settlement of the building are calculated. Since on the vertical, beneath the edge A of the foundation, there is a smaller stress than beneath edge B, the foundation settles and tilts.

The case where the load in the foundation line acts at an angle in a plane at right angles to the longitudinal axis of the foundation, is often found in technical practice. The resulting tilt of the foundation can be avoided if the foundation is designed in such a way that the resultant of the inclined load acts eccentrically. According to Garnier (1973) the foundation will not tilt if the resultant of the inclined load intersects the axis of the foundation below the foundation line at a depth $z = 0,058B$ in the case of a strip foundation and $z = 0,035B$ in the case of a square foundation, if Poisson's ratio $\nu = 0,040$. For $\nu = 0,2$ we get $z = 0,131B$ for a strip foundation and $z = 0,080B$ for a square foundation.

According to Boussinesq, Newmark (1935) determined the vertical-load increment $\Delta\sigma_z$ at point $M(x, z)$ due to the load on the surface. The basic relationships are

$$\Delta\sigma_z = (1 - \cos^3 \alpha)/m; \tan \alpha = x/z \quad (4.29)$$

A circular diagram is constructed, which consists of n annuli and m sectors of a circle of the same size. The radii of the dividing circles, which are equal to the lengths x , are calculated in such a way that the expression $(1 - \cos^3 \alpha)$ grows uniformly from 0 to 1, for example by 0.05 for a specific z , from circle to circle. The depths z acts as a scale of the diagram. When determining the vertical stress at point M , the diagram is placed on the plan of the building in such a way that the centre of the diagram lies on point M . The plan of the building must be drawn to the same scale as the diagram. For each depth z of the point M from the surface, it is necessary to draw the plan of the foundation on a different scale, so that the abscissa z (marked on the diagram) corresponds to another depth of the foundation considered. The number N of the elements on the diagram covered by the plan of the loaded surface is determined. In each element N_i of the influence grid, a mean acting load q_i is assumed. In the adjacent elements a load of a different size may be applied and this enables the graded replacement of the non-uniform load on the foundation surface. The elements of the grid of the diagram are influence surfaces with values of $1/m \cdot n$. The total load increment $\Delta\sigma_z$ due to the load on the surface

$$\Delta\sigma_z = \frac{1}{m \cdot n} \sum N_i q_i \quad (4.30)$$

In Fig. 4.7 there is a diagram, constructed for an influence value of an element of the grid $1/m \cdot n = 0.002$. The number of sectors chosen is $m = 25$ and the number of the annuli $n = 20$. The radii of the circles, shown in the illustration, correspond to the gradient of the expression $(1 - \cos^3 \alpha)$ by a factor 0,05. The abscissa z , which acts as a scale for the diagram, is marked by a heavy line.

Example 4.2

The vertical stress at point M , which lies on the axis of the longer side of the foundation at a distance of 1 m away from it and at a depth $z = 2.5$ m below the surface, is to be determined for a yielding foundation, whose dimensions are 2×3 m and in whose foundation line there is an approximately uniform stress $q = 350 \text{ kN/m}^2$ (Fig. 4.7). The density of the soil is 20 kN/m^3 . The number of the covered elements $N_i = 61.5$. According to equation (4.30) the vertical-load increment $\Delta\sigma_z = 61.5 \cdot 350/25 \cdot 20 = 43 \text{ kN/m}^2$. The vertical stress

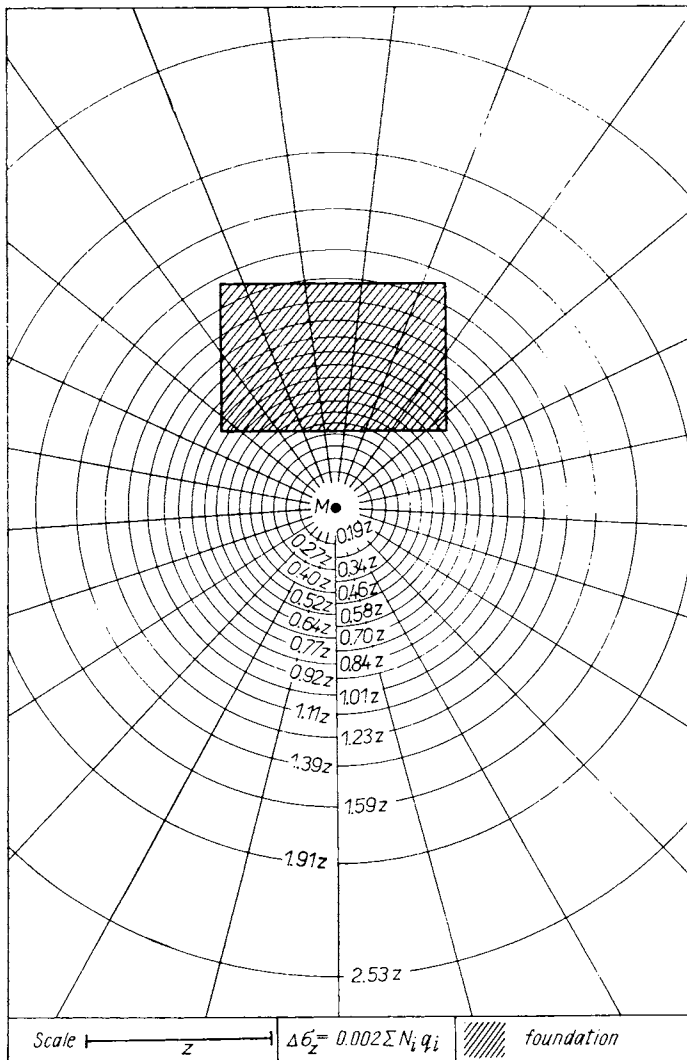


Fig. 4.7 Nomogram for the determination of the vertical stress in a homogeneous soil loaded on the surface

at point M from the dead weight $z \cdot \gamma = 2.5 \cdot 20 = 50 \text{ kN/m}^2$, so that after loading by the building we get a total vertical stress at the point considered $\sigma_z = 50 + 43 = 93 \text{ kN/m}^2$.

If we want to calculate the vertical stresses due to the load in a double-layer subgrade, whose upper layer has a deformation modulus E_{01} and lower layer has a deformation modulus E_{02} , we replace the depth of the upper layer h by

$$h_{eq} = h^{2.5} \sqrt{\frac{E_{01}}{E_{02}}}$$

and for this new surface we try to find the stress at a depth z , as though in the subgrade there was only soil of the lower layer. The stress at the top of the lower layer, whose $E_{02} < E_{01}$, is smaller then if the soil was homogeneous and had a constant deformation modulus E_{02} . (See also Appendix I.)

Up to now in the calculation of the stress in the subgrade of a building we have assumed a load acting on the surface of the area. The influence of the depth of foundation on the size of the vertical stress σ_z was studied by Melan (1932), Mindlin (1936), Széchy (1963), Kézdi (1964) and others. From published works it follows that, for foundation based below the surface, there is a reduction of the vertical stresses in the soil beneath the foundations as a result of the interacting of the soil above and below the foundation line. This reduction in the axis of a strip foundation, has for cohesive soils a maximum value at a depth approximately equal to the width of the foundation. The vertical stress at a depth $D = B/2$ is approximately 75 %, and at a depth $D = 2.5B$ about 50 % of the vertical stress which would be created in the soil by the same load, if it were applied on the surface ($D = 0$). At a greater depth the vertical stress gradually approaches the stress caused in the soil by a load on the surface irrespective of the depth of foundation.

To the sides of the axis of the strip foundation for a separation $x \doteq 0.8(z - D)$ of the examined point and the axis of the foundation, where z is the depth of this point below the surface and D is the depth of foundation, the depth of foundation has barely any influence on the size of the vertical stress in the soil. If the examined point is at a depth $(z - D)$ below the foundation, nearer to the axis of the foundation, the vertical stress caused by the surface load is greater than the stress caused by the load acting at a depth $D > 0$. For a separation $x > 0.8(z - D)$ of the examined point and the axis of the foundation, the vertical stress caused by the surface load is smaller than the stress caused by a load acting at a greater depth. In the case of cohesionless soils, the influence of the depth of foundation on the size of the vertical stress is substantially smaller than in the case of cohesive soils.

Tables for the calculation of the stress in the soil in some cases are given in Appendix I.

TABLES

(SUPPLEMENT TO CHAPTER 2.4)

Diagram of notations and legend to tables	177
Tables of factors α_γ , α_q of the interaction of adjacent foundations:	
I. For B_I/B_{II} from 0.25 to 4.0 if $S/B = 0$	179
II. For $S/B \geq 0.6$; $B_I/B_{II} = 4 : 1$ and various angles ϕ	180
III. For $S/B \geq 0.6$; $B_I/B_{II} = 2 : 1$ and various angles ϕ	188
IV. For $S/B \geq 0.6$; $B_I/B_{II} = 1 : 1$ and various angles ϕ	196
V. For $S/B \geq 0.6$; $B_I/B_{II} = 1 : 2$ and various angles ϕ	206
VI. For $S/B \geq 0.6$; $B_I/B_{II} = 1 : 4$ and various angles ϕ	214

DIAGRAM OF NOTATIONS AND LEGEND TO TABLES

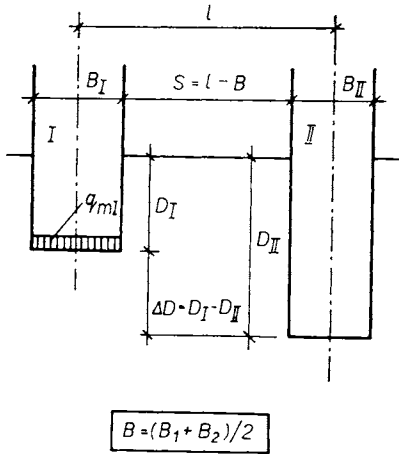


Fig. T.1 Notation for adjacent foundations

The diagram showing the designations of the dimensions of two adjacent foundations is in Fig. T.1. Foundation I is the foundation for which the ultimate bearing capacity is being determined. The adjacent foundation is designated II. The following relationships are valid:

$$B = (B_1 + B_{II})/2$$

The auxiliary function $f(D_1 - D_{11})$ is:

1. $(D_1 - D_{11})/D_1$ for $D_1/B_1 > 1$, if $(D_1 - D_{11}) > 0$
2. $(D_1 - D_{11})/B_1$ in the other cases

For intermediate values B_1/B_{11} , Φ , S/B , $f(D_1 - D_{11})$ not given in the tables, the values of factors α_y and α_q are determined by linear interpolation. In Tables II to VI the factor α_y is always given in the upper row and the factor α_q in the bottom row.

For example: For the proposed foundations in a soil with an angle of internal shearing resistance $\Phi = 30^\circ$ the following dimensions were chosen: $B_1 = 0.8$ m; $D_1 = 1.5$ m; $B_{11} = 1.6$ m; $D_{11} = 1.2$ m; $S = 2.4$ m. The factors of interaction of the two foundations α_y , α_q are sought.

We calculate:

$$B_1/B_{11} = 0.8/1.6 = 1 : 2$$

$$B = (0.8 + 1.6)/2 = 1.2 \text{ m}$$

$$S/B = 2.4/1.2 = 2$$

$$D_1/B_1 = 1.5/0.8 = 1.875$$

$$D_1 - D_{11} = 1.5 - 1.2 = 0.3 \text{ m}$$

Because $D_1/B_1 > 1$ and simultaneously $(D_1 - D_{11}) > 0$, the value of function $f(D_1 - D_{11})$ is determined from the relationship $(D_1 - D_{11})/D_1 = (1.5 - 1.2)/1.5 = 0.2$.

From Tables V. (the group for $B_1/B_{11} = 1 : 2$) we use the table for the angle of internal shearing resistance $\Phi = 30^\circ$. For $S/B = 2$ and $f(D_1 - D_{11}) = 0.2$ we find in the table values $\alpha_y = 2.339$ and $\alpha_q = 1.071$. For the simple determination of the factor α_c the following Table T 1 was drawn up, using equation (2.74) and Table 2.10. Values of factors α_c are a function of Φ and α_q .

TABLE T1

Factor α_c as a function of Φ and α_q

Φ	α_q						
	0.40	0.60	0.80	1.00	1.20	1.40	1.60
0°	1.00	1.00	1.00	1.00	1.00	1.00	1.00
10°	—	—	0.68	1.00	1.32	—	—
20°	—	0.54	0.77	1.00	1.23	1.46	—
$\geq 25^\circ$	0.40	0.60	0.80	1.00	1.20	1.40	1.60

3.0	3.5	4.0	5.0	6.5	10.0
1.000	1.000	1.000	1.000	1.000	1.000
1.000	1.000	1.000	1.000	1.000	1.000
1.032	1.021	1.011	0.999	0.995	1.000
1.000	1.000	1.000	1.000	1.000	1.000
1.059	1.039	1.021	0.999	0.991	1.000
1.000	1.000	1.000	1.000	1.000	1.000
1.083	1.054	1.030	0.998	0.988	1.000
1.000	1.000	1.000	1.000	1.000	1.000
1.101	1.066	1.036	0.998	0.985	1.000
1.000	1.000	1.000	1.000	1.000	1.000
1.111	1.073	1.040	0.997	0.983	1.000
1.000	1.000	1.000	1.000	1.000	1.000
1.101	1.066	1.036	0.998	0.985	1.000
1.000	1.000	1.000	1.000	1.000	1.000
1.083	1.054	1.030	0.998	0.988	1.000
1.000	1.000	1.000	1.000	1.000	1.000
1.059	1.039	1.021	0.999	0.991	1.000
1.000	1.000	1.000	1.000	1.000	1.000
1.032	1.021	1.011	0.999	0.995	1.000
1.000	1.000	1.000	1.000	1.000	1.000
1.000	1.000	1.000	1.000	1.000	1.000
1.000	1.000	1.000	1.000	1.000	1.000
0.944	0.948	0.953	0.963	0.976	0.991
0.935	0.941	0.948	0.961	0.975	0.991
0.915	0.921	0.928	0.944	0.964	0.987
0.902	0.912	0.922	0.941	0.963	0.987
0.906	0.913	0.921	0.938	0.960	0.986
0.892	0.902	0.913	0.934	0.959	0.985
0.909	0.916	0.924	0.941	0.962	0.986
0.896	0.906	0.916	0.937	0.960	0.986
0.935	0.940	0.945	0.957	0.973	0.990
0.925	0.932	0.940	0.955	0.972	0.990
0.964	0.967	0.970	0.976	0.985	0.994
0.959	0.963	0.967	0.975	0.984	0.994
0.998	0.998	0.998	0.999	0.999	1.000
0.998	0.998	0.998	0.999	0.999	1.000

TABLE II (cont.)

Angle of internal friction of the soil $\Phi = 20.0^\circ$
 Group $B_I/B_{II} = 4 : 1$

$f(D_I - D_{II})$	S/B					
	0.6	0.9	1.2	1.5	2.0	2.5
1.0	1.000 1.000	1.000 1.000	1.000 1.000	1.000 1.000	1.000 1.000	1.000 1.000
0.8	1.082 1.000	1.098 1.000	1.108 1.000	1.111 1.000	1.105 1.000	1.087 1.000
0.6	1.154 1.000	1.184 1.000	1.203 1.000	1.209 1.000	1.197 1.000	1.164 1.000
0.4	1.214 1.000	1.257 1.000	1.283 1.000	1.292 1.000	1.275 1.000	1.229 1.000
0.2	1.261 1.000	1.314 1.000	1.345 1.000	1.356 1.000	1.335 1.000	1.280 1.000
0.0	1.287 1.000	1.345 1.027	1.379 1.020	1.391 1.000	1.368 1.000	1.307 1.000
-0.2	1.261 1.000	1.314 1.000	1.345 1.000	1.356 1.000	1.335 1.000	1.280 1.000
-0.4	1.214 1.000	1.257 1.000	1.283 1.000	1.292 1.000	1.275 1.000	1.229 1.000
-0.6	1.154 1.000	1.184 1.000	1.203 1.000	1.209 1.000	1.197 1.000	1.164 1.000
-0.8	1.082 1.000	1.098 1.000	1.108 1.000	1.111 1.000	1.105 1.000	1.087 1.000
-1.0	1.000 1.000	1.000 1.000	1.000 1.000	1.000 1.000	1.000 1.000	1.000 1.000
-1.5	0.887 0.838	0.883 0.839	0.880 0.840	0.877 0.842	0.876 0.847	0.878 0.856
-2.0	0.830 0.756	0.823 0.757	0.818 0.758	0.815 0.762	0.813 0.770	0.816 0.782
-2.5	0.812 0.729	0.804 0.730	0.799 0.733	0.795 0.736	0.792 0.745	0.796 0.759
-3.0	0.819 0.740	0.812 0.741	0.806 0.743	0.803 0.746	0.800 0.755	0.804 0.768
-4.0	0.870 0.813	0.865 0.814	0.861 0.815	0.858 0.817	0.857 0.824	0.859 0.833
-5.0	0.928 0.897	0.925 0.897	0.923 0.898	0.922 0.899	0.921 0.903	0.922 0.908
-7.0	0.996 0.994	0.996 0.994	0.996 0.994	0.996 0.994	0.995 0.994	0.996 0.995

3.0	3.5	4.0	5.0	6.5	10.0
1.000	1.000	1.000	1.000	1.000	1.000
1.000	1.000	1.000	1.000	1.000	1.000
1.065	1.043	1.023	0.998	0.990	1.000
1.000	1.000	1.000	1.000	1.000	1.000
1.122	1.080	1.044	0.997	0.982	1.000
1.000	1.000	1.000	1.000	1.000	1.000
1.171	1.112	1.061	0.996	0.974	1.000
1.000	1.000	1.000	1.000	1.000	1.000
1.208	1.136	1.074	0.995	0.969	1.000
1.000	1.000	1.000	1.000	1.000	1.000
1.229	1.150	1.082	0.994	0.966	1.000
1.000	1.000	1.000	1.000	1.000	1.000
1.208	1.136	1.074	0.995	0.969	1.000
1.000	1.000	1.000	1.000	1.000	1.000
1.171	1.112	1.061	0.996	0.974	1.000
1.000	1.000	1.000	1.000	1.000	1.000
1.122	1.080	1.044	0.997	0.982	1.000
1.000	1.000	1.000	1.000	1.000	1.000
1.065	1.043	1.023	0.998	0.990	1.000
1.000	1.000	1.000	1.000	1.000	1.000
1.000	1.000	1.000	1.000	1.000	1.000
1.000	1.000	1.000	1.000	1.000	1.000
0.884	0.892	0.902	0.924	0.951	0.982
0.867	0.879	0.893	0.919	0.949	0.982
0.824	0.837	0.852	0.885	0.926	0.973
0.799	0.818	0.838	0.878	0.923	0.973
0.806	0.819	0.836	0.872	0.918	0.970
0.777	0.798	0.821	0.864	0.915	0.970
0.813	0.826	0.843	0.877	0.921	0.971
0.786	0.806	0.828	0.870	0.918	0.971
0.866	0.875	0.887	0.912	0.943	0.979
0.846	0.860	0.876	0.906	0.941	0.979
0.926	0.931	0.937	0.951	0.969	0.989
0.915	0.923	0.931	0.948	0.968	0.988
0.996	0.996	0.996	0.997	0.998	0.999
0.995	0.996	0.996	0.997	0.998	0.999

3.0	3.5	4.0	5.0	6.5	10.0
1.000	1.000	1.000	1.000	1.000	1.000
1.000	1.000	1.000	1.000	1.000	1.000
1.103	1.068	1.037	0.997	0.984	1.000
1.000	1.000	1.000	1.000	1.000	1.000
1.194	1.127	1.069	0.995	0.971	1.000
1.000	1.000	1.000	1.000	1.000	1.000
1.271	1.178	1.097	0.993	0.959	0.999
1.000	1.000	1.000	1.000	1.000	1.000
1.330	1.216	1.118	0.992	0.950	0.999
1.000	1.000	1.000	1.000	1.000	1.000
1.363	1.238	1.129	0.991	0.945	0.999
1.000	1.000	1.000	1.000	1.000	1.000
1.330	1.216	1.118	0.992	0.950	0.999
1.000	1.000	1.000	1.000	1.000	1.000
1.271	1.178	1.097	0.993	0.959	0.999
1.000	1.000	1.000	1.000	1.000	1.000
1.194	1.127	1.069	0.995	0.971	1.000
1.000	1.000	1.000	1.000	1.000	1.000
1.103	1.068	1.037	0.997	0.984	1.000
1.000	1.000	1.000	1.000	1.000	1.000
1.000	1.000	1.000	1.000	1.000	1.000
1.000	1.000	1.000	1.000	1.000	1.000
0.815	0.829	0.845	0.879	0.922	0.972
0.788	0.808	0.830	0.871	0.919	0.971
0.721	0.741	0.765	0.817	0.882	0.957
0.681	0.711	0.743	0.806	0.878	0.957
0.692	0.714	0.740	0.798	0.870	0.953
0.646	0.680	0.715	0.785	0.865	0.952
0.703	0.725	0.750	0.805	0.875	0.954
0.660	0.692	0.726	0.793	0.871	0.954
0.787	0.802	0.820	0.860	0.910	0.967
0.755	0.779	0.803	0.851	0.907	0.967
0.882	0.891	0.901	0.923	0.950	0.982
0.865	0.878	0.891	0.918	0.949	0.982
0.993	0.994	0.994	0.996	0.997	0.999
0.992	0.993	0.994	0.995	0.997	0.999

TABLE II (cont.)

Angle of internal friction of the soil $\Phi \geq 37.5^\circ$ Group $B_I/B_{II} = 4 : 1$

$f(D_I - D_{II})$	S/B					
	0.6	0.9	1.2	1.5	2.0	2.5
1.0	1.000	1.000	1.000	1.000	1.000	1.000
	1.000	1.000	1.000	1.000	1.000	1.000
0.8	1.172	1.207	1.227	1.235	1.221	1.184
	1.000	1.000	1.000	1.000	1.000	1.000
0.6	1.324	1.389	1.428	1.441	1.415	1.347
	1.058	1.090	1.082	1.047	1.000	1.000
0.4	1.452	1.543	1.597	1.616	1.579	1.484
	1.263	1.307	1.296	1.247	1.119	1.000
0.2	1.551	1.661	1.728	1.751	1.706	1.590
	1.422	1.475	1.461	1.402	1.246	1.066
0.0	1.605	1.726	1.799	1.824	1.776	1.647
	1.508	1.567	1.552	1.487	1.316	1.118
-0.2	1.551	1.661	1.728	1.751	1.706	1.590
	1.422	1.475	1.461	1.402	1.246	1.066
-0.4	1.452	1.543	1.597	1.616	1.579	1.484
	1.263	1.307	1.296	1.247	1.119	1.000
-0.6	1.324	1.389	1.428	1.441	1.415	1.347
	1.058	1.090	1.082	1.047	1.000	1.000
-0.8	1.172	1.207	1.227	1.235	1.221	1.184
	1.000	1.000	1.000	1.000	1.000	1.000
-1.0	1.000	1.000	1.000	1.000	1.000	1.000
	1.000	1.000	1.000	1.000	1.000	1.000
-1.5	0.762	0.753	0.746	0.741	0.738	0.743
	0.658	0.660	0.663	0.667	0.678	0.696
-2.0	0.641	0.628	0.617	0.609	0.605	0.612
	0.485	0.487	0.491	0.497	0.515	0.541
-2.5	0.603	0.588	0.576	0.567	0.562	0.570
	0.429	0.432	0.436	0.443	0.463	0.492
-3.0	0.618	0.603	0.592	0.584	0.579	0.587
	0.451	0.454	0.458	0.465	0.483	0.511
-4.0	0.725	0.715	0.707	0.701	0.698	0.703
	0.605	0.607	0.610	0.615	0.629	0.649
-5.0	0.848	0.842	0.838	0.835	0.833	0.836
	0.782	0.783	0.784	0.787	0.795	0.806
-7.0	0.991	0.991	0.991	0.991	0.990	0.991
	0.988	0.988	0.988	0.988	0.988	0.989

3.0	3.5	4.0	5.0	6.5	10.0
1.000	1.000	1.000	1.000	1.000	1.000
1.000	1.000	1.000	1.000	1.000	1.000
1.137	1.090	1.049	0.997	0.979	1.000
1.000	1.000	1.000	1.000	1.000	1.000
1.258	1.169	1.092	0.994	0.961	0.999
1.000	1.000	1.000	1.000	1.000	1.000
1.360	1.236	1.129	0.991	0.946	0.999
1.000	1.000	1.000	1.000	1.000	1.000
1.439	1.288	1.157	0.989	0.934	0.999
1.000	1.000	1.000	1.000	1.000	1.000
1.482	1.316	1.172	0.988	0.927	0.999
1.000	1.000	1.000	1.000	1.000	1.000
1.439	1.288	1.157	0.989	0.934	0.999
1.000	1.000	1.000	1.000	1.000	1.000
1.360	1.236	1.129	0.991	0.946	0.999
1.000	1.000	1.000	1.000	1.000	1.000
1.258	1.169	1.092	0.994	0.961	0.999
1.000	1.000	1.000	1.000	1.000	1.000
1.137	1.090	1.049	0.997	0.979	1.000
1.000	1.000	1.000	1.000	1.000	1.000
1.000	1.000	1.000	1.000	1.000	1.000
1.000	1.000	1.000	1.000	1.000	1.000
0.755	0.772	0.793	0.839	0.896	0.962
0.719	0.745	0.774	0.829	0.893	0.962
0.630	0.656	0.688	0.757	0.844	0.943
0.575	0.616	0.659	0.742	0.838	0.943
0.590	0.619	0.655	0.731	0.827	0.937
0.530	0.574	0.622	0.714	0.821	0.936
0.606	0.634	0.668	0.741	0.834	0.939
0.548	0.591	0.636	0.725	0.828	0.939
0.717	0.737	0.761	0.814	0.880	0.956
0.675	0.706	0.739	0.802	0.876	0.956
0.843	0.855	0.868	0.897	0.934	0.976
0.820	0.837	0.855	0.891	0.932	0.976
0.991	0.992	0.992	0.994	0.996	0.999
0.990	0.991	0.992	0.994	0.996	0.999

3.0	3.5	4.0	5.0	6.5	10.0
1.000	1.000	1.000	1.000	1.000	1.000
1.000	1.000	1.000	1.000	1.000	1.000
1.039	1.024	1.013	0.999	0.995	1.000
1.000	1.000	1.000	1.000	1.000	1.000
1.073	1.046	1.024	0.998	0.991	1.000
1.000	1.000	1.000	1.000	1.000	1.000
1.102	1.064	1.034	0.998	0.987	1.000
1.000	1.000	1.000	1.000	1.000	1.000
1.124	1.078	1.041	0.997	0.984	1.000
1.000	1.000	1.000	1.000	1.000	1.000
1.136	1.086	1.045	0.997	0.982	1.000
1.000	1.000	1.000	1.000	1.000	1.000
1.124	1.078	1.041	0.997	0.984	1.000
1.000	1.000	1.000	1.000	1.000	1.000
1.102	1.064	1.034	0.998	0.987	1.000
1.000	1.000	1.000	1.000	1.000	1.000
1.073	1.046	1.024	0.998	0.991	1.000
1.000	1.000	1.000	1.000	1.000	1.000
1.039	1.024	1.013	0.999	0.995	1.000
1.000	1.000	1.000	1.000	1.000	1.000
1.000	1.000	1.000	1.000	1.000	1.000
1.000	1.000	1.000	1.000	1.000	1.000
0.940	0.945	0.950	0.962	0.976	0.991
0.935	0.941	0.948	0.961	0.975	0.991
0.909	0.916	0.925	0.942	0.963	0.987
0.902	0.912	0.922	0.941	0.963	0.987
0.899	0.907	0.917	0.936	0.960	0.985
0.892	0.902	0.913	0.934	0.959	0.985
0.903	0.911	0.920	0.939	0.961	0.986
0.896	0.906	0.916	0.937	0.960	0.986
0.930	0.936	0.943	0.956	0.972	0.990
0.925	0.932	0.940	0.955	0.972	0.990
0.961	0.965	0.968	0.976	0.985	0.994
0.959	0.963	0.967	0.975	0.984	0.994
0.998	0.998	0.998	0.999	0.999	1.000
0.998	0.998	0.998	0.999	0.999	1.000

3.0	3.5	4.0	5.0	6.5	10.0
1.000	1.000	1.000	1.000	1.000	1.000
1.000	1.000	1.000	1.000	1.000	1.000
1.080	1.050	1.027	0.998	0.990	1.000
1.000	1.000	1.000	1.000	1.000	1.000
1.150	1.095	1.050	0.997	0.981	1.000
1.000	1.000	1.000	1.000	1.000	1.000
1.210	1.132	1.070	0.995	0.973	1.000
1.000	1.000	1.000	1.000	1.000	1.000
1.256	1.161	1.085	0.994	0.967	1.000
1.000	1.000	1.000	1.000	1.000	1.000
1.281	1.177	1.094	0.994	0.964	1.000
1.000	1.000	1.000	1.000	1.000	1.000
1.256	1.161	1.085	0.994	0.967	1.000
1.000	1.000	1.000	1.000	1.000	1.000
1.210	1.132	1.070	0.995	0.973	1.000
1.000	1.000	1.000	1.000	1.000	1.000
1.150	1.095	1.050	0.997	0.981	1.000
1.000	1.000	1.000	1.000	1.000	1.000
1.080	1.050	1.027	0.998	0.990	1.000
1.000	1.000	1.000	1.000	1.000	1.000
1.000	1.000	1.000	1.000	1.000	1.000
1.000	1.000	1.000	1.000	1.000	1.000
0.875	0.886	0.897	0.921	0.950	0.982
0.867	0.879	0.893	0.919	0.949	0.982
0.812	0.828	0.845	0.881	0.925	0.973
0.799	0.818	0.838	0.878	0.923	0.973
0.792	0.809	0.829	0.868	0.917	0.970
0.777	0.798	0.821	0.864	0.915	0.970
0.800	0.816	0.835	0.874	0.920	0.971
0.786	0.806	0.828	0.870	0.918	0.971
0.856	0.868	0.882	0.909	0.942	0.979
0.846	0.860	0.876	0.906	0.941	0.979
0.920	0.927	0.935	0.950	0.968	0.989
0.915	0.923	0.931	0.948	0.968	0.988
0.995	0.996	0.996	0.997	0.998	0.999
0.995	0.996	0.996	0.997	0.998	0.999

3.0	3.5	4.0	5.0	6.5	10.0
1.000	1.000	1.000	1.000	1.000	1.000
1.000	1.000	1.000	1.000	1.000	1.000
1.127	1.080	1.042	0.997	0.984	1.000
1.000	1.000	1.000	1.000	1.000	1.000
1.239	1.150	1.079	0.995	0.969	1.000
1.000	1.000	1.000	1.000	1.000	1.000
1.333	1.210	1.111	0.993	0.957	0.999
1.000	1.000	1.000	1.000	1.000	1.000
1.406	1.256	1.135	0.991	0.948	0.999
1.000	1.000	1.000	1.000	1.000	1.000
1.446	1.281	1.148	0.990	0.943	0.999
1.000	1.000	1.000	1.000	1.000	1.000
1.406	1.256	1.135	0.991	0.948	0.999
1.000	1.000	1.000	1.000	1.000	1.000
1.333	1.210	1.111	0.993	0.957	0.999
1.000	1.000	1.000	1.000	1.000	1.000
1.239	1.150	1.079	0.995	0.969	1.000
1.000	1.000	1.000	1.000	1.000	1.000
1.127	1.080	1.042	0.997	0.984	1.000
1.000	1.000	1.000	1.000	1.000	1.000
1.000	1.000	1.000	1.000	1.000	1.000
1.000	1.000	1.000	1.000	1.000	1.000
0.802	0.819	0.837	0.875	0.921	0.972
0.788	0.808	0.830	0.871	0.919	0.971
0.702	0.726	0.755	0.812	0.880	0.957
0.681	0.711	0.743	0.806	0.878	0.957
0.670	0.697	0.728	0.791	0.868	0.952
0.646	0.680	0.715	0.785	0.865	0.952
0.682	0.709	0.739	0.799	0.873	0.954
0.660	0.692	0.726	0.793	0.871	0.954
0.772	0.791	0.812	0.856	0.909	0.967
0.755	0.779	0.803	0.851	0.907	0.967
0.874	0.884	0.896	0.920	0.949	0.982
0.865	0.878	0.891	0.918	0.949	0.982
0.993	0.993	0.994	0.995	0.997	0.999
0.992	0.993	0.994	0.995	0.997	0.999

TABLE III (cont.)

Angle of internal friction of the soil $\Phi \geq 35.0^\circ$
 Group $B_I/B_{II} = 2 : 1$

$f(D_I/D_{II})$	S/B					
	0.6	0.9	1.2	1.5	2.0	2.5
1.0	1.000	1.000	1.000	1.000	1.000	1.000
	1.000	1.000	1.000	1.000	1.000	1.000
0.8	1.270	1.305	1.318	1.312	1.274	1.216
	1.000	1.000	1.000	1.000	1.000	1.000
0.6	1.509	1.574	1.598	1.587	1.516	1.407
	1.013	1.042	1.034	1.002	1.000	1.000
0.4	1.710	1.801	1.834	1.820	1.720	1.568
	1.200	1.240	1.230	1.185	1.069	1.000
0.2	1.865	1.976	2.017	1.999	1.877	1.692
	1.345	1.393	1.381	1.327	1.184	1.020
0.0	1.950	2.072	2.117	2.097	1.963	1.760
	1.424	1.477	1.463	1.404	1.248	1.068
-0.2	1.865	1.976	2.017	1.999	1.877	1.692
	1.345	1.393	1.381	1.327	1.184	1.020
-0.4	1.710	1.801	1.834	1.820	1.720	1.568
	1.200	1.240	1.230	1.185	1.069	1.000
-0.6	1.509	1.574	1.598	1.587	1.516	1.407
	1.013	1.042	1.034	1.002	1.000	1.000
-0.8	1.270	1.305	1.318	1.312	1.274	1.216
	1.000	1.000	1.000	1.000	1.000	1.000
-1.0	1.000	1.000	1.000	1.000	1.000	1.000
	1.000	1.000	1.000	1.000	1.000	1.000
-1.5	0.740	0.736	0.733	0.732	0.735	0.745
	0.688	0.690	0.692	0.696	0.707	0.722
-2.0	0.608	0.601	0.597	0.595	0.600	0.615
	0.530	0.532	0.535	0.541	0.557	0.581
-2.5	0.565	0.558	0.554	0.552	0.558	0.574
	0.479	0.481	0.485	0.492	0.510	0.536
-3.0	0.582	0.575	0.571	0.569	0.575	0.590
	0.499	0.501	0.505	0.512	0.529	0.554
-4.0	0.700	0.695	0.691	0.690	0.694	0.705
	0.640	0.641	0.644	0.649	0.661	0.679
-5.0	0.834	0.831	0.829	0.829	0.831	0.837
	0.801	0.802	0.803	0.806	0.813	0.823
-7.0	0.991	0.990	0.990	0.990	0.990	0.991
	0.989	0.989	0.989	0.989	0.989	0.990

3.0	3.5	4.0	5.0	6.5	10.0
1.000	1.000	1.000	1.000	1.000	1.000
1.000	1.000	1.000	1.000	1.000	1.000
1.154	1.097	1.051	0.997	0.980	1.000
1.000	1.000	1.000	1.000	1.000	1.000
1.289	1.183	1.096	0.994	0.963	1.000
1.000	1.000	1.000	1.000	1.000	1.000
1.404	1.255	1.135	0.991	0.948	0.999
1.000	1.000	1.000	1.000	1.000	1.000
1.492	1.310	1.164	0.989	0.937	0.999
1.000	1.000	1.000	1.000	1.000	1.000
1.541	1.341	1.180	0.988	0.930	0.999
1.000	1.000	1.000	1.000	1.000	1.000
1.492	1.310	1.164	0.989	0.937	0.999
1.000	1.000	1.000	1.000	1.000	1.000
1.404	1.255	1.135	0.991	0.948	0.999
1.000	1.000	1.000	1.000	1.000	1.000
1.289	1.183	1.096	0.994	0.963	1.000
1.000	1.000	1.000	1.000	1.000	1.000
1.154	1.097	1.051	0.997	0.980	1.000
1.000	1.000	1.000	1.000	1.000	1.000
1.000	1.000	1.000	1.000	1.000	1.000
1.000	1.000	1.000	1.000	1.000	1.000
0.760	0.780	0.803	0.849	0.904	0.965
0.743	0.768	0.794	0.844	0.902	0.965
0.638	0.668	0.702	0.771	0.855	0.948
0.613	0.649	0.688	0.764	0.853	0.948
0.599	0.633	0.670	0.747	0.839	0.942
0.571	0.612	0.655	0.739	0.837	0.942
0.615	0.647	0.683	0.757	0.846	0.944
0.588	0.627	0.668	0.749	0.843	0.944
0.723	0.746	0.772	0.825	0.889	0.960
0.703	0.731	0.761	0.820	0.887	0.960
0.847	0.860	0.874	0.903	0.939	0.978
0.836	0.852	0.868	0.900	0.938	0.978
0.991	0.992	0.993	0.994	0.996	0.999
0.991	0.992	0.992	0.994	0.996	0.999

3.0	3.5	4.0	5.0	6.5	10.0
1.000	1.000	1.000	1.000	1.000	1.000
1.000	1.000	1.000	1.000	1.000	1.000
1.048	1.029	1.015	0.999	0.995	1.000
1.000	1.000	1.000	1.000	1.000	1.000
1.089	1.054	1.028	0.998	0.990	1.000
1.000	1.000	1.000	1.000	1.000	1.000
1.125	1.076	1.039	0.998	0.986	1.000
1.000	1.000	1.000	1.000	1.000	1.000
1.152	1.092	1.047	0.997	0.983	1.000
1.000	1.000	1.000	1.000	1.000	1.000
1.167	1.102	1.052	0.997	0.982	1.000
1.000	1.000	1.000	1.000	1.000	1.000
1.152	1.092	1.047	0.997	0.983	1.000
1.000	1.000	1.000	1.000	1.000	1.000
1.125	1.076	1.039	0.998	0.986	1.000
1.000	1.000	1.000	1.000	1.000	1.000
1.089	1.054	1.028	0.998	0.990	1.000
1.000	1.000	1.000	1.000	1.000	1.000
1.048	1.029	1.015	0.999	0.995	1.000
1.000	1.000	1.000	1.000	1.000	1.000
1.000	1.000	1.000	1.000	1.000	1.000
1.000	1.000	1.000	1.000	1.000	1.000
0.935	0.941	0.948	0.961	0.975	0.991
0.935	0.941	0.948	0.961	0.975	0.991
0.902	0.912	0.922	0.941	0.963	0.987
0.902	0.912	0.922	0.941	0.963	0.987
0.892	0.902	0.913	0.934	0.959	0.985
0.892	0.902	0.913	0.934	0.959	0.985
0.896	0.906	0.916	0.937	0.960	0.986
0.986	0.906	0.916	0.937	0.960	0.986
0.925	0.932	0.940	0.955	0.972	0.990
0.925	0.932	0.940	0.955	0.972	0.990
0.959	0.963	0.967	0.975	0.984	0.994
0.959	0.963	0.967	0.975	0.984	0.994
0.998	0.998	0.998	0.999	0.999	1.000
0.998	0.998	0.998	0.999	0.999	1.000

3.0	3.5	4.0	5.0	6.5	10.0
1.000	1.000	1.000	1.000	1.000	1.000
1.000	1.000	1.000	1.000	1.000	1.000
1.098	1.060	1.031	0.998	0.989	1.000
1.000	1.000	1.000	1.000	1.000	1.000
1.185	1.112	1.057	0.996	0.980	1.000
1.000	1.000	1.000	1.000	1.000	1.000
1.258	1.157	1.080	0.995	0.972	1.000
1.000	1.000	1.000	1.000	1.000	1.000
1.314	1.191	1.098	0.994	0.965	1.000
1.000	1.000	1.000	1.000	1.000	1.000
1.345	1.210	1.107	0.993	0.962	1.000
1.000	1.000	1.000	1.000	1.000	1.000
1.314	1.191	1.098	0.994	0.965	1.000
1.000	1.000	1.000	1.000	1.000	1.000
1.258	1.157	1.080	0.995	0.972	1.000
1.000	1.000	1.000	1.000	1.000	1.000
1.185	1.112	1.057	0.996	0.980	1.000
1.000	1.000	1.000	1.000	1.000	1.000
1.098	1.060	1.031	0.998	0.989	1.000
1.000	1.000	1.000	1.000	1.000	1.000
1.000	1.000	1.000	1.000	1.000	1.000
1.000	1.000	1.000	1.000	1.000	1.000
0.867	0.879	0.893	0.919	0.949	0.982
0.867	0.879	0.893	0.919	0.949	0.982
0.799	0.818	0.838	0.878	0.923	0.973
0.799	0.818	0.838	0.878	0.923	0.973
0.777	0.798	0.821	0.864	0.915	0.970
0.777	0.798	0.821	0.864	0.915	0.970
0.786	0.806	0.828	0.870	0.918	0.971
0.786	0.806	0.828	0.870	0.918	0.971
0.846	0.860	0.876	0.906	0.941	0.979
0.846	0.860	0.876	0.906	0.941	0.979
0.915	0.923	0.931	0.948	0.968	0.988
0.915	0.923	0.931	0.948	0.968	0.988
0.995	0.996	0.996	0.997	0.998	0.999
0.995	0.996	0.996	0.997	0.998	0.999

TABLE IV (cont.)

Angle of internal friction of the soil $\phi = 25.0^\circ$
 Group $B_I/B_{II} = 1 : 1$

$f(D_I - D_{II})$	S/B					
	0.6	0.9	1.2	1.5	2.0	2.5
1.0	1.000	1.000	1.000	1.000	1.000	1.000
	1.000	1.000	1.000	1.000	1.000	1.000
0.8	1.310	1.329	1.324	1.303	1.248	1.185
	1.000	1.000	1.000	1.000	1.000	1.000
0.6	1.583	1.619	1.610	1.570	1.467	1.348
	1.000	1.000	1.000	1.000	1.000	1.000
0.4	1.814	1.863	1.851	1.796	1.652	1.486
	1.000	1.006	1.000	1.000	1.000	1.000
0.2	1.992	2.052	2.037	1.970	1.795	1.593
	1.076	1.108	1.100	1.064	1.000	1.000
0.0	2.090	2.156	2.139	2.066	1.873	1.651
	1.129	1.164	1.155	1.115	1.011	1.000
-0.2	1.992	2.052	2.037	1.970	1.795	1.593
	1.076	1.108	1.100	1.064	1.000	1.000
-0.4	1.814	1.863	1.851	1.796	1.652	1.486
	1.000	1.006	1.000	1.000	1.000	1.000
-0.6	1.583	1.619	1.610	1.570	1.467	1.348
	1.000	1.000	1.000	1.000	1.000	1.000
-0.8	1.310	1.329	1.324	1.303	1.248	1.185
	1.000	1.000	1.000	1.000	1.000	1.000
-1.0	1.000	1.000	1.000	1.000	1.000	1.000
	1.000	1.000	1.000	1.000	1.000	1.000
-1.5	0.792	0.793	0.795	0.798	0.805	0.815
	0.792	0.793	0.795	0.798	0.805	0.815
-2.0	0.687	0.688	0.691	0.694	0.705	0.721
	0.687	0.688	0.691	0.694	0.705	0.721
-2.5	0.653	0.655	0.657	0.662	0.673	0.691
	0.653	0.655	0.657	0.662	0.673	0.691
-3.0	0.667	0.668	0.671	0.675	0.686	0.703
	0.667	0.668	0.671	0.675	0.686	0.703
-4.0	0.760	0.761	0.763	0.766	0.774	0.787
	0.760	0.761	0.763	0.766	0.774	0.787
-5.0	0.867	0.868	0.869	0.871	0.875	0.882
	0.867	0.868	0.869	0.871	0.875	0.882
-7.0	0.992	0.992	0.993	0.993	0.993	0.993
	0.992	0.992	0.993	0.993	0.993	0.993

3.0	3.5	4.0	5.0	6.5	10.0
1.000	1.000	1.000	1.000	1.000	1.000
1.000	1.000	1.000	1.000	1.000	1.000
1.126	1.076	1.039	0.998	0.986	1.000
1.000	1.000	1.000	1.000	1.000	1.000
1.237	1.144	1.074	0.995	0.974	1.000
1.000	1.000	1.000	1.000	1.900	1.000
1.330	1.201	1.103	0.994	0.964	1.000
1.000	1.000	1.000	1.000	1.000	1.000
1.402	1.245	1.125	0.992	0.956	0.999
1.000	1.000	1.000	1.000	1.000	1.000
1.442	1.269	1.138	0.991	0.951	0.999
1.000	1.000	1.000	1.000	1.000	1.000
1.402	1.245	1.125	0.992	0.956	0.999
1.000	1.000	1.000	1.000	1.000	1.000
1.330	1.201	1.103	0.994	0.964	1.000
1.000	1.000	1.000	1.000	1.000	1.000
1.237	1.144	1.074	0.995	0.974	1.000
1.000	1.000	1.000	1.000	1.000	1.000
1.126	1.076	1.039	0.998	0.986	1.000
1.000	1.000	1.000	1.000	1.000	1.000
1.000	1.000	1.000	1.000	1.000	1.000
1.000	1.000	1.000	1.000	1.000	1.000
0.829	0.845	0.862	0.896	0.935	0.977
0.829	0.845	0.862	0.896	0.935	0.977
0.742	0.766	0.792	0.843	0.902	0.965
0.742	0.766	0.792	0.843	0.902	0.965
0.714	0.741	0.770	0.826	0.891	0.961
0.714	0.741	0.770	0.826	0.891	0.961
0.725	0.751	0.779	0.833	0.896	0.963
0.725	0.751	0.779	0.833	0.896	0.963
0.802	0.821	0.841	0.880	0.925	0.973
0.802	0.821	0.841	0.880	0.925	0.973
0.891	0.901	0.912	0.934	0.958	0.985
0.891	0.901	0.912	0.934	0.958	0.985
0.994	0.994	0.995	0.996	0.998	0.999
0.994	0.994	0.995	0.996	0.998	0.999

3.0	3.5	4.0	5.0	6.5	10.0
1.000	1.000	1.000	1.000	1.000	1.000
1.000	1.000	1.000	1.000	1.000	1.000
1.156	1.095	1.048	0.997	0.983	1.000
1.000	1.000	1.000	1.000	1.000	1.000
1.293	1.178	1.091	0.994	0.968	1.000
1.000	1.000	1.000	1.000	1.000	1.000
1.409	1.248	1.127	0.992	0.955	0.999
1.000	1.000	1.000	1.000	1.000	1.000
1.498	1.303	1.155	0.990	0.945	0.999
1.000	1.000	1.000	1.000	1.000	1.000
1.547	1.332	1.170	0.989	0.940	0.999
1.000	1.000	1.000	1.000	1.000	1.000
1.498	1.303	1.155	0.990	0.945	0.999
1.000	1.000	1.000	1.000	1.000	1.000
1.409	1.248	1.127	0.992	0.955	0.999
1.000	1.000	1.000	1.000	1.000	1.000
1.293	1.178	1.091	0.994	0.968	1.000
1.000	1.000	1.000	1.000	1.000	1.000
1.156	1.095	1.048	0.997	0.983	1.000
1.000	1.000	1.000	1.000	1.000	1.000
1.000	1.000	1.000	1.000	1.000	1.000
1.000	1.000	1.000	1.000	1.000	1.000
0.788	0.808	0.830	0.871	0.919	0.971
0.788	0.808	0.830	0.871	0.919	0.971
0.681	0.711	0.743	0.806	0.878	0.957
0.681	0.711	0.743	0.806	0.878	0.957
0.646	0.680	0.715	0.785	0.865	0.952
0.646	0.680	0.715	0.785	0.865	0.952
0.660	0.692	0.726	0.793	0.871	0.954
0.660	0.692	0.726	0.793	0.871	0.954
0.755	0.779	0.803	0.851	0.907	0.967
0.755	0.779	0.803	0.851	0.907	0.967
0.865	0.878	0.891	0.918	0.949	0.982
0.865	0.878	0.891	0.918	0.949	0.982
0.992	0.993	0.994	0.995	0.997	0.999
0.992	0.993	0.994	0.995	0.997	0.999

TABLE IV (cont.)

Angle of internal friction of the soil $\Phi \geq 35.0^\circ$ Group $B_I/B_{II} = 1 : 1$

$f(D_I - D_{II})$	S/B					
	0.6	0.9	1.2	1.5	2.0	2.5
1.0	1.000	1.000	1.000	1.000	1.000	1.000
	1.000	1.000	1.000	1.000	1.000	1.000
0.8	1.466	1.494	1.486	1.455	1.373	1.278
	1.000	1.000	1.000	1.000	1.000	1.000
0.6	1.876	1.929	1.915	1.856	1.702	1.523
	1.013	1.042	1.034	1.002	1.000	1.000
0.4	2.223	2.296	2.277	2.195	1.979	1.730
	1.200	1.240	1.230	1.185	1.069	1.000
0.2	2.490	2.580	2.557	2.457	2.193	1.890
	1.345	1.393	1.381	1.327	1.184	1.020
0.0	2.637	2.735	2.710	2.600	2.311	1.977
	1.424	1.477	1.463	1.404	1.248	1.068
-0.2	2.490	2.580	2.557	2.457	2.193	1.890
	1.345	1.393	1.381	1.327	1.184	1.020
-0.4	2.223	2.296	2.277	2.195	1.979	1.730
	1.200	1.240	1.230	1.185	1.069	1.000
-0.6	1.876	1.929	1.915	1.856	1.702	1.523
	1.013	1.042	1.034	1.002	1.000	1.000
-0.8	1.466	1.494	1.486	1.455	1.373	1.278
	1.000	1.000	1.000	1.000	1.000	1.000
-1.0	1.000	1.000	1.000	1.000	1.000	1.000
	1.000	1.000	1.000	1.000	1.000	1.000
-1.5	0.688	0.690	0.692	0.696	0.707	0.722
	0.688	0.690	0.692	0.696	0.707	0.722
-2.0	0.530	0.532	0.535	0.541	0.557	0.581
	0.530	0.532	0.535	0.541	0.557	0.581
-2.5	0.479	0.481	0.485	0.492	0.510	0.536
	0.479	0.481	0.485	0.492	0.510	0.536
-3.0	0.499	0.501	0.505	0.512	0.529	0.554
	0.499	0.501	0.505	0.512	0.529	0.554
-4.0	0.640	0.641	0.644	0.649	0.661	0.679
	0.640	0.641	0.644	0.649	0.661	0.679
-5.0	0.801	0.802	0.803	0.806	0.813	0.823
	0.801	0.802	0.803	0.806	0.813	0.823
-7.0	0.989	0.989	0.989	0.989	0.989	0.990
	0.989	0.989	0.989	0.989	0.989	0.990

3.0	3.5	4.0	5.0	6.5	10.0
1.000	1.000	1.000	1.000	1.000	1.000
1.000	1.000	1.000	1.000	1.000	1.000
1.189	1.115	1.059	0.996	0.979	1.000
1.000	1.000	1.000	1.000	1.000	1.000
1.355	1.216	1.111	0.993	0.961	1.000
1.000	1.000	1.000	1.000	1.000	1.000
1.496	1.301	1.154	0.990	0.945	0.999
1.000	1.000	1.000	1.000	1.000	1.000
1.604	1.367	1.188	0.988	0.933	0.999
1.000	1.000	1.000	1.000	1.000	1.000
1.664	1.403	1.207	0.987	0.927	0.999
1.000	1.000	1.000	1.000	1.000	1.000
1.604	1.367	1.188	0.988	0.933	0.999
1.000	1.000	1.000	1.000	1.000	1.000
1.496	1.301	1.154	0.990	0.945	0.999
1.000	1.000	1.000	1.000	1.000	1.000
1.355	1.216	1.111	0.993	0.961	1.000
1.000	1.000	1.000	1.000	1.000	1.000
1.189	1.115	1.059	0.996	0.979	1.000
1.000	1.000	1.000	1.000	1.000	1.000
1.000	1.000	1.000	1.000	1.000	1.000
1.000	1.000	1.000	1.000	1.000	1.000
0.743	0.768	0.794	0.844	0.902	0.965
0.743	0.768	0.794	0.844	0.902	0.965
0.613	0.649	0.688	0.764	0.853	0.948
0.613	0.649	0.688	0.764	0.853	0.948
0.571	0.612	0.655	0.739	0.837	0.942
0.571	0.612	0.655	0.739	0.837	0.942
0.588	0.627	0.668	0.749	0.843	0.944
0.588	0.627	0.668	0.749	0.843	0.944
0.703	0.731	0.761	0.820	0.887	0.960
0.703	0.731	0.761	0.820	0.887	0.960
0.836	0.852	0.868	0.900	0.938	0.978
0.836	0.852	0.868	0.900	0.938	0.978
0.991	0.992	0.992	0.994	0.996	0.999
0.991	0.992	0.992	0.994	0.996	0.999

3.0	3.5	4.0	5.0	6.5	10.0
1.000	1.000	1.000	1.000	1.000	1.000
1.000	1.000	1.000	1.000	1.000	1.000
1.058	1.034	1.017	0.999	0.994	1.000
1.000	1.000	1.000	1.000	1.000	1.000
1.110	1.064	1.032	0.998	0.990	1.000
1.000	1.000	1.000	1.000	1.000	1.000
1.153	1.090	1.045	0.997	0.986	1.000
1.000	1.000	1.000	1.000	1.000	1.000
1.187	1.109	1.054	0.997	0.982	1.000
1.000	1.000	1.000	1.000	1.000	1.000
1.205	1.120	1.060	0.996	0.981	1.000
1.000	1.000	1.000	1.000	1.000	1.000
1.187	1.109	1.054	0.997	0.982	1.000
1.000	1.000	1.000	1.000	1.000	1.000
1.153	1.090	1.045	0.997	0.986	1.000
1.000	1.000	1.000	1.000	1.000	1.000
1.110	1.064	1.032	0.998	0.990	1.000
1.000	1.000	1.000	1.000	1.000	1.000
1.058	1.034	1.017	0.999	0.994	1.000
1.000	1.000	1.000	1.000	1.000	1.000
1.000	1.000	1.000	1.000	1.000	1.000
1.000	1.000	1.000	1.000	1.000	1.000
0.931	0.938	0.946	0.959	0.975	0.991
0.935	0.941	0.948	0.961	0.975	0.991
0.896	0.907	0.918	0.939	0.962	0.987
0.902	0.912	0.922	0.941	0.963	0.987
0.884	0.897	0.909	0.932	0.958	0.985
0.892	0.902	0.913	0.934	0.959	0.985
0.889	0.901	0.913	0.935	0.960	0.986
0.896	0.906	0.916	0.937	0.960	0.986
0.920	0.928	0.937	0.953	0.971	0.990
0.925	0.932	0.940	0.955	0.972	0.990
0.956	0.960	0.965	0.974	0.984	0.994
0.959	0.963	0.967	0.975	0.984	0.994
0.997	0.998	0.998	0.999	0.999	1.000
0.998	0.998	0.998	0.999	0.999	1.000

TABLE V (cont.)

Angle of internal friction of the soil $\Phi = 20.0^\circ$
 Group $B_I/B_{II} = 1 : 2$

$f(D_I - D_{II})$	S/B					
	0.6	0.9	1.2	1.5	2.0	2.5
1.0	1.000	1.000	1.000	1.000	1.000	1.000
	1.000	1.000	1.000	1.000	1.000	1.000
0.8	1.417	1.415	1.387	1.345	1.264	1.186
	1.000	1.000	1.000	1.000	1.000	1.000
0.6	1.784	1.781	1.729	1.649	1.496	1.350
	1.000	1.000	1.000	1.000	1.000	1.000
0.4	2.094	2.090	2.017	1.906	1.693	1.488
	1.000	1.000	1.000	1.000	1.000	1.000
0.2	2.334	2.329	2.239	2.104	1.844	1.595
	1.000	1.000	1.000	1.000	1.000	1.000
0.0	2.465	2.459	2.361	2.213	1.927	1.653
	1.000	1.027	1.020	1.000	1.000	1.000
-0.2	2.334	2.329	2.239	2.104	1.844	1.595
	1.000	1.000	1.000	1.000	1.000	1.000
-0.4	2.094	2.090	2.017	1.906	1.693	1.488
	1.000	1.000	1.000	1.000	1.000	1.000
-0.6	1.784	1.781	1.729	1.649	1.496	1.350
	1.000	1.000	1.000	1.000	1.000	1.000
-0.8	1.417	1.415	1.387	1.345	1.264	1.186
	1.000	1.000	1.000	1.000	1.000	1.000
-1.0	1.000	1.000	1.000	1.000	1.000	1.000
	1.000	1.000	1.000	1.000	1.000	1.000
-1.5	0.806	0.811	0.815	0.821	0.831	0.843
	0.838	0.839	0.840	0.842	0.847	0.856
-2.0	0.707	0.714	0.722	0.730	0.745	0.763
	0.756	0.757	0.758	0.762	0.770	0.782
-2.5	0.676	0.683	0.692	0.701	0.718	0.738
	0.729	0.730	0.733	0.736	0.745	0.759
-3.0	0.688	0.696	0.704	0.712	0.728	0.748
	0.740	0.741	0.743	0.746	0.755	0.768
-4.0	0.776	0.781	0.787	0.793	0.805	0.819
	0.813	0.814	0.815	0.817	0.824	0.833
-5.0	0.876	0.879	0.882	0.886	0.892	0.900
	0.897	0.897	0.898	0.899	0.903	0.908
-7.0	0.993	0.993	0.993	0.993	0.994	0.994
	0.994	0.994	0.994	0.994	0.994	0.995

3.0	3.5	4.0	5.0	6.5	10.0
1.000	1.000	1.000	1.000	1.000	1.000
1.000	1.000	1.000	1.000	1.000	1.000
1.121	1.071	1.035	0.998	0.989	1.000
1.000	1.000	1.000	1.000	1.000	1.000
1.227	1.133	1.066	0.996	0.979	1.000
1.000	1.000	1.000	1.000	1.000	1.000
1.316	1.185	1.092	0.995	0.970	1.000
1.000	1.000	1.000	1.000	1.000	1.000
1.386	1.226	1.112	0.993	0.964	1.000
1.000	1.000	1.000	1.000	1.000	1.000
1.424	1.248	1.123	0.993	0.960	1.000
1.000	1.000	1.000	1.000	1.000	1.000
1.386	1.226	1.112	0.993	0.964	1.000
1.000	1.000	1.000	1.000	1.000	1.000
1.316	1.185	1.092	0.995	0.970	1.000
1.000	1.000	1.000	1.000	1.000	1.000
1.227	1.133	1.066	0.996	0.979	1.000
1.000	1.000	1.000	1.000	1.000	1.000
1.121	1.071	1.035	0.998	0.989	1.000
1.000	1.000	1.000	1.000	1.000	1.000
1.000	1.000	1.000	1.000	1.000	1.000
1.000	1.000	1.000	1.000	1.000	1.000
0.857	0.872	0.888	0.916	0.948	0.982
0.867	0.879	0.893	0.919	0.949	0.982
0.784	0.807	0.830	0.874	0.922	0.973
0.799	0.818	0.838	0.878	0.923	0.973
0.761	0.786	0.812	0.860	0.914	0.970
0.777	0.798	0.821	0.864	0.915	0.970
0.770	0.795	0.820	0.866	0.917	0.971
0.786	0.806	0.828	0.870	0.918	0.971
0.835	0.852	0.870	0.903	0.940	0.979
0.846	0.860	0.876	0.906	0.941	0.979
0.909	0.918	0.928	0.947	0.967	0.988
0.915	0.923	0.931	0.948	0.968	0.988
0.995	0.995	0.996	0.997	0.998	0.999
0.995	0.996	0.996	0.997	0.998	0.999

TABLE V (cont.)

Angle of internal friction of the soil $\Phi = 30.0^\circ$
 Group $B_I/B_{II} = 1:2$

$f(D_I - D_{II})$	S/B					
	0.6	0.9	1.2	1.5	2.0	2.5
1.0	1.000 1.000	1.000 1.000	1.000 1.000	1.000 1.000	1.000 1.000	1.000 1.000
0.8	1.661 1.000	1.659 1.000	1.614 1.000	1.547 1.000	1.418 1.000	1.295 1.000
0.6	2.244 1.000	2.239 1.000	2.156 1.000	2.030 1.000	1.787 1.000	1.555 1.000
0.4	2.736 1.084	2.729 1.117	2.613 1.109	2.437 1.072	2.099 1.000	1.774 1.000
0.2	3.116 1.203	3.108 1.243	2.966 1.233	2.752 1.189	2.339 1.071	1.943 1.000
0.0	3.324 1.269	3.315 1.313	3.159 1.301	2.924 1.252	2.471 1.124	2.036 1.000
-0.2	3.116 1.203	3.108 1.243	2.966 1.233	2.752 1.189	2.339 1.071	1.943 1.000
-0.4	2.736 1.084	2.729 1.117	2.613 1.109	2.437 1.072	2.099 1.000	1.774 1.000
-0.6	2.244 1.000	2.239 1.000	2.156 1.000	2.030 1.000	1.787 1.000	1.555 1.000
-0.8	1.661 1.000	1.659 1.000	1.614 1.000	1.547 1.000	1.418 1.000	1.295 1.000
-1.0	1.000 1.000	1.000 1.000	1.000 1.000	1.000 1.000	1.000 1.000	1.000 1.000
-1.5	0.692 0.743	0.700 0.744	0.707 0.746	0.716 0.749	0.732 0.758	0.751 0.771
-2.0	0.535 0.612	0.547 0.614	0.558 0.617	0.571 0.622	0.595 0.635	0.624 0.655
-2.5	0.485 0.571	0.498 0.572	0.511 0.576	0.525 0.581	0.552 0.596	0.584 0.618
-3.0	0.505 0.587	0.517 0.589	0.530 0.592	0.543 0.597	0.569 0.611	0.600 0.632
-4.0	0.644 0.703	0.653 0.704	0.662 0.707	0.672 0.710	0.690 0.721	0.713 0.736
-5.0	0.803 0.836	0.808 0.837	0.813 0.838	0.818 0.840	0.829 0.845	0.841 0.854
-7.0	0.989 0.991	0.989 0.991	0.989 0.991	0.990 0.991	0.990 0.991	0.991 0.992

3.0	3.5	4.0	5.0	6.5	10.0
1.000	1.000	1.000	1.000	1.000	1.000
1.000	1.000	1.000	1.000	1.000	1.000
1.191	1.112	1.056	0.997	0.982	1.000
1.000	1.000	1.000	1.000	1.000	1.000
1.360	1.210	1.105	0.994	0.966	1.000
1.000	1.000	1.000	1.000	1.000	1.000
1.502	1.294	1.146	0.991	0.953	0.999
1.000	1.000	1.000	1.000	1.000	1.000
1.612	1.358	1.178	0.989	0.942	0.999
1.000	1.000	1.000	1.000	1.000	1.000
1.672	1.393	1.195	0.988	0.937	0.999
1.000	1.000	1.000	1.000	1.000	1.000
1.612	1.358	1.178	0.989	0.942	0.999
1.000	1.000	1.000	1.000	1.000	1.000
1.502	1.294	1.146	0.991	0.953	0.999
1.000	1.000	1.000	1.000	1.000	1.000
1.360	1.210	1.105	0.994	0.966	1.000
1.000	1.000	1.000	1.000	1.000	1.000
1.191	1.112	1.056	0.997	0.982	1.000
1.000	1.000	1.000	1.000	1.000	1.000
1.900	1.000	1.000	1.000	1.000	1.000
1.000	1.000	1.000	1.000	1.000	1.000
0.773	0.797	0.822	0.867	0.918	0.971
0.788	0.808	0.830	0.871	0.919	0.971
0.658	0.694	0.731	0.800	0.876	0.957
0.681	0.711	0.743	0.806	0.878	0.957
0.621	0.661	0.702	0.778	0.863	0.952
0.646	0.680	0.715	0.785	0.865	0.952
0.636	0.674	0.714	0.787	0.868	0.954
0.660	0.692	0.726	0.793	0.871	0.954
0.738	0.766	0.794	0.847	0.905	0.967
0.755	0.779	0.803	0.851	0.907	0.967
0.855	0.871	0.886	0.915	0.948	0.982
0.865	0.878	0.891	0.918	0.949	0.982
0.992	0.993	0.994	0.995	0.997	0.999
0.992	0.993	0.994	0.995	0.997	0.999

TABLE V (cont.)

Angle of internal friction of the soil $\Phi \geq 35.0^\circ$
 Group $B_I/B_{II} = 1 : 2$

$f(D_I - D_{II})$	S/B					
	0.6	0.9	1.2	1.5	2.0	2.5
1.0	1.000	1.000	1.000	1.000	1.000	1.000
	1.000	1.000	1.000	1.000	1.000	1.000
0.8	1.802	1.799	1.745	1.664	1.507	1.357
	1.000	1.000	1.000	1.000	1.000	1.000
0.6	2.508	2.503	2.402	2.249	1.955	1.673
	1.013	1.042	1.034	1.002	1.000	1.000
0.4	3.105	3.097	2.956	2.743	2.332	1.939
	1.200	1.240	1.230	1.185	1.069	1.000
0.2	3.566	3.556	3.384	3.125	2.624	2.144
	1.345	1.393	1.381	1.327	1.184	1.020
0.0	3.818	3.808	3.619	3.333	2.784	2.257
	1.424	1.477	1.463	1.404	1.248	1.068
-0.2	3.566	3.556	3.384	3.125	2.624	2.144
	1.345	1.393	1.381	1.327	1.184	1.020
-0.4	3.105	3.097	2.956	2.743	2.332	1.939
	1.200	1.240	1.230	1.185	1.069	1.000
-0.6	2.508	2.503	2.402	2.249	1.955	1.673
	1.013	1.042	1.034	1.002	1.000	1.000
-0.8	1.802	1.799	1.745	1.664	1.507	1.357
	1.000	1.000	1.000	1.000	1.000	1.000
-1.0	1.000	1.000	1.000	1.000	1.000	1.000
	1.000	1.000	1.000	1.000	1.000	1.000
-1.5	0.626	0.636	0.645	0.655	0.675	0.698
	0.688	0.690	0.692	0.696	0.707	0.722
-2.0	0.436	0.450	0.464	0.480	0.509	0.545
	0.530	0.532	0.535	0.541	0.557	0.581
-2.5	0.376	0.391	0.407	0.424	0.457	0.496
	0.479	0.481	0.485	0.492	0.510	0.536
-3.0	0.400	0.415	0.430	0.446	0.478	0.515
	0.499	0.501	0.505	0.512	0.529	0.554
-4.0	0.568	0.579	0.590	0.602	0.624	0.651
	0.640	0.641	0.644	0.649	0.661	0.679
-5.0	0.761	0.767	0.773	0.780	0.792	0.807
	0.801	0.802	0.803	0.806	0.813	0.823
-7.0	0.986	0.987	0.987	0.987	0.988	0.989
	0.989	0.989	0.989	0.989	0.989	0.990

3.0	3.5	4.0	5.0	6.5	10.0
1.000	1.000	1.000	1.000	1.000	1.000
1.000	1.000	1.000	1.000	1.000	1.000
1.232	1.136	1.067	0.996	0.978	1.000
1.000	1.000	1.000	1.000	1.000	1.000
1.436	1.255	1.127	0.992	0.959	1.000
1.000	1.000	1.000	1.000	1.000	1.000
1.609	1.356	1.177	0.989	0.943	0.999
1.000	1.000	1.000	1.000	1.000	1.000
1.742	1.434	1.216	0.987	0.930	0.999
1.000	1.000	1.000	1.000	1.000	1.000
1.815	1.477	1.237	0.986	0.923	0.999
1.000	1.000	1.000	1.000	1.000	1.000
1.742	1.434	1.216	0.987	0.930	0.999
1.000	1.000	1.000	1.000	1.000	1.000
1.609	1.356	1.177	0.989	0.943	0.999
1.000	1.000	1.000	1.000	1.000	1.000
1.436	1.255	1.127	0.992	0.959	1.000
1.000	1.000	1.000	1.000	1.000	1.000
1.232	1.136	1.067	0.996	0.978	1.000
1.000	1.000	1.000	1.000	1.000	1.000
1.000	1.000	1.000	1.000	1.000	1.000
1.000	1.000	1.000	1.000	1.000	1.000
0.725	0.754	0.784	0.839	0.901	0.965
0.743	0.768	0.794	0.844	0.902	0.965
0.585	0.629	0.674	0.757	0.850	0.947
0.613	0.649	0.688	0.764	0.853	0.948
0.541	0.589	0.639	0.731	0.834	0.942
0.571	0.612	0.655	0.739	0.837	0.942
0.558	0.605	0.653	0.741	0.840	0.944
0.588	0.627	0.668	0.749	0.843	0.944
0.682	0.716	0.750	0.814	0.885	0.960
0.703	0.731	0.761	0.820	0.887	0.960
0.824	0.843	0.862	0.897	0.937	0.978
0.836	0.852	0.868	0.900	0.938	0.978
0.990	0.991	0.992	0.994	0.996	0.999
0.991	0.992	0.992	0.994	0.996	0.999

3.0	3.5	4.0	5.0	6.5	10.0
1.000	1.000	1.000	1.000	1.000	1.000
1.000	1.000	1.000	1.000	1.000	1.000
1.072	1.040	1.019	0.999	0.994	1.000
1.000	1.000	1.000	1.000	1.000	1.000
1.135	1.076	1.037	0.998	0.989	1.000
1.000	1.000	1.000	1.000	1.000	1.000
1.188	1.106	1.051	0.997	0.985	1.000
1.000	1.000	1.000	1.000	1.000	1.000
1.230	1.129	1.062	0.996	0.981	1.000
1.000	1.000	1.000	1.000	1.000	1.000
1.252	1.142	1.068	0.996	0.980	1.000
1.000	1.000	1.000	1.000	1.000	1.000
1.230	1.129	1.062	0.996	0.981	1.000
1.000	1.000	1.000	1.000	1.000	1.000
1.188	1.106	1.051	0.997	0.985	1.000
1.000	1.000	1.000	1.000	1.000	1.000
1.135	1.076	1.037	0.998	0.989	1.000
1.000	1.000	1.000	1.000	1.000	1.000
1.072	1.040	1.019	0.999	0.994	1.000
1.000	1.000	1.000	1.000	1.000	1.000
1.000	1.000	1.000	1.000	1.000	1.000
1.000	1.000	1.000	1.000	1.000	1.000
0.926	0.935	0.943	0.958	0.975	0.991
0.935	0.941	0.948	0.961	0.975	0.991
0.888	0.901	0.914	0.937	0.962	0.987
0.902	0.912	0.922	0.941	0.963	0.987
0.876	0.891	0.905	0.930	0.958	0.985
0.892	0.902	0.913	0.934	0.959	0.985
0.881	0.895	0.908	0.933	0.959	0.986
0.896	0.906	0.916	0.937	0.960	0.986
0.914	0.924	0.934	0.952	0.971	0.990
0.925	0.932	0.940	0.955	0.972	0.990
0.953	0.958	0.964	0.973	0.984	0.994
0.959	0.963	0.967	0.975	0.984	0.994
0.997	0.998	0.998	0.998	0.999	1.000
0.998	0.998	0.998	0.999	0.999	1.000

3.0	3.5	4.0	5.0	6.5	10.0
1.000	1.000	1.000	1.000	1.000	1.000
1.000	1.000	1.000	1.000	1.000	1.000
1.148	1.083	1.040	0.998	0.988	1.000
1.000	1.000	1.000	1.000	1.000	1.000
1.278	1.157	1.076	0.996	0.978	1.000
1.000	1.000	1.000	1.000	1.000	1.000
1.389	1.219	1.105	0.994	0.969	1.000
1.000	1.000	1.000	1.000	1.000	1.000
1.474	1.267	1.129	0.993	0.962	1.000
1.000	1.000	1.000	1.000	1.000	1.000
1.520	1.293	1.141	0.992	0.958	1.000
1.000	1.000	1.000	1.000	1.000	1.000
1.474	1.267	1.129	0.993	0.962	1.000
1.000	1.000	1.000	1.000	1.000	1.000
1.389	1.219	1.105	0.994	0.969	1.000
1.000	1.000	1.000	1.000	1.000	1.000
1.278	1.157	1.076	0.996	0.978	1.000
1.000	1.000	1.000	1.000	1.000	1.000
1.148	1.083	1.040	0.998	0.988	1.000
1.000	1.000	1.000	1.000	1.000	1.000
1.000	1.000	1.000	1.000	1.000	1.000
1.000	1.000	1.000	1.000	1.000	1.000
0.847	0.865	0.882	0.914	0.948	0.982
0.867	0.879	0.893	0.919	0.949	0.982
0.769	0.796	0.823	0.870	0.921	0.973
0.799	0.818	0.838	0.878	0.923	0.973
0.744	0.774	0.803	0.856	0.912	0.970
0.777	0.798	0.821	0.864	0.915	0.970
0.754	0.783	0.811	0.861	0.916	0.971
0.786	0.806	0.828	0.870	0.918	0.971
0.823	0.844	0.864	0.900	0.939	0.979
0.846	0.860	0.876	0.906	0.941	0.979
0.902	0.914	0.925	0.945	0.966	0.988
0.915	0.923	0.931	0.948	0.968	0.988
0.994	0.995	0.996	0.997	0.998	0.999
0.995	0.996	0.996	0.997	0.998	0.999

TABLE VI (cont.)

Angle of internal friction of the soil $\phi = 30.0^\circ$
 Group $B_I/B_{II} = 1 : 4$

$f(D_I - D_{II})$	S/B					
	0.6	0.9	1.2	1.5	2.0	2.5
1.0	1.000	1.000	1.000	1.000	1.000	1.000
	1.000	1.000	1.000	1.000	1.000	1.000
0.8	2.138	2.066	1.941	1.798	1.569	1.379
	1.000	1.000	1.000	1.000	1.000	1.000
0.6	3.142	3.005	2.770	2.502	2.071	1.713
	1.000	1.000	1.000	1.000	1.000	1.000
0.4	3.989	3.798	3.470	3.096	2.495	1.995
	1.084	1.117	1.109	1.072	1.000	1.000
0.2	4.643	4.411	4.011	3.555	2.822	2.213
	1.203	1.243	1.233	1.189	1.071	1.000
0.0	5.001	4.746	4.306	3.806	3.001	2.332
	1.269	1.313	1.301	1.252	1.124	1.000
-0.2	4.643	4.411	4.011	3.555	2.822	2.213
	1.203	1.243	1.233	1.189	1.071	1.000
-0.4	3.989	3.798	3.470	3.096	2.495	1.995
	1.084	1.117	1.109	1.072	1.000	1.000
-0.6	3.142	3.005	2.770	2.502	2.071	1.713
	1.000	1.000	1.000	1.000	1.000	1.000
-0.8	2.138	2.066	1.941	1.798	1.569	1.379
	1.000	1.000	1.000	1.000	1.000	1.000
-1.0	1.000	1.000	1.000	1.000	1.000	1.000
	1.000	1.000	1.000	1.000	1.000	1.000
-1.5	0.631	0.647	0.663	0.678	0.703	0.729
	0.743	0.744	0.746	0.749	0.758	0.771
-2.0	0.443	0.468	0.491	0.514	0.552	0.592
	0.612	0.614	0.617	0.622	0.635	0.655
-2.5	0.383	0.411	0.436	0.461	0.504	0.548
	0.571	0.572	0.576	0.581	0.596	0.618
-3.0	0.407	0.433	0.458	0.482	0.523	0.565
	0.587	0.589	0.592	0.597	0.611	0.632
-4.0	0.574	0.593	0.610	0.628	0.657	0.687
	0.703	0.704	0.707	0.710	0.721	0.736
-5.0	0.764	0.775	0.785	0.794	0.810	0.827
	0.836	0.837	0.838	0.840	0.845	0.854
-7.0	0.987	0.987	0.988	0.988	0.989	0.990
	0.991	0.991	0.991	0.991	0.991	0.992

3.0	3.5	4.0	5.0	6.5	10.0
1.000	1.000	1.000	1.000	1.000	1.000
1.000	1.000	1.000	1.000	1.000	1.000
1.235	1.132	1.064	0.996	0.981	1.000
1.000	1.000	1.000	1.000	1.000	1.000
1.442	1.249	1.120	0.993	0.964	1.000
1.000	1.000	1.000	1.000	1.000	1.000
1.616	1.347	1.167	0.991	0.950	0.999
1.000	1.000	1.000	1.000	1.000	1.000
1.751	1.423	1.204	0.988	0.939	0.999
1.000	1.000	1.000	1.000	1.000	1.000
1.825	1.465	1.224	0.987	0.933	0.999
1.000	1.000	1.000	1.000	1.000	1.000
1.751	1.423	1.204	0.988	0.939	0.999
1.000	1.000	1.000	1.000	1.000	1.000
1.616	1.347	1.167	0.991	0.950	0.999
1.000	1.000	1.000	1.000	1.000	1.000
1.442	1.249	1.120	0.993	0.964	1.000
1.000	1.000	1.000	1.000	1.000	1.000
1.235	1.132	1.064	0.996	0.981	1.000
1.000	1.000	1.000	1.000	1.000	1.000
1.000	1.000	1.000	1.000	1.000	1.000
1.000	1.000	1.000	1.000	1.000	1.000
0.757	0.786	0.813	0.863	0.917	0.971
0.788	0.808	0.830	0.871	0.919	0.971
0.634	0.677	0.718	0.794	0.874	0.956
0.681	0.711	0.743	0.806	0.878	0.957
0.594	0.642	0.688	0.771	0.861	0.952
0.646	0.680	0.715	0.785	0.865	0.952
0.610	0.656	0.700	0.780	0.866	0.954
0.660	0.692	0.726	0.793	0.871	0.954
0.720	0.752	0.785	0.842	0.904	0.967
0.755	0.779	0.803	0.851	0.907	0.967
0.845	0.863	0.881	0.913	0.947	0.982
0.865	0.878	0.891	0.918	0.949	0.982
0.991	0.992	0.993	0.995	0.997	0.999
0.992	0.993	0.994	0.995	0.997	0.999

3.0	3.5	4.0	5.0	6.5	10.0
1.000	1.000	1.000	1.000	1.000	1.000
1.000	1.000	1.000	1.000	1.000	1.000
1.312	1.176	1.085	0.995	0.975	1.000
1.000	1.000	1.000	1.000	1.000	1.000
1.587	1.331	1.159	0.991	0.953	0.999
1.000	1.000	1.000	1.000	1.000	1.000
1.819	1.462	1.222	0.987	0.934	0.999
1.000	1.000	1.000	1.000	1.000	1.000
1.999	1.563	1.271	0.985	0.919	0.999
1.000	1.000	1.000	1.000	1.000	1.000
2.097	1.618	1.298	0.983	0.911	0.999
1.000	1.000	1.000	1.000	1.000	1.000
1.999	1.563	1.271	0.985	0.919	0.999
1.000	1.000	1.000	1.000	1.000	1.000
1.819	1.462	1.222	0.987	0.934	0.999
1.000	1.000	1.000	1.000	1.000	1.000
1.587	1.331	1.159	0.991	0.953	0.999
1.000	1.000	1.000	1.000	1.000	1.000
1.312	1.176	1.085	0.995	0.975	1.000
1.000	1.000	1.000	1.000	1.000	1.000
1.000	1.000	1.000	1.000	1.000	1.000
1.000	1.000	1.000	1.000	1.000	1.000
0.677	0.715	0.752	0.818	0.889	0.962
0.719	0.745	0.774	0.829	0.893	0.962
0.513	0.570	0.626	0.726	0.833	0.942
0.575	0.616	0.659	0.742	0.838	0.943
0.461	0.524	0.586	0.696	0.815	0.936
0.530	0.574	0.622	0.714	0.821	0.936
0.482	0.542	0.602	0.708	0.822	0.938
0.548	0.591	0.636	0.725	0.828	0.939
0.627	0.671	0.714	0.790	0.872	0.956
0.675	0.706	0.739	0.802	0.876	0.956
0.794	0.818	0.842	0.884	0.929	0.976
0.820	0.837	0.855	0.891	0.932	0.976
0.988	0.990	0.991	0.993	0.996	0.999
0.990	0.991	0.992	0.994	0.996	0.999

APPENDIX I

TABLES FOR THE DETERMINATION OF THE VERTICAL STRESS IN THE SOIL

It is often necessary to determine the vertical stress in the soil, especially during the calculation of the settlement of buildings according to Sec. 1.3. If several foundations are near to each other, then the stresses in the soil they cause are added (Fig. I.1). Tables have been prepared for the simpler calculation of the vertical stresses in the soil beneath a foundation caused not only by the load acting on the foundation but also by the loads acting on the adjacent foundations. Solutions are presented for a homogeneous subgrade (a homogeneous subgrade is one whose properties do not change in the active zone—see Appendix II), for a vertical load also the case of a double-layer subgrade and the case of an earth cushion beneath a foundation.

a) Vertical load at various depths of a homogeneous soil

In the foundation line there is an average load increment

$$\Delta q = Q'/BL \quad \text{for a strip foundation} \quad (\text{I.1})$$

$$\Delta q = Q'/B^2 \quad \text{for a square foundation} \quad (\text{I.2})$$

$$\Delta q = Q'/\pi R^2 \quad \text{for a circular footing with a radius } R \quad (\text{I.3})$$

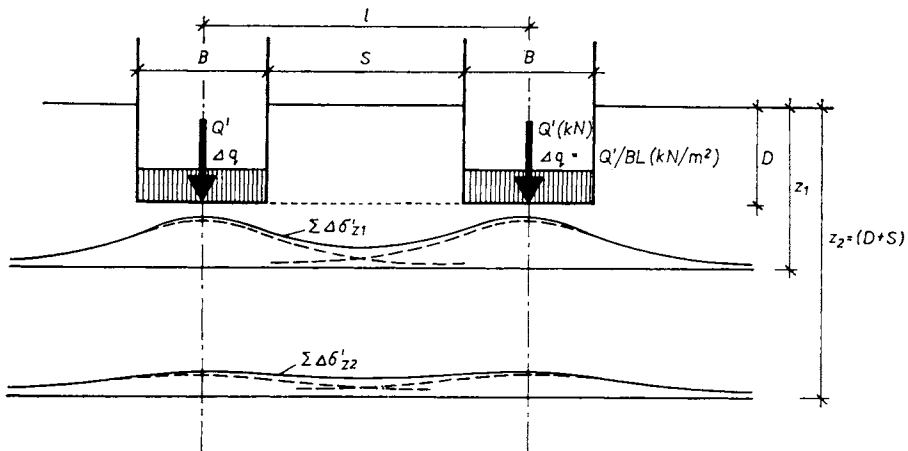


Fig. I.1 Superposition of stresses under strip foundation

if Q' is a vertical central resultant of the forces acting on the foundation, reduced by the weight of the soil excavated to make room for the foundation. The diagram of the designations is in Fig. I.2. The vertical stress at point M from the load increment in the foundation line is

$$\Delta\sigma_z = \Delta q K_1 \quad (I.4)$$

The values of coefficient K_1 are given in Table I.1 for various depths ($z - D$) below the foundation and for various distances x from the axis of the foundation, which is based at a depth D below the ground surface.

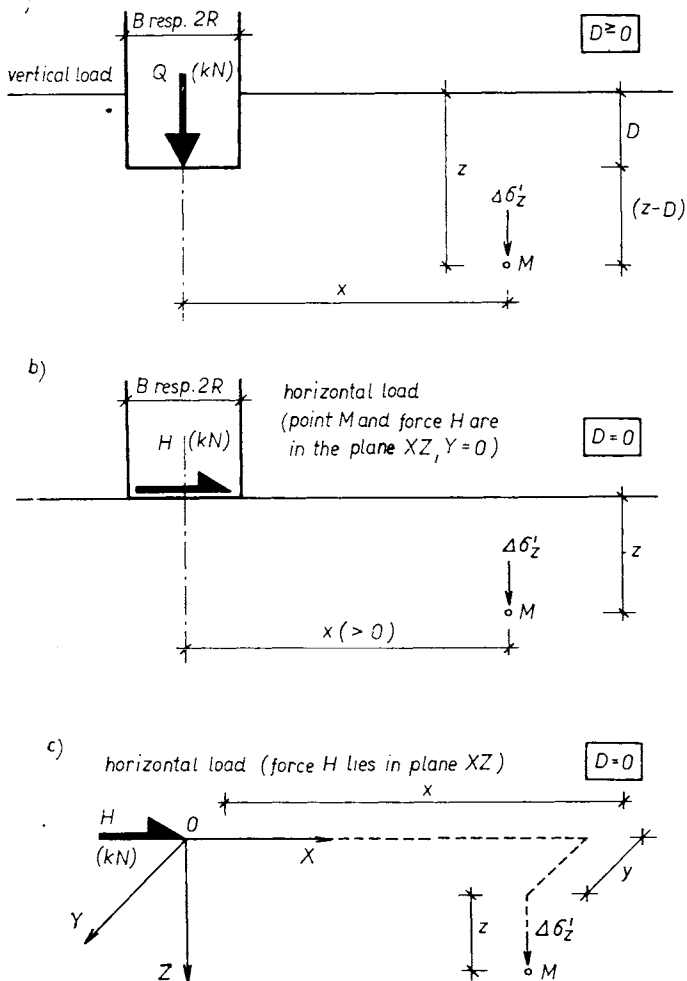


Fig. I.2 Notation for the calculation of the vertical stresses in the soil caused by the load of a strip foundation (a, b) or a footing (a, b, c)

TABLE I.1

Values of coefficient K_1 for the calculation of the vertical stress in the soil if the foundation, which is loaded vertically, is based at various depths D and if there is a homogeneous soil in the subgrade

$(z - D)/B$ or $(z - D)/2R$	D/B or $D/2R$	x/B for a strip foundation					x/B or $x/2R$ for a footing		
		0	2	3	4	5	0	2	3
0	≥ 0	1	0	0	0	0	1	0	0
0.25	0	0.96	0	0	0	0	0.92	0	0
	0.5	0.86	0.02	0	0	0	0.75	0	0
	1	0.79	0.07	0	0	0	0.65	0.01	0
	2	0.68	0.19	0.11	0.03	0	0.54	0.01	0
	4	0.57	0.23	0.19	0.16	0.12	0.48	0	0
0.50	0	0.82	0.01	0	0	0	0.67	0	0
	0.5	0.71	0.03	0	0	0	0.50	0.01	0
	1	0.61	0.08	0	0	0	0.42	0.01	0
	2	0.52	0.13	0.08	0.04	0	0.35	0.01	0
	4	0.43	0.14	0.12	0.09	0.07	0.34	0	0
1.00	0	0.54	0.03	0.01	0	0	0.31	0.01	0
	0.5	0.44	0.06	0.02	0	0	0.22	0.01	0
	1	0.38	0.09	0.03	0	0	0.18	0.01	0
	2	0.31	0.11	0.07	0.04	0.02	0.16	0.01	0.01
	4	0.27	0.10	0.08	0.06	0.05	0.15	0.01	0
1.50	0	0.40	0.06	0.02	0.01	0	0.16	0.01	0
	0.5	0.32	0.09	0.03	0.01	0	0.11	0.02	0
	1	0.28	0.10	0.05	0.02	0	0.09	0.02	0.01
	2	0.23	0.10	0.07	0.04	0.02	0.08	0.01	0.01
	4	0.20	0.09	0.07	0.06	0.04	0.08	0.01	0
2.00	0	0.31	0.08	0.03	0.01	0.01	0.09	0.02	0.01
	0.5	0.25	0.10	0.04	0.02	0.01	0.06	0.02	0.01
	1	0.21	0.11	0.06	0.03	0.01	0.05	0.02	0.01
	2	0.18	0.10	0.07	0.04	0.03	0.05	0.01	0.01
	4	0.15	0.09	0.07	0.05	0.04	0.04	0.01	0
3.00	0	0.21	0.10	0.05	0.03	0.02	0.04	0.02	0.01
	0.5	0.17	0.11	0.06	0.03	0.02	0.03	0.02	0.01
	1	0.14	0.11	0.07	0.04	0.02	0.02	0.01	0.01
	2	0.12	0.10	0.07	0.05	0.04	0.02	0.01	0.01
	4	0.10	0.09	0.07	0.05	0.04	0.02	0.01	0.01
5.00	0	0.13	0.09	0.07	0.05	0.03	0.02	0.01	0.01
	0.5	0.10	0.09	0.07	0.05	0.04	0.01	0.01	0.01
	1	0.09	0.09	0.07	0.05	0.04	0.01	0.01	0.01
	2	0.07	0.07	0.07	0.05	0.04	0.01	0.01	0.01
	4	0.07	0.07	0.06	0.05	0.04	0.01	0.01	0

Coefficient K_1 for a strip foundation from Table I.1 can be used for practical calculations of strip foundations, whose length $L \leq 3B$. The values of K_1 in the table are calculated for $L = 4B$.

The coefficient K_1 given in the table for a footing can be used both for a square and circular footing. The exact values differ from the values in Table I.1 at most by 10% for $x/B = 0$, $(z - D)/B = 1.5$, $D/B = 0$.

During the calculation of the vertical stresses in the soil the influence of the distribution of the stress in the foundation line is apparent only in the near vicinity of the foundation. For $x/B > 1$ or $(z - D)/B > 1.5$ the stress in the soil from the foundation footing can be calculated as though due to a point load and the stress from a strip foundation as though due to a line load. The error thus created does not exceed 2%.

b) The vertical load on the surface of a stratified subgrade ($D = 0$)

During the calculation of vertical stresses in the soil beneath a foundation the influence of stratification is incorporated in the calculation approximately by replacing the upper layer of soil by an equivalent layer of the soil of the lower layer. The stress is then calculated as for a homogeneous subgrade for an equivalent depth

$$z_{eq} = z\lambda \quad (I.5)$$

In this way a multilayered subgrade can be gradually transformed into a substitute homogeneous subgrade, which is formed only by the soil of the lowest layer. The coefficient for a double-layer subgrade

$$\lambda \doteq \sqrt[2.5]{E_{01}/E_{02}} \quad (I.6)$$

and for a soil cushion below the foundation

$$\lambda \doteq \sqrt[3.5]{E_{01}/E_{02}} \quad (I.7)$$

Equation (I.7) is valid in the case of a soil cushion which is only a little wider than the foundation (up to $1.4B$) and reaches from the foundation line to a depth

$$h = B \frac{\sin(\beta^\circ + \Phi_2/2)}{\sin(90 - \Phi_2/2)} \exp(\beta^\circ \tan(\Phi_2/2)) \quad (I.8)$$

if

$$\beta^\circ = 45^\circ \left(1 - \frac{\beta}{\Phi_2}\right) - \frac{\beta}{2} \quad (I.9)$$

Usually we find $h = 0.75B$ to $h = 1.3B$.

In the equations Φ_2 is the angle of internal shearing resistance of the cushion

E_{01} is the deformation modulus of the upper layer (cushion)

E_{02} is the deformation modulus of the lower layer of soil

β is the inclination of the resultant of the central load on the foundation from the vertical.

Using equation (I.5) we can determine the vertical stress in the soil beneath the foundation to a maximum distance $x = B/2$ from the axis of the foundation. Expressions (I.6) and (I.7) were derived for a load acting on the surface ($D = 0$), but they can be used with sufficient accuracy even for shallow foundations. The coefficient λ according to equation (I.6) and (I.7) is calculated for various ratios E_{01}/E_{02} in Table I.2.

TABLE I.2

Value of coefficient λ for various ratios of the deformation moduli E_{01}/E_{02}

E_{01}/E_{02} (C_1/C_2)	0.02	0.10	0.25	0.50	1.00	2.00	4.00	6.00	10.00
double layer subgrade	0.21	0.40	0.57	0.76	1.00	1.32	1.74	2.05	2.51
λ soil cushion	0.33	0.52	0.67	0.82	1.00	1.22	1.49	1.67	1.93

c) The horizontal load on the surface of a homogeneous soil ($D = 0$)

If a horizontal force H , parallel with axis X , acts in the foundation line, then there is created at point M , which is at a distance x , a stress

$$\Delta\sigma_z = \frac{x}{|x|} \frac{H}{B} K_2 \quad (\text{I.10})$$

for a strip foundation or a square footing

$$\Delta\sigma_z = \frac{x}{|x|} \frac{H}{2R} K_2 \quad (\text{I.11})$$

for a circular footing

The axis X is at right angles to the length of the strip. The diagram of the designations is in Fig. I.2. The values of coefficient K_2 are given in Table I.3 for various depths z and various distances x from the axis of the foundation if $D = 0$. The vertical stress in the soil caused by a square or circular footing loaded horizontally, can be determined even in the case where point $M(x, y, z)$ at which we are determining the vertical stress, is at a distance y from the

TABLE I.3

Values of coefficient K_2 ($D = 0$)

z/B or $z/2R$	$ x /B$ for a strip foundation					$ x /B$ or $ x /2R$ for a footing		
	0	2	3	4	5	0	2	3
0	0	0	0	0	0	0	0	0
0.25	0	0.01	0	0	0	0	0	0
0.50	0	0.02	0.01	0	0	0	0.01	0
1.00	0	0.06	0.02	0.01	0	0	0.01	0
1.50	0	0.08	0.04	0.02	0.01	0	0.02	0.01
2.00	0	0.08	0.05	0.03	0.02	0	0.02	0.01
3.00	0	0.07	0.05	0.04	0.03	0	0.01	0.01
5.00	0	0.04	0.04	0.04	0.03	0	0	0

TABLE I.4

Values of coefficient K_3 ($D = 0$)

$ x /z$	$ x /z$								
	0	0.20	0.40	0.60	0.80	1.0	2.00	3.00	5.0
0	0	0.02	0.05	0.08	0.09	0.08	0.03	0.01	0
0.2	0	0.02	0.05	0.07	0.08	0.08	0.03	0.01	0
0.4	0	0.01	0.04	0.06	0.07	0.07	0.03	0.01	0
0.6	0	0.01	0.03	0.04	0.05	0.06	0.03	0.01	0
0.8	0	0.01	0.02	0.03	0.04	0.04	0.03	0.01	0
1.0	0	0	0.01	0.02	0.03	0.03	0.02	0.01	0
1.5	0	0	0	0.01	0.01	0.01	0.01	0.01	0
2.0	0	0	0	0	0	0	0	0	0

vertical plane XZ in which the horizontal force H lies (Fig. I.2c). At point M given by coordinates (x, y, z) there is a vertical stress due to force H

$$\Delta\sigma_z = \frac{x}{|x|} \frac{H}{z^2} K_3 \quad (\text{I.12})$$

The origin O of the rigid-angled coordinate system is at the centre of the horizontal foundation surface of the footing. The values of coefficient K_3 are given in Table I.4. The calculation according to equation (I.12) can be used if the point at which the vertical stress is being determined is at a distance of at least $2R$ or B from the centre of the circular or square footing.

effective depth, depends mainly on the depth of foundation, the width of the foundation, the compressibility of the soil and the size of the load. When, during the calculation of the vertical stresses in the soil, we also consider the effect of the adjacent foundations¹⁾ and other similar influences, the active zone can be determined from the condition

$$\Delta\sigma_z \geq 0.3\sigma_z \quad (\text{II.1})$$

where σ_z is the initial stress in the soil at a depth z

$\Delta\sigma_z$ is the load increment in depth z caused above the point by the foundation, by adjacent foundations, by the lowering of the groundwater level, etc.

The determination of the active zone is shown in Fig. II.1. In equation (II.1) a coefficient smaller than 0.3 was used previously, but recent measurements show that the value 0.3 is more realistic.

1) Very approximately, it is also possible to determine the vertical stress in the soil under shallow foundations ($0 < D \leq 4B$) as for $D = 0$, but then it is not possible to add the effect of the adjacent foundations.

BIBLIOGRAPHY

- [1] Barkan, D.: Dynamics of Bases and Foundations, 1st ed., McGraw-Hill Book Company, London, 1962.
- [2] Bažant, Z.: Metody zakládání staveb, Prague, NČSAV, 1973.
- [3] De Beer, E.: Foundation Problems of Petroleum Tanks, Annales de l'Institut Belge, 1969.
- [4] Brinch Hansen, J.: 1) A General Formula for Bearing Capacity (Bulletin No. 11), Copenhagen, Geoteknisk Institut Akademiet for de Tekniske Videnskaber, 1961.
2) A Revised and Extended Formula for Bearing Capacity, Reprint of lecture in Japan, 1968.
- [5] Borowicka, H.: Die Einbruchlast eines Streifenfundamentes als Stabilitäts Problem. Mitt. des Institutes für Grundbau und Bodenmechanik Technische Hochschule Wien, 1973.
- [6] Caquot, A. and Kerisel, J.: Sur la terme de surface dans le calcul des fondations eu milieu pulvérulent. In: Proceedings of the 3rd International Conference on Soil Mechanics and Foundation Engineering, Zürich 1953, p. 336.
- [7] Caquot, A. and Kerisel, J.: Grundlagen der Bodenmechanik, 1st ed. Springer Verlag, Berlin, 1967.
- [8] Code of Practice for Foundation Engineering. The Danish Geotechnical Institute. Bulletin 22. Copenhagen, 1966.
- [9] Cytovič, N.: Mechanika gruntow. 4th ed. Gosudarstvennoje izdatelstvo po strojitelstvu, architekture i strojitelnyh materialam, Moscow, 1970.
- [10] Dembicki, E. et al.: Load Tests on Slurry — trench Walls. In: Proceedings of the 4th Budapest Conference on Soil Mechanics and Foundation Engineering. Budapest, 1971, p. 533.
- [11] Dembicki, E. et al.: Stateczność pojedynczych fundamentów słupowych. 1st ed. Państwowe wydawnictwo naukowe, Warsaw, 1971.
- [12] Ducháček, J. et al.: Nauka o pružnosti a pevnosti ve stavitelství. SNTL Prague, 1963.
- [13] Fischer, K.: Beispiele zur Bodenmechanik. Verlag von Wilhelm Ernst & Sohn, Berlin-München, 1965.
- [14] Garnier, J.: Tassement et contraintes. Influence de la rigidité de la fondation et de l'anisotropie du massif (Doctorate thesis). Grenoble, 1973. L'Université Scientifique et Médicale de Grenoble.
- [15] Giroud, J.: Bearing Capacity of Footings on a Stratified Scil. In: Proceedings of the 4th Budapest Conference on Soil Mechanics and Foundation Engineering, Budapest, 1971 (p. 551).
- [16] Goodman, R. and Seed, H.: Earthquake-induced Displacements in Sand Embankments. Journal of the Soil Mechanics and Foundation Division, 92, Proceedings of the American Society of Civil Engineers, 1966, SM 2.
- [17] Grasshoff, H. et al.: Die Berechnung elastischer Gründungsbalken auf nachgiebigem Untergrund. 1st ed. Westdeutscher Verlag, Köln, 1966.
- [18] Grasshoff, H.: Das steife Bauwerk auf nachgiebigem Untergrund. Ein Näherungsverfahren zur Berechnung von Flächengründungen. Verlag von Wilhelm Ernst & Sohn Berlin, 1966.

- [19] Haedicke, K. and Fuchs, E.: Gründungen. 1st ed. VEB Verlag für Bauwesen Berlin 1968, 2 vol.
- [20] Houska, J.: Inženýrské stavby, 7, Prague 1959 (p. 442).
- [21] Janbu, N.: Settlement Calculation Based on the Tangent Modulus Concept. TU Norway. Mitt. 1967.
- [22] Jeske, T. and Przedeci, T. and Rossinski, B.: Mechanika gruntów. 1st ed. Państwowe wydawnictwo naukowe, Warsaw, 1966.
- [23] Jelinek, R.: Der Einfluss von Gründungstiefe auf bekreuzter Schichtmächtigkeit und die Druckausbreitung in Baugrund. Bautechnik 1951.
- [24] Jelinek, R. and Ranke, A.: Berechnung der Spannungsverteilung in einem Zweischichten system. Bau'technik 1970.
- [25] Kézdi, A.: Bočnice mechanik. 1st ed. VEB Verlag für Bauwesen and Verlag der Ungarischen Akademie der Wissenschaften Berlin—Budapest, 1964. 2 vol.
- [26] Koloušek, V. et al.: Stavebné konštrukcie namáhané dynamickými účinkmi. Slovenské vydavateľstvo technickej literatúry, Bratislava, 1st. ed. 1967.
- [27] Król, W.: Die Statik der Stahlbetonfundamente unter Berücksichtigung der Steifigkeit des Überbaues. 1st ed. Verlag von Wilhelm Ernst & Sohn, Berlin—München—Düsseldorf, 1970.
- [28] Kysela, Z.: Únosnost vrstevnatého podloží. (Diploma treatise). Prague, 1965. Technical University of Prague, Faculty of Building Technology.
- [29] Kysela, Z.: Vzájemné spolupůsobení stejných sousedních základů. (Candidature treatise). Prague, 1971. Technical University of Prague, Faculty of Building Technology — ÚTAM ČSAV.
- [30] Kysela, Z. and Fiřt, V.: Stabilita zemních svahů při zemětřesení a pohyb svahů. (Research report). Prague, Institute for Theoretical and Applied Mechanics, ČSAV 1972.
- [31] Kysela, Z. and Fiřt, V.: Shear Failure on Slip Surfaces by Dynamic Load. In: Proceedings of the 4th Danube-European Conference on Soil Mechanics and Foundation. Eng. Bled, 1974 (p. 193).
- [32] Lebegue Y.: Pouvoir portant du sol sous une charge inclinée. In: Annales de l'institut technique du bâtiment et des travaux publics. No 292. Paris, 1972 (p. 1).
- [33] L'Hermier, R., Tcheng, Y. and Lebegue, Y.: Expérimentation en laboratoire de la capacité portante des sols. In: Proceedings of the 6th International Conference on Soil Mechanics and Foundation Engineering. vol. 2. Montreal, 1965 (p. 117).
- [34] Livneh, M.: The Theoretical Bearing Capacity of Soils on a Rock Foundation. In: Proceedings of the 6th International Conference on Soil Mechanics and Foundation Engineering, vol. 2. Montreal, 1965 (p. 122).
- [35] Mandel, J. and Salencon, J.: Poinçonnement d'un bicouche à interface lisse eu déformation plane. CRAS vol. 263, sér. A, Paris, 1969.
- [36] Mandel, J.: Interférence plastique de semelle filantes. In: Proceedings of the 6th International Conference on Soil Mechanics and Foundation Engineering, vol. 2. Montreal, 1965 (p. 127).
- [37] Meyerhof, G.: The Ultimate Bearing Capacity of Foundations on Slopes. In: Proceedings of the 4th Conference on Soil Mechanics and Foundation Engineering. London, 1957 (p. 384).
- [38] Meyerhof, G.: The Bearing Capacity of Foundations under Eccentric and Inclined Loads. Proceedings of the 3rd International Conference on Soil Mechanics and Foundation Engineering, Zürich 1953
- [39] Muhs, H.: Die Experimentelle Untersuchung der Grenztragfähigkeit nichtbindigen Böden bei lotrecht mittiger Belastung. Mitt. DEGEBO, 1971.

- [40] Muhs, H.: Shallow Foundations and Pavements. In: Proceedings of the 6th International Conference on Soil Mechanics and Foundation Engineering. Montreal, 1965 (p. 419, fig. 17).
- [41] Muhs, H. and Weiss, K.: Versuche über die Standsicherheit flach gegründeter Einzel-fundamente in nichtbindigen Böden. Mitt. DEGEBO, 1972.
- [42] Myslivec, A.: Mechanika zemin. Revised edition, SNTL, Prague, 1968.
- [43] Myslivec, A.: Die Grenztragfähigkeit des zwischichtigen Baugrundes. In: Proceedings of the 4th Budapest Conference on Soil Mechanics and Foundation Engineering. Budapest, 1971 (p. 677).
- [44] Myslivec, A. and Eichler, J. and Jesenák, J.: Mechanika zemin. 1st ed. SNTL/ALFA, Prague, 1970.
- [45] Myslivec, A. and Kysela, Z.: Effect of Adjacent Foundations on Bearing Capacity. In: Acta Technica Academiae Scientiarum Hungaricae. 64. Budapest, 1969 (p. 183).
- [46] Myslivec, A. and Kysela, Z.: Výpočet únosnosti základového podloží s písكوšterkovým polštářem. Inženýrské stavby, 20, 1972, p. 417.
- [47] Myslivec, A. and Kysela, Z.: Interaction of Neighbouring Foundations. In: Proceedings of the 8th International Conference on Soil Mechanics and Foundation Engineering. Moscow, 1973 (Vol. 1, 3, p. 181).
- [48] Myslivec, A. and Vaniček, I.: Vliv příčného tvaru základu v sypkých zeminách na jeho mezní zatížení (Research report). Prague, ÚTAM ČSAV, 1970.
- [49] Newmark, N. M.: Simplified Computation of Vertical Pressures in Elastic Foundations. Univ. of Illinois, Bull. No. 24, 1935.
- [50] Obin, J. P.: Force portante en deformation plane d'un sol verticalement non-homogene. (Doctorate thesis). Grenoble 1972. L'Universite scientifique et medicale de Grenoble 1972. L'Universite scientifique et medicale de Grenoble.
- [51] PN-491/B-03 020
- [52] Rossiński, B. and Przedeci, T.: Badania modelowe nośności granicznej osrodków sypkich. Archiwum inżynierii ładowej, vol. 7, Warsaw, 1961, p. 171 (sec. 3.4.5.).
- [53] Seed, H. and Chan, C.: Clay Strength Under Earthquake Loading Conditions. Journal of the Soil Mechanics and Foundation Division, Proceedings of the American Society of Civil Engineers, 92, 1966, SM 2.
- [54] Schibert, K.: Böschungen, Dämme, Hulden, Kippen. Leipzig, 1972.
- [55] Schultze, E.: Distribution of Stress Beneath Rigid Foundations. In: Proceedings of the 5th International Conference on Soil Mechanics and Foundation Engineering, 1st vol. Paris, 1961 (p. 807).
- [56] Schultze, E.: Die Grundbaunormung in der Bundesrepublik. Mitt. des Inst. für Grundbau. Wien, 1973.
- [57] Schultze, E.: Der Widerstand des Baugrundes gegen schräge Sohlpressungen. Bautechnik 1952.
- [58] Schultze, E.: Erdstatische Berechnungen. Mitteilungen aus dem Institut für Verkehrswasserbau, Grundbau und Bodenmechanik der Technischen Hochschule, Aachen, 1950.
- [59] Schultze, E. and Muhs, H.: Bodenuntersuchungen für Ingenieur-bauten. Berlin, 1967.
- [60] Siemer, H.: Gründung auf Schluff. Mitteilungen aus dem Institut für Verkehrswasserbau, Grundbau und Bodenmechanik der Technischen Hochschule Wuppertal, 1973.
- [61] Sobotka, Z.: Mezní stavy rovnováhy zemin a jiných souvislých hmot. 1st ed. SNTL Prague, 1956.
- [62] Stuart, J.: Geotechnique, 12, 1962, p. 15.

- [63] Széchy, K.: Der Grundbau. 1st ed. Springer Verlag, Wien, 1963, 3 vols.
- [64] Šimek, J.: Řešení pružného podkladu od zatížení působícího uvnitř v polovině. Inženýrské stavby, 10, 1962, p. 348.
- [65] Šimek, J., Vaníček, I. and Fanta, R.: Kritický přehled současných znalostí o vývoji a rozdělení kontaktních napětí v základové spáře. (Research report), Prague, Technical University of Prague.
- [66] Terzaghi, K.: Teoria mechaniky gruntov. (Theoretical Soil Mechanics.) 1st ed. Gosudarstvennoe izdatelstvo literatury po stroitelstve, architekture i stroitelnyh materialam, Moscow 1961.
- [67] Šuklje, L.: Rheological Aspects of Soil Mechanics. Wiley Interscience, London, 1969.
- [68] Žemočkin, B. N. and Sinicin, A. N.: Praktičeskije metody rasčeta fundamentnyh balok i plyt na uprugom osnovanii bez gipotesy Winklera. Gosudarstvennoe izdatelstvo stroitelnoj literatury (GISL), Moscow, 1947.

Bibliography used for the Appendixes

- [I] Ducháček, J.: Nauka o pružnosti a pevnosti II. Teoretická část. SNTL, Prague, 1964.
- [II] Florin, V. A.: Osnovy mechaniky gruntov. 1st vol. Gosudarstvennoe izdatelstvo literatury po stroitelstve, architekture i stroitelnyh materialam, Moscow, 1959.
- [III] Kysela, Z. and Drdácký, M.: Racionalizace některých výpočtů mechaniky zemin využitím počítače Hewlett-Packard. (Internal report). ÚTAM ČSAV, Prague, 1974.
- [IV] Šimek, J.: Příspěvek k navrhování plošných základů. Inženýrské stavby, 22, Bratislava, 1974, p. 280.
- [V] Sneddon, I. N.: Fourier Transforms. 1st ed. McGraw-Hill Book Company, New York, 1951.
- [VI] Valenta, V.: Výpočet napětí v půdě pod bytovkou založenou na pásech. Pozemní stavby, 22, Prague, 1974, p. 160.

INDEX

- absolute coefficient of compressibility 27
- absorbed water 52
- acceleration 66, 155
- active soil pressure 72, 77, 84
- active zone 30, 229
- adhesion 68, 86
- adjacent foundations 93, 132
- alternate soils 150
- amplitude 66, 155
- angle of friction 54, 59, 61
- angle of wall friction 67

- base failure 14, 16, 17, 94, 116, 119
- base slab 19, 71, 75, 80, 85, 88, 93, 152, 160, 223, 229
- batter pile 133
- bearing capacity 54
 - graphical method 88, 126
 - method of Brinch Hansen 80
 - method of Caquot and Kérisel 85
 - method of Mayerhof 75
 - method of Terzaghi 71
- bearing-value coefficient 72, 75, 78, 87
- bedrock 140
- box shear apparatus 54
- building period 49
- bulking 49

- capillary height 21
- capillary level 20, 229
- capillary tension 20
- capillary water 20, 229
- cast-in-situ pile 80, 85
- coefficient of active soil pressure 72
- coefficient of earth pressure at rest 171
- coefficient of friction 67
- coefficient of oedometric compressibility 24
- coefficient of passive soil pressure 72
- coefficient of permeability 28, 47
- cohesion 54, 61, 86
- collapse mechanism according to Mayerhof 17
 - — — to Prandtl 14
 - — — to Terzaghi 16
 - — of adjacent foundations 94
- compaction 172
- compressibility 24
- compression curve 24
- concrete 160
- confidence 93
- consolidation coefficient for primary settlement 45, 47
 - — for secondary settlement 44
- consolidation stress 23, 29
- contact stress 160
- continuous footing 19, 71, 75, 80, 85, 88, 93, 116, 119, 134, 152, 160, 223, 229, Coulomb's equation 54
- critical yield surface 14, 16, 17, 88, 94, 116, 119, 126, 143
- cross section influence 116
- cushion 143

- deep foundation 76
- deformation modulus 24, 25, 26, 27, 28
- deformation work 61, 62
- degree of consolidation 45, 46
- degree of mobilisation of shearing 78
- depth factors 81
- direct box shear apparatus 54
- distribution of load 160
- double layer subgrade 134
- drawing-out 158
- drying out of soil 49

- earth pressure 72, 77, 84, 171
- earth pressure at rest 171
- earthquake 65
- earthquake acceleration 66
- earthquake amplitude 66
- eccentricity 166, 167
- effective depth 86, 229
- effective part of foundation 84
- equivalent layer 148

- equivalent part of foundation 84
- expansion 52

- factor of safety 128, 130, 156
- factor of slope stability 120
- flat foundation 19, 71, 75, 80, 85, 88, 93, 116, 119, 134, 152, 160, 223, 229
- floating pile 80, 85, 127
- footing 19, 71, 75, 80, 85, 93, 116, 119, 134, 152, 160, 223, 229
- forced vibrations 63, 155
- foundations in a group 93, 132
- foundation non-rigid circular 115
- foundation rigid circular 32, 167
- foundation slab or strip 19, 71, 75, 80, 85, 88, 93, 152, 160, 223, 229
- freezing 52, 60
- freezing zone 52
- frequency 64, 155
- friction angle 54, 67
- friction between soil and structure 67
- friction cohesion 68
- friction pile 80, 85, 127
- frost heave 52
- frost zone 52

- grading curves 135
- graphical method 88, 126, 146
- gravel-sand cushion 143
- groundwater elevation, -level, -surface, -table 20, 85, 229

- harmonic motion 155
- height of plastic range 86
- homogeneous foundation soil 29, 31, 69
- horizontal force, load 127, 227

- inclination factors 81
- inclined force 74, 81, 89
- inclined foundation 74
- incompressible subgrade 141
- independent footing 19, 71, 75, 80, 85, 88, 93, 119, 134, 152, 160, 223, 229
- influence factors 163, 164
- influence of adjacent foundations 93
- influence of cross section 116
- influence of groundwater 19, 29, 85
- influence of slope 79
- influence of vertical moment 36

- initial shear strength 60
- intensity °MCS 66
- intrinsic curve 55
- isolated foundation 19, 71, 75, 80, 85, 88, 93, 119, 134, 152, 160, 223, 229

- landslide 119, 123
- land upheaval 52
- line load 170, 172
- load carrying capacity 54
- loading disc 13,28
- loading of slope 79
- layered subgrade 134
- loading test 14, 28, 93, 132

- mat foundation 19, 71, 75, 80, 85, 88, 93, 152, 160, 223, 229
- Mises criterion 56
- mobilisation moduli 62, 63
- model test 89, 93, 116, 130, 132, 134
- Mohr—Coulomb criterion 55, 56
- Mohr's circle 55
- Mohr's envelope 55
- mobilisation work 61, 62
- moisture content 49
- multilayered subgrade 150, 226

- natural frequency 64, 155
- neutral air pressure 19
- neutral stress of water 19
- non-elastic compression 24
- non-uniform lifting 52
- non-uniform soil 134
- normal stress 172
- number of rigidity 160

- oedometer modulus 24
- oscilations 155
- overcompaction 171
- overconsolidation 23, 24, 52, 57, 60

- passive earth pressure 72, 84
- period of drought 51
- permafrost 60
- permissible amplitudes 155
- permissible differences 152
- permissible eccentricity 85
- permissible load 152
- permissible settlement 152

- pier footing 80, 85, 127
- pile 80, 85, 127
- pile group 132
- plate loading test 14, 28
- point load 225
- Poisson's ratio 26
- porosity 27, 52
- pressure at rest 171
- primary settlement 42
- protective filter 150
- pulses 64

- raft foundation 19, 71, 75, 80, 85, 88, 93, 152, 160, 223, 229
- reinforced concrete 160
- raising 52, 158
- raking pile 133
- real settlement 31
- redistribution of stress 30
- reference plane 128
- repeated load 44, 63, 155
- revolutions 155
- rigid foundation 28, 32, 160
- rigidity coefficient 160
- rigidity number 160
- rigidity of foundation 30, 160
- rotation of foundation 130
- rotation slip 119
- row of piles 132

- safety factor 128, 130, 156
- sand cushion 143
- secondary settlement 42, 44
- self frequency 64, 155
- settlement analysis 29, 31
 - of non-rigid circular foundation 115
 - of rigid circular foundation 32
- shallow foundations 29, 31, 36, 42, 49, 69, 93, 116, 118, 134, 152, 160, 223, 229
- shear box 54
- shearing 158
- shearing resistance 54
- shear strength 54
- shrinkage limit 49
- sinking 158
- skin friction 67
- slab foundation 19, 71, 75, 80, 85, 88, 93, 152, 160, 223, 229
- sliding 158
- slip surface 14, 16, 17, 88, 94, 116, 119, 126, 143
- slope 79, 119
- slope factors 81, 87
- slope failure 119, 123
- soft soil 134
- soil pressure 72, 84, 171
- soil shrinkage 49
- spot loading 225
- stability number 158
- stratified soil 29, 33, 226
- stress in soil 18, 160
- strip foundation 19, 71, 75, 80, 85, 88, 93, 116, 119, 134, 152, 160, 223, 229
- Student's distribution 93
- subsidence of soil 49
- surface level difference 100
- surface of sliding 14, 16, 17, 88, 94, 116, 119, 126, 143
- swell, to 52
- swelling pressure 52

- time factor 28, 45, 46
- time-settlement curve 42
- total settlement 29
- traffic shock 65
- Tresco criterion 56
- triaxial shearing apparatus 55
- turning over 158

- ultimate bearing capacity 54
- ultimate load 71, 130
- ultimate settlement 154
- uprooting 158

- velocity 155
- vertical stress in soil 19, 148, 176, 223
- vibrations 64, 65
- void ratio 27, 59
- void water 20, 21, 22, 229

- wall friction 67, 77
- water content 50
- water menisci 20, 229
- weak soil 134

- yield surfaces 14, 16, 17, 88, 94, 116, 119, 126, 143
- Young's modul 31